



City Research Online

City, University of London Institutional Repository

Citation: Vasilakos, I. (2017). Cavitation in the cylinder-liner and piston-ring interaction in internal combustion engines. (Unpublished Doctoral thesis, City, University of London)

This is the accepted version of the paper.

This version of the publication may differ from the final published version.

Permanent repository link: <https://openaccess.city.ac.uk/id/eprint/19265/>

Link to published version:

Copyright: City Research Online aims to make research outputs of City, University of London available to a wider audience. Copyright and Moral Rights remain with the author(s) and/or copyright holders. URLs from City Research Online may be freely distributed and linked to.

Reuse: Copies of full items can be used for personal research or study, educational, or not-for-profit purposes without prior permission or charge. Provided that the authors, title and full bibliographic details are credited, a hyperlink and/or URL is given for the original metadata page and the content is not changed in any way.

CITY, UNIVERSITY OF LONDON

Cavitation in the Cylinder-liner and Piston-ring Interaction in Internal Combustion Engines

Doctor of Philosophy Thesis

Ioannis Vasilakos

December 11th, 2017



This thesis is submitted for the fulfilment of the requirements for the Degree of Doctor of
Philosophy

ACKNOWLEDGMENTS

I would like to deeply thank my supervisor Prof Nouri. His expertise, understanding and support guided me through the course of the PhD. I would also like to express my gratitude to Dr Yan for her valuable assistance and time. Also, I would like to thank Dr Reyes-Aldasoro for his valuable input and time in developing the Matlab algorithm.

A big thank you goes to Dr Gold, Dr Pearson, Dr Brett and BP Castrol for their continuous support, motivation and encouragement.

I must also acknowledge the valuable help of our technical staff Mr R Cherry and J Ford who played a critical part in the progress of the project.

I would also like to thank Dr Mitroglou for his time and assistance.

I like to thank my family for their unconditional support throughout my studies and I recognise that without their encouragement and assistance I would have never reached that far.

DECLARATION

I declare that this thesis is the result of my own work. Wherever contributions have been made by others every effort has been made to indicate this clearly. Parts of this report where pieces of work were used that have not been produced by me have been referenced accordingly.

Mr Ioannis Vasilakos

.....

Date.....

ABSTRACT

The emissions control regulations introduced by governments are set to improve the quality of the engines and reduce the impact automobiles have on the planet. The regulations imposed on the manufactures have proven very difficult to meet, with some of the leading names in the industry investing significant part of their funding in research and development. Their goal is to reduce the fuel consumption and exhaust emissions while increasing the engine performance and durability. The piston-ring and cylinder-liner interaction is the major source of frictional losses for reciprocating internal combustion engines. The failure of the piston-rings to effectively control the transportation of oil from the sump onto the cylinder walls results among others to lubricant consumption.

The objective of this project is to assist with the investigation of phenomena that occur in the cylinder liner and piston ring interaction under different operating conditions. To achieve these the following investigations have been carried, flow and cavitation visualisation in a model lubricant rig, and cavitation visualisation in a newly designed optical engine. The main focus of the project was the design, manufacturing and assembly of an optical internal combustion reciprocating engine. The new engine has been based on the design of a 450cc Ricardo Hydra, where many parts had to be redesigned or modified. The engine was fitted with a custom cylinder liner designed to accommodate custom made windows that covers almost the full length of the liner over a width of 25mm; this visibility allows access not only into the contact point over the entire length of the liner, but also provides access to the combustion chamber to allow for flow visualisation and flow field measurements. The cooling system was modified to allow for the accurate control and maintaining of the engine temperature. The control of the engine is performed with a new custom engine management system build in LabView which allowed for the precise control of the engine and of all the auxiliary systems such as fuel, ignition, sensors and optical equipment. The new control system and the optical engine were tested successfully up to 3000 RPM with the same specification as the unmodified engine in terms of in cylinder pressure and maintaining the original engine tolerances. The design of the new optical engine was a great success and it would offer a useful and valuable testing device that would allow further investigation to be carried out.

In parallel to the design of the engine, a parametric experimental study was undertaken and performed on 6 lubricant samples of different formulations at two lubricant flow rate of 0.02

and 0.05 L/min, three speeds at 100, 300 and 600 RPM, and two different temperatures at 30oC and 70oC. The study was performed on an existing test-rig to visualise lubricants cavitation using two high speed cameras coupled with three ARRI high intensity light sources. This optical test device is a quick, efficient and effective way to test different lubricant samples and compare their in-between performance. The captured video images were processed through a custom build algorithm designed around the lubrication rig. This algorithm allowed for the extraction of matrices such as cavity length, cavity width, area of cavitation and number of cavities present in the area between the piston ring and the cylinder liner interaction. This parametric study offered a set of valuable results from which the performance of each lubricant can be assessed and a direct link between the lubricant formulation and the operating conditions can be established.

Cavitation visualisation of the lubricant in the new optical engine was performed under motorised and firing condition up to an engine speed of 300 RPM and produced high quality images from the usually inaccessible piston ring and cylinder liner interaction. This unique design allowed to investigate a number of phenomena around that specific area like cavitation, blow-by, fuel spray, flame propagation and oil transportation. The parametric study results investigated in the test-rig have been linked with those obtained in the conventional internal combustion engines while providing a very useful and very powerful piece of software.

TABLE OF CONTENTS

ACKNOWLEDGMENTS	1
DECLARATION	2
ABSTRACT.....	3
LIST of FIGURES	8
LIST of TABLES.....	12
NOMECLATURE	13
CHAPTER 1: INTRODUCTION	15
1.1 Aims and Objectives	17
1.2 Thesis Outline	18
CHAPTER 2: HISTORICAL BACKGROUND and LITERATURE REVIEW.....	19
2.1 History of Lubricants	19
2.2 History of Lubrication Systems	20
2.3 Internal Combustion Engines.....	22
2.4 Engine Types	24
2.4.1 Types of Ignition.....	24
2.5 Four Stroke Engine Cycles	25
2.5.1 Four-Stroke Spark Ignition Engine Cycle.....	25
2.5.2 Four-Stroke Compress Ignition Engine Cycle	26
2.6 Internal Combustion Engines, Emissions and Air Pollution.....	28
2.7 Internal Combustion Engines and Cavitation	29
2.8 Cavitation in Supersaturated Liquids.....	32
2.9 Positive Effects of Cavitation	34
2.10 Measuring Techniques	35
2.10.1 Optical Techniques	35
2.10.2 Electrical Techniques.....	36
2.11 Lubricants	36
2.12 Piston-ring-pack.....	40
2.13 Lubrication Regimes	45
2.14 Lubricants and Internal Combustion Engines	46
2.14.1 Oil Transport Mechanisms Forces	48
2.14.2 Oil Consumption and Emissions.....	48
2.15 Relevant Work	49
2.16 Previous Work on Oil Film Thickness, Pressure, Load and Friction in Relation to the Cavity Behaviour.....	53
2.17 Critical Review on previous work	54

CHAPTER 3: LUBRICATION TEST-RIG	58
3.1 Test-rig Setup.....	60
3.2 Test-rig Sensors	61
3.3 Cavity Formation	65
3.4 Cleaning and Flushing Between the Test Runs	66
3.5 Piston-ring Profile.....	67
3.6 Processing Software.....	68
CHAPTER 4: OPTICAL ENGINE AND ENGINE DESIGN	74
4.1 Optical-Engine and Engine Design.....	74
4.2 Relevant Previous Work	76
4.3 Cylinder Block and Window Design	78
4.4 Engine Control Software.....	91
4.5 Testing.....	93
4.6 Summary	95
CHAPTER 5: RESULTS AND DISCUSSION.....	96
5.1 Lubrication Test-Rig.....	96
5.1.1 Velocity and Acceleration.....	101
5.1.2 Data Matrix	103
5.1.3 Data	107
5.2 Repeatability Test of E1003A_021A.....	161
5.3 Optical-Engine and Lubrication Test-Rig Correlation.....	164
5.4 General Characteristics of the Cavity Flow	167
5.4.1 Reynolds Number	167
5.4.2 Weber Number.....	168
5.4.3 Cavitation Number.....	168
5.4.4 Young-Laplace.....	169
5.5 Optical-Engine	170
5.5.1 Intake/Exhaust Cycle	181
5.5.2 Power Cycle	186
5.5.3 Cavity Generation	191
5.5.4 Temperature Effect	193
5.5.5 Speed Effect	197
5.5.6 Blow-by Effect.....	199
5.5.7 Ring Rap and Blow-By	204
5.5.8 Firing.....	209
5.6 Error Analysis	214

CHAPTER 6: CONCLUSIONS AND FURTHER DISCUSSION	216
6.1 Summary discussions and conclusions of test-rig measurements.....	216
6.2 Summary of Design of the Optical Engine	219
6.3 Summary discussions and conclusions of Optical Engine measurements	221
6.4 Contribution to knowledge.....	221
6.5 Aims and Objectives Assessment	223
6.6 Critical Assessment of experimental process.....	225
6.7 Recommendations for Future work.....	226
REFERENCE.....	228

LIST of FIGURES

Figure 1 – Castrol Lubricants Range (BP-Castrol, 2015)	19
Figure 2 - Internal Combustion Reciprocating Engine (What-When-How, 2015)	22
Figure 3 - Corvette LT1 6.2-liter V8 450hp with Cylinder Deactivation (Hill, 2015)	23
Figure 4 - Jet Engine, Piston less Engine (Sobester, 2015)	23
Figure 5 - The Lenoir Engine (Greene, 2015).....	24
Figure 6 – Spark Ignition VS Compression Ignition (Gitlin, 2015)	25
Figure 7 – Four Stroke Cycle (Moin, 2015).....	27
Figure 8 – Emission standards from 1993 to 2014 (pi-innovo, 2015)	29
Figure 9 - Hydraulic pump valve plate damaged by cavitation (hydraulicspneumatics, 2015).....	30
Figure 10 - Cavitation Damage on Propeller of Personal Watercraft (SonicCavitation, 2015).....	31
Figure 11 – Solubility of carbon dioxide as a function of temperature, at 105 Pa (Heywood, 1998)...	33
Figure 12 – Rectangular Ring (Grant Piston-rings, 2015)	41
Figure 13 – Taper Faced Ring (Grant Piston-rings, 2015).....	41
Figure 14 – Internally Bevelled or Stepped Ring (Grant Piston-rings, 2015).....	41
Figure 15 – Tapped Faced Ring with Inside Bottom Bevel or Step (Grant Piston-rings, 2015)	42
Figure 16 – Keystone Ring (Grant Piston-rings, 2015)	42
Figure 17 – Half Keystone Ring (Grant Piston-rings, 2015)	43
Figure 18 – L-Shaped Compression Ring (Grant Piston-rings, 2015).....	43
Figure 19 – Commercially available piston-ring types (Grant Piston-rings, 2015).....	44
Figure 20 – Lubrication Regimes and Stribeck curve (Subtech, 2015)	45
Figure 21 – Lubrication engine regimes (Tian, T. and V. W. Wong, 2000).....	47
Figure 22 - Inagaki’s (1995) single cylinder optical-engine.....	50
Figure 23 - Optical test-rig as used by Ostovar (Ostovar, 1996)	52
Figure 24 – Optical Test-rig, top view of the liner	60
Figure 25 – Modified optical liner with additional capacitance plate.....	61
Figure 26 - Friction sensor mounting positions (PCB Piezotronic, 2015).....	62
Figure 27 - Friction sensor calibration chart, derived by Ostovar	62
Figure 28 - Optical test-rig capacitance probe and setup.....	63
Figure 29 - Capacitance plate for optical and oil film thickness measurements.....	63
Figure 30 - Optical liner's capacitance plate drawing	64
Figure 31 - Capacitance calibration sample chart and calibration equation	65
Figure 32 - Development of cavities as they appear on the surface on the ring (Dhunput, 2009).....	66
Figure 33 - Piston-ring Profile, Up-Stroke (Left) - Piston-ring Profile, Down-Stroke (Right)	67
Figure 34 - Cavity width and Length, down-stroke	69
Figure 35 - Matlab image processing software	70
Figure 36 - Visual Basic algorithm, Cavitating area calculation example, 800RPM, 70C.....	71
Figure 37 - Correlation between processing software and raw data, 600RPM, 70C, 0-180 Degrees...	72
Figure 38 - Correlation between processing software and raw data, 600RPM, 70C, 270 & 348 Degrees	73
Figure 39 - Ricardo Hydra engine.....	74
Figure 40 - Model of Thermocouples in Solid Cylinder Block (Ricardo, 2011).....	75
Figure 41 - Schematic of thermocouple locations on Hydra engines cylinder and piston (Ricardo, 2011).....	75
Figure 42 - Thirouard's Kubota diesel optical-engine.....	77
Figure 43 - Thirouard's Peugeot gasoline Peugeot XUL10Ar optical-engine	77
Figure 44 - MOHS hardness scale	79

Figure 45 - First design iteration of the cylinder block assembly	80
Figure 46 - Initial Ricardo Hydra optical-engine 2D design.....	81
Figure 47 - Ricardo Hydra optical-engine 3D design	82
Figure 48 - Ricardo Hydra optical-engine 2D second design	83
Figure 49 - Ricardo Hydra optical-engine 3D final design.....	84
Figure 50 - Ricardo Hydra optical-engine 3D final design cut-out.....	85
Figure 51 - Window imperfections in the first batch of optical windows.....	86
Figure 52 - Ricardo Hydra optical-engine new cylinder block assembly	86
Figure 53 - Window, window housing and flange assembly	87
Figure 54 - Ricardo Hydra optical-engine piston-ring modification (Ricardo, 2011)	89
Figure 55 - Ricardo Hydra optical-engine piston-ring setup (Ricardo, 2011)	89
Figure 56 - Ricardo Hydra optical-engine manufactured parts.....	90
Figure 57 - Side and top view of the cylinder block and optical window assembly.....	91
Figure 58 - Engine control and acquisition software	93
Figure 59 - Photron Fastcam SA1-1 high speed camera (Photron, 2015).....	94
Figure 60 - Optical test-rig measurements of flow rate vs. supply pressure at 40C	100
Figure 61 - lubrication test-rig Optical Liner Velocity	102
Figure 62 - lubrication test-rig Optical Liner Acceleration	103
Figure 63 - Polynomial trend line and equation fitted for 40, 70 and 150C	106
Figure 64 - Kinematic viscosities at 70C	107
Figure 65 - E1003A, 300rpm, 0.05L/Min, 70C, 0-20deg	108
Figure 66 - E1003A, 300rpm, 0.05L/Min, 70C, 40-60deg	108
Figure 67 - E1003A, 300rpm, 0.05L/Min, 70C, 80-100deg	109
Figure 68 - E1003A, 300rpm, 0.05L/Min, 70C, 120-140deg	109
Figure 69 - E1003A, 300rpm, 0.05L/Min, 70C, 160-180deg	110
Figure 70 - E1003A, 300rpm, 0.05L/Min, 70C, 200-220deg	110
Figure 71 - E1003A, 300rpm, 0.05L/Min, 70C, 240-260deg	111
Figure 72 - E1003A, 300rpm, 0.05L/Min, 70C, 280-300deg	112
Figure 73 - E1003A, 300rpm, 0.05L/Min, 70C, 320-360deg	112
Figure 74 - E1003A, 300rpm, 0.05L/Min, 70C, 360-380deg	113
Figure 75 – Area Covered, E1003A_003A, 0.005L/Min, 70C, 300RPM.....	116
Figure 76 – Area Covered, E1003A_004A, 0.005L/Min, 70C, 300RPM.....	117
Figure 77 – Area Covered, E1003A_008A, 0.005L/Min, 70C, 300RPM.....	118
Figure 78 – Area Covered, E1003A_009A, 0.005L/Min, 70C, 300RPM.....	119
Figure 79 – Area Covered, E1003A_016A, 0.005L/Min, 70C, 300RPM.....	120
Figure 80 – Area Covered, E1003A_020A, 0.005L/Min, 70C, 300RPM.....	121
Figure 81 – Area Covered, E1003A_003A, 0.005L/Min, 70C, 600RPM.....	121
Figure 82 – Area Covered, E1003A_004A, 0.005L/Min, 70C, 600RPM.....	122
Figure 83 – Area Covered, E1003A_008A, 0.005L/Min, 70C, 600RPM.....	123
Figure 84 – Area Covered, E1003A_009A, 0.005L/Min, 70C, 600RPM.....	123
Figure 85 – Area Covered, E1003A_016A, 0.005L/Min, 70C, 600RPM.....	124
Figure 86 – Area Covered, E1003A_020A, 0.005L/Min, 70C, 600RPM.....	125
Figure 87 – Number of Cavities, E1003A_003A, 0.005L/Min, 70C, 300RPM	126
Figure 88 – Number of Cavities, E1003A_004A, 0.005L/Min, 70C, 300RPM	127
Figure 89 – Number of Cavities, E1003A_008A, 0.005L/Min, 70C, 300RPM	127
Figure 90 – Number of Cavities, E1003A_009A, 0.005L/Min, 70C, 300RPM	128
Figure 91 – Number of Cavities, E1003A_016A, 0.005L/Min, 70C, 300RPM	129
Figure 92 – Number of Cavities, E1003A_020A, 0.005L/Min, 70C, 300RPM	129

Figure 93 – Number of Cavities, E1003A_003A, 0.005L/Min, 70C, 600RPM	131
Figure 94 – Number of Cavities, E1003A_004A, 0.005L/Min, 70C, 600RPM	132
Figure 95 – Number of Cavities, E1003A_008A, 0.005L/Min, 70C, 600RPM	132
Figure 96 – Number of Cavities, E1003A_009A, 0.005L/Min, 70C, 600RPM	133
Figure 97 – Number of Cavities, E1003A_016A, 0.005L/Min, 70C, 600RPM	134
Figure 98 – Number of Cavities, E1003A_020A, 0.005L/Min, 70C, 600RPM	135
Figure 99 – Cavity Width, E1003A_003A, 0.005L/Min, 70C, 300RPM	136
Figure 100 – Cavity Width, E1003A_004A, 0.005L/Min, 70C, 300RPM	137
Figure 101 – Cavity Width, E1003A_008A, 0.005L/Min, 70C, 300RPM	137
Figure 102 – Cavity Width, E1003A_009A, 0.005L/Min, 70C, 300RPM	138
Figure 103 – Cavity Width, E1003A_016A, 0.005L/Min, 70C, 300RPM	139
Figure 104 – Cavity Width, E1003A_020A, 0.005L/Min, 70C, 300RPM	139
Figure 105 – Cavity Width, E1003A_003A, 0.005L/Min, 70C, 600RPM	140
Figure 106 – Cavity Width, E1003A_004A, 0.005L/Min, 70C, 600RPM	141
Figure 107 – Cavity Width, E1003A_008A, 0.005L/Min, 70C, 600RPM	142
Figure 108 – Cavity Width, E1003A_009A, 0.005L/Min, 70C, 600RPM	142
Figure 109 – Cavity Width, E1003A_016A, 0.005L/Min, 70C, 600RPM	143
Figure 110 – Cavity Width, E1003A_020A, 0.005L/Min, 70C, 600RPM	144
Figure 111 – Cavity Length, E1003A_003A, 0.005L/Min, 70C, 300RPM	145
Figure 112 – Cavity Length, E1003A_004A, 0.005L/Min, 70C, 300RPM	145
Figure 113 – Cavity Length, E1003A_008A, 0.005L/Min, 70C, 300RPM	146
Figure 114 – Cavity Length, E1003A_009A, 0.005L/Min, 70C, 300RPM	147
Figure 115 – Cavity Length, E1003A_016A, 0.005L/Min, 70C, 300RPM	148
Figure 116 – Cavity Length, E1003A_020A, 0.005L/Min, 70C, 300RPM	149
Figure 117 – Cavity Length, E1003A_003A, 0.005L/Min, 70C, 600RPM	150
Figure 118 – Cavity Length, E1003A_004A, 0.005L/Min, 70C, 600RPM	151
Figure 119 – Cavity Length, E1003A_008A, 0.005L/Min, 70C, 600RPM	151
Figure 120 – Cavity Length, E1003A_009A, 0.005L/Min, 70C, 600RPM	152
Figure 121 – Cavity Length, E1003A_016A, 0.005L/Min, 70C, 600RPM	153
Figure 122 – Cavity Length, E1003A_020A, 0.005L/Min, 70C, 600RPM	153
Figure 123 – Repeatability between different test runs, E1003_021A, 600RPM, 70C, 0.05L/Min ...	162
Figure 124 – Mean and Standard Deviation for 8 consecutive cycles E1003_21A, 600RPM, 70C, 0.05L/Min	163
Figure 125 - Side by Side optical-engine and lubrication test-rig Cavity Comparison	165
Figure 126 - Side by Side optical-engine and lubrication test-rig Cavity Comparison	165
Figure 127 - Side by Side optical-engine and lubrication test-rig Cavity Comparison	166
Figure 128 - Typical Cavitation of the Model Rig (Dhunput, 2006)	170
Figure 129 - The Camera Positions used for capturing the visual data.....	173
Figure 130 - Firing vs Motorised operation, 800RPM, 70C	174
Figure 131 - The optical-engine pressure trace, Motorised, 1000RPM, 70C, 720deg.....	175
Figure 132 - The optical-engine pressure, Firing, 1000RPM, 70C, 720deg	175
Figure 133 - Optical Engine Piston Velocity Profile	176
Figure 134 - Optical Engine Piston Acceleration Profile.....	176
Figure 135 - Aerosol effect, 208rpm, 70C, Motorised.....	178
Figure 136 - Aerosol effect, 208rpm, 70C, Motorised.....	179
Figure 137 - Aerosol effect, 208rpm, 70C, Motorised.....	179
Figure 138 - Aerosol effect, 208rpm, 70C, Motorised.....	180
Figure 139 - Exhaust/Intake Cycle VS Power Cycle	180

Figure 140 - BTDC, 1000rpm, 70C, Motorised.....	182
Figure 141 - BTDC, 1000rpm, 70C, Motorised.....	183
Figure 142 - BTDC, 1000rpm, 70C, Motorised.....	184
Figure 143 - ATDC, 1000rpm, 70C, Motorised.....	184
Figure 144 - ATDC, 1000rpm, 70C, Motorised.....	185
Figure 145 - ATDC, 1000rpm, 70C, Motorised.....	185
Figure 146 - BTDC, 1000rpm, 70C, Motorised.....	188
Figure 147 - BTDC, 1000rpm, 70C, Motorised.....	188
Figure 148 - BTDC, 1000rpm, 70C, Motorised.....	189
Figure 149 - ATDC, 1000rpm, 70C, Motorised.....	189
Figure 150 - ATDC, 1000rpm, 70C, Motorised.....	190
Figure 151 - ATDC, 1000rpm, 70C, Motorised.....	190
Figure 152 - BTDC, 2000rpm, 70C, Motorised.....	192
Figure 153 - BTDC, 2000rpm, 70C, Motorised.....	193
Figure 154 - Temperature Effect 30C VS 40C, 800RPM.....	195
Figure 155 - Temperature Effect 40C VS 50C, 800RPM.....	196
Figure 156 - Temperature Effect 50C VS 60C, 800RPM.....	196
Figure 157 - Temperature Effect 60C VS 70C, 800RPM.....	197
Figure 158 - 208RPM VS 1000RPM, Speed Effect, 70C.....	198
Figure 159 - 1000RPM VS 2000RPM, Speed Effect, 70C.....	198
Figure 160 - 2000RPM VS 3000RPM, Speed Effect, 70C.....	199
Figure 161 - ATDC, 1000rpm, 70C, Motorised.....	200
Figure 162 - ATDC, 1000rpm, 70C, Motorised.....	201
Figure 163 - ATDC, 1000rpm, 70C, Motorised.....	202
Figure 164 - 1000rpm, 70C, Motorised	205
Figure 165 - 1000rpm, 70C, Motorised	206
Figure 166 - 1000rpm, 70C, Motorised	206
Figure 167 - 1000rpm, 70C, Motorised	207
Figure 168 - 1000rpm, 70C, Motorised	207
Figure 169 - 1000rpm, 70C, Motorised	208
Figure 170 – 1000rpm, 70C, Firing	210
Figure 171 – 1000rpm, 70C, Firing	212
Figure 172 – 1000rpm, 70C, Firing	213
Figure 173 – 1000rpm, 70C, Firing	213
Figure 174 – 1000rpm, 70C, Firing	214

LIST of TABLES

Table 1 - Full Lubricant Matrix and testing conditions carried out on the Lubrication test-rig	97
Table 2 - Test operating conditions. Speed, fps, Flow-rate and Temperature	98
Table 3 - Data Collection Equipment	99
Table 4 - Lubricant Sample Matrix.....	104
Table 5 – Repeatability between different test runs, E1003_021A, 600RPM, 70C, 0.05L/Min	161
Table 6 - optical-engine specifications	171
Table 7 - Lubricant specification used on optical-engine	171
Table 8 - High Speed camera used for the optical-engine testing.....	172
Table 9 - Motorised Test Conditions	172
Table 10 - Firing Test Conditions	173
Table 11 – Fully firing optical engine test conditions.....	210

NOMECLATURE

2-D	Two-dimensional
3-D	Three-dimensional
ABDC	After bottom dead centre
AFR	Air to fuel ratio
ATDC	After top dead centre
b	Ring width
BDC	Bottom dead centre
CA	Crank angle
CI	Compression ignition
CO/CO ₂	Carbon monoxide/dioxide
DAQ	Data acquisition
DI	Direct injection
DISI	Direct injection spark ignition
F	Friction force
g	gravity acceleration
GDI	Gasoline direct injection
HC	Hydro carbons
HTHS	High temperature high shear viscosity
I _o	Intensity
KV	Kinematic viscosity
KV100	Kinematic viscosity at 100°C
KV40	Kinematic viscosity at 40°C
LIF	Laser induced fluorescence
n	Refractive index
NO _x	Nitrogen oxides
n _s	Molecular density
OCR	Oil control ring
OFT	Oil film thickness
P	Oil film pressure
P _{atm}	Atmospheric pressure
P _{back}	Back pressure, pressure at the diverging wedge of ring
P _{comp}	Combustion chamber pressure at the converging wedge of the ring
PM	Particulate matter
P _{MAX}	Maximum pressure at combustion chamber

ppm	Parts per million
ppr	Pulses per revolution
R_a	Average roughness
R_{crank}	Crank radius
R_q	RMS roughness
SD	Standard deviation
SI	Spark ignition
T	Temperature
TDC	Top dead centre
TML	Transducer Measurement Limit
U	Axial piston velocity
V	Sample volume
VI	Viscosity index
$W(\theta)$	Load acting on the ring
ρ	Lubricant density
$\omega(\theta)$	crank angular velocity

CHAPTER 1: INTRODUCTION

In the modern world, internal combustion engines have found their way into a wide range of applications. They hold a key role in the propulsion of vehicles and are the main source of power in many industrial applications. The internal combustion engine is a machine designed to convert the chemical energy stored inside a fuel into kinetic energy. The fuel enters the combustion chamber where in the presence of an oxidiser, usually air, it combusts and releases energy. There are many types of internal combustion engines, but this report will mainly focus on automotive gasoline powered reciprocating engines. This type of engine uses a single or multiple piston to harness the energy released by the combusting fuel. The high-temperature and high-pressure gasses produced by the combustion apply a direct force onto the engine's internal components. Following the combustion, the piston and the other components are designed in such a way that will transform the chemical energy into kinetic energy and will set the engine into motion. Each piston features a set of rings also known as the ring-pack. The piston-rings seal off the combustion chamber and restrict the combustion products from passing down into the engine sump. The piston-rings are also responsible of controlling of the oil supply onto the cylinder walls, a task vital to the correct operation of the engine. Automotive engines can reach thousands of revolutions per minute. The high speeds and pressures combined with the extreme temperatures make the interaction between the piston-ring and the cylinder-liner one of the most hostile areas inside an engine. To avoid critical engine failure, it is important that this specific area is sufficiently lubricated. The lubricants used in automotive engines are designed to operate under extreme conditions such as heavy loads, high temperatures and pressures. The main role of a lubricant is to interfere between the sliding surfaces and provide a fine film which will prevent the components from wearing one another while minimising friction. The job of a lubricant extends further than lubrication, lubricants are also responsible for the cooling and cleaning of the engine's components. It is very important that the lubricant can maintain its properties throughout the engine's full operating range. Equally important is the ability of the piston-rings to control the amount of the lubricant present between the piston-ring and the cylinder-liner interaction. The cylinder-liner and piston-ring interaction is the major source of frictional losses inside an internal combustion engine. Lubricants are available in a wide range of formulations. The use of different additives can have a significant effect on the properties of a lubricant. There is a wide selection of different additives available for automotive applications, few of them are listed below.

- Antioxidants
- Anti-Wear
- Detergent
- Metal Deactivators
- Corrosion Inhibitors
- Friction Modifiers
- Extreme Pressure
- Anti-Foaming Agents
- Viscosity Index Improvers
- Depressants
- Pour Point Depressants

The sufficient control of lubricant supply within an engine is crucial to the performance and reliability of that engine. Low lubricant supply could offer increased performance and fuel efficiency but decreased wear protection. Excess lubrication could have a negative impact on the performance and the output emissions of an engine but will offer better component protection. The objective of this project is to deliver an internal combustion engine that will allow for optical access to the area where the piston-ring meets the cylinder-liner. The study will then focus on the visualisation of the oil film present in that area while the engine operates at speeds close to the ones experienced by commercial automotive engines. The optical-engine will allow for the study of the phenomenon of cavitation as this takes place inside an internal combustion engine. Cavitation is believed to play a crucial part in the transportation of the lubrication oil from the sump into the combustion chamber. It is also linked to the wear of internal components. Cavitation is a phenomenon which usually occurs at high speed flow applications. Few of these applications are internal combustion engines, marine propulsion systems, injector nozzles, journal bearings and hydraulic pumps, cavitation has also been described as “boiling”. During cavitation, the generated cavities force the oil film to break and increase the risk of moving engine components wearing one another. The cavities that collapse are capable of causing serious damage to the nearby mechanical components. There are many cases where cavitation was the main cause of severe engine damage. The cavities created during cavitation might be of a very small scale but the energy they release when they collapse combined with the small focus area, can damage even the toughest of components. The initial stage of the project involved the design and manufacture of an optical-engine that allows for the investigation of the effect that cavitation has on

internal combustion engines. The design and manufacture of the engine run in parallel with a proposed parametric study. The parametric study has been based on a lubrication test-rig capable of investigating cavitation at a range of operating conditions. The test-rig has been designed so it can replicate the operation of a reciprocating internal combustion engine. The parametric study offered a better understanding of the behaviour of lubricants and how these are affected by the different lubricant formulations. Additionally, the study offered knowledge that could be directly applied on the engine project and the testing of the further testing of the lubricants. Both the engine project and the parametric study focused on the phenomenon of cavitation and how this develops in lubricants that are operated within internal combustion engines. The testing of the engine and the test-rig was finally concluded with the analysis of all the collected data. This was performed with the use of custom algorithms built in-house specifically for the needs of the project. The findings are presented and analysed while drawing conclusions and offering suggestions for future studies that would benefit from the knowledge gained through the course of this project.

1.1 Aims and Objectives

- Design, manufacture and assembly of an optical internal combustion engine that would allow for the investigation of the phenomenon of cavitation while this takes place in the cylinder liner and piston-ring interaction. Key feature of the engine needs to be the use of metal piston-rings similar to the ones used on automotive production engines.
- Use the optical equipment installed on the engine to collect data from the piston ring and cylinder liner interaction.
- Process the data collected on the optical engine to extract information that would reveal a link between cavitation and the operating conditions of an engine.
- The completion of the parametric study that would use an existing test-rig, currently property of City, University of London to test a set of 19 lubricants. These 19 lubricants were received by BP while their formulations were withheld and protected by a confidentiality agreement. Key point is the investigation of the phenomena of cavitation and the extraction of information that had not been investigated by the work performed on the test-rig by previous researchers.
- The data from the test-rig must be compared to the data from the engine and their in-between correlation must be investigated.
- Finally, a report must be produced that would summarise and discuss the findings of the project along with suggestions for future work.

1.2 Thesis Outline

The thesis is composed by 5 main chapters. The order of the chapters is based solely on their content under the effort to follow a systematic and coherent structure. The main chapters are as follows.

CHAPTER 1: INTRODUCTION

This Chapter gives an overview of the project as well as insight to some of the aims and objectives that drove the initiative.

CHAPTER 2: HISTORICAL BACKGROUND and LITERATURE REVIEW

The second chapter follows with an extensive reference to historic information relevant to the project. The information is lined to various aspects of the project from internal combustion engines to the history of lubricants. It also contains additional historic reference to relevant work performed in the past. This is an attempt to investigate and gain valuable knowledge by previous projects.

CHAPTER 3: LUBRICATION TEST-RIG

This chapter details and analyses the setup used for the experiments for both the test-rig and the optical engine. This chapter also makes a link between the lubrication test-rig and the optical engine. The link is important in order to establish a correlation between the optical engine and the lubrication test-rig.

CHAPTER 4: OPTICAL ENGINE AND ENGINE DESIGN

This chapter gives information in relation to the design of the optical engine and the modifications that had to be applied so that a conventional internal combustion engine is given optical access capabilities. The optical access is to the piston ring and cylinder liner interaction.

CHAPTER 5: RESULTS AND DISCUSSION

This chapter is one of the core chapters as it details the data captured during the course of the project. The data are then analysed, and the results are discussed in order to provide useful information that will give a better understanding of the cavitation phenomenon with an internal combustion engine.

CHAPTER 6: CONCLUSIONS AND FURTHER DISCUSSION

The final chapter summarises the conclusions derived from the experimental data. In this chapter there is also a review of the aims and objectives and suggestions for future work.

CHAPTER 2: HISTORICAL BACKGROUND and LITERATURE REVIEW

The nature of the project dictates that it is important to investigate the development of lubricants and internal combustion engines to date. Lubricants are crucial to the operation of internal combustion engines and should come as no surprise that the development of the internal combustion engines has greatly been affected by the development of lubricants.

2.1 History of Lubricants

The first record of a lubricant dates to the birth of civilization, these lubricants were manufactured out of animal fat or vegetable oils and were used on machinery or in transportation. As early as the 1400bc, records show examples of lubricants which were used on chariot wheels and axes. These early lubricants were made from tallow and mainly composed of animal fats. These early discoveries show the importance of lubricants and the effort to find a way of reducing friction and wear even with those early inventions. In the next two thousand years and through the middle ages there was a steady development in lubricants. It was not until the early 17th century though, that the true value of lubricants was recognised. The 17th century and the industrial revolution created a demand for a new type of lubricants. Lubricants that would successfully satisfy the needs of this newly invented machinery (Dowson, D. 1993).



Figure 1 – Castrol Lubricants Range (BP-Castrol, 2015)

In 1859 Edwin Laurentine Drake pioneered a new method of extracting oil from the ground that made use of piping to prevent the extraction holes from collapsing. This allowed for deeper penetration into the ground. Drake's new method accelerated the move towards the

use of mineral based lubricants while signalled the birth of the petroleum industry. The first petroleum based lubricants were not accepted at first as they did not perform as good as the animal based products available at the time (Dowson, D. 1979). With the birth of the automobile though, the demand for high performance lubricant grew and the newly introduced petroleum based lubricants started catching up and rapidly replaced the animal based products. At the beginning of the 20th century lubrication manufacturers started investigating new ways of improving their lubricants by changing their physical properties. This led the Society of Automotive Engineers to introduce for the first time the classification of engine oils by viscosity. These early lubricants had no additives and their performance was poor compared to modern lubricants. In the 1920s lubricants had to be changed after every 1000 miles of use. In the 1930s lubricant manufacturers started experimenting with the use of additives to improve the performance of their lubricants. By the 1940s additives were widely used by lubricant manufacturers, this change would significantly extend the time between the oil changing intervals. In the 1950s multi grade oils were first introduced, which improved the cold and hot performance of the lubricants. For the next few decades the lubricant industry continued to improve the performance of their products with the use of new and more sophisticated additives. The 1970s and the Arab oil embargo brought a new momentum to the development of synthetic engine oils in both passenger and commercial vehicles. Lubrication companies promoted the use of synthetic oils because these were not dependent upon crude oil resources. Lubricants in the 1950s used additives in an attempt to solve problems partially faced even nowadays but modern additives have seen a great advance in their technology since those early examples. Modern lubricants are formulated from a wide range of base fluids with use of additives. Figure 1 shows a few examples of modern lubricants for automotive applications. Lubricants undertake several roles inside an engine, ranging from lubricating and preventing wear to cooling and cleaning the engine parts (Grice, N. and I. Sherrington. 1993).

2.2 History of Lubrication Systems

Lubrication systems are used in a wide range of applications and their core purpose is to deliver the lubricant that will prevent moving parts from wearing each other to the point of failure. Modern lubrication systems use pressure fed oil systems with either dry or wet sumps though that was not always the case. Back in the 1840s and before the development of the petroleum based lubricants, lubrication was achieved with the use of animal or vegetable oils. Early locomotives used animal fat for their lubrication. The animal fat was brushed over

the axles to keep them in a good working order and prevent component failure (Dowson, D. 1979). Tallow was used not only on the axles but also on the mechanical parts to reduce friction. These early machines had to be lubricated by hand and every single part had to be individually looked after by a dedicated worker, which made the lubrication of those machines a complicated and time-consuming task.

A few years later as Drake redefined the extraction of crude oil out of the ground and along with the advances in technology a new generation of lubricants was developed. Henry Ford industrialised the Automobile and made it available to the masses and along with the automotive industry and the newly developed petroleum based lubricants came the need for lubrication systems that would allow the lubrication of the automobiles without the need of dedicated workers. The combination of all these factors later turned the operation of an automobile vehicle into a one-man job (Dowson, D. 1979).

The Ford T model much like many industrial engines used a splash lubrication system for the internal components and bearings. This system relies on the rotating motion of the crankshaft to splash oil on the internal components. Small grooves on the crankshaft and connection rods, scoop oil from the sump and splash it around the inside of the engine, achieving in that way the lubrication of all the internal components. These systems were not very effective as the oil was not targeted on specific areas and lubrication was not efficient (Dowson, D. 1979).

The evolution of lubrication systems leads to the development of pressurised oiling systems that could guide the lubricants through tubing directly to the affected areas thus, allowing a more precise metering of the lubricants onto important parts while improving performance, reliability and longevity. Pressurized lubrication systems use power off the crank shaft to operate a small pump which circulates the oil around the engine. These new systems solved one of the main problems older systems had where components were faced with oil starvation when moving uphill, downhill or around corners. Eventually more sophisticated systems allowed the direct and effective lubrication of more internal components inside an engine. Grooved bearings and drilled passages made automobiles more powerful, more reliable and more affordable to the public (Dowson, D. 1979).

These sophisticated hydraulic circuits lead to the development of new more sophisticated automotive engines. Pressure fed bearings could operate in a hydrodynamic mode resulting in increased life span. The additional cooling that these systems offered improved the longevity of key components such as the pistons, which usually are subjected to high temperatures. In

addition to the water cooling systems, oil coolers were also implemented offering a more effective cooling. The following years engines were equipped with new and more sophisticated systems such as self-adjusting valve tappets, variable timing camshafts and cylinder deactivation systems, which gave to this new generation of engines improved fuel economy, performance and durability. These engines had reduced maintenance requirements compared to their predecessors while offering much better overall performance and efficiency. Despite the latest advances in technology, engines can still face failure under extreme conditions. Modern engines have become more demanding and lubrication systems continue to evolve in order to meet the industry requirements (Dowson, D. 1979).

2.3 Internal Combustion Engines

The internal combustion engine is a type of heat engine that converts the chemical energy stored in a fuel into mechanical energy through the combustion of the fuel in the presence of an oxidizer, usually air.

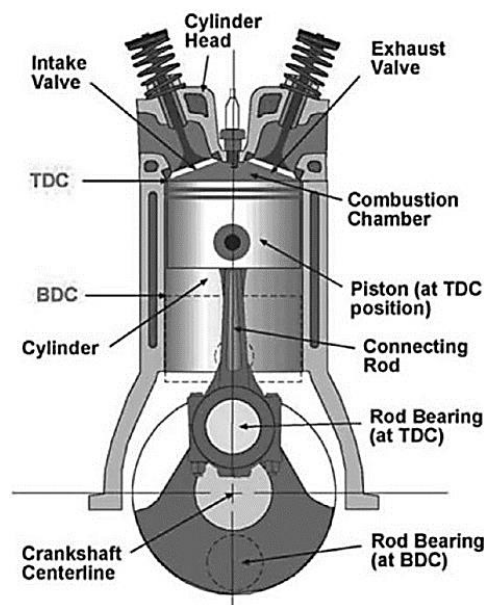


Figure 2 - Internal Combustion Reciprocating Engine (What-When-How, 2015)

The chemical energy stored in the fuel is converted at first to thermal energy by the means of combustion. This takes place inside a sealed off chamber similar to the one illustrated in figure 2, an automotive engine as represented in figure 3 can feature multiple of these cylinders. The thermal energy raises the temperature and pressure of the gases inside the chamber and the high-energy gasses expand against the internal components on the engine. The main components are the cylinder and the piston, the piston is connected through a set of



Figure 3 - Corvette LT1 6.2-liter V8 450hp with Cylinder Deactivation (Hill, 2015)

mechanical linkages to the crankshaft which delivers the power output of the engine. The operational range of internal combustion engines is limited when compared to the variety of applications they need to be of use. The means of adjusting the same engine to fit a wide range of applications is made possible with the use of a gearbox. The crankshaft is connected to the gearbox which then delivers the power to the desired application. Gearboxes find their application from commercial vehicles to lawn mowers. The majority of internal combustion engines available worldwide are reciprocating engines. Other types of internal combustion engines are jet engines and rocket engines, figure 4. These types of engines might not use a piston, but they still rely on fuel combusting internally to generate power. Internal combustion engines can feature one, two or multiple cylinders and they are available in numerous different geometric configurations.

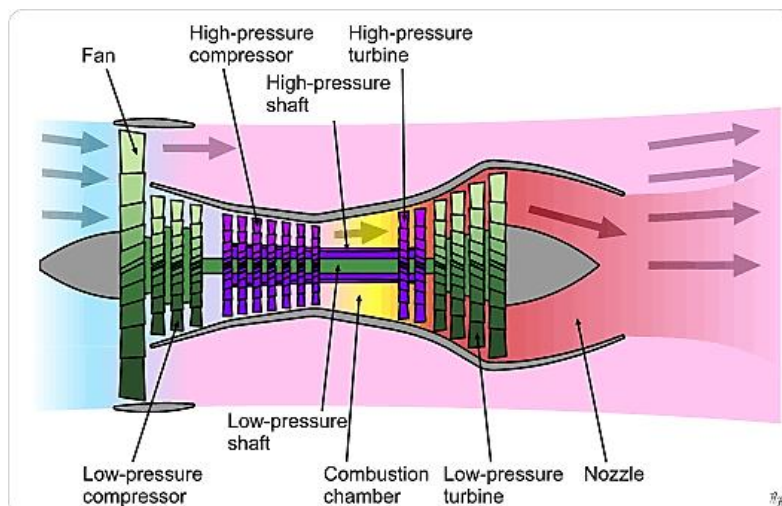


Figure 4 - Jet Engine, Piston less Engine (Sobester, 2015)

They differ according to the type of fuel they use and the way they deliver it to the combustion chamber. They also come in a range of power ratings capable of powering a

small chain saw up to an oil tanker, weighting hundreds of thousands of tons. The first commercially successful engine was made available in the 1850s by E. Lenoir, figure 5. Records show that the history of internal combustion engines started much earlier than Lenoir's engine, the first records date back to the 17th century. Most of these early examples were never practical, nor were fully operational. Internal combustion engines played a leading part to the way the world is shaped to date.

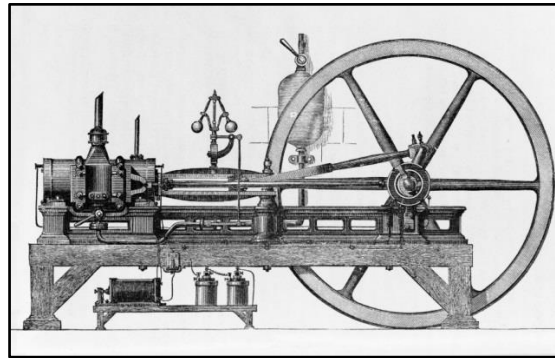


Figure 5 - The Lenoir Engine (Greene, 2015)

2.4 Engine Types

Internal combustions engines come in many different configuration, the most common engine types are detailed, analysed and explained in the following pages of this chapter. The different engine types are classified by either their primary operating principles or by their specific operating components.

2.4.1 Types of Ignition

There are two ignition systems mainly available in modern engines, these are the Spark Ignition and the Compression Ignition systems, figure 6. Spark ignition engines ignite the fuel on each cycle by the use of a spark plug, the spark plug is a device capable of delivering a high electric current generated in the ignition system to the combustion chamber in order to ignite the air fuel mixture. The fuel is ignited by the current which is discharged between two electrodes. Compression ignition systems are used with high compression engines such as Diesel engines, the combustion starts when the air-fuel mixture self-ignites inside the combustion chamber due to the pressure generated by the high compression.

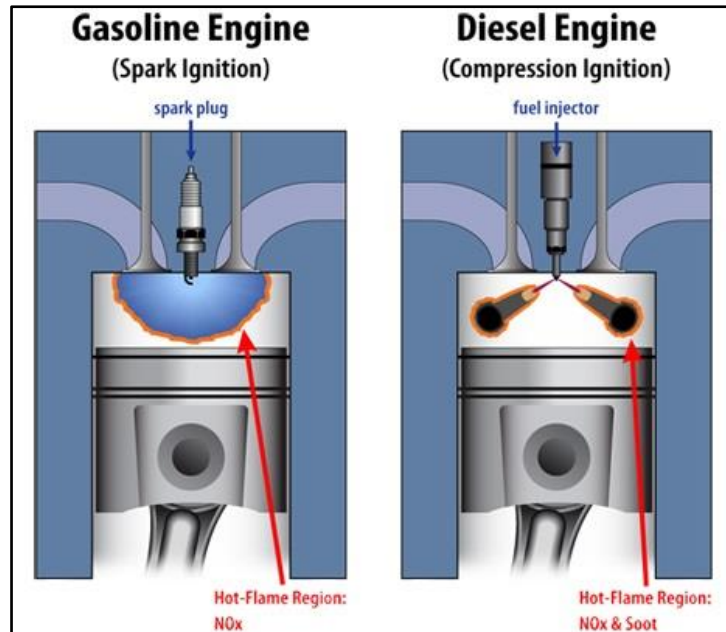


Figure 6 – Spark Ignition VS Compression Ignition (Gitlin, 2015)

2.5 Four Stroke Engine Cycles

Most internal combustion engines operate on either a four-stroke cycle or a two-stroke cycle. These basic cycles are company standard for all engines with slight variations found in individual designs. This chapter will analyse the operation of four stroke engines as the project focuses mainly on engines operating on that principle. Four-stroke engines perform four piston movements for every two revolutions to complete one cycle, figure 7.

2.5.1 Four-Stroke Spark Ignition Engine Cycle

- a) **First Stroke:** The Intake Stroke or Induction. The piston travels from TDC to BDC with the intake valves open and the exhaust valves closed. This creates an increasing volume in the combustion chamber, which generates a vacuum. The resulting pressure differential through the intake system causes air to be sucked into the cylinder. As the air passes through the intake system, fuel is added to it by either a fuel injector or a carburettor.
- b) **Second Stroke:** The Compression Stroke. When the piston reaches BDC, the intake valves close and the piston travels back to TDC, with all the valves closed now. This compresses the air-fuel mixture, raising both the pressure and temperature inside the cylinder. The time required to close the intake valves means that the actual compression doesn't start until ABDC. Near after the end of the compression stroke, the spark plug is used to ignite the fuel and combustion is initiated.
- c) **Combustion:** The Combustion of the air-fuel mixture occurs in a very short time with the piston near TDC (i.e., nearly constant-volume combustion) and it starts at or right after

the end of the compression stroke. The combustion changes the composition of the fuel into a high-energy mixture of gas that rapidly increases the temperature and the pressure inside the cylinder.

- d) **Third Stroke:** The Expansion Stroke or Power Stroke. With all valves closed the high pressure created by the combusting fuel pushes the piston away from TDC. This is the stroke which produces the work output of the engine. As the piston travels from TDC to BDC the cylinder volume increases causing pressure and temperature to drop.
- e) **Exhaust Blowdown:** Late in the power stroke, the exhaust valve is opened, and exhaust blow down occurs. Pressure and temperature inside the cylinder are still high, relative to the surroundings, and a pressure differential is created through the exhaust system which is open to the atmospheric pressure. This pressure differential causes much of the hot exhaust gas to be pushed out of the cylinder and through the exhaust system when the piston is near BDC. This exhaust gas carries away a high amount of enthalpy, which lowers the cycle thermal efficiency. Opening the exhaust valve before BDC reduces the work obtained during the power stroke but is required due to the short time available for exhausting the combustion products.
- f) **Fourth Stroke:** The Exhaust Stroke. By the time the piston reaches BDC, exhaust blowdown is complete, but the cylinder still contains exhaust gases at approximately atmospheric pressure. With the exhaust valve open the piston now travels from BDC to TDC. This pushes most of the remaining exhaust gases out of the cylinder and into the exhaust system. Near the end of the exhaust stroke at TDC, the intake valves start to open, and the exhaust valves are almost closed. This period when both the intake and exhaust valves are open is called valve overlap (Heywood, 2004).

2.5.2 Four-Stroke Compress Ignition Engine Cycle

- a) **First Stroke:** The Intake Stroke. The Intake Stroke or Induction. The piston travels from TDC to BDC with the intake valves open and exhaust valves closed. This creates an increasing volume in the combustion chamber, which generates a vacuum. The resulting pressure differential through the intake system causes air to be sucked into the cylinder. This intake stroke is the same between the SI and CI engines with one major difference: no fuel is added to the incoming air.

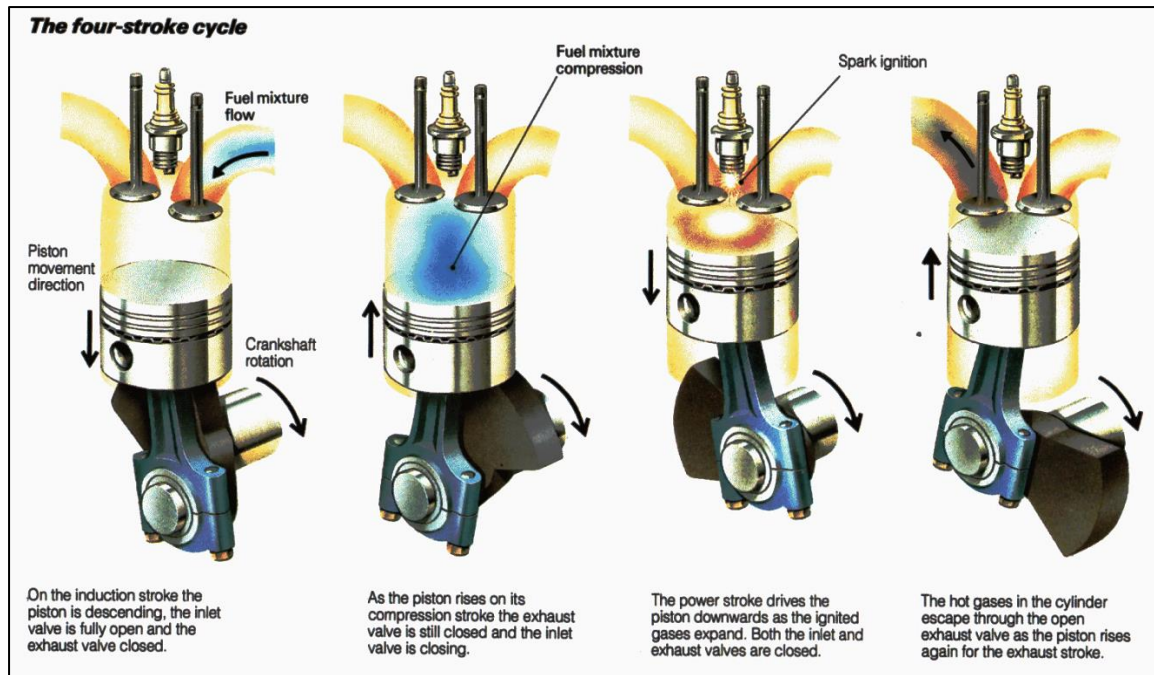


Figure 7 – Four Stroke Cycle (Moin, 2015)

- b) **Second Stroke:** The compression Stroke. The air is compressed at a very high pressure. Multiple times higher than a conventional SI engine. This high compression does not only increase the pressure but also the temperature within the cylinder. Later in the compression stroke fuel is injected directly into the combustion chamber, where it mixes with the very hot compresses air. This causes the fuel to evaporate and self-ignite, initiating combustion.
- c) **Combustion:** The combustion is fully developed by TDC and continues at about constant volume until fuel injection is complete and the piston has started moving towards BDC.
- d) **Third Stroke/Power Stroke:** The power stroke continues as combustion ends and the large cylinder pressure pushes the piston towards BDC.
- e) **Exhaust Blowdown:** Later in the power stroke, the exhaust valve opens, and exhaust blow down occurs. Pressure and temperature in the cylinder are still high relative to the surroundings and a pressure differential is created through the exhaust system which is open to atmospheric pressure. This pressure differential causes much of the hot exhaust gas to be pushed out of the cylinder and through the exhaust system when the piston is near BDC. This exhaust gas carries away a high amount of enthalpy, which lowers the cycle's thermal efficiency. Opening the exhaust valve before BDC reduces the work obtained during the power stroke but is required due to the short time available for exhaust.

f) **Fourth Stroke:** The Exhaust Stroke. By the time the piston reaches BDC, exhaust blow-down is complete, but the cylinder still contains exhaust gases at approximately atmospheric pressure. With the exhaust valve remaining open, the piston now travels from BDC to TDC in the exhaust stroke. This pushes most of the remaining exhaust gases out of the cylinder into the exhaust system at about atmospheric pressure, leaving trapped only the gasses in the clearance volume when the piston reaches TDC. Near the end of the exhaust stroke at BTDC, the intake valves start to open, so that they are fully open by TDC when the new intake stroke starts in the next cycle. The exhaust valves start to close near TDC and are fully closed at a point ATDC. This interval when both the intake valve and exhaust valve are open is called valve overlap (Heywood, 2004).

2.6 Internal Combustion Engines, Emissions and Air Pollution

The exhaust products of automobiles are a leading cause of the greenhouse effect and a major contributor to the pollution of air. To limit the impact of internal combustion engines to the environment, governments have introduced emission standards that engine manufacturers need to comply with. Even with the latest emission regulations the problem is still ongoing and a core issue that will be faced in the years to come. This is partially the outcome of the growing number of vehicles put on the roads. During the early 1900s the automobile emissions were not recognised as a problem, one of the main reasons was the low number of vehicles, as the number of vehicles increased the problem started to surface. The issue was first identified in the Los Angeles area in the 1940's, this specific area due to the high density of people and automobiles faced an air pollution problem which was first perceived as a unique weather condition. By the 1970's air pollution was recognised as a major environmental issue, the identification of the problem resulted into new laws that would for the first time control the output of exhaust emissions of internal combustion engines. These laws have been established in most of the industrialized countries, the emission laws and the continuous development of new more environmental friendly engines has resulted to an emission reduction of more than 90% since those first laws were introduced. The problem though is still present and is still a major environmental concern, the four major products of the internal combustion engines are Hydrocarbons (HC), Carbon Monoxide (CO), Oxides of Nitrogen (NOx) and Solid Particles (PPM). Figure 8 shows the development of the emission standards from 1992 to 2014 (pi-innovo, 2015). Hydrocarbons are fuel molecules which have not taken part into the combustion or have partially combusted. Carbon monoxide occurs when not enough oxygen is present to fully react with all the fuel. Nox emissions do not form

in significant amounts until flame temperatures reach 1500°C. Once that threshold is passed, any further rise in temperature causes a rapid increase in the rate of Nox formation.

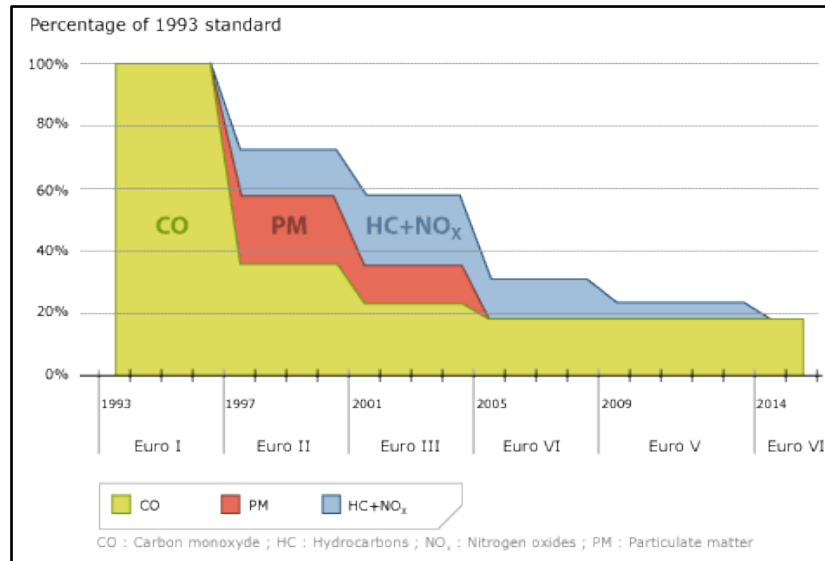


Figure 8 – Emission standards from 1993 to 2014 (pi-innovo, 2015)

Nox production is highest at a fuel-to-air combustion ratio of 5–7% O₂ (25–45% excess air). Lower excess air levels starve the reaction of oxygen, and higher excess air levels drive down the flame temperature, slowing the rate of reaction (Allied Environmental Technologies, 2016). Solid particles are mainly formed in compression ignition engines (diesel engines) and can be seen out of the exhaust in the form of black smoke. Other emissions that are found in the exhaust products of engines include aldehydes, sulphur, lead and phosphorus. The two methods used to reduce the harmful engine emissions are to improve the fuels and engines to achieve better and more complete combustion and by also improving the after-treatment. The after-treatment usually involves a series of devices such as catalytic converters that promote chemical reactions within the exhaust to reduce harmful emissions. These chemical reactions convert the harmful emissions into the more acceptable CO₂, N₂O and N₂ (Heywood, 2004).

2.7 Internal Combustion Engines and Cavitation

Cavitation was first observed by Newton in 1669. Cavitation is the formation of cavities in a liquid. The cavities are areas free of liquid zones where the liquid separates due to the forces that act upon it. Cavitation is a phenomenon which usually occurs in high speed flow applications such as internal combustion engines, marine propulsion systems, injector nozzles, journal bearings and hydraulic pumps, cavitation can also be described as “boiling”. While these two are very similar phenomena, their main difference is that they follow different thermodynamic paths that lead to the formation of vapour. When the local saturated

vapour pressure rises above the local ambient pressure then the liquid starts to boil. On the other hand, cavitation occurs when local pressure falls below the saturated vapour pressure of the liquid at the given temperature. Cavitation is the formation of gas or vapour bubbles inside the volume of the liquid when the pressure of the liquid falls below the atmospheric pressure. Whether the formed cavities are gaseous or vaporous depends on the way they are formed. Vaporous cavitation is a boiling type process that takes place if the bubble grows explosively in an unbounded manner as liquid rapidly changes into vapour. This situation occurs when the pressure drops below the vapour pressure of the liquid. Gaseous cavitation is a diffusion process that occurs whenever the pressure falls below the saturation pressure of the non-condensable gas dissolved in the liquid. While vaporous cavitation is a rapid process, gaseous cavitation is much slower, the time it takes depends upon the degree of fluid circulation (convection).



Figure 9 - Hydraulic pump valve plate damaged by cavitation (hydraulicspneumatics, 2015)

Cavitation has the ability to directly generate wear only under vaporous cavitation, where the shock waves and the micro jets can erode the surfaces. Gaseous cavitation does not cause damage to the surface of the material. It only creates noise, generates high temperatures and affects the chemical composition of the fluid (oxidation). Cavitation wear is also known as cavitation erosion, vaporous cavitation, cavitation pitting, cavitation fatigue, liquid impact erosion and wire-drawing. Cavitation wear is a fluid-to-surface type of wear that occurs when a portion of the fluid is first exposed to tensile stresses that causes the fluid to boil and then exposed to compressive stresses that cause the vapour bubbles to collapse. This collapse produces a mechanical shock and micro jets that could attack the nearby surfaces. Any system including internal combustion engines that can repeat this tensile and compressive stress pattern is subject to cavitation wear and all the complications accompanying such an activity. Cavitation wear is similar to surface fatigue wear, materials that can resist surface

fatigue can also resist cavitation damage. Cavitation is a major cause of component wear in internal combustion engines and contributes to the reduction of performance while increasing the engines output emissions. The phenomenon of cavitation can occur in two forms. These two forms are “Inertial” and “Non-Inertial” cavitation. Inertial cavitation is the phenomenon where the formed cavities collapse while releasing significant amounts of energy to their surroundings. Inertial cavitation is usually initiated by pre-exciting bubbles in the volume of the liquid. Oil minerals usually have 8-15% by volume of dissolved air, these pre-existing bubbles will grow until the point when they will collapse (Boness, R. J. and H. M. Hawthorne, 1995). Non-inertial cavitation follows the same path as inertial cavitation until the point of collapse. This form of cavitation usually causes less damage to the engine components as the bubbles do not collapse but oscillate, as the energy absorption is not high enough to cause them to collapse. Cavitation is a phenomenon that finds its use in many industrial applications. Few of these sectors are Chemical Engineering, Healthcare and the Cleaning industry. Many industrial mixing machines base their operation on cavitation. One of many examples is the paint mixing machines which are based on this design principle to mix or to dissolve paint.

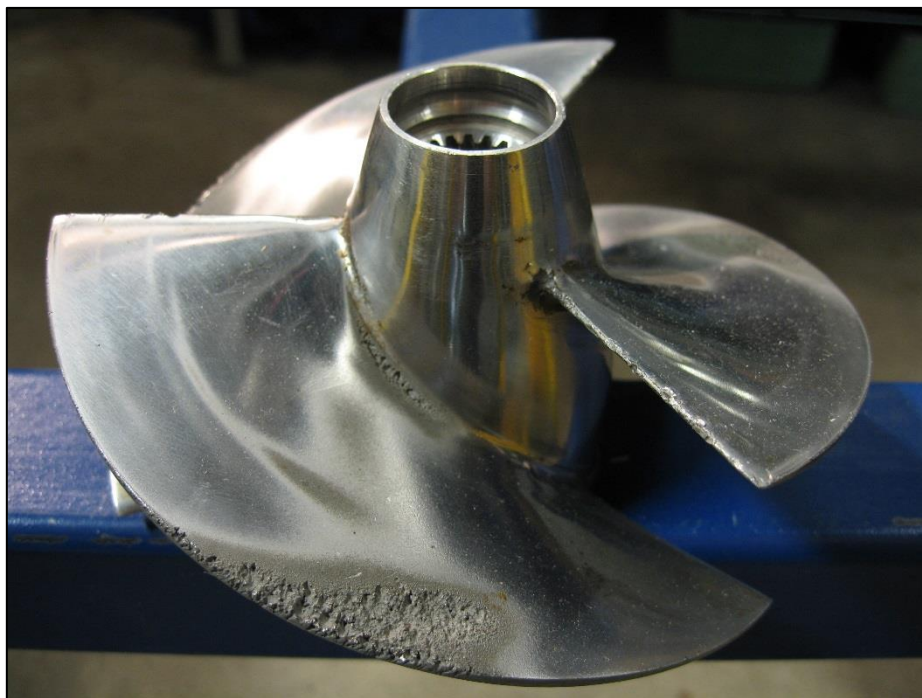


Figure 10 - Cavitation Damage on Propeller of Personal Watercraft (SonicCavitation, 2015)

Doctors perform lithotripsy on patients with Kidney stones, a method where cavitation is used for the distraction of the kidney stones. Cavitation in internal combustion engines is in most cases but not always an undesirable effect. When cavitation occurs, it causes a great

deal of noise, vibration and damage to the engine components. Furthermore, the formation of cavities will result to performance loss, as it will negatively interfere with the engines components. The leading cause of cavitation is the sudden pressure drop at a constant temperature. The area of the engine that mainly offers great and rapid changes in pressure is the piston-ring and cylinder-liner interaction. Cavitation is a naturally occurring phenomenon of a lubricant film that is forced through a converging-diverging wedge, one of these areas is the interface of the piston-ring and the cylinder liner interaction. When cavitation bubbles collapse, they force small volumes of liquid onto the engine components, this results into many small high-pressure and high-temperature spots. If the force applied at these spots exceeds the strength of the material the component will fail. Figure 9 and Figure 10, show the damage caused on a valve plate of an axial piston pump due to the generation of cavities in the working fluid. Easily spotted is the way the material was “attacked” by the small volumes of energetic liquid which were generated by the collapse of the in-liquid formed cavities. Cavitation is also related to the eroding of metals and to the wear of components which can dramatically shorten the component’s life. As soon as the surface of the component starts failing the rate that the damage spreads to the rest of the components will increase at an accelerating pace thanks to the formation of pits which increase the turbulence of the fluid flow, thus increasing the cavity generation (B.Christopher E, 1995).

2.8 Cavitation in Supersaturated Liquids

There are numerous industrial applications and natural processes that involve supersaturated or superheated liquids that promote cavitation. Cavitation or else nucleation involves the formation and growth of bubbles. A tragic example that came as a result of cavitation is the eruption of Lake Nyos in Cameroon in 1986 which resulted in the loss of more than thousand lives. The disaster was caused by the carbon dioxide which was dissolved in the waters of the lake and which suddenly released causing the eruption of the lake (Boness, R. J., S. L. McBride and M. Sobczyk, 1990). Cavitation does not have only negative effects. Cavitation is important in many commercial applications. Some of them are: Electrolytic Processes, Carbonated Drinks, Electric Power Generation, Liquid Waste Treatment etc. Cavities are formed when a purely homogeneous liquid undergoes a phase change at low levels of super saturation where pre-existing gas causes the formation of cavities. These cavities exist at various levels of stability and are affected by the changes that occur in the thermodynamic state of the solution. The term super saturation is used to quantify the tendency of the system to produce cavities. To help the understanding of the way the term is used, figure 11 shows

the saturation data as a function of temperature for a system consisting of carbon dioxide dissolved inside water at a pressure equal to 1.1013×10^5 Pa. Super saturation can be achieved by raising the temperature of the system.

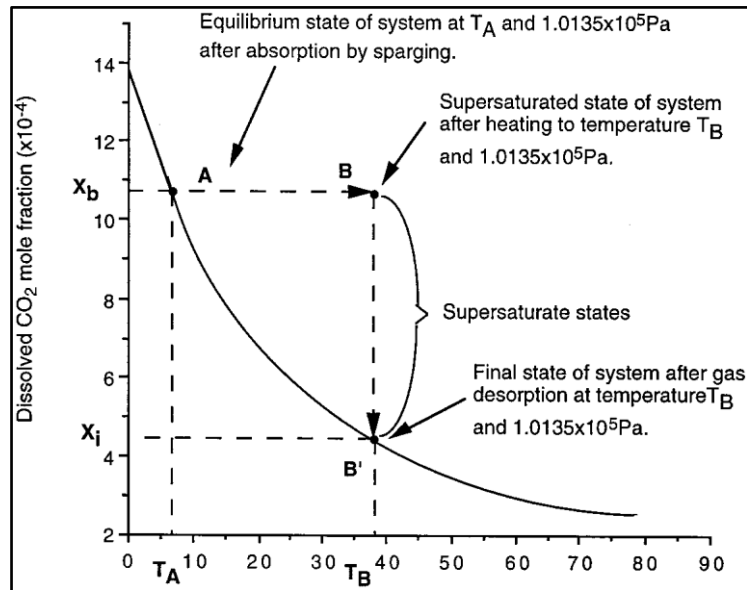


Figure 11 – Solubility of carbon dioxide as a function of temperature, at 105 Pa (Heywood, 1998)

The point {A} in figure 11 represents a saturated solution at temperature $\{T_A\}$ and $\{X_B\}$ the saturation mole fraction for that temperature. If the temperature of the solution is raised to $\{T_B\}$ at the point {B} then the system will reach a supersaturated state with $\{X_B\}$ being the dissolved mole fraction of carbon dioxide inside water. The release of carbon dioxide from water causes the system to move from state {B} to $\{B'\}$, where the new saturation mole fraction is equal to $\{X_i\}$. The saturation ratio as it was defined by Lubetkin and Blackwell is as follows,

$$\alpha = \frac{X_B}{X_i} \quad (1)$$

While the super saturation as,

$$\sigma = \alpha - 1 \quad (2)$$

Then, according to Henry's Law,

$$H = \frac{P_i}{X_i} \quad (3)$$

Henry's Law shows that the value of Henry's Law constant $\{H\}$ varies as a function of temperature according to the changes of $\{X_i\}$ which is the equilibrium concentration shown

in figure 11. By introducing the Henry's Law constant, it is possible to relate the equation 1 and equation 2 to pressure.

Now at temperature $\{T_B\}$ the difference in the contents equilibrium pressure for $\{B\}$ and $\{B'\}$ is,

$$\Delta P = P_b - P_i = H(X_b - X_i) = P_i \left(\frac{X_b}{X_i} - 1 \right) = P_i \sigma \quad (4)$$

If P_b is the equilibrium pressure at $\{B\}$ of carbon dioxide then the difference in pressure can be described by Laplace equation,

$$\Delta P = \frac{2\gamma}{R'} \quad (5)$$

Where R' is the radius of the cavity and γ the interface tension between the gas and the solution. By equating equation 4 and 5 and by assuming that the vapour pressure of the solvent is negligible then a bubble in the solution for a level of super saturation σ is in equilibrium with the solution if the radius is equal to the critical radius (Heywood, 2004).

2.9 Positive Effects of Cavitation

Contradictory views exist concerning whether the presence of cavitation has a positive or negative effect on engine performance, emission or reliability. Cavitation affects more than one areas within internal combustion engines. Internal combustion engines rely on multiple working fluids to maintain good operation. From the fuel to the lubricants all these working fluids are subjected to high pressures and temperatures while they are transported throughout the engine. Due to the nature of their use these fluids are subjected to cavitation and on one side cavitation in fuel injectors reduces the effective cross-sectional flow area and complicates the injection of large masses of fuel through small nozzles and on the other, cavitation enhances mixture formation and cleans the exit of the nozzle holes from deposits that are caused by carbonisation. In a similar way cavitation of lubricants in internal combustion engines can have catastrophic effects on the internal components. Collapsing cavities can damage even the toughest of the components but the presence of cavities can also have a positive effect in the performance and efficiency of engines. The cavities can reduce the amount of lubricant present within the engines sliding surfaces which could reduce their in-between friction offering benefits to fuel consumption.

2.10 Measuring Techniques

Sherrington and Smith, back in 1985 divided the measuring techniques that can be used in a scientific research into two major categories; Optical and Electrical. Years later and after the continuous advance of technology in 2006, Sherrington and Söchting added one extra member to the measuring techniques. As of today, the measuring techniques can be divided into three main categories. These are Optical, Acoustic and Electrical techniques. Only two of these three measuring techniques were used in the course of this project.

2.10.1 Optical Techniques

Optical techniques rely on visualisation equipment to acquire data. The visualisation is not possible without the use of a see-through window which allows for optical access to the area of interest. Usually engines that are tested with this method are equipped with optical windows or see-through cylinders usually made from Fused Silica (Quartz) or Sapphire for good optical access and increased scratch resistance. Green (1969) used a transparent cylinder which he manufactured to the same roughness as the original optical liner of the engine he modified. He used and applied two optical methods. At first Green applied an ultra-violet light source to illuminate the oil film and then used a fluorescence compound mixed in the oil, which emitted an intense blue fluorescence. The results were captured by a high-speed camera at 800 frames per second. The second method involved the use of scattered light to visualise the behaviour of the lubricant onto the cylinder walls. The results Green derived indicated that the piston and the cylinder-liner were separated always by a constantly changing small film of lubrication oil.

- **1993**, Sanda et al used a Laser Induced Fluorescence to capture two dimensional images of the oil film.
- **1995**, Inagaki et al used a Xenon Flash lamp along with a fluorescence dye to capture images from the oil film lubrication in internal combustion engines. Inagaki et al used two different cylinders to achieve that. They first used a full Quartz liner for the non-firing runs and then they used a cast iron liner with small windows for the firing runs. Inagaki et al observed and captured oil moving up into the cylinder and passing inside the combustion chamber.
- **1995**, Nakashima et al used a cast iron cylinder equipped with a small Quartz window along with a red dye which was diluted inside the lubrication oil and with the use of a video camera they managed to capture the flow of the lubrication oil through the ring-

pack. Later on, in 1996 Nakashima repeated his tests using greater pressure differences and speeds and observed that the lubrication oil was flowing through the ring-gaps.

- **1995**, Kim et al decided to manufacture an experimental test-rig that would be able to simulate the piston-ring/liner lubrication.
- **1998**, Thirouard et al used two different types of engines. The first one was a diesel engine equipped with a Quartz window and the second one a gasoline engine that was used with a Sapphire window. Both engines were tested using Laser Induced Fluorescence and a CCD Camera. Thirouard et al confirmed that the lubrication oil fluid flow is greatly affected by the gasses that flow through the lands and piston-rings (Thirouard, B. P., T. Tian and D. P. Hart, 1998).

2.10.2 Electrical Techniques

Capacitance is a technique based on the fundamental principles of the capacitor operation. Capacitance is the ability of a capacitor to store energy in an electric field. The most common capacitor is the parallel plate capacitor. In a parallel plate capacitor, the capacitance is linked, and it is directly proportional to the surface area of the conductor plates and inversely proportional to the distance between these two plates. For a given plate size, the voltage of the system will change depending on the distance between the plates. For many years, capacitance has been the most popular technique for measuring the oil film thickness in several applications (Thirouard, B. 2001). Hamilton and Moore (1974) measured the oil film thickness by mounting capacitance transducers on the cylinder-liner of an engine. They were able to measure films as small as 10 μ m. Further modification to their test-rig allowed for more accurate measurements close to 0.4 μ m. One year later Parket et al (1975) used probes in the rings of an operational engine and were able to investigate the oil film thickness throughout the engine's cycle. Dhunpant (2006) used the capacitance technique to measure the oil film thickness of different lubricants on an idealised test-rig capable of simulating the operation of conventional internal combustion engines. The capacitance technique is fairly accurate and easy to implement.

2.11 Lubricants

Lubricants are widely used to prevent wear of the engine components and to increase the performance. The first lubricants were organic and were the products of plants, animals or other organisms through natural metabolic processes. During the Second World War the limited availability of natural oil to supply the German air force and the increased

performance requirements lead to the development of new lubricants that would feature all the properties of natural oils without the tendency to gel or gum as natural oils did in internal combustion engines. The first synthetic lubricants were used during the Second World War by Germany and the United States and its main use was for aircraft engines. Synthetic lubricants improved cold engine start in the winter while offering an improved and cleaner operation. The majority of synthetic oils are mineral oils and are by-products of the distillation of petroleum to produce gasoline. Motor oils are composed out of a heavier petroleum hydrocarbon stock derived from crude oil, then with the use of additives it is possible the enchantment of certain properties. The first and most important property of lubricants is to maintain a lubrication film between the engines components and especially the moving parts. Then the additives will improve the remaining of its properties (Care and H.E.G. Powrie, 2006). Some of the major additive families are:

- Antioxidants
- Anti-Wear
- Detergent
- Metal Deactivators
- Corrosion Inhibitors
- Friction Modifiers
- Extreme Pressure
- Anti-Foaming Agents
- Viscosity Index Improvers
- Depressants
- Pour Point Depressants

a) Antioxidant Additives

Antioxidants is one of the most important additives in modern lubricants. Mineral oils have the tendency to react with oxygen and form organic acids. The oxidation of the oil causes an increase of the oils viscosity, formation of sludge and contributes to the corrosion of metallic parts. The antioxidants are added in lubricant to reduce sludge formation. The antioxidants improve the thermal stability, performance and life of the lubricant. They also reduce thickening and inhibit acid formation. Most widely used antioxidants are;

- Zinc Dithiophosphate
- Alkyl Sulphides
- Aromatic Sulphides

- Aromatic Amines
- Hindered Phenols

b) Anti-Wear Additives

The main property of the anti-wear additives is to prevent the metal on metal contact between the engine parts when the oil film is broken down. Anti-wear additives dramatically increase the engine's life and they provide a higher wear resistance to the components. The way the anti-wear additives work is by reacting with the metal's surface and forming a film, which is able to reduce friction and prevent wear. Some of the most commonly used additives are;

- Zinc Dithiophosphate
- Zinc Dialkyldithiophosphate
- Tricresylphosphate

c) Detergents

Detergents are mainly used in engines to protect the carburettor and the injector components in order to prevent fouling. Detergent additives in lubricants serve a similar cause. They are responsible for the neutralisation of strong acids present in the lubricant. Some of these acids are sulphuric and nitric acids produced in internal combustion engines as part of the combustion process. Some of the detergents used in today's lubricants are;

- Phenolates
- Sulphonates
- Calcium (Ca)
- Magnesium (Mg)
- Sodium (Na)
- Barium (Ba)

d) Metal Deactivators

Metal Deactivators also known as Metal Deactivating Agents are used to stabilise the lubricants by deactivating the metal's ions, which are generated in the lubricant during the oxidation that takes place with the metallic parts of the engine when they come in contact.

e) Corrosion Inhibitors

Corrosion and Rust Inhibitors are chemical compounds that decrease the corrosion rate of metals or alloys. The inhibitors are also absorbed on the components surface and can form a layer that will protect the part from oxygen, water and other chemical active substances. Some corrosion and rust inhibitors are;

- Alkaline Compounds
- Organic Acids
- Esters
- Amino-acid Derivatives

f) Friction Modifiers

Friction Modifiers are added to lubricants in order to enhance their ability to reduce surface friction. Friction modifier additives in lubricants have a positive impact on the fuel efficiency of engines. The following are the most commonly used friction modifiers;

- Graphite
- Molybdenum Disulfide
- Boron Nitride
- Tungsten Disulfide
- Polyterafluoroethylene

g) Extreme Pressure Modifiers

Extreme Pressure Additives decrease the wear of components that are subjected to very high pressures. They prevent seizure caused by direct metal on metal contact between parts that experience very high loads. The extreme pressure additives work in the same way as anti-wear additives. The additive will form a coating over the component's surface that will offer protection and prevent direct contact with other parts. Extreme pressure additives reduce wear and increase the life cycle of an engine. The following materials are used as Extreme Pressure Additives;

- Chlorinated Paraffin's
- Sulphurized Fats
- Esters
- Zinc Dialkyldithiophosphate
- Molybdenum Disulfide

h) Anti-Foaming Agents

The agitation and aeration of the lubricants which occurs in engine oils, gearbox oils and compressor oils may result in the formation of air bubbles in the oil. That phenomenon is also known as foaming. Foaming is capable of decreasing the lubrication properties by causing starvation while enhancing the oil oxidation. The most commonly used anti-foaming agent in lubricants is Dimethylsilicones.

i) Viscosity Index Improvers

The high operational temperatures of internal combustion engines have a huge impact on the viscosity of the lubrication oils, the high temperatures decrease the lubricants viscosity. The viscosity index-improvers keep the viscosity of the oil at an acceptable level for the correct operation of the engine, it maintains a stable oil film even at high temperatures. Viscosity index improvers are used in multi-grade oils, the viscosity of which is specified both at low and high temperatures. The viscosity index also determines the quality of the oil. The higher the viscosity index (VI) the better the oil. The original VI scale is 0 to 100 with 0 being the worst and 100 the best. Synthetic oils usually score in the range of 80 to 400 on the VI scale. Since the VI scale was introduced, the viscosity index additives have improved so much that the scale had to be extended. The most common viscosity index-improvers are Acrylate Polymers.

j) Dispersants

Dispersants keep the foreign particles such as sludge, varnish, dirt, products of oxidation etc. present in a lubricant finely divided and uniformly dispersed throughout the oil. Long grain hydrocarbons and succinimides are used as dispersants in lubricants.

k) Pour Point Depressants

Pour Point is the lowest temperature that the oil can flow. Pour point depressants can further lower that temperature. Pour point depressants are polymers that are designed to control the wax crystal formation that occurs when lubricants are subjected to low temperatures which reduces the lubricants fluidity. The pour point depressants used in lubrication oils are co-polymers of polyalkyl methacrylates.

2.12 Piston-ring-pack

The piston-rings found in internal combustion engines are of two types, Compression Rings and Oil Control Rings. The main function of the compression rings is to seal the compression chamber from the crank case and prevent combustion gases from moving pass the piston. The oil control rings are mainly responsible for controlling the amount of oil left on the cylinder-liner by scraping any excess amount. Both compression and control rings are partially responsible for maintaining the compression inside the cylinder and for controlling the supplied oil though their primary function is dictated by the position they hold on the piston. Most of the piston-ring types commercially available are shown in figure 19, from those the most common are analysed below (S. Hochgreb et al, 2001).

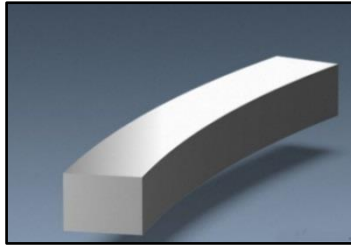


Figure 12 – Rectangular Ring (Grant Piston-rings, 2015)

The rectangular ring, figure 12 features the simplest geometrical shape available for a piston-ring. It can perform simple sealing functions under normal operating conditions and is commonly used in passenger cars fuelled by either gasoline or diesel. This type of ring due to its large contact area is commonly equipped with peripheral coating for reduced friction and increased durability. The rectangular piston-ring is one of the first types of metal piston-rings ever used on an internal combustion engine. Its simple design still classes it as one of the most popular piston-rings even in modern applications.

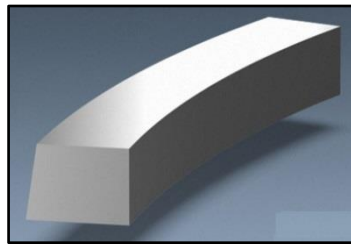


Figure 13 – Taper Faced Ring (Grant Piston-rings, 2015)

The taper faced ring, figure 13 is similar to the rectangular ring with an angled outer face, this ring comes in contact with the cylinder only with its bottom outer edge. These feature offers reduced friction as the area of contact is reduced which also improves its oil scraping capabilities. Taper faced rings are usually positioned at the second groove of a piston-ring in gasoline and diesel engines. Their design provides a degree of pressure relief as the gas forces act initially at the angled face. Some engines use them as a top ring, but their special design makes them ideal for performing both oil-controlling and pressure-sealing functions.

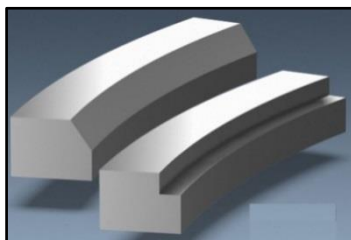


Figure 14 – Internally Bevelled or Stepped Ring (Grant Piston-rings, 2015)

Internally Bevelled or Stepped Rings in figure 14 features an angle corner or a step on the inside diameter on the top side of the ring. The taper faced rings offer a twist effect without any gas pressure loading. The angled corner allows the ring to twist and to contact the cylinder-liner with only its outer bottom edge. This helps to improve the oil consumption as the ring acts like a combination of a rectangular and a taper faced ring. Plus, under operating conditions the gasses act on the inside of the ring, thus improving its dynamic behaviour. This type of rings can be used in diesel or gasoline engines and due to their special design, they can be placed at both top and second piston groves.

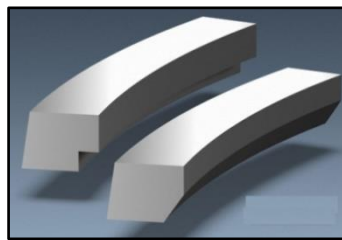


Figure 15 – Tapped Faced Ring with Inside Bottom Bevel or Step (Grant Piston-rings, 2015)

Tapped faced ring in figure 15 with an inside bottom bevel or a step is capable of causing a negative twist opposite to the twist that the internally bevelled or stepped ring does. The ring contacts the cylinder-liner with only its bottom outer edge and ensures minimum oil consumption. At the same time, its ability to twist brings its full face in contact with the cylinder-liner to offer better seal. This is often a second groove ring for gasoline or diesel automotive applications.

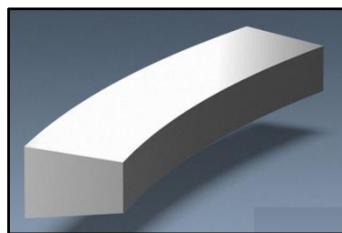


Figure 16 – Keystone Ring (Grant Piston-rings, 2015)

The keystone ring in figure 16 is a ring with a wedged cross section. Due to its unique design this ring always operates “freely”. The ring is moving inside the groove which prevents combustion residuals from sticking on it. This type of ring is not very common in passenger cars and is only used in the top groove if ring sticking is an issue.

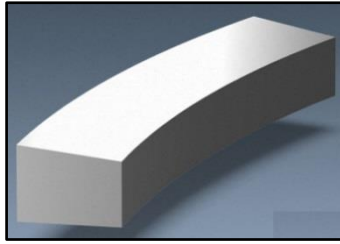


Figure 17 – Half Keystone Ring (Grant Piston-rings, 2015)

The half Keystone Ring in figure 17 is a compression ring with only one side tapered. The geometry of a half keystone ring is similar to the keystone ring with the only difference that both of its top and bottom sides are angled. The reason for this specific design is the same as with the design of the keystone ring and it is to avoid ring sticking. Half keystone ring is very common in two-stroke engines.

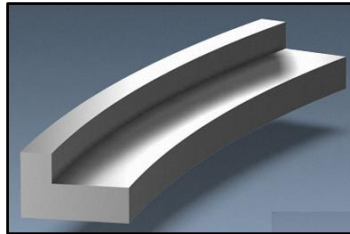


Figure 18 – L-Shaped Compression Ring (Grant Piston-rings, 2015)

The L-Shaped Compression Ring in figure 18 is mainly used in small two-stroke engines. L-Shaped Rings are mostly used on the top groove of a piston as compression rings. When compression gasses act on the L-shaped arm they force the ring on the cylinder liner which offers improved sealing.

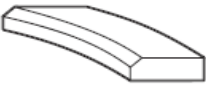
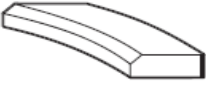
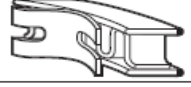
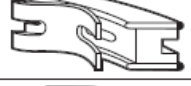
Compression Rings		PISTON RING TYPES		Oil Rings	
TORSIONAL TWIST CAST IRON	PL		*SS* EXPANDER SPACER w/ CHROME RAILS	CO	
TORSIONAL TWIST CAST IRON CHROME	CH		"SIDEWINDER" EXPANDER SPACER w/ CHROME RAILS	OH	
SQUARE CAST IRON	SQ		*PC98* EXPANDER SPACER w/ CHROME RAILS	PC98	
SQUARE STEEL CHROME	SC		"WMRE LATCH" EXPANDER SPACER w/ CHROME RAILS (Rails not shown)	WL	
TORSIONAL TWIST STEEL CHROME	SCT		EXPANDER SPRING & SEPARATOR w/ CHROME RAILS	B	
TORSIONAL TWIST CAST IRON PLASMA MOLY	PM		CAST IRON SPACER & SPRING EXPANDER w/ CHROME RAILS	X	
SQUARE CAST IRON 3 SIDES CHROME	IC		SPRING LOADED OIL RING, SYMMETRIC BEVEL CAST IRON CHROME	CS	
HALF KEYSTONE STEEL/DUCTILE IRON CHROME	HK		SPRING LOADED OIL RING, SYMMETRIC BEVEL CAST IRON NO CHROME	PS	
FULL KEYSTONE STEEL/DUCTILE IRON CHROME	FK		SPRING LOADED OIL RING, SYMMETRIC BEVEL CAST IRON CHROME INSIDE GROOVE	PSI	
STEP SCRAPER CAST IRON	DS		SPRING LOADED OIL RING, w/ BEVEL CAST IRON	GS	
NAPIER CAST IRON	N		SLOTTED OIL RING, GROOVED w/ BEVEL CAST IRON	GB	
BEVELED STEP SCRAPER CAST IRON	BS		SLOTTED OIL RING, GROOVED CAST IRON	W	
REVERSE TORSIONAL TAPER FACE CAST IRON	RTTF		SLOTTED OIL RING, GROOVED w/ SYMMETRIC BEVEL CAST IRON	WA	
TAPER FACE CAST IRON	TF				
TORSIONAL TWIST TAPER FACE CAST IRON	TTF				

Figure 19 – Commercially available piston-ring types (Grant Piston-rings, 2015)

2.13 Lubrication Regimes

Lubricated friction is characterised by the presence of a thin film of lubricant between two sliding surfaces. The ratio of the oil film thickness “ h ” to the surface roughness “ R_a ” determines the type of the lubrication regime. There are three major lubrication regimes; Boundary lubrication when $h < R_a$, Mixed lubrication when $h \approx R_a$ and Hydrodynamic Lubrication when $h > R_a$. All three regimes are explained and analysed below. Figure 20 shows the lubrication regimes and the Stribeck curve (S. Söchting, 2006).

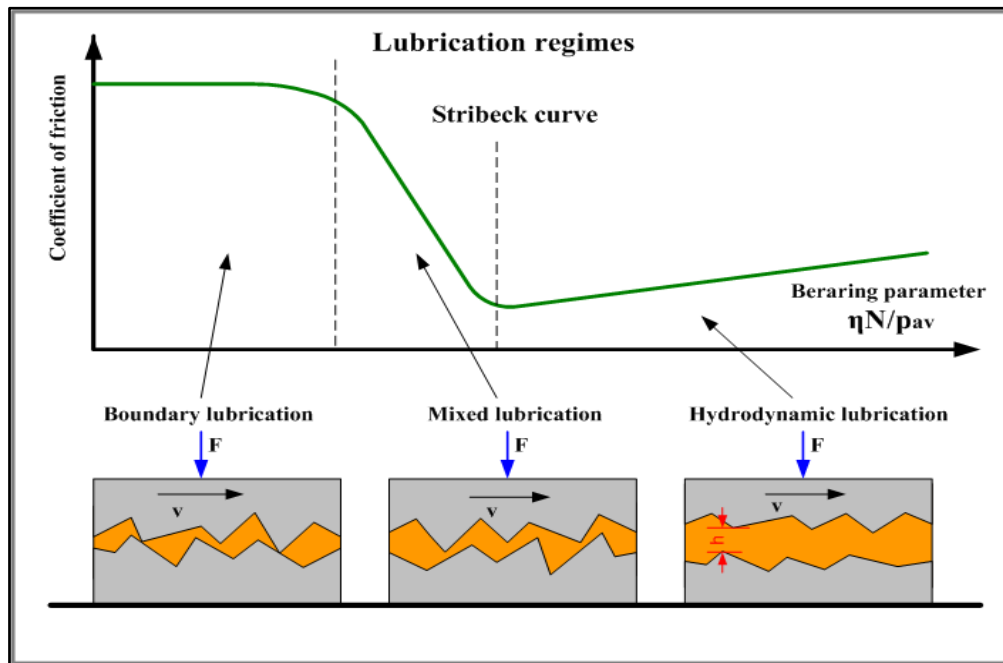


Figure 20 – Lubrication Regimes and Stribeck curve (Subtech, 2015)

a) Boundary Lubrication

At boundary lubrication, there is a contact between the high surface points of the two surfaces that slide on top of each other. This type of regime is highly undesirable in automotive applications, it increases wear and the possibility of component failure. Severe engine failures have been caused by boundary lubrication. Boundary lubrication usually occurs at low engine speeds while as start-up or at very high loads. Modern lubricants use high pressure additives, to protect the engine components, from metal to metal contact, at boundary lubrication.

b) Mixed Lubrication

At mixed lubrication, the contact between the two sliding surfaces occurs only at a very few high edges. This stage is an intermediate step when moving from the Boundary Lubrication regime to the Hydrodynamic Lubrication regime

c) Hydrodynamic Lubrication

The Crankshaft, the crankpin and the crankshaft bearings are only a few components that operate on hydrodynamic lubrication. It is very important that those components operate in hydrodynamic lubrication or else they might fail. In this regime, no contact is made between the two sliding surfaces. The oil film keeps the surfaces apart due to a force known as hydrodynamic lift and which is generated by the lubricant being squeezed through a narrow gap between two sliding surfaces.

2.14 Lubricants and Internal Combustion Engines

Internal combustion engines rely on piston-rings to seal off the cylinder and maintain the in-cylinder pressure. As the rings slide on the cylinder walls, a lubricant is used to minimise component wear and friction. The piston-ring and cylinder-liner setup is the major source of frictional losses inside an internal combustion engine. It is important that sufficient lubricant is supplied at all times between the contact regions and especially near the compression ring (top ring). It is important to maintain sufficient lubrication for good engine operation. Equally important is to make sure that the supply does not exceed the minimum amount of lubricant required for the correct operation. By optimizing the oil transportation through the ring-pack it is possible to minimize the oil consumption which leads to undesirable side effects such as increased emissions and oil consumption. Due to the way, the piston-rings are designed and operate, the piston-ring-liner setup offers various paths from where oil can enter the combustion chamber. Oil can pass from one side of the piston to the other using the ring grooves, ring-gaps and connections. These gaps open and close following the reciprocating motion of the piston. Rabute and Tian (2001) investigated the oil transportation mechanisms for a number of pistons and piston-rings at various geometries. They concluded that the oil consumption is highly affected by the geometry of the piston and the ring-pack. Figure 21 shows the different lubrication regimes along the stroke of the piston (Tian, T. and V. W. Wong, 2000).

Even though the ring-pack is responsible of retaining the combustion gasses inside the combustion chamber there are always gasses that manage to escape into the crank case. There has been a lot of research in order to determine whether these gasses affect the oil consumption. The main passages for these gasses are through the ring-gaps, the back of the rings and the front of the rings when not in full contact with the cylinder walls. When the pressurised gasses pass through the top ring, they get trapped between the following rings while the piston is in motion, the low in-cylinder pressure will force the pressurised gasses to

flow back into the cylinder. This backward flow of gasses will force lubrication oil over the top ring and into the cylinder. This flow of gasses has been the focus of many research groups in the attempt to reduce oil consumption in internal combustion engines.

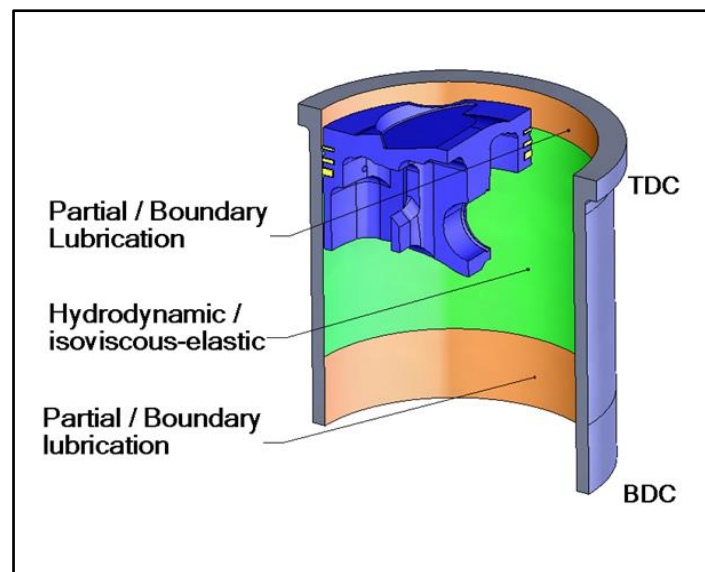


Figure 21 – Lubrication engine regimes (Tian, T. and V. W. Wong, 2000)

The engine pistons are usually equipped with three rings. These rings are designed to perform different and distinct operations by either acting as a seal for the combustion gasses or by controlling the oil delivered onto the cylinder walls. The rings and the cylinder walls are designed with a circular profile. The reality is that regardless of how advanced or sophisticated is a manufacturing technique the finished product will never be ideal and will deviate from the design. The small inconsistencies on the component geometries might not be visible in most of the cases but do affect the operation of an engine. When the piston-rings are used in an engine they are subjected to very high speeds which force them to move inside their grooves by either oscillating or rotating. Since the cylinder liners and the piston rings are not perfectly circular, the lubrication control will change depending on the movement of the piston-rings. Min et al (1998) investigated the ring rotation and the way that it affects the oil consumption inside an engine. Min et al concluded that at low speeds the top ring will rotate at a rate of 0.3 to 0.4rpm were the other two will just oscillate. When the tests were repeated at higher speeds it appeared that all the rings started to oscillate. The results they obtained were all based on steady speed engine operation. When the tests were repeated in a range of variable speeds closer to automotive operating conditions the behaviour of the rings was unpredictable and followed no specific pattern (R. Kai and M. Sato, 2000). The ring pack is vital to the operation of an engine. The design of the rings can affect the operation of an

engine with regards to its performance, reliability and efficiency. A number of studies have showed that the design of the ring-pack can significantly influence the oil consumption and the blow-by of an engine.

2.14.1 Oil Transport Mechanisms Forces

There are four main factors that contribute to the transportation of the oil through the pistons ring-pack and into the combustion chamber, these are; Mechanical, Inertia, Pressure or Shear Stresses.

- a) Mechanical: The piston follows a reciprocating motion at very high speeds which is relative to the linear movement of the pistons and the movement of the piston-rings inside their groove which subsequently results to the displacement of lubricant.
- b) Inertia: While the piston is moving, the lubricant present on its surface is moving at relatively the same speed. The rings and the lubricant present on the piston follow an alternating motion, which involves rapid changes in the direction and velocity. As the piston starts to decelerate towards TDC the inertia of the lubricant will force it to leave the piston and continue its path into the cylinder.
- c) Pressure: The significant changes in the in-cylinder pressure and the pressure differential between the crankcase and the combustion chamber may cause rapid exchange of air and gases between the crankcase and the combustion chamber. These moving gasses are capable of carrying oil which can enter the combustion chamber.
- d) Shear Stresses: The flow of gasses through the ring-pack causes shear stress at the interface between the gas and the oil layers. These stresses are capable of contributing to the transportation of oil into the combustion chamber.

2.14.2 Oil Consumption and Emissions

Oil consumption has been the main focus of study among many engine manufacturers and many research groups. While the engine is in operation, oil can enter the combustion chamber and take part in the combustion while leaving the system as exhaust emissions. With the latest emission laws, manufacturers are in a race to find the contributors that raise the exhaust emissions. One of the leading factors that contributes to increased carbon dioxide emissions is the parasitic frictional losses occurring inside the engine. Other areas include:

- The Crankcase breather systems
- The Valve stem seals
- The Turbocharger seals
- The Piston-ring / Cylinder-liner interactions

The interaction between the cylinder-liner and the piston-ring is the biggest source of frictional losses and accounts for approximately 20% of the total mechanical losses that occur inside an engine. Insufficient lubrication will allow for the metal surfaces to contact against each other which will affect the engines performance. A thick oil film will reduce wear, but the increased oil supply will have a negative impact on the engines output emissions. The excess oil can enter the cylinder and take part in the combustion. Appropriate control of the lubricant present between the piston-rings and the cylinder-liner is crucial to the operation and performance of the engine.

2.15 Relevant Work

1969 – Greene manufacture a rig to visualise lubrication on the piston-rings at conditions close to the induction and compression strokes of an engine. His work continued at a range of operating conditions, which he captured on film. The results obtained were not sufficient to document the lubricant transportation mechanisms that take place between the cylinder-liner and piston-ring assembly.

1995 – Inagaki Modified a single cylinder gasoline engine by installing two sapphire windows into the liner, figure 22. The windows were glued inside the liner to prevent popping-out due to the high in-cylinder pressures. The engine was tested both under firing and motoring conditions. The engine had been equipped with a cylinder head pressure transducer, an oil film pressure transducer and a shaft encoder. The data acquisition was performed with the use of LIF.

1996 – Ostovar manufactured a single ring test-rig capable of simulating the operating conditions of a piston-ring and cylinder-liner setup under idealised conditions. The test-rig was developed in such a way that would allow for simultaneous pressure, oil film thickness and friction measurements. The pressure measurements were obtained through a pressure transducer installed on the cylinder-liner near the surface. The oil film thickness was captured using a capacitance device. A numerical method was developed for the prediction of the lubricant film parameters based on the Swift-Stieber separation. Ostovar also developed a dual laser induced fluorescence technique that could be used to permit the dynamic calibration of the oil film thickness in an engine.

1999 – Duszynski used the dual laser induced fluorescence technique developed by Ostovar on a firing four-stroke diesel engine which was later proved to be unsuitable for the application. The measurements were obtained by optic fibres installed on the cylinder-liner.

The measuring equipment was calibrated with a static calibration technique developed by Duszynski. Duszynski recorded all the calibration coefficients for the oils he tested at different temperatures. Furthermore, he also constructed a calibration device based on his measurements. The device was made by fused silica and had a rectangular shape with groves on its surface. The groves were carefully cut in depths from 2 to 10 μm in steps of 2 μm . Duszynski examined a variety of oils with different concentration of additives at different viscosities. Duszynski at a later date tried to repeat his measurements on a two-stroke engine.

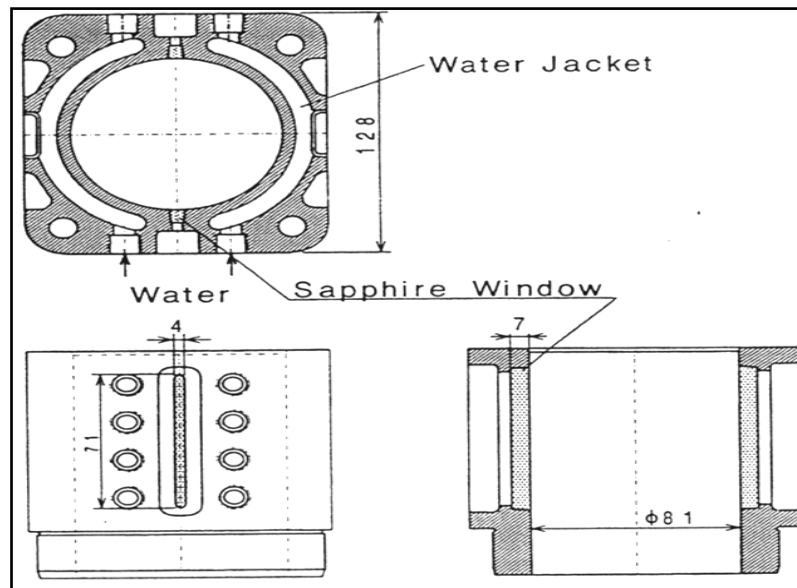


Figure 22 - Inagaki's (1995) single cylinder optical-engine

1999 – Takamitsu et al investigated the variation in oil film thickness of a piston-ring-pack using the LIF technique. The authors conducted simultaneous measurements of the oil film thickness at the centre stroke on both the thrust and the anti-thrust sides of the piston. It was found that the oil film thickness on the thrust side differs from the anti-thrust side. All the measurements were acquired by four optic fibres inserted in the cylinder-liner. During the study, it was observed that the amount of lubrication oil around each ring increases greatly with the decrease in engine load, but the effect on the oil film thickness is small.

2000 – Pyke applied the LIF technique on a test-rig and a diesel engine in order to measure the oil film thickness between the cylinder-liner and the piston-ring. The use of LIF on a diesel engine proved to be difficult as the results were affected by the engine's temperature. Despite the difficulties, the results showed trends that linked the oil film thickness with the engines operating conditions. Pyke used an optic fibre in an attempt to measure the cavitation

between the ring and the cylinder-liner. There was also another attempt to establish a relation between the roughness orientation and its effect on friction.

2001 –Newaz et al used a bench friction test system to investigate the piston-ring and liner contact interface. The test-rig had a high stroke length and large contact width. The effects of the load, the speed, the temperature and the surface roughness were investigated for conventional cast iron cylinder bores.

2001 – Thirouard tried to address the fundamental aspects of oil transportation in the ring-pack through experiments and modelling. He used a two-dimensional multiple dye Laser Induced Fluorescence Technique to visualise the piston-ring – cylinder-liner interaction for both a diesel and a gasoline engine. The outcome was high resolution images of the ring-pack's oil distribution. The measurements were repeated at a range of operating conditions. The analysis of the data revealed major oil flow patterns which were identified and characterised. A theoretical model was developed which offered results that matched those obtained on the engine. This work offered a comprehensive investigation of the oil transportation mechanisms that affect the ring-pack inside internal combustion engines.

2004 – Bolander et al developed an experimental and analytical model to investigate and determine the lubrication frictional losses at the interface between the piston-ring and the cylinder-liner. The test-rig featured dual-fibre optic-displacement sensors to measure the oil film thickness and a tri-axial force transducer to measure the friction. The effects of boundary and mixed lubrication at the end of the stroke were investigated with the use of an analytical model that featured the Elrod and Stochastic/Deterministic approach for asperity contact. The final experimental and analytical results were found to be very close. They also accurately illustrated the transportation of the oil through the different lubrication regimes that the piston-ring and cylinder-liner experience during a stroke.

2005 –Tamminen used a four-stroke diesel engine to determine the gas pressure acting on the ring-pack area. The experimental part of the study was carried on a firing engine with an instrumented piston and cylinder-liner. The experimental results were compared to computer simulations. The two methods when later compared found to be a very close match

2005 – Dellis used Ostovar's test-rig to measure the oil film thickness by adopting both the capacitance and the LIF techniques. He employed various methods to calibrate the LIF technique. Ending his project Dellis concluded that the most appropriate technique is using a groove of known depth on a piston-ring specimen to achieve dynamic calibration while

eliminating the uncertainties of the static calibration and compensating for the oil film, temperature and property variations. The calibrating techniques used were later compared with the results obtained by the capacitance method and none of them proved to be effective. The test-rig was modified to allow optical access to the piston-ring and cylinder-liner interaction. The metal liner was replaced with an optical one made from quartz and the oil film behaviour was captured with a CCD camera. Dellis could visualise the behaviour of the oil film on the piston-ring and capture images of the different stages of cavitation as they formed. He continued by installing a quartz window on the same engine that Pyke used and performed tests under motorised conditions. He could capture similar images as he did earlier on the test-rig. The only drawback was the lack of in-cylinder pressure measurements to support the optical data.

2008 – Dhar et al used the capacitance method to measure the minimum oil film thickness at the piston-ring and cylinder-liner interaction. Two probes were required for the capacitance to work. The two probes were one on the piston-ring and one on the cylinder-liner. The oil film thickness was measured on a motorised engine at three different locations. These locations were the Top-Dead-Centre, the Mid-Stroke and the Bottom-Dead-Centre. The lubrication oil film was found to range from $0.2\mu\text{m}$ to $8\mu\text{m}$. The data on the up-stroke and the down-stroke stroke showed significant variations due to the tilt of the piston.



Figure 23 - Optical test-rig as used by Ostovar (Ostovar, 1996)

2009 – Dhunput used Ostovars test-rig, figure 23 to develop a methodology to assess the rheological behaviour of various base-oils and additives. Dhunput with a use of high speed equipment managed to capture the cavitation occurring between the liner and the piston-ring specimen. His research continued on a modified engine on which he installed two optical windows that would allow access to the inside of the cylinder. Moreover, the engine was modified in such a way that two pressure transducers were implemented at mid-stroke, bottom and TDC. The engine tests unfortunately did not extract any useable information.

2.16 Previous Work on Oil Film Thickness, Pressure, Load and Friction in Relation to the Cavity Behaviour

Work performed by previous researchers has mainly focused on the investigation and establishment of a link between oil film thickness, pressure and friction in relation to cavity behaviour. This section summarizes the findings of previous research projects and presents them in order to give a better understanding of the aspects that have been previously covered and where the current project has contributed towards the better understanding of the phenomenon. The findings are presented below in bullet points as these have been detailed by previous researchers. (A.Dhunput, 2009). All the work below has been performed on City University's optical test rig.

- Oil film thickness as measure by the capacitance probe decreases with increasing load and increases with increasing speed.
- Viscosity of the oils found to be an important factor in the characterization of the oil films; the more viscous oil gave rise to a higher oil film thickness.
- Friction results were found to be repeatable with their symmetry during upstroke and downstroke reflection the design and manufacturing of the test rig.
- Friction results close to the dead centres where peaks were recorded have been validated by the capacitance results.
- The frictional force at the ring/liner contact is mainly attributed to asperity contact and viscous drag; when asperity contact is present, it plays the dominant role.
- For the very viscous oils no asperity interaction was noted and hence the friction measurements have been dominated by viscous drag.
- Higher oil film pressure occurs on the smaller curvature side of the ring.
- The depletion of the oil film as obtained by the LIF corresponds to the sub-atmospheric pressure measured locally. This lead to the conclusion that cavitation occurs in the sub-atmospheric pressure region within the diverging section of the ring.

- Higher speeds and loads increase the hydrodynamic pressure, but the negative pressure remains practically unchanged especially in the larger curvature of the ring.
- Higher viscosity oil gives rise to higher oil film pressure higher oil temperature reduces the oil film pressure; the pressure of the oil film is related to the oil film thickness available between the contacts.
- The higher the load, the earlier in the stroke the fern cavities appear and the smaller their size and the higher the number of strings.
- The higher the viscosity, the later in the stroke the cavities appear, the larger their size and the smaller their numbers.
- It has been observed that the higher the load is, the sooner in the stroke the fern cavities appear and the smaller their size is.
- The number of string cavities increases when the applied load increases.
- Both load and speed have an influence on the number of string cavities.
- The load and speed do influence the number of string cavities quite considerably. At higher loads, the number of string cavities increases and the width of the string decreases. On the other hand, at higher speeds the number of string cavities decreases and the width of the string increases.

2.17 Critical Review on previous work

This section is dedicated into detailing and analysing previous research projects and is accompanied by a commentary and a critical evaluation. This exercise is a continuation of the literature and it is not meant as a negative review but as a discussion of the work performed and where gaps could be bridged with additional investigation. This is also an assessment of the strengths and weaknesses of the literature and it is performed in relation to the scope of the current project. The previous work carried within the research group of City, University of London has been based on a test-rig first constructed by Ostovar and developed back in 1996. The test-rig Ostovar developed features a single ring and simulates the lubricating conditions between the cylinder liner and piston-ring interaction of a reciprocating engine under idealised conditions. The test-rig allowed for the simultaneous measurement of oil film thickness and friction, with the use of a capacitance probe and a friction transducer. A numerical method was developed in parallel and proposed for the prediction of the lubricant film parameters. These include the Swift-Stieber, Separation, Coyne and Elrod and Flower boundary conditions. The model was assessed against the measurements obtained on the single ring test rig. A crucial observation was a cavitation delay mechanism that was found to

be responsible for a thinner film, after the reversal points were compared to the predictions made by the Reynolds boundary condition. Another point worth noting is that the roughness parameters used were found to affect at a very high level the surface roughness models which proved to be relatively sensitive.

Ostovar also developed a dual Laser Florescence and Interferometric technique that would permit the dynamic calibration and acquisition of the oil film thickness within an engine. A few years later in 1999 Duszynski employed the Laser Induced Fluorescence technique developed by Ostovar in a firing four-stroke diesel engine to acquire oil film thickness measurements. Unfortunately, the technique was proven to be inadequate and no useful data were extracted. Duszynski installed optical fibres in fused silica blocks and the system was calibrated at a static state. He performed a study that quantified the temperature effect on the calibration coefficients of the engines oils he tested. The way he performed the calibration is by cutting grooves of known depth and then filling those grooves with oil and taking measurements from each individual specimen. Fused silica was chosen for its low thermal expansion. The grooves on the side of the blocks were in multiple depths between $2\mu\text{m}$ and $10\mu\text{m}$, in $2\mu\text{m}$ steps. The increment and the range chosen was determined in earlier tests which concluded that the piston-rings within an operating internal combustion engine vary within that range. Duszynski considered a wide range of lubricants that featured various additives and viscosities. Following the diesel engine test runs, Duszynski continued the tests on a two-stroke engine. The results showed higher oiling rates associated with thicker oil films.

Following Duszynski the next year Pyke (2000) carried out experiments both on Ostovars test-rig and on a firing diesel engine. The oil film thickness was measured on the liner with the use of LIF techniques. The tests were carried out on a plethora of a different operating conditions. Weight was put on the repeatability of the measurements though this was not achieved on the diesel engine, while the measurements on the test-rig were proven to be much more consistent. The main issues that Pyke faced were the comparability of the different samples mainly due to the issues faced with the calibration process of the LIF technique. Despite all the difficulties faced, Pyke was still able to identify the expected trends. The final part of the project involved the repetition of the tests at cold runs and at engine start up. The build-up of the oil film thickness was identified as a four-stage process and the effect of engine speed, cylinder pressure and temperature were all visible only during the first two hundred cycles. Pyke also continued the development of Ostovar's test-rig by

inserting an optical fibre on the rigs metal liner where the LIF technique was used to measure the oil film thickness while cavitation occurred for a range of lubricants. Pyke faced many difficulties when tried to compare the different runs between them. He also carried an investigation on the surface roughness orientation and its effects on friction. Finally, concluded that the crosswise oriented roughness produces less friction.

In 2005 Dellis was another one of the researcher that used Ostovar's test-rig to investigate the oil film thickness between the cylinder liner and piston-ring interaction. Dellis attempt to add value to the already rich literature by investigating and comparing the capacitance and the LIF techniques. He tried to calibrate the LIF method through a series of various techniques. A dynamic technique was implemented that had many similarities with Duszynski calibration techniques. This technique made use of a groove of a known depth on a piston-ring specimen which was used for the calibration of different oil samples. The second technique used a micrometre that allowed for a static calibration. The gap between the two mating surfaces of the micrometre represented the gap that the oil would penetrate, and the measurement would then be taken. Deli also took under consideration the power output of the fibres and the background noise generated and the resident voltage of the fluorescence detector. Delis concluded that none of the investigated techniques proved to be sufficient or satisfactory when compared with the capacitance technique. Finally, he proceeded by concluding his research on Ostovars test-rig with the use of the capacitance technique in combination with the friction sensor and the pressure sensor on the test rig. That allowed him to acquire measurements related to the phenomenon of cavitation between the two sliding surfaces. Delis also used the installed heater to control the temperature and even went a step further by performing tests with different ring profiles. Once the tests were competed Delis used a metal liner with an optical window that had been manufactured for the specific test-rig and continued his measurements with the acquisition of optical images. For the visualisation, Delis used a CCD camera which had to be precisely timed with the rotating position of the test rig. Pyke also tried to modify a diesel engine in order to incorporate an optical window to allow for visual measurements. The tests were run only under motorised conditions and they did not feature a pressure transducer, thus no pressure measurements were acquired.

After Delis, Dhunput performed extensive measurements on the same test rig. The main focus was on the oil film thickness and the friction generated when lubricants are tested under certain conditions. He used a variety of different measuring techniques to achieve his objectives. The project generated a sizable database on the oil film thickness and the friction

of lubricants when these are present between the “piston-ring – cylinder liner” interaction. The study has provided a good dataset that supports the link between the oil film thickens and the friction with the lubricant composition.

Dhunput’s research was used as a stepping stone to further continue and investigate the link between the lubricant composition and the lubricant performance. As the oil film thickness and the friction had been extensively investigated a new approach had to be implemented for the current project. An approach that would allow for new information had to be extracted from the tested lubricants. This study made use of the latest advances in technology both in optical equipment and computer processing power. A brand-new set of data was captured in the form of optical data and computer algorithms were compiled in order to assist with the processing. For the first time, physical properties were measured such as cavity length, cavity width, cavitating area and number of cavities. These new set of data has been the extra step in order to get a better insight into the link between lubricant composition and lubricant performance and to get a better understanding of the phenomenon of cavitation. This new approach opened new paths to the investigation of the phenomena of cavitation. The project delivered a set of data which offer a better insight on the way cavities generate and develop in the piston-ring and cylinder liner interaction. The test-rig experiments were run in parallel to the main project. The core of the project involved the design, manufacture and testing of an operational, fully firing optical engine. This part of the project took under consideration previous work done in order to identify problems and limitations faced before. This approach of the investigation of cavitation in internal combustion engines offered for a set of images that clearly illustrates the development and behaviour of cavities in the cylinder liner and piston-ring interaction.

CHAPTER 3: LUBRICATION TEST-RIG

The test-ring and the optical engine experimental setups are both documented and analysed in the following paragraphs of this chapter. The setup of each experimental device was derived as a result of the experience gained during the course of the project. The settings and the layout chosen for each of the experiments has been the result of research combined with testing observations. The correct setup is important to the acquisition of the output data. An incorrect setup could render the results unusable. Significant part of the project was dedicated to the identification of the optimum setup considering the available equipment and the desirable outcome.

The investigation of the phenomenon of cavitation was performed with the use of City University's in-house test-rig and was focused on the area between the piston-ring and the cylinder-liner interaction. This test-rig offers a simple way of assessing the behaviour of different lubricants. Its design makes it easy to test different types of lubricants at multiple operating conditions in a fraction of the time that would usually be required on an engine. The test-rig uses a flat cylinder-liner which slides on a single fixed piston-ring. The test-rig is capable of collecting data related to the oil film thickness, the friction, the pressure and the flow rate of the lubricant.

The test-rig was designed to function on the same basic principles as a full sized automotive engine. The cylinder-liner was manufactured out of a solid block of polished stainless steel. The liner is capable of reciprocating over the piston-ring which is unable to move on any of the three axes. The ring can rotate along the central line to introduce a degree of freedom in their in-between interaction. The test-rig is powered by an electric motor capable of speeds up to 1400rpm. The speed of the liner is controlled by the voltage supplied to the electric motor. An electric pump is responsible for the continuous oil supply. The test-rig operates on a closed oil supply system where the pump re-circulates the oil from the reservoir to the oil-filter, through the heat exchanger. The heat exchanger can either maintain or increase the temperature. The oil after the heat exchanger enters the injection nozzles which directs it onto the piston-ring and liner interaction. The oil is then collected in the sump under the piston-ring and is returned back to the oil reservoir. The length of the stroke is adjustable ($\pm 50\text{mm}$). The stroke is adjustable through a removable link located in the middle of the connection rod (Arcoumanis, C., M. Duszynski, H. Flora and P. Ostovar, 1995). The oil film thickness measurements can be obtained by either LIF or capacitance, while the LIF sensor is in the

middle of the cylinder-liner. The stroke length can be adjusted by the use of different length connection rods.

The injection nozzles are located on both sides of the piston-ring. These are drilled on two cylindrical tubes installed in parallel and very close to the ring. Each tube has four injection nozzles ensuring a constant and uniform oil feed during operation. One of the injection tubes features a hollow end where a K-type thermocouple is located for accurate oil temperature monitoring. The system's temperature is controlled by the heat exchanged which can maintain a temperature of up to 80°C. The electric motor which powers the test-rig is located on a flexible coupling to minimise the transmitted vibrations. The main shaft that transfers the power from the electric motor to the connection rod was designed using counterweights, similar to the ones used on the crank shaft of an internal combustion engine. The liner and the majority of the moving parts is made out of aluminium with the only exception being the sliding surfaces which are made from a heat-treated steel in order to increase durability and scratch resistance. The axial friction is measured with a force transducer which is located on the holder of the piston-ring. The cylinder-liner is kept in place by two high precision linear bearings. The linear bearings are located on a stationary metal holder which acts as the frame where the liner can reciprocate. The frame allows for extra weight to be added on its free end in order to increase the total load on the system. The Load of the ring from the additional weight is a function of the crank angle and the reciprocating speed. The load on the TDC is greater than the load on the BDC for the same amount of weight. The force on the ring can be calculated by the following equation;

$$W_{(\theta)} = \frac{0.1830g + 0.25gm_h(0.089 - R_{crank} \cos \theta) + 5.78 * 10^{-3}R_{crank} \cos \theta \omega^2(\theta)}{(0.088 + 0.5b)B}$$

g = gravity acceleration, m_h = mass applied to the hanging point, R_{crank} = the crank radius, ω (θ) = crank angular velocity, b = ring width, B = bearing length.

The test-rig is built in such a way that the following parameters can be controlled; Speed, Temperature and Pressure. While the following can be monitored: Nozzle Temperature, System Flow Rate, Oil Film Thickness, Friction, Oil Film Pressure and Oil Film Visualisation. The need to visualise the behaviour of the oil film between the piston-ring and the cylinder-liner interaction lead to the manufacture of an optical-liner that would replace the metal one, the new liner was made from Quartz (Fused Silica). Most optical applications use Quartz due to its durability and the fact that the material behaves in a predictable manner

very close to steel. This allows for a very smooth finish and successful mating with the other steel components. Quartz offers much better optical properties than lenses made by common glass formulas. The optical images were captured with the use of a high-speed camera. (Arcoumanis, C., M. Duszynski and H. Preston, 1998b).

3.1 Test-rig Setup

The test-rig as developed by Arcoumanis et al, can be seen in figures 24 and 25. It uses a single ring on a flat surfaced quartz window in an aluminium frame to simulate the principle operation of a piston-ring and cylinder-liner setup. The non-optical liner featured a pressure transducer capable of measuring the oil film pressure and an optic fibre for LIF measurements.

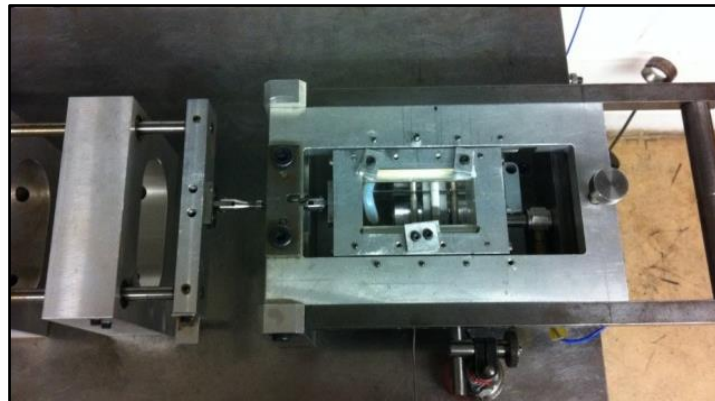


Figure 24 – Optical Test-rig, top view of the liner

The non-optical liner is also capable of providing capacitance measurements. Previous work performed on the test-rig was concluded in two steps. The first step was with the use of the non-optical liner to acquire pressure, film thickness and friction readings while and second used the optical liner for the flow visualisation. The need to find a way to better link the optical measurements with the data acquired by the sensors, lead to the modification of the current optical liner to allow for film-thickness and optical-measurements to be taken simultaneously.

The modification included a new capacitance plate that was attached on the housing of the existing optical liner. The plate was designed is such a way that it would be a direct fit on the test-rig without any additional modifications. Figure 25 shows the new capacitance plate fitted on the frame of the optical window. Again, in the same figure the optical liner was marked with a permanent marker to give a more accurate indication of the liners movement. After the first set of optical data was acquired it was noticed that the movement of the liner is

not clear and the TDC and BDC point could not be identified. The solution was to mark the optical liner using a permanent marker at 1mm increments to get a clear view of the liners movement. The chosen increments were set at 1mm due to the camera setup having a minimum optical frame of 1mm long, this ensures that when a line from the scale leaves the ring surface the next one enters.

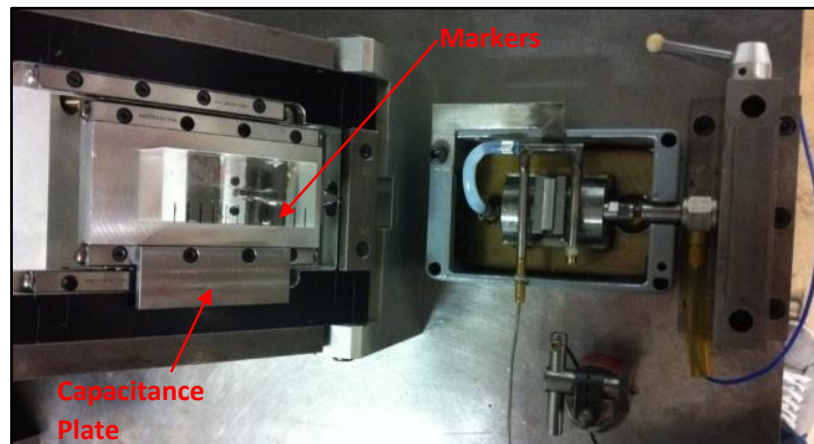


Figure 25 – Modified optical liner with additional capacitance plate

3.2 Test-rig Sensors

The test-rig through the various projects had been equipped with a plethora of sensors. These sensors were capable of extracting valuable information out of the tested specimens and were responsible of generating most the data captured.

The friction sensor used on the test-rig is the PBC 208B force sensor. The Series 208 general purpose sensors are designed to measure compression and impact forces from 44.48N to 22.24kN and tension forces up to 2.224kN. This sensor is extremely sensitive and capable of reacting even to the slightest displacement changes. The 208B force series sensors are very flexible and offer many mounting options. Figure 26 shows the mounting possibilities available for the 208B force series sensors. The friction sensor was first calibrated by Ostovar (1996) using a set of weights (Arcoumanis, C., P. Ostovar and R. Mortier, 1997). The friction sensor calibration chart as this was derived by Ostovar is shown in figure 27.

The two thousand pulses shaft encoder used on the lubrication test-rig was mounted on the base of the electric motor. This type of encoder is equipped with two one-thousand pulses-channels. These channels are useful for detecting at which direction the encoder is rotating at any given time. The channel A and the channel B depending on which one is ahead of the other will indicate the direction of the rotation.

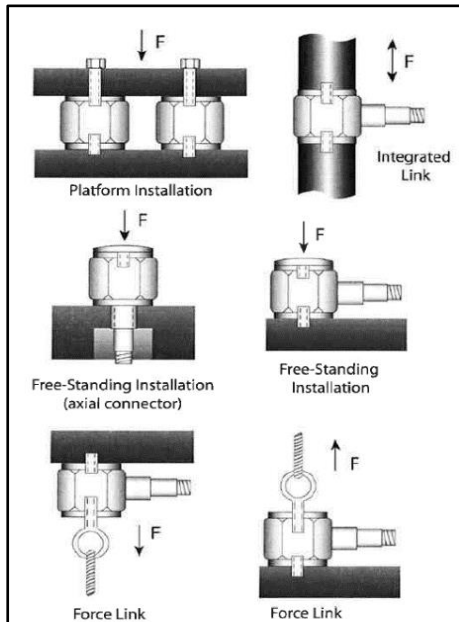


Figure 26 - Friction sensor mounting positions (PCB Piezotronic, 2015)

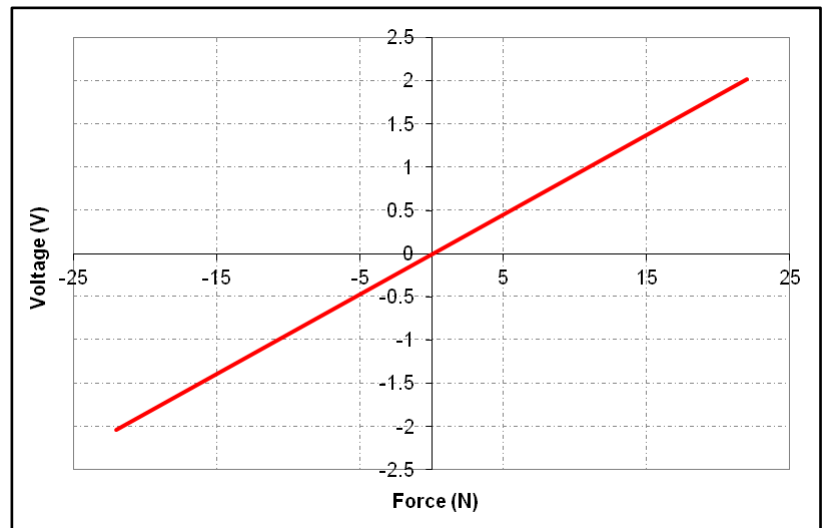


Figure 27 - Friction sensor calibration chart, derived by Ostovar

The shaft encoder is connected onto a custom data signal conditioning box which collects the two channels and adds them up in order to get a two-thousand-pulses per revolution encoder. The signal from the signal conditioning box is then sent to a 2839 NI (National Instruments) data acquisition card which translates the analogue signal into digital for the computer to process it. The rest of the test-rig's sensors rely on the shaft encoder to initiate acquisition. Each sensor acquires one measurement for every pulse of the encoder that the NI card receives. The capacitance method used for measuring the oil film thickness on the lubrication test-rig is based on the capacitance principle. The capacitance measuring technique uses a probe placed under the test-rig's liner and which measures the changes between the liner-probe distance by measuring the voltage fluctuations. The output of the capacitor is sent to a Capacitec unit which converts the signal output to a voltage. The analogue signal is read by the NI data acquisition card which is then translated to a digital signal for the computer to process it. One of the capacitance probes is shown in figure 28, when installed on the test-rig it was placed right next to the ring at around 30 microns lower than its flat surface. The distance is very small but ideal for the capacitor to take accurate readings.

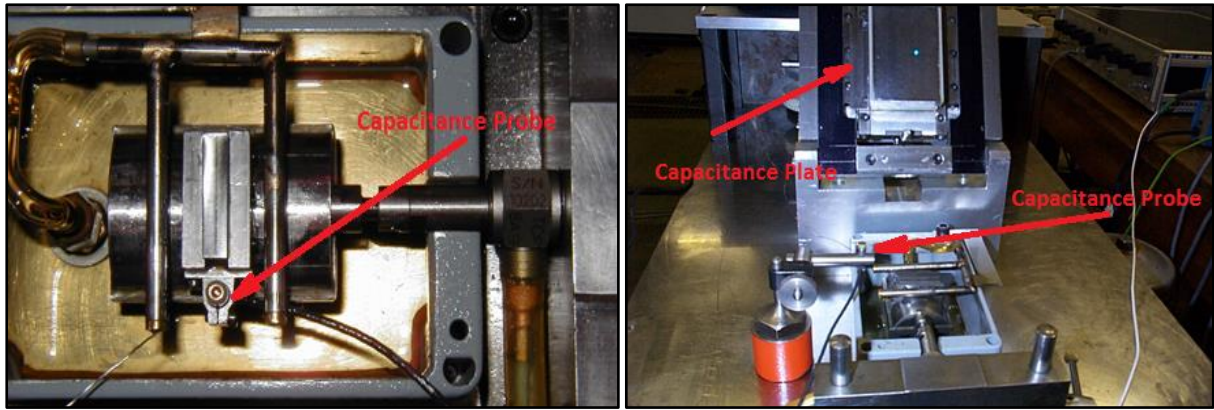


Figure 28 - Optical test-rig capacitance probe and setup

The main problem with this arrangement was that oil would splash and get in the gap between the capacitance-probe and the liner and would conduct the two terminals which would interfere with the readings. The major problem was that the tested lubricants at high speeds would form cavities which interfered with the results as they changed the dielectric properties of the lubricant (Arcoumanis, C., M. Duszynski, H. Lindenkamp and H. Preston, 1998a). The probe as shown in figure 28 is mounted onto the powerful Eclipse E909 magnet which secures it on to the test-rig's bed under the liners capacitance plate. The magnet, the capacitance plate and the area where the magnet is placed have been carefully polished and levered. The capacitance readings were collected by the NI card from where they could be recorded and processed to get the oil film thickness. One of the major advantages of this test-rig is that it offers optical access to the area where the ring and the liner come in contact.

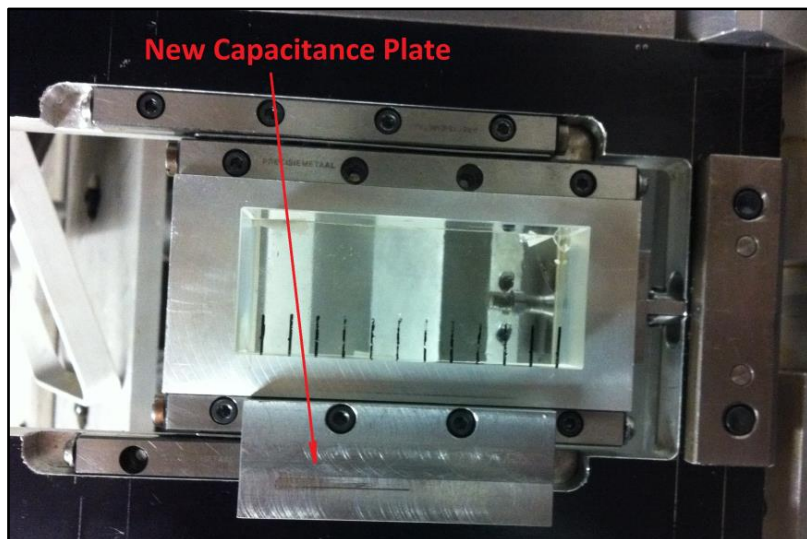


Figure 29 - Capacitance plate for optical and oil film thickness measurements

One of its disadvantages was that the visual data and the oil film thickness were acquired using two different liners and the measurements were taken at different instances. This meant that the correlation between them was not very accurate. The need to better link the images captured by the camera and the data collected by the sensors lead to the installation of a capacitance plate on the test-rig's optical liner. The new plate was designed in such a way so that it could be used without modifying the original capabilities of the test-rig. Figures 29 and 30 show the new capacitance plate fitted on the optical liner ready for operation. The new capacitance plate is securely located on the journal bearings on the side of the windows casing. The bearings have four holes across their length from where they can be mounted onto the rig's casing. All these holes come with counter sinks in order to prevent the bolts from interfering with any of the moving parts. The new capacitance plate is designed in such a way that uses two of the four counter sinks to secure onto the current liner. The new setup allows for simultaneous optical and oil film thickness measurements. The capacitance is an accurate method of measuring the changes in the oil film thickness but in order to do that in an accurate way it needs to be calibrated after every time the capacitance probe is relocated. The calibration of the capacitance is a simple and straightforward technique. The calibration is performed with the calibration screw attached onto the liner and with a dial gauge capable of measuring small displacements in microns.

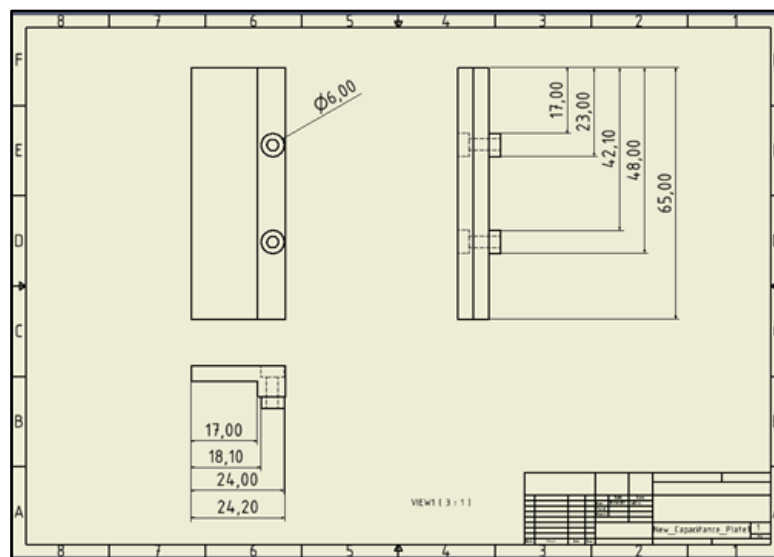


Figure 30 - Optical liner's capacitance plate drawing

The calibration screw is placed at the free end of the line and is capable of manually lifting the liner in small intervals. The dial is then placed under the capacitance plate and its scale is set to zero. Then the user lifts the liner at 2 μ m increments by using the calibration screw and

by monitoring the lift with the dial. The user must note the output voltage of the capacitance for every 2µm increments. This process is repeated eleven times to complete a set of calibration readings. Then each set is repeated five more times to successfully perform the calibration. After all the calibration data are collected the rest of the process according to Pyke (2000) is to derive a chart that will provide the equation from which the voltage can be converted into length. A sample calibration chart can be found in figure 31.

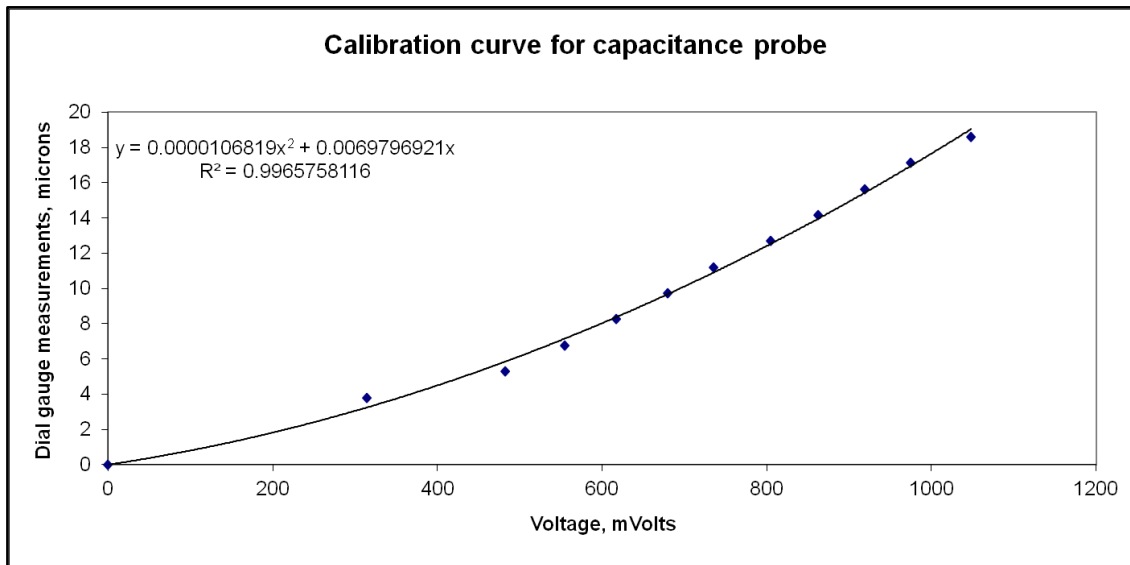


Figure 31 - Capacitance calibration sample chart and calibration equation

3.3 Cavity Formation

The cavities as shown in figure 32 will pass through 4 main stages in their life cycle. These stages are the following; generation and development of fern cavities, fern growth, fissure cavities and string or finger cavities. There is one more stage that is related to the point in time where the cavities have formed bubbles and are at the end of their lifecycle before they collapse, and which comes after the string cavities stage. In the first stage at generation the cavities are initiated and start to appear on the piston-ring surface. These cavities are related to sub-figures 'A' to 'H' in figure 32. After the cavities, have initiated they next pass in the fern growth stage. These are sub-figures 'I' to 'K' in figure 32. During that stage, the cavities grow in size up to the point where they will enter the next stage and develop fissure cavities. Sub-figures 'L' to 'N' in figure 32 show the schematic of fissure cavities as these appear in the piston-ring and cylinder liner interaction. Finally, the fissure cavities pass into the next stage and develop string or finger cavities which are the last stage before the cavities start reducing in size, form bubbles and finally collapse. The string cavities can be seen in figure 32 as the sub-figures 'O and 'P'.

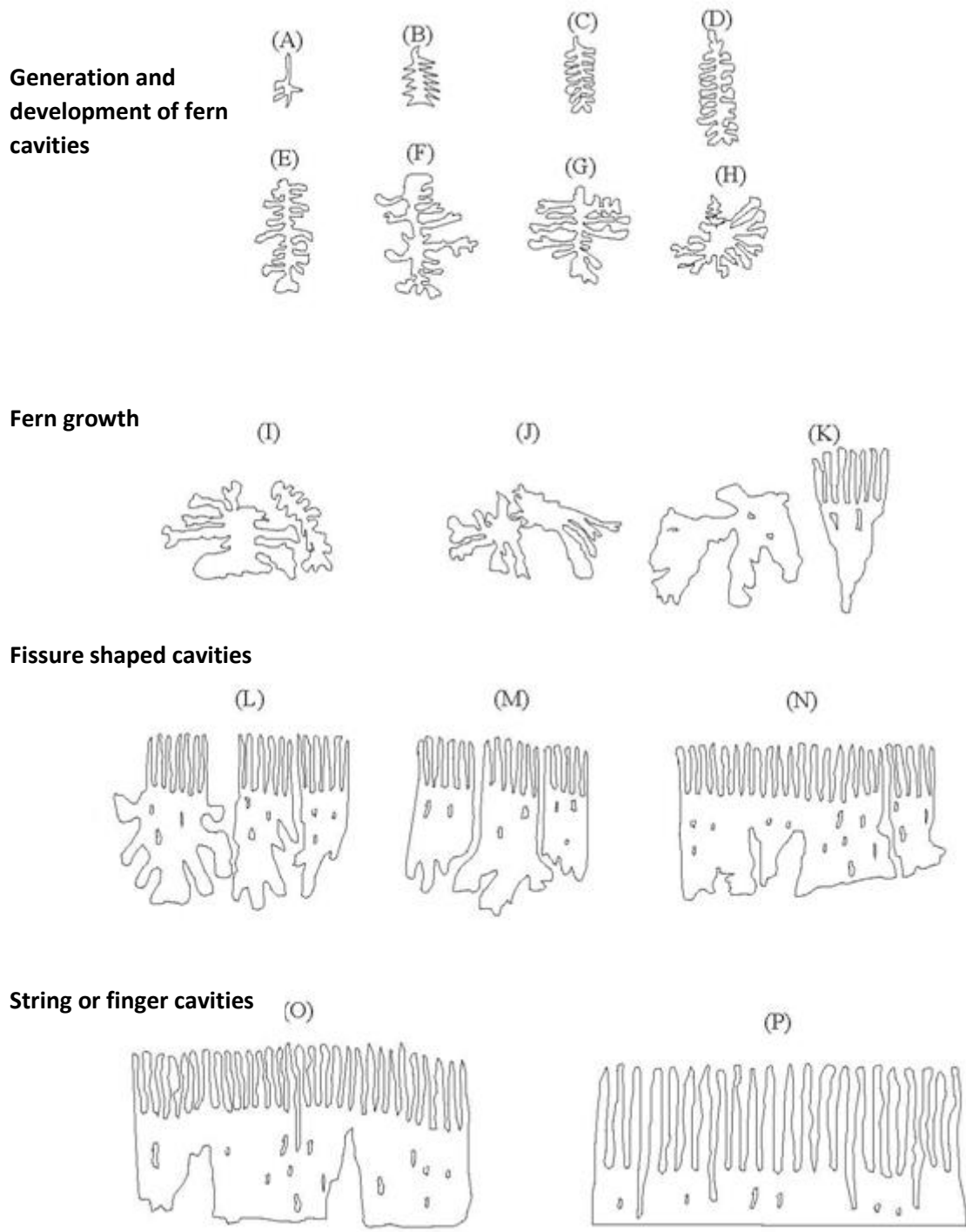


Figure 32 - Development of cavities as they appear on the surface on the ring (Dhunput, 2009)

3.4 Cleaning and Flushing Between the Test Runs

The lubrication test-rig has been used for the testing of the entire lubrication matrix. Each lubricant of the matrix has been run through the test-rig and then flushed before the next run. The correct flushing of each lubricant is important to the validity of the results. The

lubrication test-rig features a reservoir where the lubricant is initially stored before it is circulated by the pump. The lubricant flows through all the components of the test-rig before it finds its way on the piston-ring and liner interaction. Each time a test run finishes the old lubricant is flushed out of the system following a procedure set to eliminate the effect of lubricant contamination. The first step is to open the exit valve located on the return feed and the pump is then run until all the lubricant is let out of the system. Once the reservoir is empty the new sample is poured in and the system is run for 30 minutes. After the 30 minutes the exit valve is opened, and the lubricant is let to drain out of the system. The pump is then switched off and the liner is lifted to allow for access to the piston-ring surface. The contact surfaces are cleaned carefully with the use of a solvent and once they have been dried out the reservoir is filled once more with the sample to be tested. The test-rig is left to run once more for another 30 minutes. Finally, the exit valve is used once more, and the lubricant is flashed out of the system before the reservoir is filled again for one last time before the new test run begins. The process had to be repeated every time a new lubricant was tested on the test rig.

3.5 Piston-ring Profile

Piston-rings come at a range of shapes and profiles. The ring that equipped the lubrication test-rig features a curved profile and the high contact point is at an offset from its centre line. Piston-rings for automotive gasoline commercial engines are close to 2mm. The rings used on the lubrication test-rig is more than double this size at 5mm.

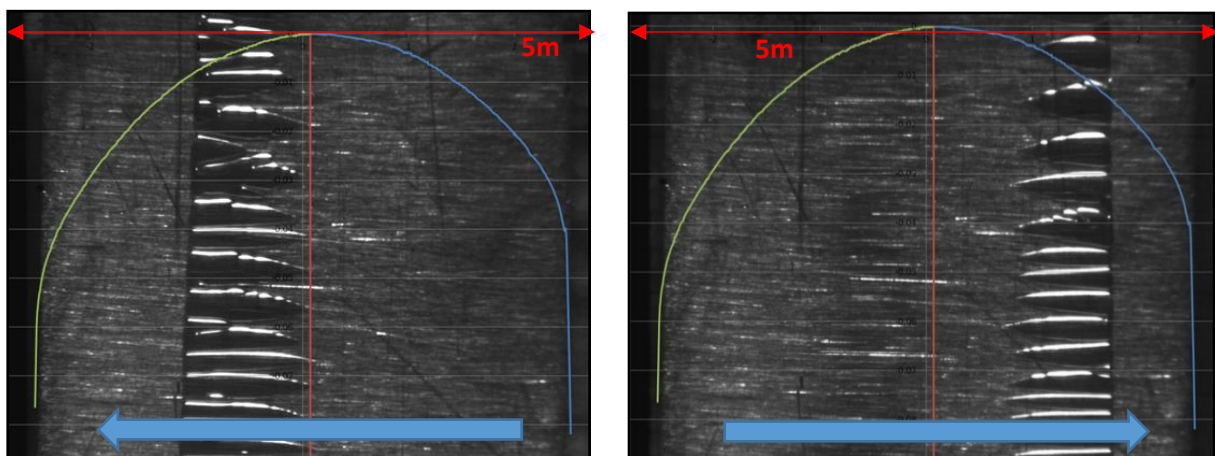


Figure 33 - Piston-ring Profile, Up-Stroke (Left) - Piston-ring Profile, Down-Stroke (Right)

Figure 33 shows the profile of the ring used on the test-rig. The images show the ring at both the up-stroke and the down-stroke while they have been enhanced with markers that draw the profile of the specimen along the face of the ring. The centre point of the ring is at an offset from its centreline and each of its sides follows a different profile, with one being steeper

than the other. This has a direct effect to the way lubricants cavitate on each of the sides as the pressure profile is highly depended on the profile of the ring.

3.6 Processing Software

The high volume of data captured during the testing made it impossible to manually process the results. The processing of the data has been performed with algorithms developed in Matlab and VBA, which allowed the translation of the images into quantified data. The algorithm was developed with the help of Dr Reyes-Aldasoro where the core of the software is based on his research on cavities occurring within capillary tubes. Matlab or else known as “the language of technical computing” is a high-level language and interactive environment for numerical computation, visualization and programming. Matlab is capable of analysing data, develop algorithms, create models and applications. Matlab can be used in a range of applications, including signal processing, communications, image and video processing, control systems, test and measurement, computational finance, and computational biology. The first step to the creation of the software was the set of certain thresholds that would specify the parameters which would be extracted out of the visual data. The physical properties that the final version of the software has been able to extract are measurements related to the following:

- a)** Width of Cavities
- b)** Length of Cavities
- c)** Area that the cavities cover
- d)** Number of cavities present

Some of the extracted values are shown in figure 34. The software extracts all the information by treating each picture as a separate matrix. Every image that is stored in a digital format is effectively a matrix with each cell containing a distinct colour value for each pixel on the screen. The matrix dimensions and contents vary depended on the resolution, colour and format of the images. While the software reads each matrix, it compares the data to a set of thresholds set to filter out unwanted information. Based on the observation that cavitating areas are recorded at a different contrast than the rest of the image the algorithm was developed on the principle of detecting those high intensity areas wherever they appeared onto the frame. Soon it was noted that the reflective properties of steel could pose a risk of misclassifying high reflective areas of the piston-ring as cavitating areas. Misclassification was rectified with the use of sophisticated filters and machine learning techniques that trained the algorithm into separating cavities from surrounding noise. After the filters were

successfully applied and all the unwanted information had been filtered out, the software could start recording and quantifying the useful information out of the raw data. In total the following metrics were captured:

- a) Relative area of cavitating region
- b) Length and width of the cavities
- c) Number of cavities.

When all the data have been extracted the software plots the results into graphs before it stores them into excel files for post processing. Even with the filters the image processing software could misread information and fine readjustment were needed for each individual sample. As a failsafe mechanism, the software would use the computer screen to give visual feedback to the user at real time. The feedback would include each image with additional markers over the areas where the algorithm was processing information.

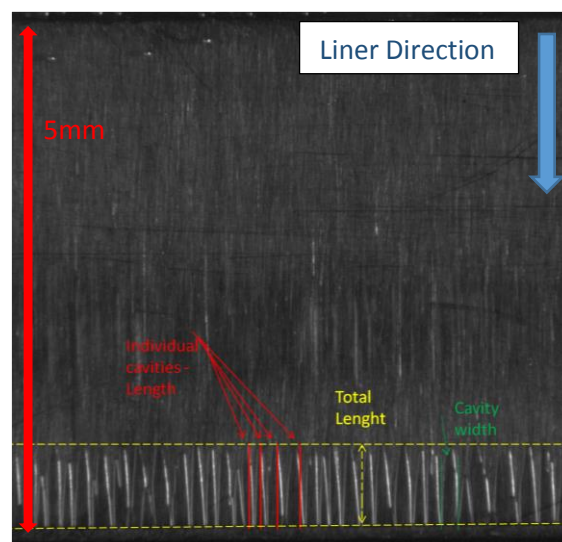


Figure 34 - Cavity width and Length, down-stroke

This gave the ability to the user to judge whether the software is processing the correct information or if the filters would need re-adjusting. Before ending the processing, the software saves the feedback in the form of a video for future reference. Figure 35 shows a snapshot of the feedback the software provides back to the user. The red cross markers indicate the individual cavities and the green markers indicate the cavitating areas. The software does not log all the marked areas as valid data, in figure 35 the software has detected two areas in the image that meet the software thresholds for cavitation. One on the top and one on the bottom of the image. In the image it is noticed that cavitation only takes place on the top of the image, but the visual feedback indicates that both areas are being logged. This

is mainly a representation as the software even though it is detecting two cavitating areas, one on the top and one on the bottom it will only log the top one where cavities exist.

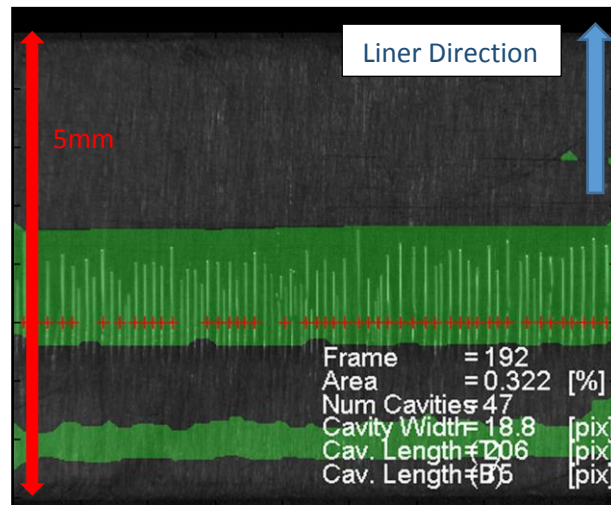


Figure 35 - Matlab image processing software

When the software runs it first identifies an area between the two cavitating regions that cavitation never takes place then splits each image into two parts and only logs data in the half that cavitation actually takes place while disregarding the other. When the software is triggered one of the first task it performs is to identify a centre line where cavitation never takes place and declares that as a non-cavitating region.

Below is a list with the individual steps the software needs to follow to process the visual data.

1. The number of the images is identified.
2. The software finds the area between the cavitating regions where cavitation never takes place and sets that as the centre line and as a non-cavitating area.
3. The software compares all the images and finds the shift and tilt between the images to accommodate for the vibrations and the movement of the ring.
4. The filters are applied. Unwanted data and the background are being discarded.
5. Software processes all the desired data and returns the feedback to the user.
6. Data are plotted on graphs and the values are stored in excel files.
7. The entire process is saved in a video file for future reference.

The project required more than one methods of extracting information out of the raw data. An additional algorithm was developed in Visual Basic and was used to calculate the area of cavitation in still images. The software can identify the circumferential area of the cavities and can calculate the total cavitating area as a percentage of the total ring area as this is

shown in figure 36. The main reason area is calculated as a percentage is due to the fact that the piston-rings and piston follow a circular profile. The approach of calculating the percentage has been classed as more reliable and valid for direct comparison between the different testing conditions. The vibrations caused by the engine operation have also caused for a slight shift between the capture images. The software will detect and adjust for that shift. The specific algorithm has been used for the area calculation in the “Temperature Effect” and “Speed effect” sections of this report.

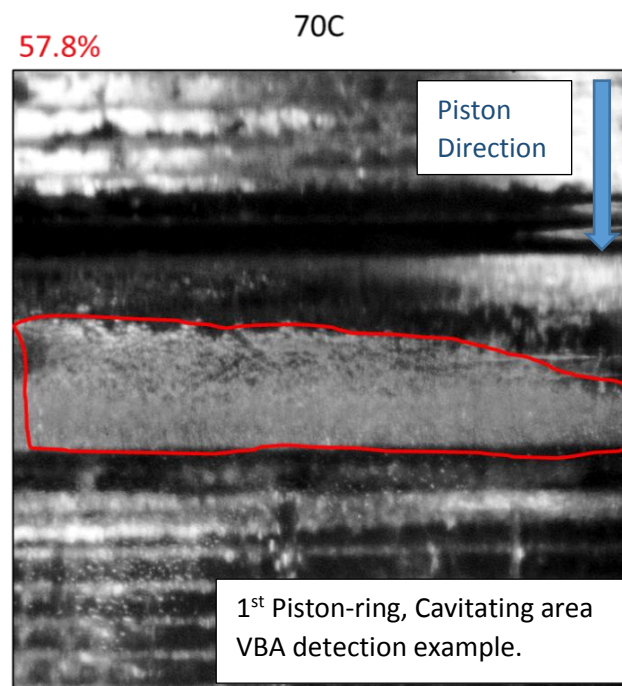
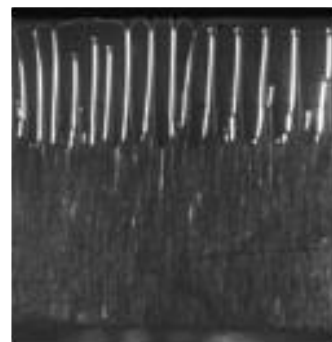
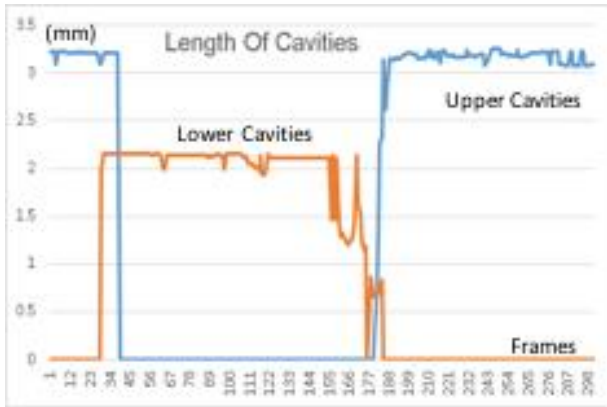


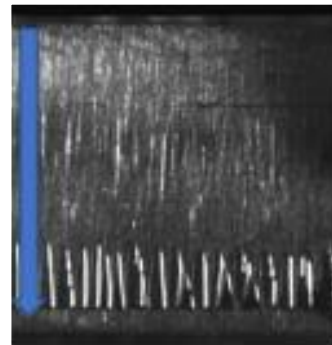
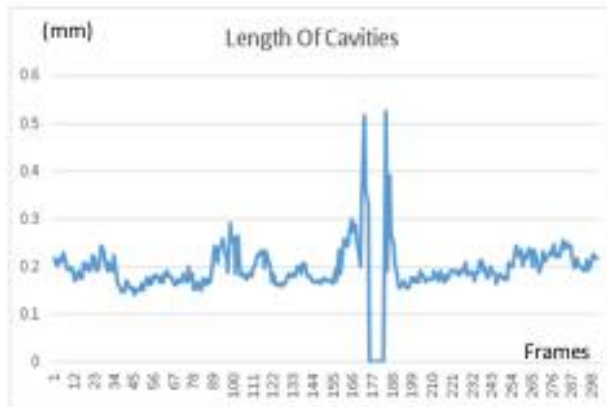
Figure 36 - Visual Basic algorithm, Cavitating area calculation example, 800RPM, 70C

The images in figure 37 and figure 38 show the correlation between the processing software and the physical properties of the cavitating lubricants. In total four main physical properties were extracted and these are the length of the cavities, the width of cavities, the number of cavities and the area covered. Each figure shows on the left the graphs plotted from the data that were extracted by the algorithm and on the right the raw data as these were captured by the high-speed imaging equipment. These images show the way that the software extracted all related properties. The individual frames are compared next to the plotted graphs to assist with the comparison. It is visible that the algorithm produced results that were very close to the actual values of the cavities.

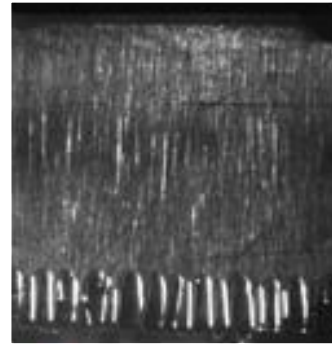
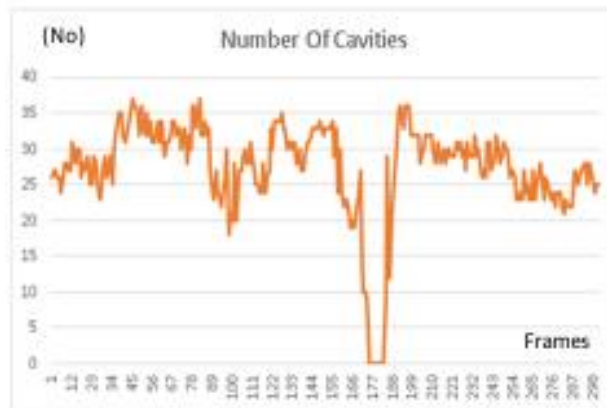


0 degrees

TDC

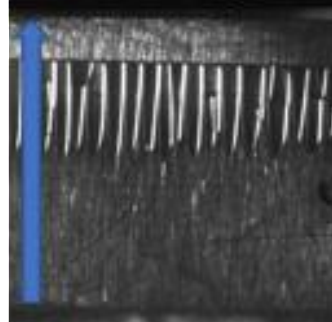
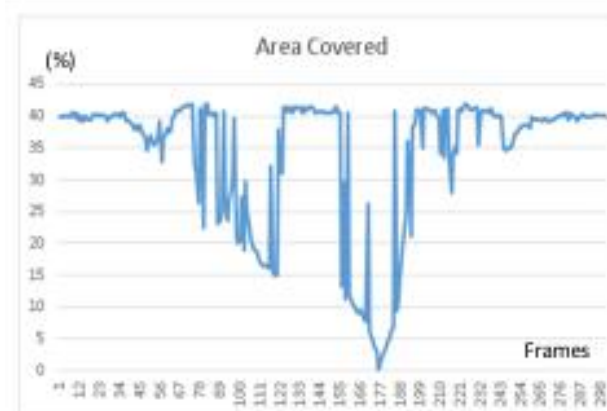


90 degrees

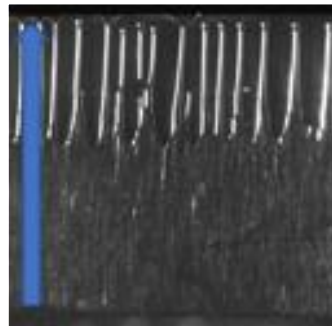


180 degrees

BDC



270 degrees



348 degrees

Figure 37 - Correlation between processing software and raw data, 600RPM, 70C, 0-180 Degrees

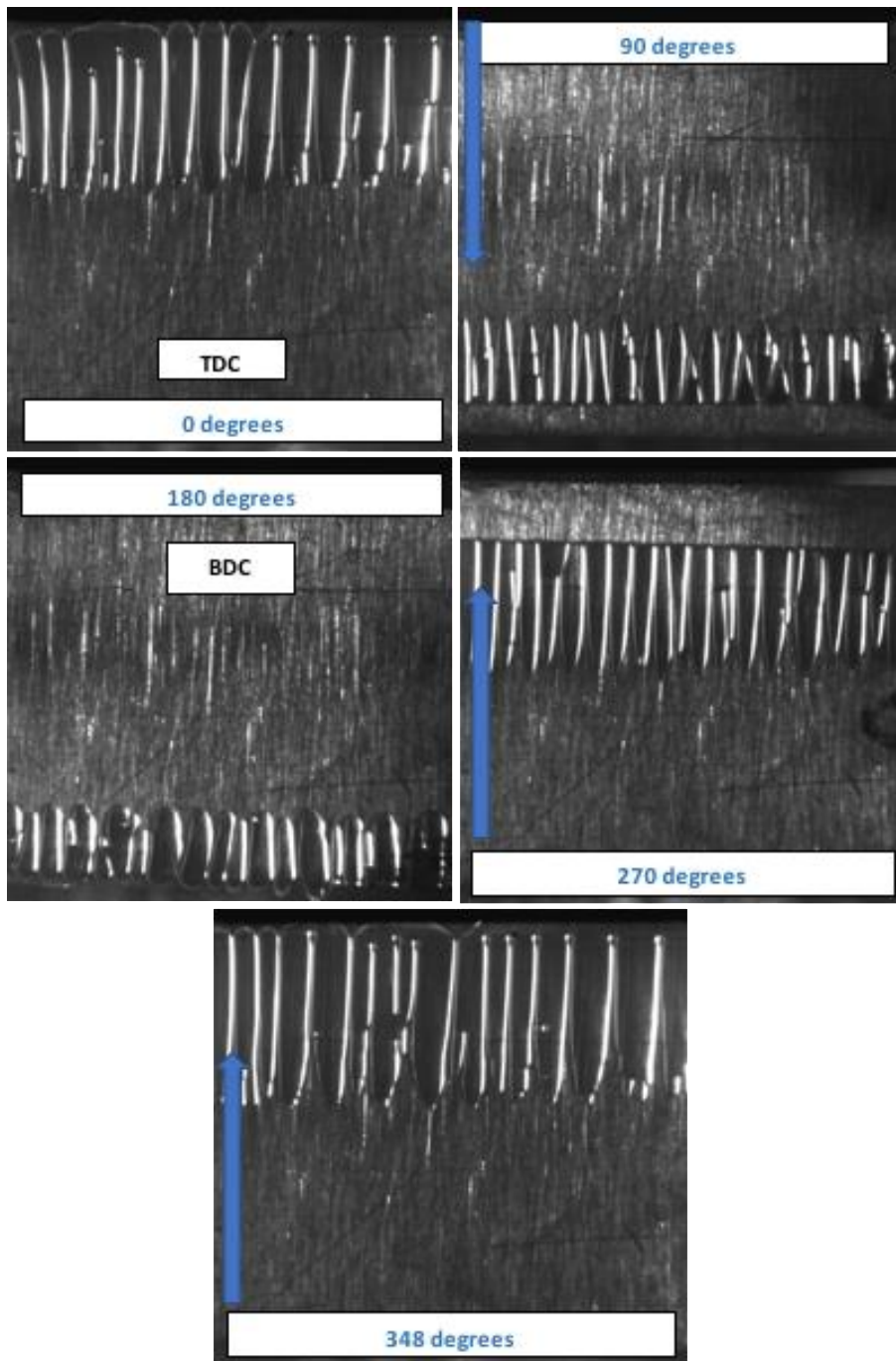


Figure 38 - Correlation between processing software and raw data, 600RPM, 70C, 270 & 348 Degrees

CHAPTER 4: OPTICAL ENGINE AND ENGINE DESIGN

4.1 Optical-Engine and Engine Design

To investigate the oil transportation mechanisms and to capture the phenomenon of cavitation as it develops on the cylinder walls, an optical engine had to be developed where a part of its cylinder would have to be replaced with an optical window which would allow for full optical access to the piston ring and cylinder liner interaction. The focus of the project has been the visualisation of the phenomenon of cavitation while this occurs in gasoline internal combustion engines. Conventional internal combustion engines do not feature an optical window for in-cylinder access ready “off the shelf” thus one had to be designed and manufacture.

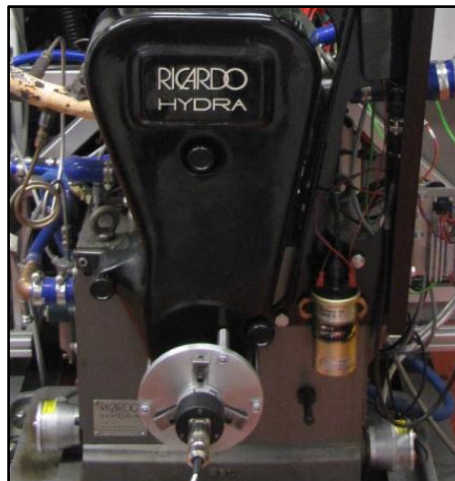


Figure 39 - Ricardo Hydra engine

The objective of the project is to study the phenomenon of cavitation that occurs in internal combustion engines between the piston-rings and the cylinder-liner interaction. It is believed that the phenomenon contributes to the transportation of oil into the combustion chamber which results in oil consumption and increased output emissions. Cavitation is dependent on pressure which means the effect of cavitation is also dependent on the speed, the load under which the engine operates and lubricant properties. It has been observed that the blow-by flow-rate of gasses in a cylinder can vary from zero to many litres per minute when the engine load increases. Transportation of oil occurs both in gasoline and diesel engines though this project focuses on the study of cavitation in gasoline engines under various operating conditions. Particular focus is given to the investigation of the effect that the engine speed and the fuel combustion have on the oil film formation and cavitation. The engine used for the testing is a Hydra model manufactured by Ricardo specifically for lab use, figure 39. This

type of engine can operate with gasoline, diesel or even bio-fuels while this particular model can be used as a port-injected or direct-injected engine. The engine used for the tests was a gasoline, spark ignition, port injected engine and the cylinder had a capacity of 450cc. The specific engine comes in two versions out of the factory, the low-pressure version and the high-pressure version. The current model is the high-pressure version that can withstand pressures of up to 160bar. This can be achieved with the use of a forged piston, a forged connection rod, a forged crankshaft and a forged set of inlet and outlet valves. The engine was also equipped with the optional thermocouple modified cylinder block which can perform a full thermal analysis with the use of thermocouples installed on the liner and the piston as shown in figure 40.



Figure 40 - Model of Thermocouples in Solid Cylinder Block (Ricardo, 2011)

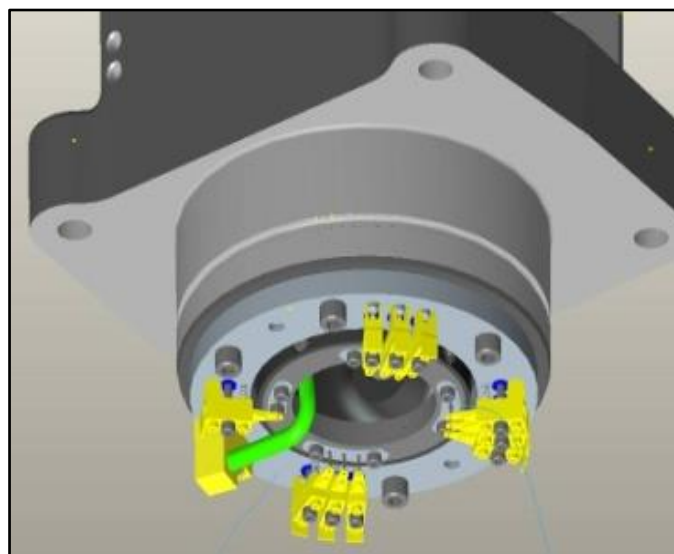


Figure 41 - Schematic of thermocouple locations on Hydra engines cylinder and piston (Ricardo, 2011)

However, this setup could not be utilised due to the malfunction of the acquisition unit which render the thermocouple system unreliable for use. Figure 41 illustrates the thermocouple setup as this was installed inside the engine cylinder block and the thermocouples installed on the piston itself. Due to the operation of the reciprocating engine and the way the piston moves inside the cylinder the thermocouples on the piston could only give point measurements every time the piston reached the BDC. On the contrary the thermocouples on the cylinder block offered real time readings and could provide a real time temperature distribution of the cylinder block. The possibility of obtaining real time temperature distribution readings from the cylinder block has been proposed later on in Chapter 6 of this report as a good topic for future studies. Cavitation is closely related to the variation of pressure and temperature within the engine and a map of the temperature and pressure distribution along the cylinder profile could give a better understanding of the cavitation distribution along the stroke of the engine. The engine has been coupled with an electric motor capable of rotating the engine at speeds of up to 3500RPM without the use of combustion. The dynamometer has been used to start, operate and put a load on the engine. Force-fed engines have seen a great rise in recent years due to the advantages they offer on efficiency and performance. Due to the fact that the engine was still in the early stages of its development the use of a force-feeding device was deemed unnecessary, thus no type of supercharger was used. The effect of turbocharging on cavitation is an area that could be investigated as a continuation of this project.

4.2 Relevant Previous Work

Optical-engines have been used by many researchers to investigate phenomena occurring inside the cylinder of an engine. While there are several different paths of visually accessing the combustion chamber the most common is by replacing a part of the cylinder with a transparent window made from Quartz or Sapphire. There have been cases where windows were manufactured out of Perspex, but its poor thermal properties do not allow testing under firing conditions. Regardless the material used for the windows it is important that optical engines are equipped with sufficient cooling to avoid unnecessary damage. The windows on optical engines often requires constant cleaning between the different runs as the combustion deposits tend to contaminate (fouling) the surface of the optical window and reduce its optical properties.

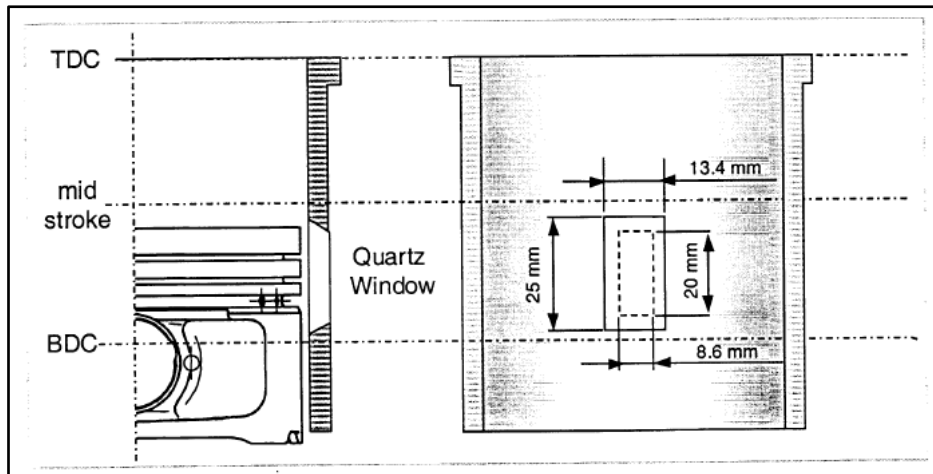


Figure 42 - Thirouard's Kubota diesel optical-engine

The average time before cleaning the window between the runs for a firing engine is usually 40 to 90 seconds, several techniques have been developed to increase the time intervals between the cleaning of the windows. Some of the most common techniques are the use of additives, the non-firing operation, the skip firing operation or the use of a leaner air/fuel mixtures. To design the engine, one of the first steps was to investigate past literature and the work performed by previous researchers. The study of previous projects presented valuable knowledge on difficulties faced and techniques used while it offered a solid background that could be used as a stepping stone. Unfortunately, the research at the time showed very limited literature and did not return many successful projects where part of the cylinder block was replaced by a window and a full metal ring pack was used to investigate cavitation.

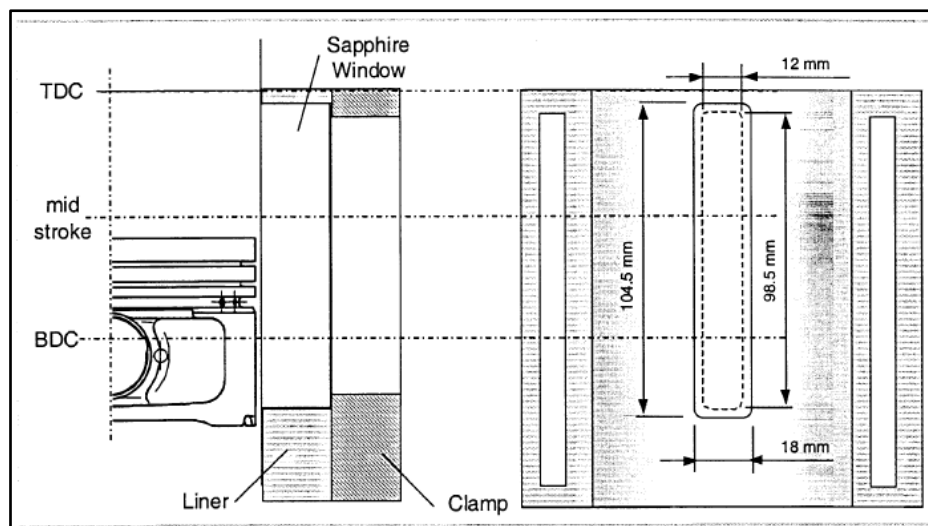


Figure 43 - Thirouard's Peugeot gasoline Peugeot XUL10Ar optical-engine

Thirouard in 2001 used two optical internal combustion engines to investigate the oil transportation mechanisms within an internal combustion engine. The engines used were a four-stroke Diesel and a four-stroke Gasoline engine. Both of these engines were modified by replacing parts of their cylinder with Quartz and Sapphire. The diesel engine was a Kubota manufactured EA300 model engine with a capacity of 300cc. This Kubota engine featured a single window between the mid-stroke and the BDC also illustrated in figure 42. The gasoline engine was a Peugeot manufactured XUL10Ar model engine with a capacity of 500cc. As shown in figure 43 the window extended through the full length of the stroke (Thirouard, B, 2001). It is evident that XUL10Ar optical engine is a better design than that of Kubota engine providing much more optical access, 12mm wide over the full stroke length against that of 8.6mmx20mm in Kubota engine. The Kubota window allowed for a better seal against pressure losses and a better alignment with the cylinder walls. Two main problems faced with these two particular designs was that each time the windows had to be cleaned the top part of the engine would have to be disassembled which increased dramatically the cleaning time between the runs. By having also, the windows inserted from the inside of the wall the windows faced the risk of getting sucked into the cylinder where even the smallest movement would cause the window to protrude within the cylinder where the window would “catch” it with catastrophic consequences for the engine. The main objective for designing the new optical engine is to provide maximum exposure to not only to lubricant flow but also optical access to the flow inside the combusting chamber when the engine is operating fully under motorised and firing conditions at different loads.

4.3 Cylinder Block and Window Design

The design of the cylinder block and of the windows went through various phases. The initial design was changed numerous times due to upcoming problems until it reached the final stage which was submitted for manufacture. Since the first design, it was clear that the area of the engine to be modified would have to be the entire cylinder block. It had to be modified in such a way that it would allow for optical access to the inside of the cylinder while maintaining its optical properties and structural integrity. The design also involved the identification of the material that would be the best fit for the optical window. The most common material used for optical engine applications is Perspex. Perspex is a transparent thermoplastic that is often used as an alternative to glass.

<u>MOHS HARDNESS SCALE</u>		
		Wax 0.2, Graphite 0.5-0.9
1	TALC	Soapstone 1, Lead 1.5, Tin 1.5-1.8, Alabaster 1.7
2	GYPSUM	Halite (Rock Salt) 2, Magnesium 2.0, Aluminum 2-2.4, Amber 2-2.5, Galena 2.5, Copper 2.5-3, Gold 2.5-3, Mica 2.8
3	CALCITE	Limestone 3, Boric Acid 3, Barite 3.3, Brass 3-4, Marble 3-4, Serpentine 3-4, Dolomite 3.5-4
4	FLUORITE	Bell Metal 4, Iron 4-5, Platinum 4.3, Soda (soft) Glass 4.5, Glass 4.8-6.6, Opal 4-6  Iron
5	APATITE	Asbestos 5, Manganese 5.0, Steel 5-5.5, Hornblende 5.5, Stainless Steel 5.5-6.3  Steel
6	ORTHOCLASE	Feldspar 6, Hematite 6, Magnetite 6, Pumice 6, Pyrite 6.3, Agate 6.5-7, Garnet 6.5-7.5
7	QUARTZ	Flint 7, Silicon 7.0, Tourmaline 7.3, Emery 7-9, Beryl 7.8  Quartz
8	TOPAZ	Case Hardened File Steel 7.8-8.5
9	CORUNDUM	Aluminum 9+, Chromium 9.0, Carborundum 9.3, Boron 9.5  Sapphire
10	DIAMOND	

Figure 44 - MOHS hardness scale

Perspex is strong, lightweight, cheap, easy to machine and features a very good optical clarity for visualisation. Perspex can transmit 92% of the visible light and has a reflective index of $n=1.490$. Even though Perspex offers better properties than most other plastics it has a melting point of 165°C . The relatively low melting point makes it unsuitable for use on a firing gasoline engine. The low melting point of plastics lead to the search of alternative materials that would have the strength, the thermal capacity and the visual clarity required for the application. Figure 44 shows the MOHS hardness scale for different materials. Two types of materials were found to match the experimental requirements, and these were Quartz and Sapphire. Quartz is a type of glass containing primary Silica and has a reflective index of $n=1.458$. Quartz or Fused Silica is manufactured by melting naturally occurring quartz crystals of high purity at approximately 2000°C , this process gives a glass of high purity and improved optical transition. Sapphire is the product of alumina powder processed using flame fusion, a process also known as Bernoulli process, Sapphire has a reflective index of $n=1.762$. Bernoulli process is the first commercially successful method used to manufacture synthetic gemstones. Sapphire has exceptional optical clarity, hardness and thermal capacity, it scores a nine out of ten on the MOHS hardness scale which makes it the second hardest mineral after the Diamond. Both Quartz and Sapphire are available in either synthetic or natural forms. The fabricated versions of the materials are relatively cheaper compared to

their naturally extracted versions but due to their increased hardness are very difficult to machine and that makes them very expensive to order in custom dimensions.

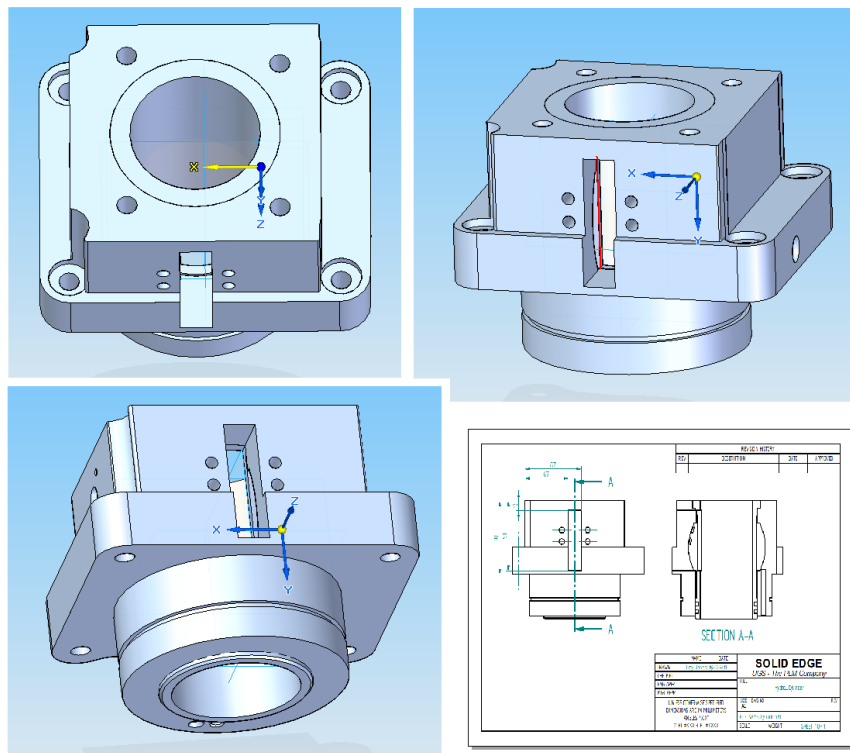


Figure 45 - First design iteration of the cylinder block assembly

The final decision was made to proceed with Quartz, its excellent optical clarity and physical properties made it an ideal material for use in an optical-engine. Another factor that led to the use of Quartz instead of Sapphire was the purchasing cost. Sapphire comes at a cost of three times the amount of Quartz and with the possibility that the engine would use several of them during the project (due to the damage to the window especially under high load and firing conditions) then the Quartz was deemed to be a more viable solution. After the material for the windows was chosen, the cylinder had to be modified in a way that it would accommodate the windows in a manner that the engine's basic operation principles remained unchanged.

The first approach was to modify the standard engine block that was received with the engine. Figure 45 shows the first design of the cylinder block which involved the machining of material out of the stock block and the insertion of a rectangular optical window that would extend from the face of the cylinder block to the face of the liner. Though the original cylinder block is made from cast iron which makes it very durable and easy to machine, there was a challenge to be faced. The cooling system of the cylinder block was located around the

iteration of the engine block design. The next design tried to solve both the leakage and the thrust and anti-thrust problems but introducing some additional features.

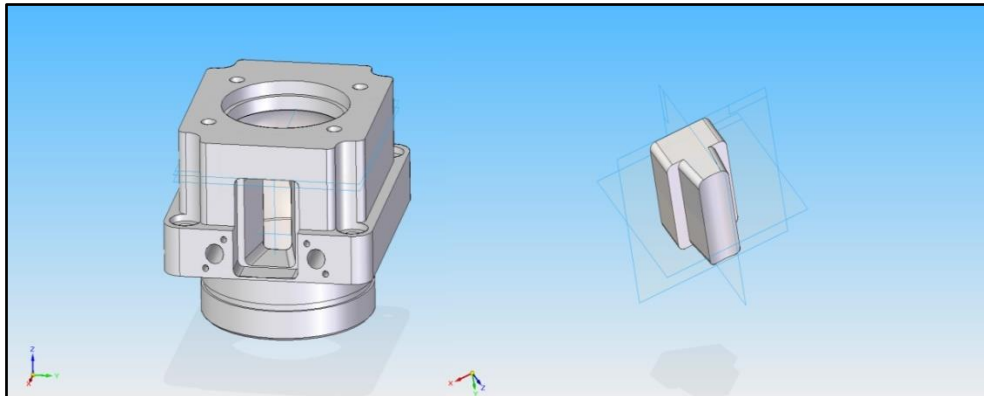


Figure 47 - Ricardo Hydra optical-engine 3D design

The next design, as shown in figure 46, offered a distinct difference when compared with the first engine design and more specifically where the first design was rectangular this next design has tapered edges. These edges would allow for a greater mating surface between the window and the cylinder block which would offer a better seal. This design would use wider windows that would offer a step around the middle of their length which would ensure that the window is inserted at the right depth and that it would not protrude inside the cylinder. The problem of the thrust and anti-thrust side was solved after the 4 mounting holes of the cylinder block were measured. It was identified that all the holes were equidistant from the centre except one. Considering the difficulty of modifying both sides of the cylinder block and the cost of the windows the idea was derived to modify two of the mounting holes which would then allow for the 180-degree rotation of the cylinder block. This solution meant that by having the optical window on one side and allowing the cylinder block to be mounted at a 180-degree rotation, both the thrust and anti-thrust sides can be investigated by installation of only one window. This design though came with its own problems. The first and most important problem was the manufacture of such a window would be very difficult. Quartz is a very hard material and very difficult to manufacture, the manufactures found it very difficult to achieve the required tolerances on the chamfered edges which meant that the design discrepancies between windows would have been that great that even if one window would have fitted in the cylinder block the other ones would not, without any major leads or protruding within the cylinder. Though this being another failed design it gave the foundation to generate the ideas used on the final version of the cylinder block. In brief, the key points that were identified were that there was no need any more for two windows on the cylinder

window was rejected is the difficulty that the window manufacturers would face to manufacture both angled sides at the same specifications.

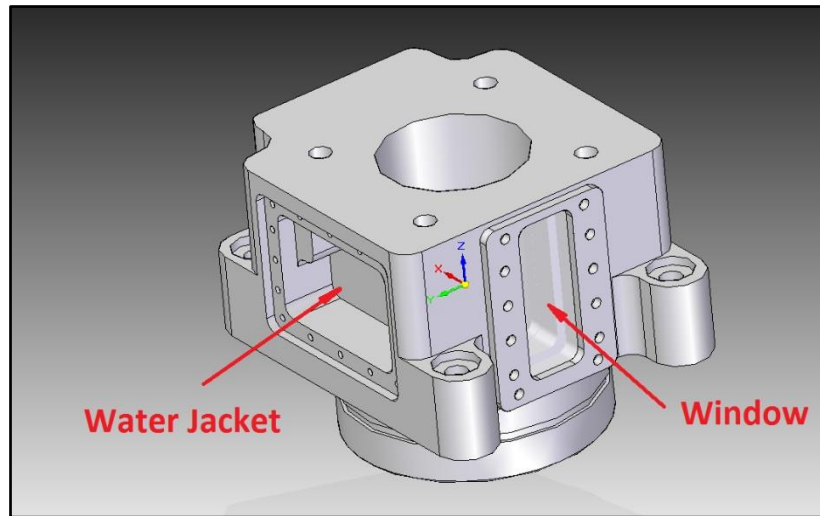


Figure 49 - Ricardo Hydra optical-engine 3D final design

At the later stages of the engine design and after a lot of iterations it was clear that the only way to optically modify the engine without compromising the integrity of the results would be to manufacture a new cylinder block. The new cylinder block like the original one would require an effective cooling system; in this design the outlets of the coolant has been diverted from the windows location and are now located on either side of the cylinder block as shown in figure 47. The use of two optical windows was also considered to be high risk for leakages and as mentioned earlier on, it was rejected as an idea. The final design was based on the use of a single window and the manufacture of the new cylinder block which allowed the use of that window for both the thrust and anti-thrust sides. The next design featured a straight cut window as this is shown in figure 48. Being easier to manufacture the straight cut window would eliminate the inconsistency problem between the different windows. After a lot of close communication with the window supplier, the window design was simplified enough for the manufacturer to be able to reach the required tolerances. The final window compared with the initial designs featured parallel surfaces and 90 degrees angles, these features are much easier to manufactured which ensured a better consistency between the windows. Experience with other types of internal combustion engine showed that these types of engines are affected by a common problem of widow fouling. This problem is the cleaning of the windows after every run due to the combustion residuals that stick on their surface and that affect their optical properties. These time intervals usually range from 30 seconds to 2 minutes. This indicated that the windows would have to be removed and cleaned regularly

which also meant that the windows could not be glued inside the cylinder block. To open the cylinder head for cleaning the window was not an option as this operation was very time consuming and required more than one person to perform. For that reason, a mechanism was manufactured, and a methodology established which would allow for the safe removal of the windows. This mechanism should also allow for the reassembly of the windows with the cylinder block while ensuring that there would be no pressure losses, damage to the window or the windows protruding into the cylinder.

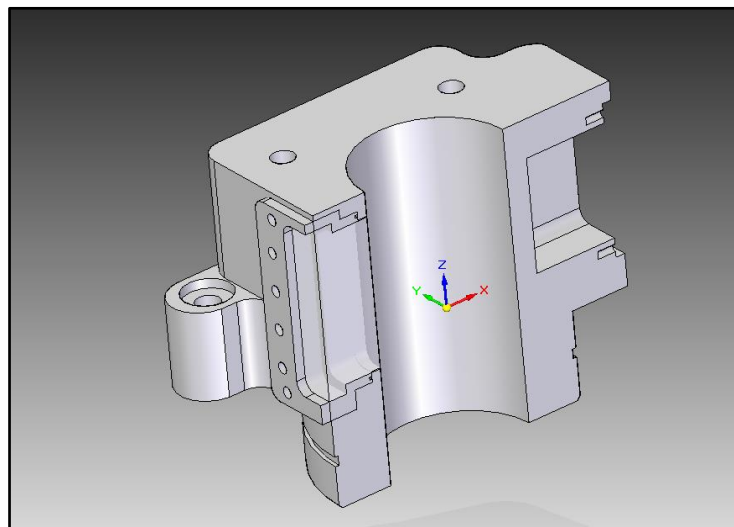


Figure 50 - Ricardo Hydra optical-engine 3D final design cut-out

Furthermore, an engine with such a limited operation cannot produce enough heat from the combusting fuel capable of causing sufficient damage to the windows. The main parameter that would affect the integrity of the window would be the high pressure and the possibility of the piston rings “catching” the edges of the windows. On the basis that the engine would only operate for short intervals, it was decided that the water jacket of the original engine could be substituted by a smaller and simpler design. The new cylinder block in figures 49 and 50 was machined from a single piece of cast iron, the same figure shows the individual water pockets located on the three sides of the block, opposite and next to the window slot. The new cylinder-liner instead of being pressed into the cylinder block, it was bored out of the block. Once the cylinder block was machined and the cylinder itself was bored at the required diameter, the surface of the cylinder was treated to reach the same surface roughness as the original cylinder block of the Ricardo Hydra engine. The final design as described above instead of a water jacket features three water pockets located on the sides of the cylinder block that are responsible for cooling the cylinder block while in operation or warm it up

before every run up. One of the water pockets can be seen in figure 50 on the opposite side of the window. The windows chamfered edges were removed and the new windows featured straight cuts, at the same time the thickness of the new window was reduced by twenty millimetres (20mm) shorter than the one initially proposed.

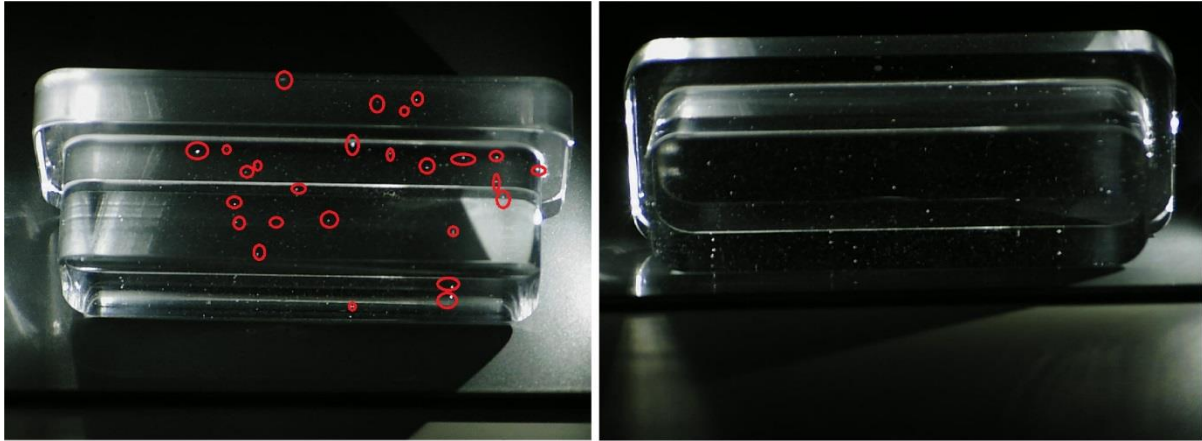


Figure 51 - Window imperfections in the first batch of optical windows

This significant reduction could be achieved as the new cylinder block did not feature a full water jacket and therefore the side where the window was fitted could be made 20mm thinner than the original hydra. The thinner windows has the great advantage of producing much better images with higher clarity/resolution since the transmitting and scattering lights needs to travel a smaller distance. The shorter window also means that the camera could be

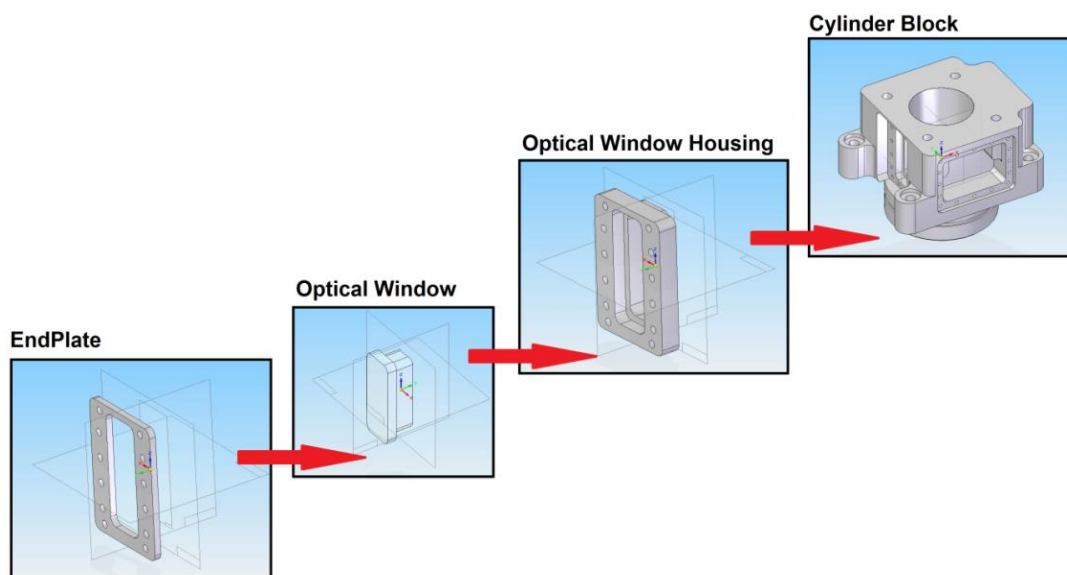


Figure 52 - Ricardo Hydra optical-engine new cylinder block assembly

mounted at a closed distance to the piston rings which with the right extension camera tubes would give a much higher magnification. The shorter window will also offer better access for the light, this is mainly due to the fact that the camera must be placed directly in front of the window. Since the camera occupies the space in front of the windows the light sources need to be mounted at an offset and would normally aim the specimen at an angle. Thus the shorter the window the smaller the angle between the window center line and the light source. Once the final design was submitted there was a constant communication with the manufacturer to make sure the windows were manufactured up to the correct specifications. Once the final products were received these were measured and checked to identify if they met the required specifications. It was quickly realised that despite the best efforts the window tolerances were not within the expectations and this was not the biggest issue. Upon inspecting the windows under light in a dark room it was found that the quality of the windows was not as expected either. It was found that the volume of the windows was not consistent and that there were air bubbles trapped in them. Figure 51 show an example of the first windows received showing the impurities in its mass. Artificial Quartz needs to follow a very slow heating process where the windows are heated at a very high temperature for several days until all the bubble initially trapped during manufacture slowly escape. It was obvious that the manufacturer had not followed the correct procedure which left air bubbles still trapped within the quartz. The windows were classed as unsuitable for use or visualisation but they were still retained to use during the initial engine test runs. The main issue with the air bubbles trapped in the windows was that the air bubbles would obstruct the view of the camera and would affect the clarity of the images.

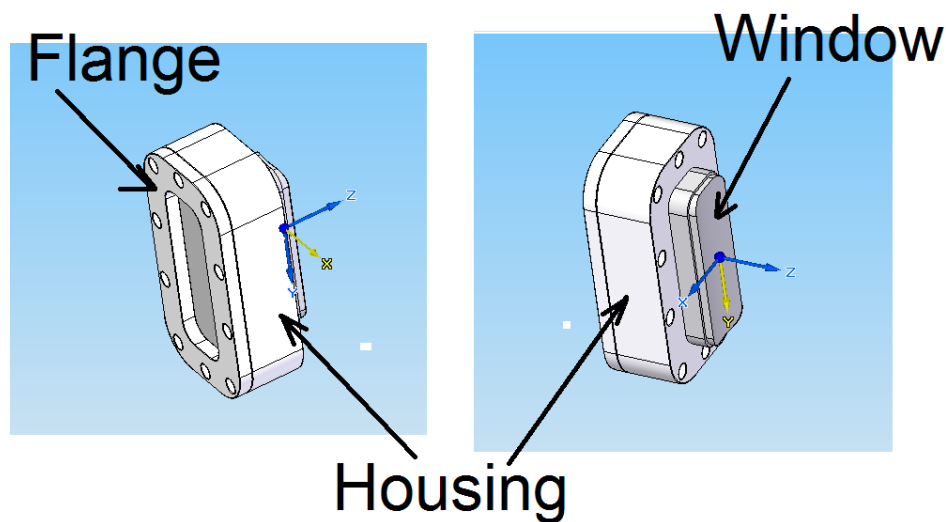


Figure 53 - Window, window housing and flange assembly

The findings were presented to the supplier and a new set of replacement windows were sent. The new windows were tested and found to be of an excellent optical quality but their dimensions were still not consistent with the tolerances that were initially specified. Since the manufacturer could not achieve better tolerances the solution was given with the use of custom window housings. The window inconsistencies were a major concern since the initial stages of the project. Quartz is a very hard material which makes it very difficult to manufacture. For that reason the manufacturing tolerances that could be achieved were not ideal. The minor dimensional differences between the different windows can be eliminated with the use of custom made housings. Figures 52 and 53 show examples of those housings along with the way that the windows were secured inside and how those fit onto the cylinder block. Steel is an easier material to machine than quartz, for that reason better tolerances can be achieved in machining steel than Quartz. These housings would be machined internally to fit each of the individual windows which would accommodate for the window inconsistencies and on the outer side they could be made at a very tight tolerance to fit the cylinder block ensuring no leaks occurred. Since the optical window housings are custom made for each window that meant that the windows could be glued onto the housings which would give an extra security against the leaks. The mating of the cylinder with the Quartz was a major issue with the design of the engine, the custom housings though allowed for an excellent fit. The windows were glued within their housings and they were machined again with the cylinder block once they were all assembled together ensuring perfect mating of the window, the housing and the cylinder. The housings also feature a very important step which prevented the window from sliding into the cylinder while it could be easily removed and installed for cleaning between the runs. The housings on the four corners featured 4 additional holes made for the window extractor. The window extractor ensured that the windows were removed evenly and securely without distorting the window channel and also assisted with the refitting of the window to avoid damaging them while they are placed back in. It is known from literature that when internal combustion engines are in operation the piston-rings located on the piston have the tendency to rotate inside their grooves. It is believed that the rotation of the piston can affect the visualisation of the lubricant flow as it can drag the lubricant at a circular path in the direction of movement. In order to prevent the rotation of the piston-rings, these could be pinned inside their grooves. The technique behind pinning the piston rings is illustrated in figure 54. The pinning of the rings had been considered at the early stages of the design phase but the final engine did not have the piston-rings pinned. This could be added at a later stage if ring rotation was proven to be an issue.



Figure 54 - Ricardo Hydra optical-engine piston-ring modification (Ricardo, 2011)

One of the core objectives of this project was the use of as many of the engine components in their original form as possible in an attempt to produce results that would be as close as possible to the operation of an unmodified engine. There are many piston-rings commercially available and each is suitable for a variety of different applications. Finally it was decided to use the ring setup that was supplied originally with the Hydra engine. The chosen setup is shown in figure 55 with the following details:

1. **Compression Ring:** Internal Beveled with Negative Twist
2. **Midle Ring:** Rectangular Ring
3. **Oil Control Ring:** Spring Loaded

The cylinder block started as a solid block of steel and the manufacturing was completed in house, the manufacturing started by first machining the lower part of the cylinder which fits inside the engine block. The lower part was machined to the exact the same specification as the original hydra block, before continuing with the manufacturing, the O-ring groves were cut on the lower part and the block was fitted onto the engine sump. Once proper fitting was ensured the mounting holes were drilled and ensured they were in line with the mounting holes of the engine block.

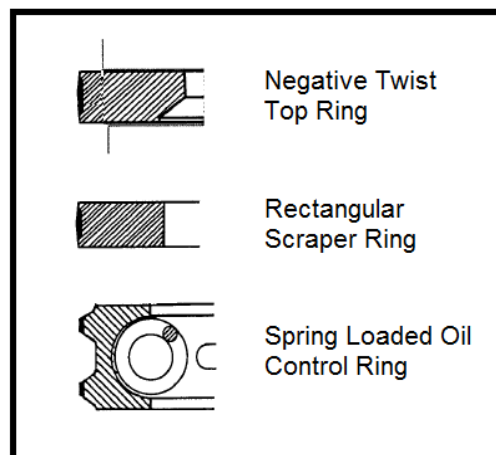


Figure 55 - Ricardo Hydra optical-engine piston-ring setup (Ricardo, 2011)

The next step was to cut the water jackets and test their seal by circulating water through them, once the water jackets were manufactured the next step was to hone out the cylinder itself. The cylinder was drilled in steps, the drilling starting in the centre of the block and the hole was slowly widened. This ensured no distortions were introduced in the block while machining. Once the cylinder reached close to its final diameter a special honing tool was used to smoothen out and treat the cylinder at the desired roughness. The cylinder was made at the exact same specifications as the original cylinder block supplied with the engine by Ricardo. The final step was to cut out the window channel and ensure all housings were a perfect fit. Initially the window channels were scheduled to be manufactured before boring out the cylinder as their machining could possibly affect the cylinder itself. The main reason the cylinder was bored before the window channel was because every window and window housing once they were placed onto the cylinder block they were re-honed to ensure perfect fitting. Following the cylinder block the windows were ordered through a manufacturer at the United States which could provide optical quality quartz windows at the required specifications. Figure 56 shows the tool used for the initial machining of the cylinder and the cylinder block at an intermediary stage. In this figure, it is observed that the cylinder has already been honed where the window slot is still to be machined. Figure 57 shows the finished window and the cylinder block along with the window and housing right before these were fitted onto the engine for the first time. The same figures clearly show the cylinder block with the window slot, the water pockets, the cylinder block mounting holes as well as the cylinder head mounting holes.



Figure 56 - Ricardo Hydra optical-engine manufactured parts



Figure 57 - Side and top view of the cylinder block and optical window assembly

4.4 Engine Control Software

The engine control unit, or ECU is responsible for controlling the smooth and correct operation of an engine. In the case of the optical engine and due to the custom design, the engine control had to be designed and manufactured for the project as there were no off the shelf solutions available that would match the project specification. The control of the engine was based on two National Instruments PCI cards that were installed on a lab desktop computer. This setup offered one acquisition and one processing cards. The acquisition card could only acquire and read signals that came from the sensors while the processing card was capable of receiving, processing and sending signals back to the engine. The computer would use the cards to acquire and send signals from and to the engine and to all the auxiliary components. The signal processing on the computer was possible with the use of LabView. LabView is a software supplied by National Instruments and is designed to work with the supplied cards. Figure 58 show the 3 pieces of software that had to be designed for the needs of the engine. All the 3 different circuits are part of the same control software and they are responsible for crucial functions of the engine such are firing and injection. The engine software was taking input from two main sensors, the crank shaft encoder and the cam shaft encoder. Both of these encoders were responsible for sending signals that would give information of crank angle and to whether the engine is exhausting or intaking. The signal from the encoders was collected by the two cards. The signals were then processed, and new signals were send back to the engine. One of the signals was sent to the ignition control unit, the ignition control unit was responsible of receiving the 5V pulse generated by the NI card and activating the ignition driver responsible of sending the charge to the spark plug. The next signal was send to the throttle control unit, the throttle control unit was a

servomechanism that controls the butterfly valve in the inlet manifold which restricts the flow of air in the engine. One more signal was sent to the injector driver, the job of the injector driver was to receive the 5V signal and operate the fuel injector. The injector driver works in two stages, the first stage is to send high voltage to the injector to ensure the injector open instantaneously but then immediately drops the voltage to ensure the circuit is not damaged. Usually injectors require a much higher voltage to open than to stay open.

There were three signals mainly required by the engine to operate but the software was designed to send out another two additional signals that would control the optical equipment. One of the additional signals was used to trigger the high-speed camera at a specific crank angle and the second to drop the intensity of the light source right after the camera would stop recording. The high-speed cameras are equipped with a limited internal memory that is usually enough for a few seconds of continuous recording. The correct timing of the camera with the engine has been crucial to the acquisition of the data. High speed cameras require a lot of light as they operate at very high shutter speeds, the light though used are so powerful that could set the engine on fire. It was important that once the camera started recording there was a way to drop the light intensity to the minimum setting in order to avoid damaging the engine components.

In addition to the signals responsible for the operation of the engine and the acquisition of the data the software provided a range of information to the user. This information which was crucial for the operation of the engine ranged from the engine speed to the load. The user had also the option to switch on and off any of the signals mentioned above and were related to the operation of the engine. All the signals were adjustable and could be set at an offset from the top dead centre (TDC). The in-cylinder pressure was monitored at a separate monitor and did not go through the NI cards. The computer as well as the engine were connected on a central control unit which was responsible of cutting the power and switching off the equipment in case the computer would crash. This was mainly designed in order to avoid the computer leaving the injector open while the sparkplug was firing in the event of a computer failure. The control unit had also a manual override where the user could activate on demand. The engine lab was protected against fire by a carbon dioxide fire suppressant mechanism which operated on a separate circuit for safety reasons.

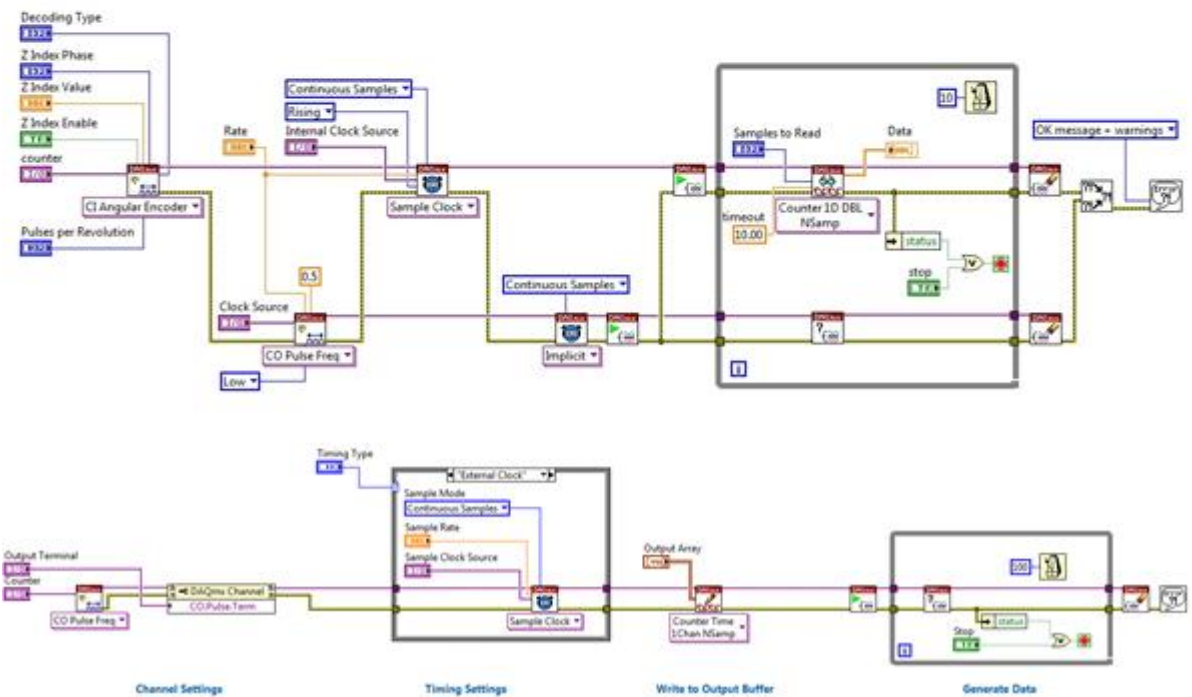
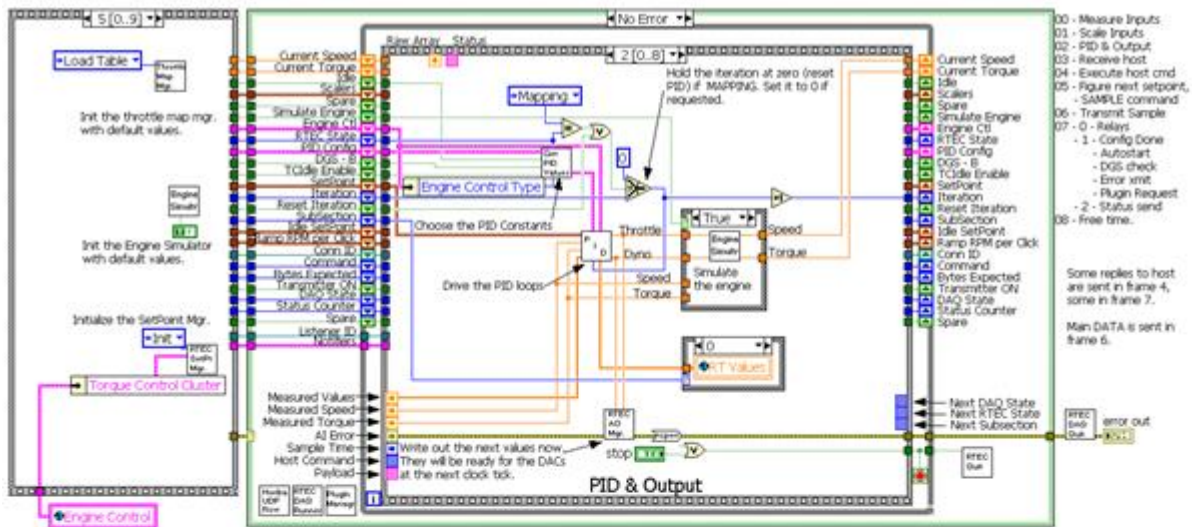


Figure 58 - Engine control and acquisition software

4.5 Testing

The aim of the project has been to visualise the flow of the lubricant on the cylinder walls of an internal combustion engine using Mie-scattering technique. The visualisation was performed with the use of a high-speed camera and appropriate lighting. The camera would be placed on the thrust side of the engine and would capture images under motorised and firing conditions. The images were captured with Photron Fastcam SA1.1 camera. Photron is a high-speed camera manufacturer that has managed to become a household name mainly due to the innovative and technologically advanced solutions they offer, one of their products can

be seen in figure 59. The SA1.1 has a 12-bit dynamic range with shutter speed down to 1 μ s. It provides 5,400 fps for the full resolution of 1024x1024 pixels, but the faster frame rate can be achieved for smaller resolution, eg, a frame rate of 67,500 fps for a resolution of 256x256 pixels. The engine was initially tested under motorised operation. That means that the engine was not fired during any cycle and it operated with the use of an electric motor connected onto the engines crank shaft. Optical-engines are very hard to manufacture and before they operate for the first time they need to be tested and carefully inspected. Any faults that might have slipped the design phase would normally surface in motorised testing. The motorised testing offers a safe way of assessing the engine's capabilities. The significantly lower operating pressure and temperature will protect the engine from getting severely damaged. If the engine was initially tested under firing operation the possibility of engine damage or failure beyond repair would be much higher. Once the engine has been rigorously tested and finely tuned the next step was to continue testing under skip-firing operation. Skip-firing operation is when the fuel is not ignited in every cycle and the engine still requires the electric motor to operate. Skip firing operation is useful to identify and further assess the limits of the engine. The tests started by skipping four cycles for every one that fired and that continued until the engine reached fully firing operation. Similar path has been followed to bring the engine at its maximum operational speed.



Figure 59 - Photron Fastcam SA1-1 high speed camera (Photron, 2015)

The use of high speed cameras for the visualisation of a lubricant's flow requires high-intensity light-sources to capture the changes in the fluid flow. All the sources of lighting used came from the high-power line of ARRI. The lights used are similar to the ones installed in football stadiums and arenas. Due to their use in stadiums and theatres these lights offer a very wide focal point. Since the window was only a few centimetres wide the light would have to be coupled with focussing lenses which could assist with the guidance of the light onto the point of interest. More precisely the light sources used were coupled with either one or two focusing lenses and along with the light source were fixed on an adjustable rail. The

adjustable rail allowed for the correct alignment of the light with the lenses and offered the freedom to adjust the distance between the two lenses and the light source. The entire assembly was mounted onto a lathe bed weighting 350kg to ensure stability.

The installation of an optical rail was also investigated, designed and manufactured for the future use of lasers and laser illuminating techniques. The lasers allow for the implementation of the Laser Induced Fluorescence (LIF) and Particle Image Velocimetry (PIV) techniques. The former can be in order to quantify the oil film thickness and therefore the amount of lubricant present on the cylinder-liner, and the latter can be used to measure the instantaneous lubricant velocity between the ring and liner gap.

4.6 Summary

Overall the design of the optical engine was a success and provided the means to fulfil the objectives of the project, the investigation of the phenomenon of cavitation within a fully firing optical-engine, and beyond. An optical engine that was designed and manufactured specifically for the needs of the project. The new design provides full access to the very hostile area where the piston-ring and the cylinder-liner interact with each other and in addition a good exposure to the combustion chamber where the charged motion, spray characteristics and combustion can be visualised or quantified using different optical diagnostics. The design process was very careful and time-consuming to ensure the new custom optical engine can stand extreme forces, temperatures and pressures and at the same time to allow for the thermal expansion and tolerances; specific considerations have been given to ensure proper matting of the optical window with the cylinder liner and the piston rings. The entire control system to operate the engine has been redesigned with new software and the ECU (as explained above) capable of controlling both the operation of the engine as well as the optical equipment that were later installed. The combined new control system and the optical engine would offer a useful and valuable testing device that would allow further investigation to be carried out.

Introduction of the optical window that covers the full length of the liner over a width of 25mm provide a great optical access, much greater than that given by XUL10Ar engine. This allow not only the investigation of lubricants cavitation and flow into the contact point over the entire length of the liner, but also provide access to combustion chamber to allow flow visualisation and flow field measurements using different laser based optical diagnostics like LDV, PIV, PDA and LIF.

CHAPTER 5: RESULTS AND DISCUSSION

This chapter includes the results for both the test-rig and the optical engine in two different sections. The results for both experimental devices are presented, analysed and discussed independently within this chapter. Furthermore, there has been an attempt to establish a correlation between the optical engine and the lubrication test rig.

5.1 Lubrication Test-Rig

The test-rig used for the parametric study can simulate the lubricating conditions between the piston-ring and the cylinder-liner which occur in a reciprocating engine in an idealised manner. An internal combustion engine operates on the basic principle of a reciprocating piston moving inside a sealed chamber that converts the energy released by the combusting fuel into kinetic energy. The test-rig operates on the same principle with the difference that the ring is stationary, and the liner reciprocates on top of it. One of the main advantages of this rig is its simple assembly which provides full optical access to the piston-ring and the cylinder-liner interaction. It is a fast way of testing different lubricants without the interference of parameters and phenomena that usually occur inside an engine.

In total nineteen lubricants were tested, all the lubricants featured different formulations. The formulations were specified and supplied by BP and they were kept confidential, relative information can be found in table 1. Each lubricant was tested at three different speeds; 100RPM, 300RPM and 600RPM. These speeds were chosen according to the testing capabilities of the test-rig and they are proportional to the speeds of an automotive engine. The first speed at 100RPM was chosen to simulate engine speeds close to idle. Idle is the state of the engine where the minimum engine speed is sustained to maintain engine operation. Usually engines do not produce any significant amount of power at these operating conditions, but it is a state where the engine can remain in a standby operation and ready to use when needed. The next speed is at 300RPM. This speed was chosen as an intermediate operating state, similar to the ones engines experience when cruising on the motorway at normal speeds. The highest speed used for the tests was 600RPM. This condition was chosen to represent the engine state where the engine speed is near the speed limiter. Usually normal engines reach this level of operation at rapid acceleration or when a vehicle is reaching its top speed. The choice of the operating conditions was such that would represent the operating conditions found in automotive engines, in an attempt to link the project to everyday applications and better understand problems that affect the performance of automotive engines. Other factors that played a significant part while choosing the operating conditions

was the physical limitations of the lubrication test-rig. This test-rig has been in the possession of City University for several years and despite the best efforts to update and enhance its capabilities, there are physical limitations that are directly linked to its original design. The speed of the test-rig cannot get past 900RPM. This is not just a design limitation but also the result of the component limitations available at the time of built. The motor can reach 1000rpm but that has been limited by the weight of the rotating components. There is also a safety limiter which ensures that components are not operated close to their limits. The testing was not based only on a range of speeds but also on a range of different flowrates.

Lubrication Rig	Temperature		Speed		
	40C	70C	100rpm	300rpm	600rpm
E1003A_003A	X	X	X	X	X
E1003A_004A	X	X	X	X	X
E1003A_005A	X	X	X	X	X
E1003A_006A	X	X	X	X	X
E1003A_007A	X	X	X	X	X
E1003A_008A	X	X	X	X	X
E1003A_009A	X	X	X	X	X
E1003A_010A	X	X	X	X	X
E1003A_011A	X	X	X	X	X
E1003A_012A	X	X	X	X	X
E1003A_013A	X	X	X	X	X
E1003A_014A	X	X	X	X	X
E1003A_015A	X	X	X	X	X
E1003A_016A	X	X	X	X	X
E1003A_017A	X	X	X	X	X
E1003A_018A	X	X	X	X	X
E1003A_019A	X	X	X	X	X
E1003A_020A	X	X	X	X	X
E1003A_021A	X	X	X	X	X

Table 1 - Full Lubricant Matrix and testing conditions carried out on the Lubrication test-rig

The flowrate is measured as the rate of supply of the lubricant in the area between the piston-ring and the cylinder-liner interaction. Engines experience a plethora of different operating conditions and they all depend on the application of the engine. When engines operate under high load the increased forces have a massive impact on the lubrication of the internal components. This is the main reason why there is a need for controlling the fluid flow of the

supplied lubricant on the optical test-rig. The control of the flow rate was achieved with the use of a control valve. The position of the valve restricts or allows the flow of lubricant through the oil feed. The oil feed is pointing directly to the area where the piston-ring and the cylinder-liner meet. The flowrates used were 0.05L/Min and 0.02L/Min. Both flow rates are in Litters per Minute. These two flowrates were selected as a result of testing and research in order find two values that would cover the majority of the operating conditions found in automotive engine. The high and the low flowrates represent the two main oil supply conditions that are most likely to be found in a modern engine. These two states are fully flooded and starvation. The fully flooded is when there is adequate oil supply and Starvation is the state where the supply of oil is limited or not sufficient. The option of controlling the flow rate of the oil is not only an add-on but a necessity. The tests covered a total of twelve operating conditions, these conditions are listed in table 2. The testing of all the different lubricants under all the operating conditions generated many interesting observations that offered a great insight to the better understanding of their behaviour inside an internal combustion engine environment. The collection of these data was performed with the use of specialised equipment fit for the project as this is shown in table 3. This equipment includes high speed cameras, high intensity light sources and sophisticated optics. The visual data were captured with the use of high-speed imaging equipment. This is specialised equipment capable of recording videos at high frame rates that allow the observation of phenomena that are generated and collapse in a fraction of a second and that would normally be impossible to observe with conventional equipment. These high-speed cameras have the capability of recording videos up to 1,000,000 frames per second.

Speed	Flow rate	Temperature
100RPM (@ 12000fps)	0.05L/Min	40C
300RPM (@ 36000fps)	0.02L/Min	70C
600RPM (@ 72000fps)		

Table 2 - Test operating conditions. Speed, fps, Flow-rate and Temperature

“Frames per second” is the unit used to measure the recording speed of these devices. It is directly linked to their ability of recording a high volume of images in the space of a second. The cameras that reach 1,000,000fps, will capture 1,000,000 images in the length of a second. These figures are also directly linked to the resolution and the shutter speed. All these aspects

are equally important to the quality of the visual data. A high resolution will give much better image quality and will result to a more solid foundation towards the processing of the data, where a high resolution ensures that the captured images are more information rich. The more information is contained inside a picture the more information will be extracted at the processing. Due to the vast amount of data captured the only way to process them accurately was with the use of sophisticated algorithms that would undertake this long and time-consuming job of extracting all this information out of the raw data. The better the quality of the image the easier and more accurate will be the job of the algorithm to process and extract the data.

Data Acquisition Equipment		
High Speed Camera	Friction	Injection Pressure
Capacitance	Flow Meter	

Table 3 - Data Collection Equipment

The shutter speed is equally important to the quality of the images, if chosen appropriately it can produce images that are clear and sharp. If set incorrectly the images will be blurry and unsuitable for processing. Video recording devices produce videos out of a sequence of consecutive images. When these images are played above a certain frame rate the individual images appear in the form of a video. When the user is pressing the record button on a video recording device the device is capturing a sequence of images at a specific frame rate. The images in modern digital cameras are captured with the use of a light sensitive micro-chip that translates light into digital data. The individual images are captured with the use of a shutter located in front of the micro-chip and every time it opens and closes an individual image is captured. The shutter is also controlling the exposure time. The exposure time is very important to the quality of the image. If the exposure is too long the excess light will burn the image and destroy all the information. If the exposure time is too short the image will appear dark and information empty. The main problem faced with high speed cameras that operate at high frame rates is that usually the shutter moves at a speed that normal light sources are proven to be insufficient. During the project the supply of sufficient light was a constant challenge, each optical setup came with different light demands. Between the many attempts to improve the quality of the images was the use of several light sources and different techniques. The cylinder-liner and piston-ring interaction is located deep inside the engine, it is one of the most difficult areas to gain access and this is not different when it

comes to the lubrication test-rig. The limited optical access made the supply of light a real challenge. The problem was tackled with the use of very bright high intensity light sources specifically designed for filming applications. These types of light sources produce a lot of high intensity light, but this comes at a cost.

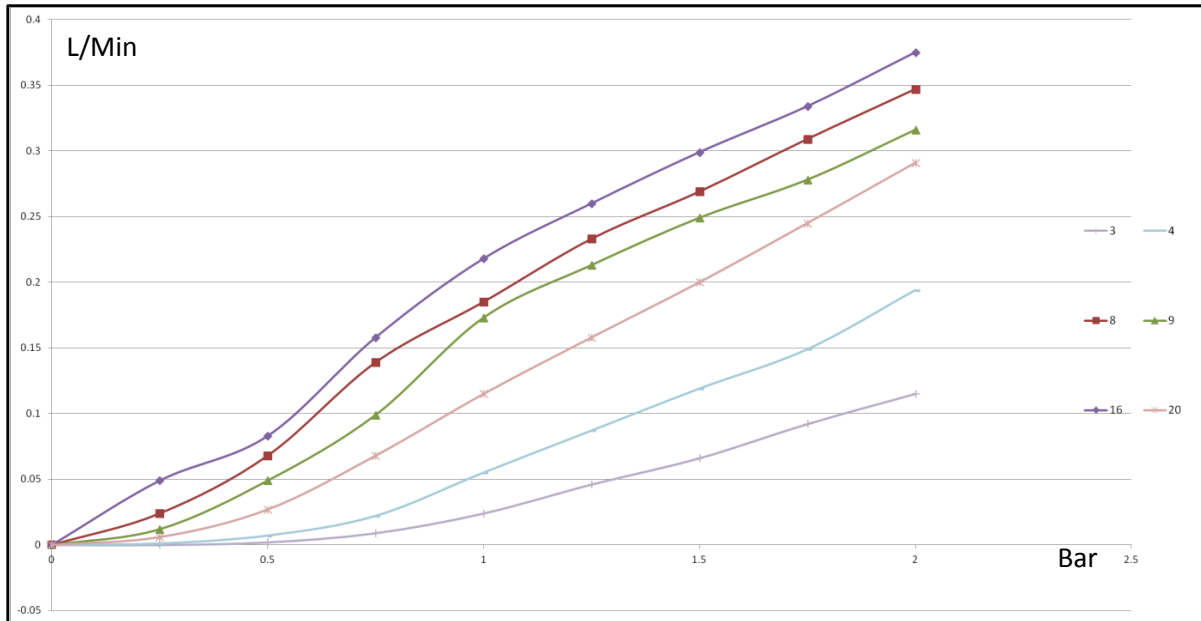


Figure 60 - Optical test-rig measurements of flow rate vs. supply pressure at 40C

The trade-off for all that power is that these lights emit high levels of heat. The amount of heat produced can easily damage the nearby equipment. In cases where the filmed object is not metallic the light source can severely damage it or even set it on fire. The light sources were never operated for extended periods of time and there was always sufficient cooling available. Cooling was provided by several cooling fans pointing directly to the filmed object. At times, even the best counter measures proved insufficient. This is the reason why temperature was always monitored with the use of laser thermometers to avoid critical component damage and prevent the likelihood of fire. The resolution, the shutter speed and the frame rate are all equally important to the successful outcome. The biggest challenge when setting up the optical equipment was to find the perfect balance between the three. Many of the test had to be repeated several times to ensure optimum image quality. This report includes the visualisation data and the oil behaviour for 6 out of the 19 lubricant formulations originally received by BP. As the formulations of the lubricants received are confidential they will be referred to by their code names. This report will present data related to 6 out of the 19 lubricants for one temperature, one flow rate and two different speeds. These lubricants are:

- E1003A_003A
- E1003A_004A
- E1003A_008A
- E1003A_009A
- E1003A_016A
- E1003A_020A

When these lubricants were tested, it was found that they are of different viscosities. When the lubricants were first received, BP did not provide any information related to their formulation. By the end of the project the company was ready to share additional information on their composition and from what it has been observed there were differences mainly in their viscosity. In an early attempt to identify differences between the samples and get an understanding of the differences between the lubricants the decision was made to identify a methodology that would reveal key facts related to their physical properties, in this attempt certain modifications had to be made on the test-rig. One of the latest additions was the introduction of a flowmeter that would give readings of the flowrate. The addition of the flowmeter allowed for the measurement of the injection flowrate which at a constant temperature could reveal information related to lubricant viscosity. The geometrical setup of the test-rig remained unchanged and while keeping the temperature steady all samples were circulated around the system. This resulted to each lubricant offering a different flowrate at a constant temperature. The different flowrates of all the different lubricants were captured and the results showed that the lubricants did not share the same viscosities. The results are presented in Figure 60, for a temperature of 40C.

5.1.1 Velocity and Acceleration

Reciprocating engines derive their power from the vertical motion of the piston. This motion is then translated into the reciprocating motion that is used to drive the vehicle. The movement of the piston extends from the Top Dead Centre to the Bottom Dead, the velocity and the acceleration of the piston are directly linked to the physical dimensions of the engine components. The test-rig may follow the same operating principles as a reciprocating engine but has a fundamental difference. In an automotive engine, the piston is the moving part of the engine and the cylinder-liner is stationary where the test-rig keeps the piston-ring stationary while the liner reciprocates on top of it.

The acceleration and velocity curves shown in figures 61 and 62 represent the liner velocity and acceleration throughout a full test-rig cycle for 3 different speeds. The velocity by

definition is the instantaneous rate of change of position with respect to a reference. The velocity of the piston is measured by how rapidly the position of the piston is changing. The velocity is known as the first derivative of the position curve. The velocity of the test-rig liner is represented in Meters per Second against the crank angle. The green, red and blue curves indicate the different speeds. Blue marks the 100RPM, red the 300RPM and green the 600RPM. The curve shows the piston velocity during a full cycle from 0 to 360 degrees. The velocity is equal to zero at 0, 180 and 360 degrees. This is a fundamental design specification of internal combustion engines and in extension of the lubrication test-rig which has been designed along the same principles.

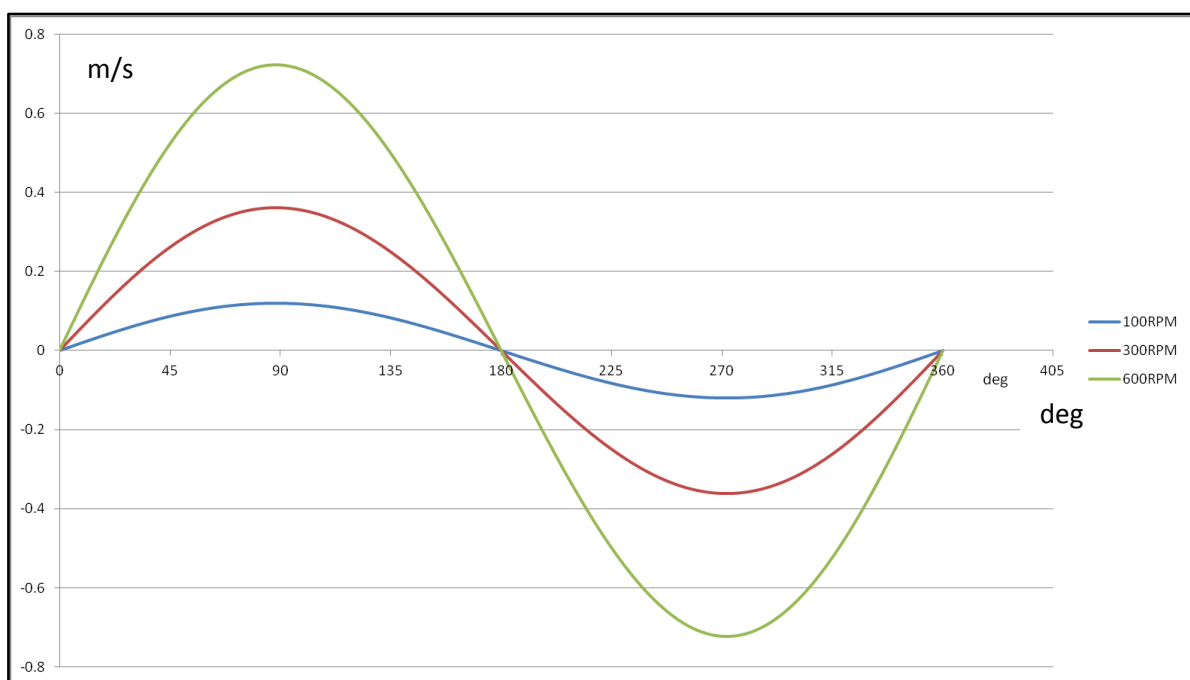


Figure 61 - lubrication test-rig Optical Liner Velocity

The zero velocity points are the points where the piston momentarily stops at TDC and BDC. In the case of the test-rig the moving part is the liner, thus the curves represent the movement of the optical liner instead of the piston. The TDC and BDC points are where the liner changes directions and moves from up-stroke to down-stroke and vice versa. The velocity peaks are the equivalent of the mid-stroke points in an internal combustion engine. At this point the liner is at the middle of its journey between the TDC and BDC. The piston will follow the same velocity profile for every consecutive cycle. Figure 62 shows the acceleration profile of the optical liner for a full 360 degrees' cycle. The acceleration profile even though is related to the velocity profile follows an entirely different pattern. The

acceleration is also known as the second derivative of the position and the first derivative of the velocity. The velocity is represented in meters per second squared.

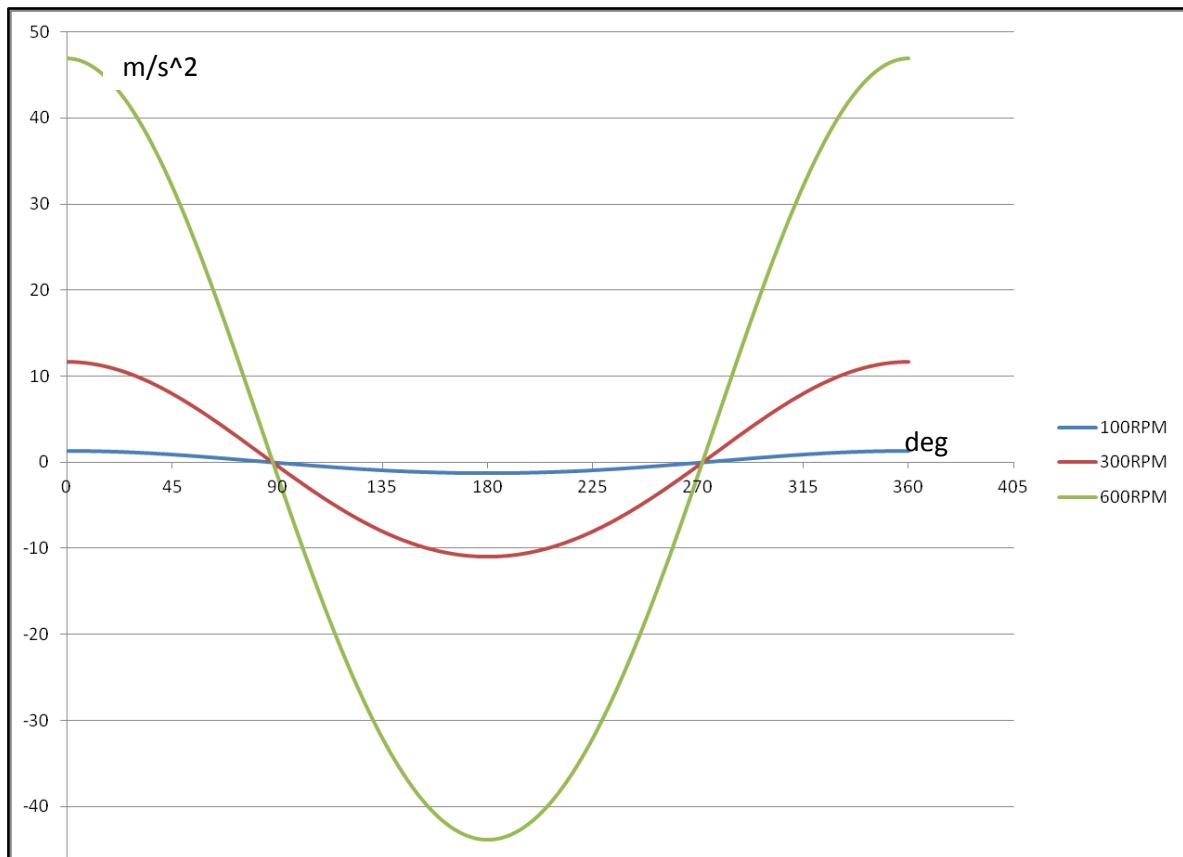


Figure 62 - lubrication test-rig Optical Liner Acceleration

5.1.2 Data Matrix

Table 4 shows the lubricant matrix received for the project and a sample of the lubricants provided by BP along with basic information on their formulations as these were specified by the company, these formulations will be kept confidential until BP decides to release them. These lubricants are related to products that BP had not released up to the point of the data processing as they were in preliminary development stages. Each petroleum company with the new European regulations must plan far ahead of the deadlines. Each lubricant manufacturer develops several lubricants and treats them all as possible successful candidates for production, which of these lubricants makes it to production depends on their individual performance. In the case of this project a total of 19 lubricants was received all in the development stages.

In total 50 liters were used from each sample to cover the needs of the project. These 50 liters covered the tests as well as the “flushes” or cleaning between the runs. A specific

amount of lubricant is used to flush any remaining lubricant before the new one is added. The flush was accompanied with the cleaning of all the test-rig components with a specific solvent that would remove any lubricant residuals before the next run. Then one additional flush was performed to remove any solvent residuals. For each test run a total of 2 liters was required to fill up the lubrication test-rig reservoir for normal operation. Every time the lubricant had to be changed the equivalent of two full fill-ups were needed to ensure the lubrication test-rig had been properly flushed. That mean that for every 2 liters used for testing another 4 liters were used to flush and clean the experimental setup.

	Lube test number	1	2	6	7	-	14	-	18
	E1003A/	003	004	008	009		016		020
Base oil	Group 1	x			x				
	Group 3			x			x		
	Group 4		x						x
	Group 5								
	Pack 1	xx	xx	xx	xx		xx		xx
	Pack 2								
	Pack 3								
Add pack	VM 1						xx		x
	VM 2								
	VM 3								
	GP	1	4	3	1		3		4
	HTHS	4.92	4.88	3.05	3.04		2.93		3.82
	KV40	176.6	128.2	57.28	65.28		43.88		90.61
KV100	17.16	16.94	9.12	9.24		9.64		13.19	
Visc +1	17.16	16.94							
VM	Group - fixed visc			9.12	9.24				
	Lower Visc			9.12					
	Add conc						9.64		
	VM conc								13.19
	VM type?								
VI	104	144	139	119		161		145	
Density	0.8944	0.8533	0.8585	0.8848		0.8542		0.8505	
Based on lube formulation	E0300A								
	011C	006A	014A	009A		New		New	

Table 4 - Lubricant Sample Matrix

To complete the testing of the entire matrix a total of 950 liters of lubricant were used either to test or flush the experimental device. The 950 liters of lubrication oil produced a large amount of data. After careful consideration and lubricant comparison, it was considered as unnecessary to include the entire database in this report. A lot of work has been dedicated in identifying the most appropriate samples, which would construct a conclusive set of data that

would illustrate in the best way possible the findings of the project. It has been considered that the set of data to be included in this report would have to represent the entire tested matrix. These samples would have to give conclusive results toward the contribution of this project to the better understanding of the phenomenon of cavitation. In conclusion, the decision was taken to narrow down the batch of 19 lubricants to 6 representative samples purely based on their formulations. Many of the 19 lubricants presented similarities in regard to their formulations and performance. From the testing and the information received by BP the lubricants were grouped into 6 categories as per their test results. One sample from each group was chosen to be included in this report. These lubricants were chosen for their distinct behaviour under testing and for the way they represented all the attributes of their group. These 6 lubricants are based on 3 main base compositions, the Base Oil Group 1, the Base Oil Group 2 and the Base Oil Group 3. All these base lubricants are enhanced with a variety of additives. Some of the lubricants have also an additional Viscous Modifier. These are referred to as VM1, VM2 and VM3. The lubricants that used Viscous Modifier only made use of VM1. All the lubricants feature different kinematic viscosities. In conclusion, the 6 lubricants used for the purpose of this report are a solid representation of the behaviour of the entire matrix received by BP and are considered to be a sample that offers a collective view and understanding of how different formulations affect the behaviour of cavitation and how this is depended of their specific additives.

The sample received from BP were accompanied with limited information regarding their performance and formulation as these are presented in Table 1. The information available presents the Kinematic Viscosity at 40C and at 100C and the HTHS (High Temperature High Shear) which is the viscosity at 150C. The tests presented on the lubrication test-rig in this report are all performed at 70C which is in between the 40C and the 100C kinematic viscosities available in the documentation. KV70 is not something that is available or commonly used by lubricant manufacturers and for that reason it would have to be calculated. The kinematic viscosity curve is not linear. The use of the two 40C and 100C data points would make a fit line using the Reynolds equation. However, the best approach would be to introduce a third point and use the Vogel equation which is the most accurate viscosity-temperature equation. HTHS can be used as the third point to allow for that calculation. The HTHS is the viscosity at 150C which is divided by density and could give the kinematic viscosity at 150C. Figure 63 shows the trend lines for all the individual lubricants as this is fitted for 40C, 100C and 150C. The trend lines given by the Vogel equation allow for the

approximate calculations of KV70. The values for KV70 are presented in figure 64 and will be used for the direct comparison of the lubricant samples in the discussion of this report.

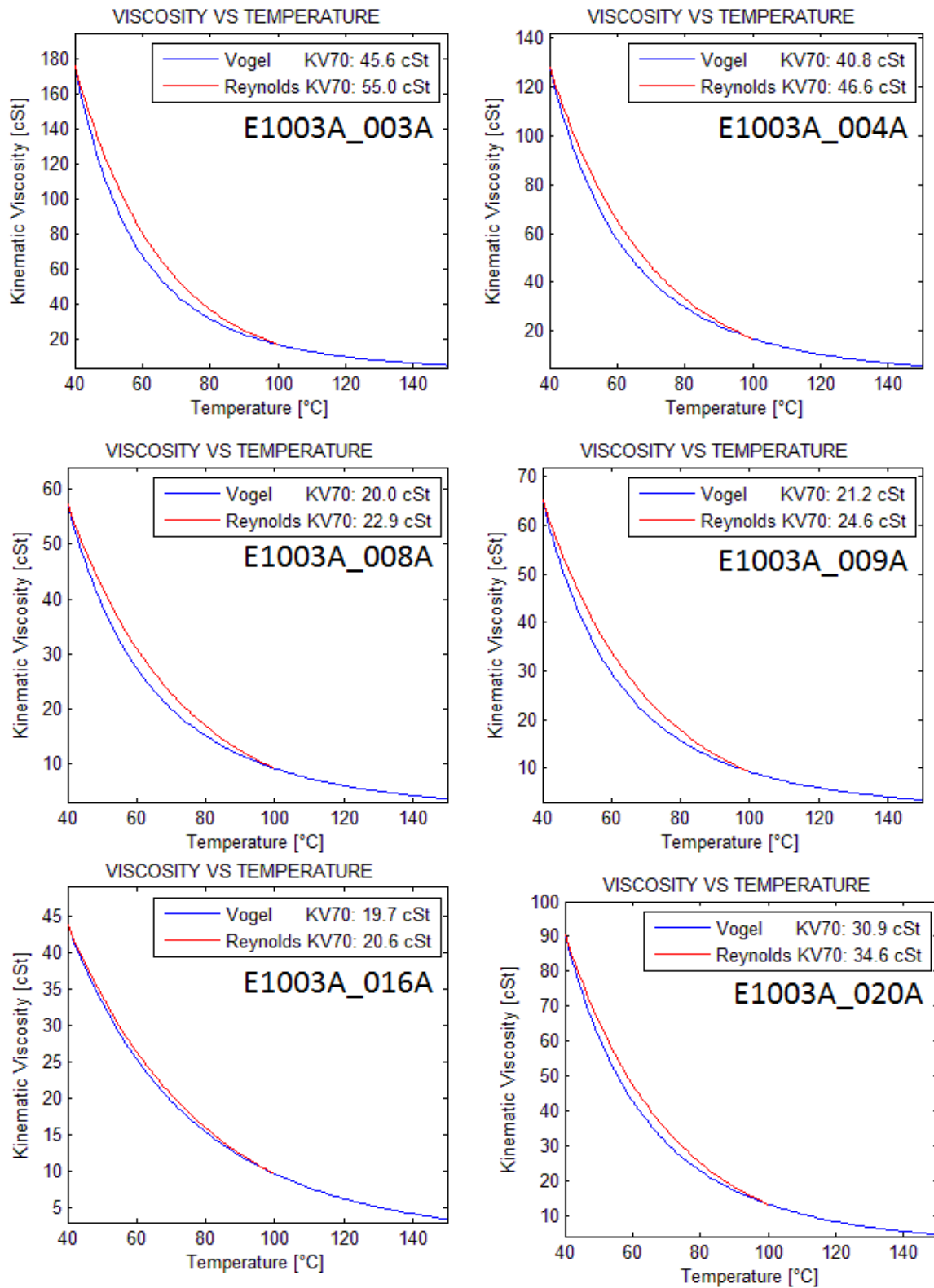
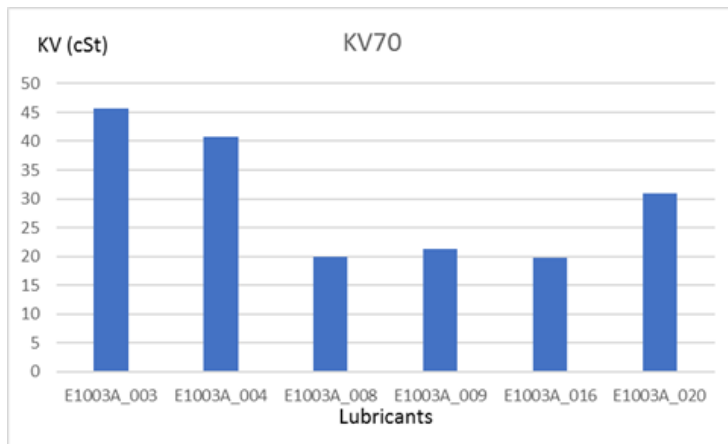


Figure 63 - Polynomial trend line and equation fitted for 40, 70 and 150C



Lubricant	KV70 (cSt)
E1003A_003	45.6
E1003A_004	40.8
E1003A_008	20
E1003A_009	21.2
E1003A_016	19.7
E1003A_020	30.9

Figure 64 - Kinematic viscosities at 70C

5.1.3 Data

This section contains a set of images captured in the course of the project while the majority of the data are in the form of a graphs extracted by the same type of data. Later the phenomena observed are linked to the physical properties of each lubricant and the results are discussed to whether these properties influence the performance of each lubricant.

5.1.3.1 Optical Data

The first sample to be analysed is lubricant E1003A_003A. The data are in a set of consecutive images where the speed is at 300rpm, the temperature at 70C, the frame rate at 36000fps and the lubricant supply flow rate at 0.05L/Min. The following set of unprocessed data offers a better understanding to why the figures plotted through the Matlab algorithms follow the trends they do. More information on the comparison between the raw and the processed data are given in earlier parts of this report where the output of the Matlab algorithm is compared next to the raw inputs. The following images illustrate the formation, development and collapse of cavities while testing lubricant samples on the test-rig. It is identified that the cavities which are generated on the top and the bottom of the ring are of different lengths. This is mainly due to the design of the ring, as the contact point with the liner is at an offset from the centreline, this is also discussed in the “Ring Profile” section of this report. The cavities shown in figure 65 to 74 pass through all the main stages of cavitation. The first stage is identified as the cavity generation, the cavities generated at this stage are also known as fern cavities.

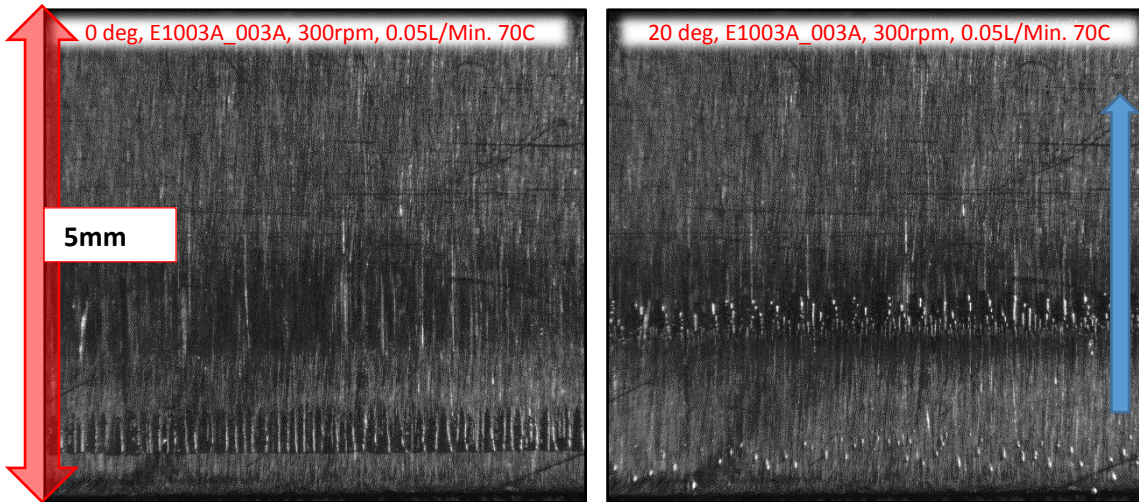


Figure 65 - E1003A, 300rpm, 0.05L/Min, 70C, 0-20deg

The next stage after the fern cavities is the development of the finger cavities. The finger cavities remain developed for the majority of the stroke until they are forced to collapse in the form of bubbles. The last stage before collapse is the formation of a cavitating sheet, this sheet is observed in certain frames as in figure 66 in the form of a large unified dark area. The captured data indicate that though the cavity behaviour is directly linked with the relative piston-ring and liner movement there is a small delay to the cavity reaction which is directly linked to each lubricant's individual viscosity.

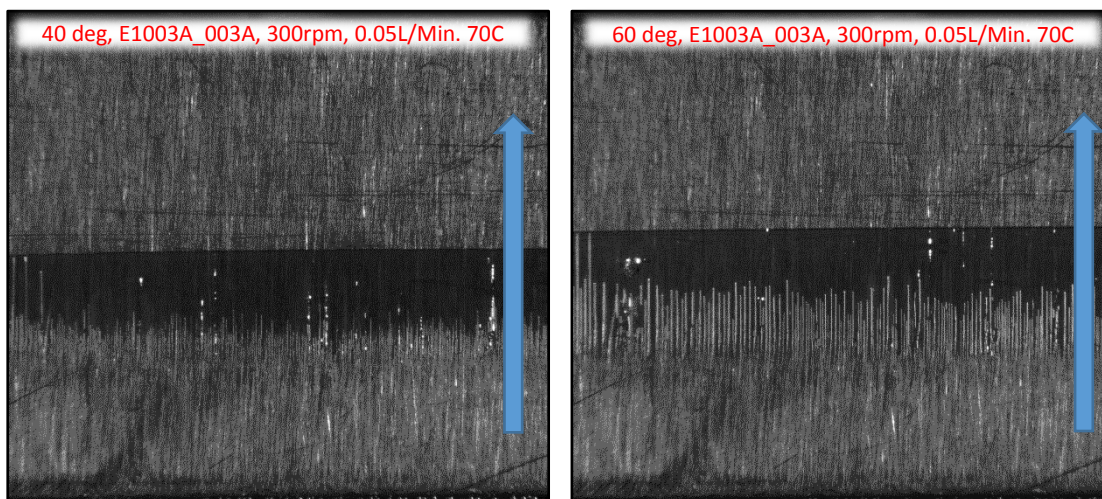


Figure 66 - E1003A, 300rpm, 0.05L/Min, 70C, 40-60deg

The following images have been enhanced with markers. The blue arrow indicates the liner movement direction in an attempt to give a better understanding of the link between the cavity behaviour and the relative liner movement, where a blue arrow is not present the liner is either at the TBC or BDC and its velocity is equal to zero.

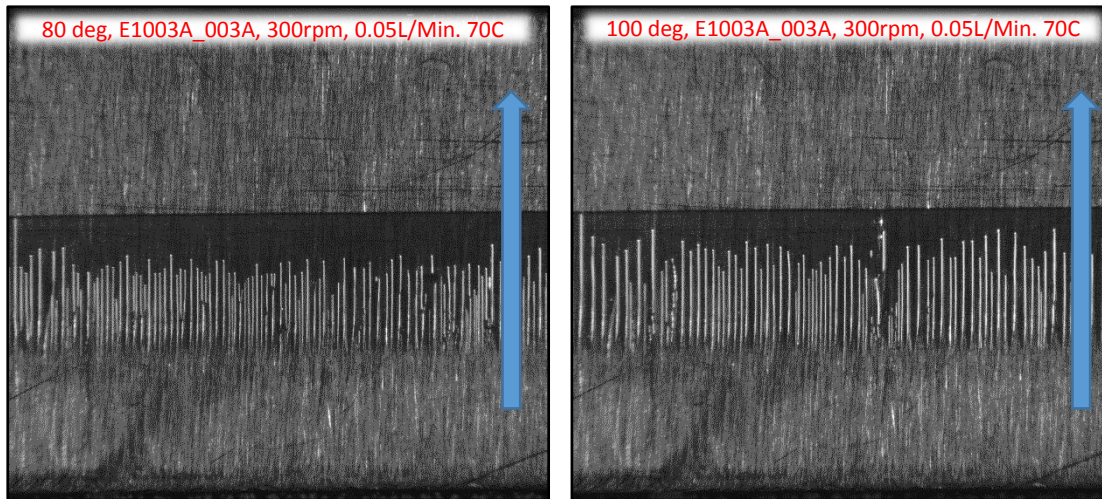


Figure 67 - E1003A, 300rpm, 0.05L/Min, 70C, 80-100deg

The red arrow indicates the length of the ring specimen. Each frame includes a caption at either the top or the bottom of the frame with information related to the specific conditions when the frame was captured. The 0 degrees' frame in figure 65 represents the beginning of a cycle at BDC, this is a point where the liner is at zero velocity relative to the piston. In the same figure, even though the liner is still, and the new cycle is about to start there are still cavities that remain from the previous cycle. The cavities that are still present seem to maintain a significant length and appear to be in the fissure cavity stage.

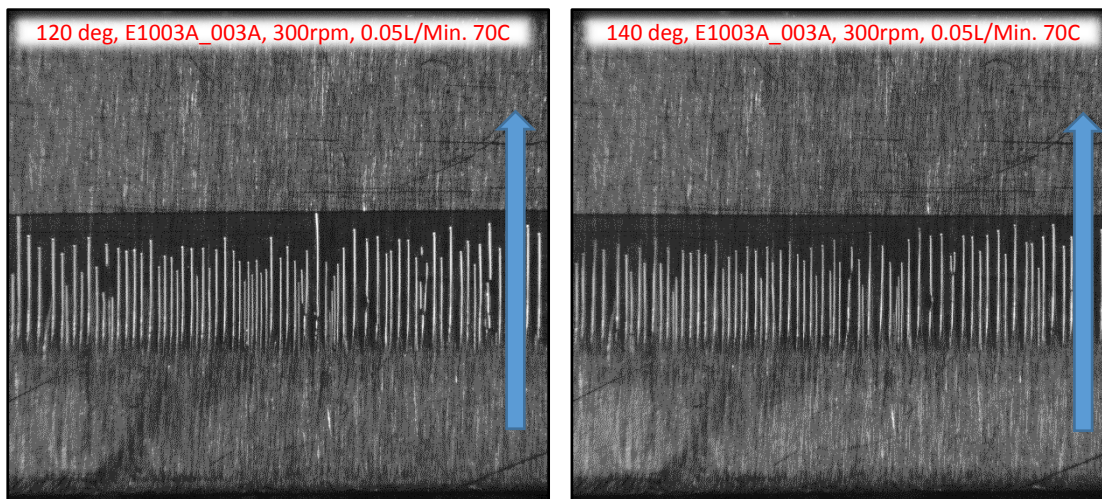


Figure 68 - E1003A, 300rpm, 0.05L/Min, 70C, 120-140deg

This phenomenon is specific to each sample where the cavities are depended on the physical properties of the lubricant and might not fully collapse before the new cycle begins. Further information of the cavity formation and the way this is affected by lubricant formulation is given at a later chapter of this report.

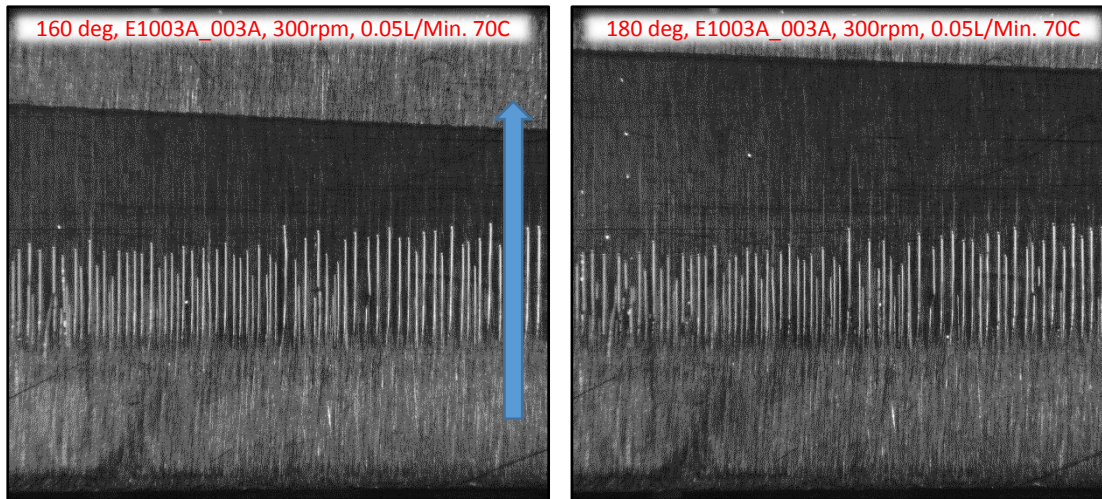


Figure 69 - E1003A, 300rpm, 0.05L/Min, 70C, 160-180deg

On the next frame in the same figure and at 20 degrees into the new cycle, the remaining cavities are either collapsing or on their path to escape the confined space between the piston-ring and the liner. At the same crank angle but on the opposite side of the ring new cavities have started to generate. These cavities are still at the early fern cavity stage. These newly generated cavities will continue to develop in the next frame at 40 degrees as shown in figure 66. At this point the cavities have passed the fern cavity stage and have developed into finger cavities through they are not fully developed yet. On the next frame at 60 degrees in the same figure, the cavities are fully developed and have reached a stage where they start to form a cavitating sheet. The cavities will remain at this state for the next four frames and figures 67 and 68. An arrow has been placed on the specific images to indicate the direction of the optical liner.

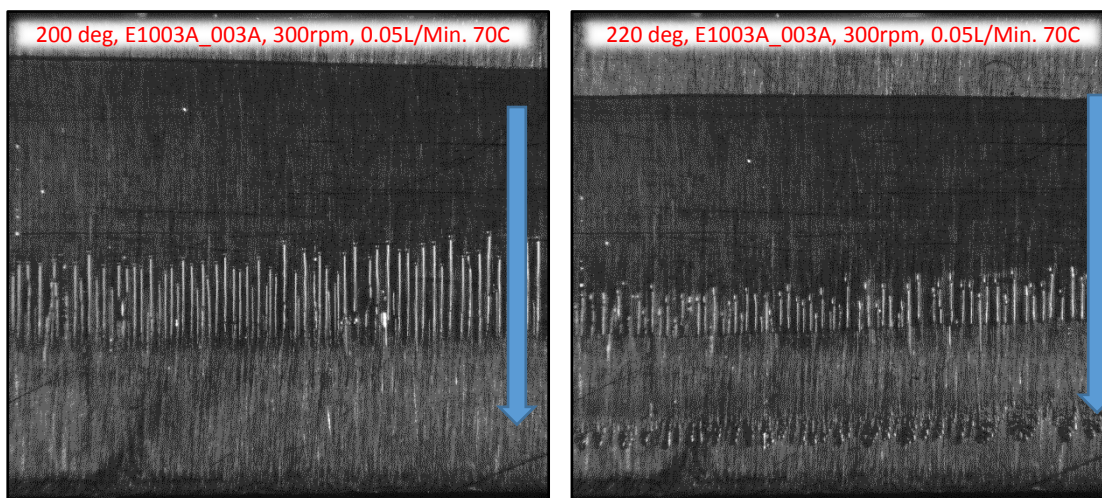


Figure 70 - E1003A, 300rpm, 0.05L/Min, 70C, 200-220deg

In these four frames, the cavities do not show any significant change in their behaviour or physical properties. The only change that is worth noting is the constant generation and collapse of finger cavities at the front of the cavitating area but there is a relatively small change in their length, width or population. Referring again to figures 61 and 62 which present the velocity and acceleration of the liner a link is observed. It is noticed that the described phenomenon is directly linked to the liner velocity and the liner acceleration. More precisely the behaviour of the cavities at any given crank angle is the result of the changes in acceleration and velocity. This phenomenon is further analysed in the later parts of this section. Moving onto the next frame in figure 69 and at 160 degrees there is a significant change in the cavity behaviour and more specifically to the values around the length of the cavities. The cavities at this stage seems that in the length of a few frames have rapidly expanded up to a length almost double the length they had in the frame before in the same figure. At this stage, the cavitating sheet covers the majority of the ring and the back of the cavitating area has reached the edges of the ring, the cavities are not separated any more by the lubricant but have all joined into what it seems to be a cavitating sheet.

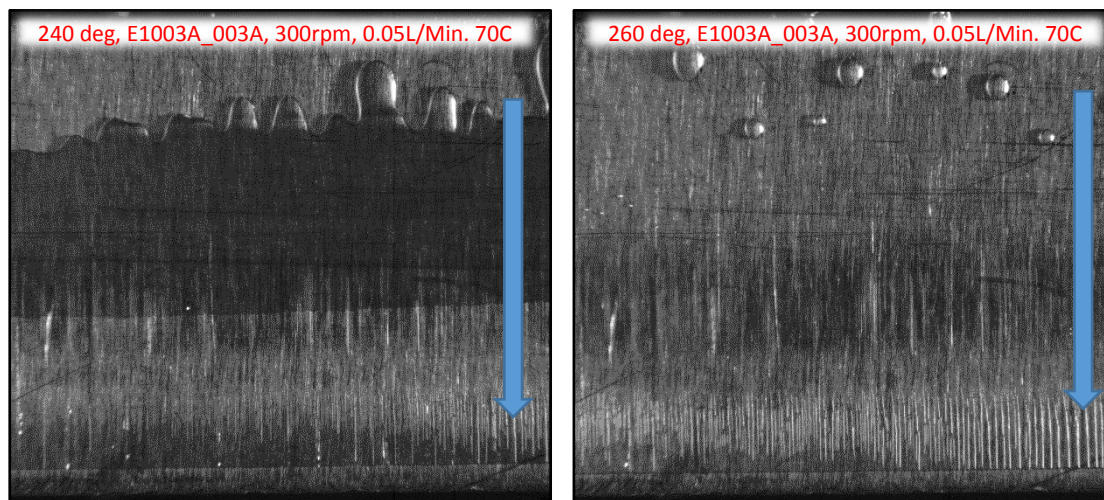


Figure 71 - E1003A, 300rpm, 0.05L/Min, 70C, 240-260deg

Further investigation is needed to clarify why this phenomenon occurs at this particular stage of the cycle and how that is linked to the pressure, the velocity and the acceleration but it can be assumed that due to the increased length of the cavities the internal tension of the lubricant has significantly decreased thus forcing the individual cavities to merge into a uniform cavity sheet.

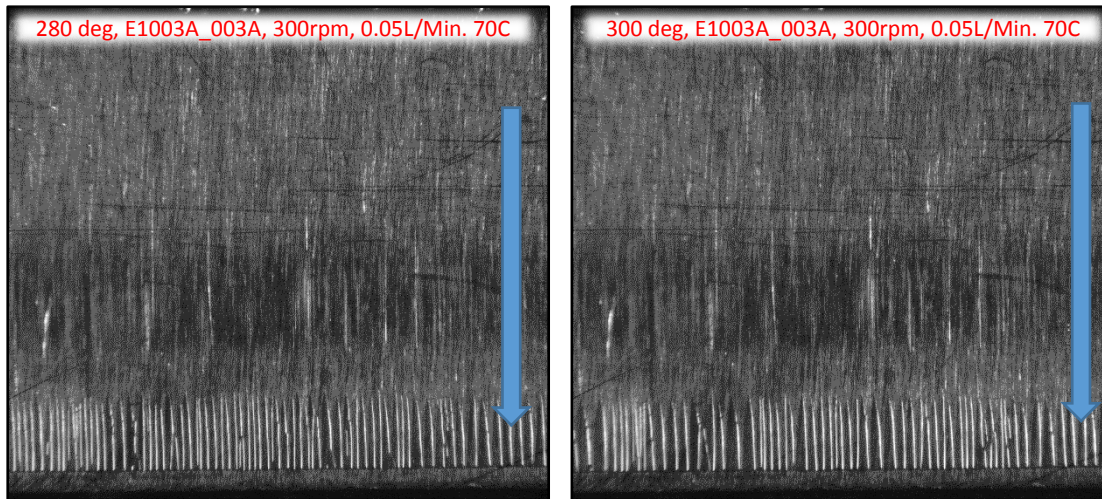


Figure 72 - E1003A, 300rpm, 0.05L/Min, 70C, 280-300deg

In the next frame at 180 degrees and figure 69 the cavities have now increased at a length almost double that of the frame before and the forth front of the cavities is not aligned anymore with the profile of the ring. The main reason of that uneven front is the profile of the specific piston-ring. To better replicate a conventional internal combustion engine the piston-ring was designed and manufactured with a circular profile. The face of the ring does not feature a flat surface, but it follows a curvature along both of its axes. An additional factor that will promote that behaviour is the fact that the ring is also allowed to pivot on a knife edge along its centreline.

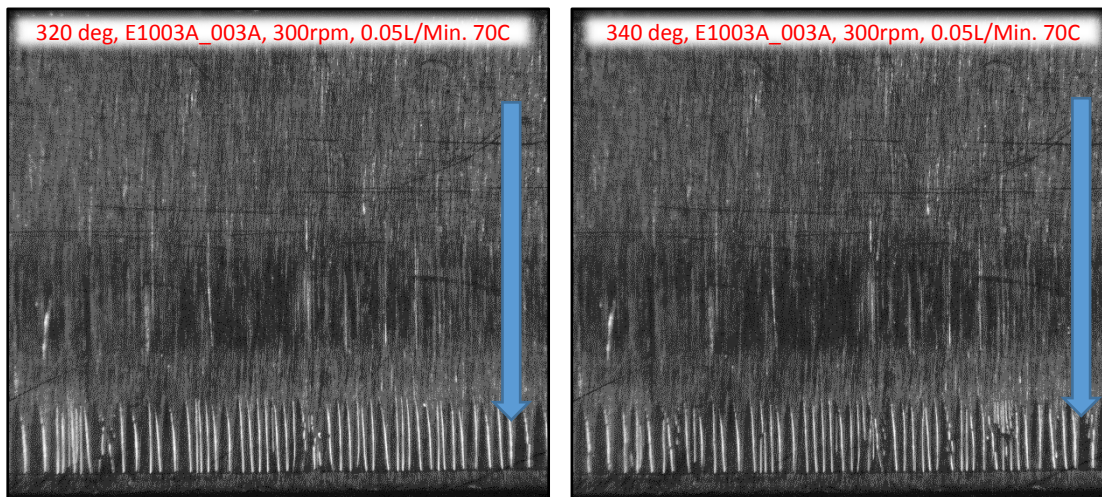


Figure 73 - E1003A, 300rpm, 0.05L/Min, 70C, 320-360deg

That movement along with the uneven profile will also cause extra abnormalities in the gap between the piston-ring and the liner. In the next frame in figure 70 the cavities have increased even further, and they now reach almost three times the length of the earlier

cavities. The majority of the cavitating area is covered by a cavitating sheet and the total cavitating area covers the majority of the ring. This phenomenon continues into the next frame in same figure even though the length of the cavities has already started to decrease. In the same figure, it is observed that even though the cavities on the top side of the frame have not fully collapsed, there are new cavities already generating on the lower part of the piston-ring. These are still at an early fern cavity stage; this phenomenon has been also observed at an earlier stage of this cycle where cavities in both sides of the ring coexisted. The relative motion of the cylinder-liner is highlighted with the blue arrow on the right of the frame. The cylinder-liner in both frames in figure 70 has started moving towards the opposite direction as in figure 69 and towards the bottom dead centre. Cavities are now present on both sides of the piston-ring. If the newly generated cavities are compared with the ones from the previous stroke obvious differences can be identified. The main reason behind these differences is once again the profile of the piston-ring. The piston-ring geometry does not only vary along the vertical axis, but also along the perpendicular axis. In the next two frames, the new cavities have developed fully and have reached their maximum length for this cycle.

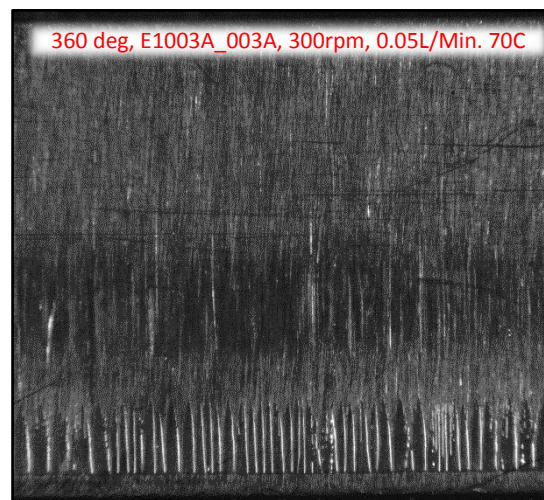


Figure 74 - E1003A, 300rpm, 0.05L/Min, 70C, 360-380deg

At this stage the collapsing cavities on the opposite side, still cover a big part of the ring and have not fully collapsed at this stage yet. At 240 degrees, the collapsing cavitating sheet occupies a larger area than the fully develop cavities on the lower part of the ring. In the next frame in figure 72, at the 280 degrees the cavities on the top part of the ring have in their majority collapsed and that ones that have not, are escaping the interaction in the form of bubbles. At the same time, the cavities on the opposite side of the piston-ring are still developed and still maintain the length and the area they occupied in the previous frames.

These cavities are going to maintain their length and area until the end of the cycle and this will continue into the next stroke. The consecutive frames give an understanding on the behaviour of the cavities in relation to the velocity, acceleration and position of the liner and also give an overview of how the cavities pass through all the different cavitating stages and how these are affected by velocity and acceleration. This knowledge is essential to the in-depth understanding of the phenomenon of cavitation and give a good foundation for the tests that were later performed on the optical engine. It is also important that a correlation is established between the lubrication test-ring and the optical-engine with the use of this data.

5.1.3.2 Software Processed Data

During the testing phase of the project a database was created to hold the acquired data. The majority of those data are in a visual form and more specifically in high speed videos. These videos are composed by a series of consecutive images. Each video contains thousands of images, thus, processing them manually would be an inefficient task to undertake. The decision to use the processing power of a computer was then considered as the only effective and efficient option to successfully process all the data. Due to the nature of the project an off-the-shelf solution was not available at a time. The software that would utilise the processing power of a computer to analyse the visual data acquired would have to be written from the beginning. There is a wide selection of programming languages available that could fit the purpose. After research based on the nature of the data and the fact that these were stored in a matrix format the decision was made to use Matlab. Matlab is a multi-paradigm, numerical computing environment and a fourth-generation programming language. Multi-paradigm programming languages are languages that allow the users to work in a variety of styles. Fourth-generation programming languages are refined languages usually away from the low-level “0101” computer language and they offer a more understandable and user-friendly environment. Matlab is a Mathworks product and is available for a range of applications. Matlab offers additional modules that can be utilised to assist with tasks such as image or sound processing. Initially Matlab was intended as a numerical computing language and users come from various backgrounds with the majority of them being engineers, economists and scientists. The derived algorithm is capable of extracting a number of information related to the phenomenon observed in the captured images. More important this information can be quantified and stored in memory for further processing. The data were processed using the newly developed software and the extractions gave information regarding the area that the cavities occupy, the length and width of the cavities and the number of

cavities present. Further processing was performed within Microsoft Excel and graphs were plotted for visualisation and comparison purposes. All the data presented in the following sections are at a 70C temperature. The tests were carried at a number of different operating conditions. These conditions included two different temperatures at 40C and 70C. The following chapters present data generated from tests performed at 70C while the oil flow rate at the supply through the injectors is constant at 0.05L/Min. The high-speed camera used for this experiment offers shutter speed and frame rate adjustability. Each video was captured at a different frame rate which depended on the engine speed. A full 360 degrees' cycle is equal to 606 frames and that is for all the three different speeds. Each of the graphs represents data derived from the physical dimensions of the generated cavities against the crank angle. The chosen range is from 0 degrees to 1080 degrees. The full cycle is 360 degrees, thus the graphs present data related to three consecutive cycles. The data processing has been performed mainly with Matlab and as with every data capturing software the generated data were affected by certain amount of "noise". Noise is the unwanted data captured by the algorithms when processing the raw data. There are a number of techniques and tools to mitigate at a certain extend these unwanted data. In some of the cases the readings were affected by external noise, the data related to those readings had to be further processed in Matlab or Excel. The Microsoft Excel software has the ability of accepting custom functions and algorithms and offers to the user a powerful and easy to use tool for data processing. Some post processing of the data has been performed with algorithms implemented within Microsoft excel and part of this filtered data are presented in the following sections. The processing of the data has been a difficult and time-consuming procedure. The development of the algorithm has been based on a mixture of software development and experimental trial and error. During the development of the software the lubricants had to be retested multiple times to achieve the required quality. The tests were in total repeated 3 times with the final results featuring the best possible clarity for the supplied equipment. The repeating of the tests for the same samples under the same conditions had to be performed in accordance to the modifications implemented within the software at each different phase of the project. The raw data had to be improved in such a way that would bridge the limitation of the algorithm. Due to confidentiality, the exact formulations of the lubricant could not be retrieved. To comply with the confidentiality agreement the lubricant samples have been masked and referred to by their product code names. These names were given to them by BP and the same applied to their formulations. All the tested samples belong to five different base Oil Groups. These groups are Group 1, Group 3, Group 4 and Group 5. Each group was available with

three different Add-Packs. These add-packs are Pack 1, Pack2 and Pack 3. Some lubricants also feature additional Viscous Modifiers, VM 1, VM 2 and VM 3. The following sections present data that have been processed through Matlab and Excel and are part of the matrix received by BP. It has to be noted that the camera recorded the first 3 cycles of every run. The first 3 runs ensured that all lubricants would have the same number of cycles due to the limited internal memory of the camera.

Area covered 0.005L/Min 70C 300rpm

The following figures present information related to the area of the ring where cavitation occurs on its surface. They cover all the six lubricants tested at a temperature of 70C and a flowrate of 0.005L/Min at a speed of 300rpm. All the data are presented as a percentage of the total ring area against the rotational crank angle. For the first lubricant E1003A_003A in figure 75, the test conditions as mentioned earlier are; flow rate of 0.005l/min, temperature at 70C and a speed of 300RPM. This specific lubricant belongs to base oil Group 1 with the addition of add-pack 1. This specific lubricant has no additional Viscous Modifiers. Figure 75 shows the area of cavitation for that specific lubricant as a sequence of three consecutive cycles. The cavitating area behaviour is repeatable on every cycle. Lubricant E1003A_003A shows a peak of maximum area of cavitation at 180, 540 and 900 degrees, for all the three cycles. These are the middle-points of every cycle and where the liner changes direction. In the same figure, it is supported that the area of cavitation is directly linked to the crank angle.

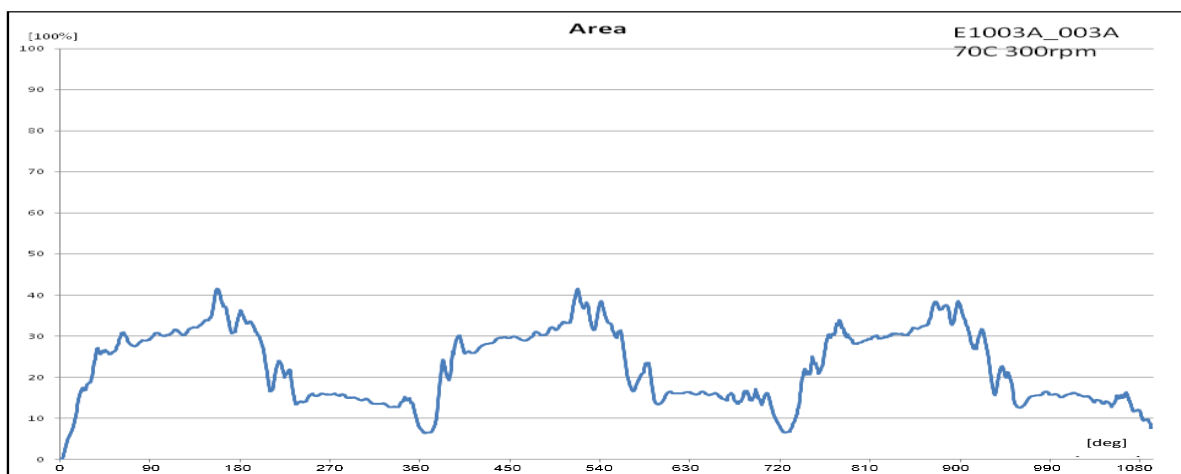


Figure 75 – Area Covered, E1003A_003A, 0.005L/Min, 70C, 300RPM

When compare to figure 76 it is noted that the area of cavitation is also linked to the lubricant formulation. Figure 76 in contrast with figure 75 presents a much more “disturbed” profile. This is mainly due to their different formulation of each lubricant. Lubricant E1003A_003A

is based on Group 1 and E1003A_004A on Group 4 and both of the samples feature an add-pack 2 additive. Lubricant 003A was calculated to have a KV70 of 45 cSt and lubricant 004A of 40 cSt. Figures 76 and 75 show that the lubricant with the higher kinematic viscosity will also offer a lower area of cavitation throughout the 3 cycles. Both of the lubricants follow the pattern detailed earlier on where the cavitating area on the ring is greater in the first part of the cycle from 0 to 180 degrees and lower at the second part from 180 to 360 degrees. The cause of this distinct behaviour is not based on the lubricant formulation but on the physical design of the ring specimen. Similar to the comparison of these two lubricants is the direct comparison between lubricants E1003A_004A and E1003A_008A. Lubricant E1003A_004A in figure 76 is again showing a rougher profile than E1003A_008A in figure 77. Lubricant E1003A_008A has a KV70 of 20 cSt. The Lower KV will indicate that the lubricant will present a lower area of cavitation than the previous sample.

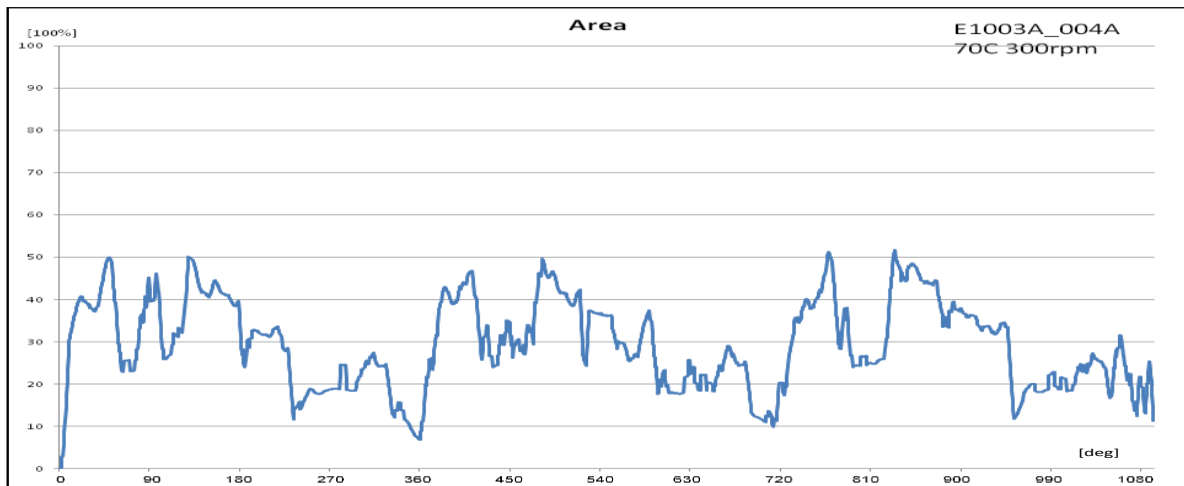


Figure 76 – Area Covered, E1003A_004A, 0.005L/Min, 70C, 300RPM

This is also confirmed by figure 77 where despite the sudden spikes it offers a generally smaller area of cavitation. Once more the relation between the different formulations and the behaviour of the phenomenon of cavitation is supported by the comparison of these graphs. Lubricant E1003A_004A belongs to the base oil Group 4 and lubricant E1003A_008A belongs to the base oil Group 3. Their different compositions play a crucial role to their in-between performance. They both share the same add pack, but their physical properties related to Kinematic Viscosity as calculated are very far apart, in fact 004A has double the kinematic viscosity of 008A. This difference in the physical properties is one of the main causes behind the differences in their individual behaviour. Despite the random spikes in figure 77 it has been noted that the main curve follows a relatively different pattern. The low

points of the curve are closer to the axes and the total area underneath the curve is smaller than the total area in figure 76. This can be linked to the higher KV70 of E1003A_004A which promotes higher area of cavitation and despite both lubricants having the same density, lubricant 008A has almost half the kinematic viscosity at 70C when compared to 004A. One distinct difference is the cavitation overlap that some samples depended on their formulation experience between the strokes. The strokes if separated to up-stroke and down-stroke, refer to the direction of the optical liner and subsequently the position of the ring where cavitation occurs. Cavitation is either generated at the upper or the lower part of the ring. Which area is affected is directly linked to the movement of the liner in relation to the ring. Each time the liner changes direction so does the cavitating side. When cavitation is generated on one side of the ring, it collapses and disappears on the other one. Despite this general rule there are some lubricants that escape that pattern. In some cases, when the liner changes direction the cavities that would normally collapse, do not and in fact continue to be present even in the next stroke. It is not an uncommon phenomenon to see cavitation simultaneously occupying both sides of the ring. Since the software is capturing the total area of cavitation in relation to the ring, in the case that cavities are present on both of the sides during each cycle the total area will never reach 0 as the total area of cavitation will be their summation. This feature of the software is not a design flaw but a design specification.

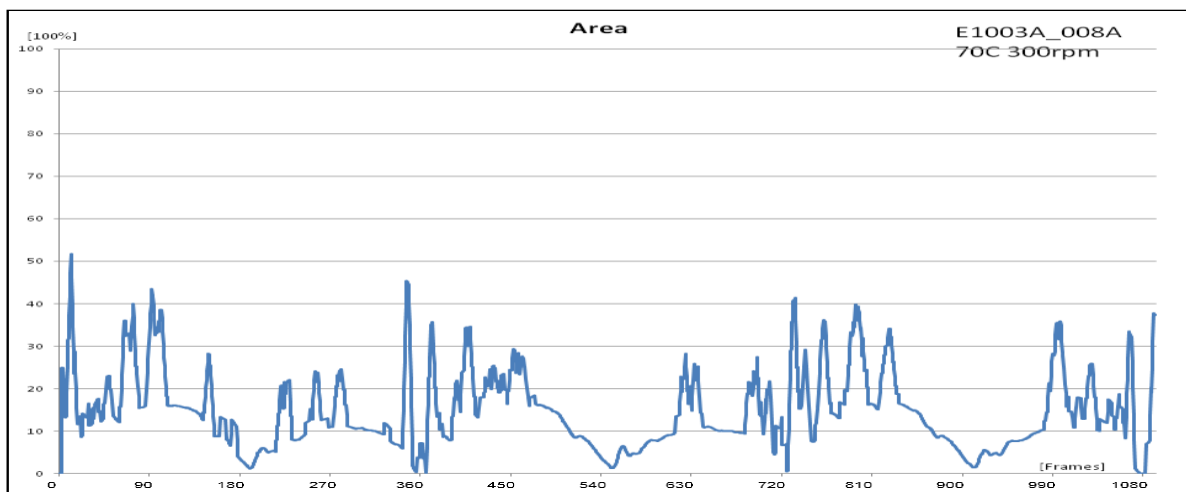


Figure 77 – Area Covered, E1003A_008A, 0.005L/Min, 70C, 300RPM

Figure 78 shows a cavity behaviour that follows an entirely different pattern than the rest of the lubricant matrix. The area under the curve covers a much larger area than the rest of the samples. This specific lubricant is affected by cavitation in a completely different way than the rest of the batch. The graph shows a significant breakage at the end of every cycle, which

is every 360 degrees. Despite the basic differences presented in relation to the rest of the samples, lubricant E1003A_009A still shows a repeated pattern which follows a frequency of 360 degrees. Lubricant 009A is quite a unique sample within the batch, it is a lubricant based on group 1, a group which included lubricant 003A which has the highest KV70 within the group and while featuring the same base group and additives, 009A has one of the lowest KV70 values within the batch, of 21 cSt. The low KV70 explains the high cavitating area and the tendency of the specific lubricant to cavitate. Figure 79 and figure 80 show lubricants E1003A_016A and E1003A_020A respectively. These lubricants follow patterns similar to the majority of the lubricants, even though they show a high number of “sudden” spikes. As shown in figure 79, lubricant 016A shows no overlap of cavitation between the different runs where 020A does. These two lubricants are the only two lubricants in the presented batch that feature a viscous modifier with the 016 having double the concentration of 020A. These lubricants are of different base groups but with the same add-pack at the same concentration. Despite these two lubricants having the same viscous modifier a very interesting observation comes when comparing lubricants 008A and 016A together in figures 77 and 79. These two lubricants are of the same group, group 3 and feature the same add-pack, with lubricant 016A having an additional viscous modifier. Despite the viscous modifier these two lubricants have similar KV70 of 19 and 20 cSt with 008A being slightly higher and density close to 0.85. This similarity is also reflected in the captured data where they both present similar curves and similar values with 008A having a small edge.

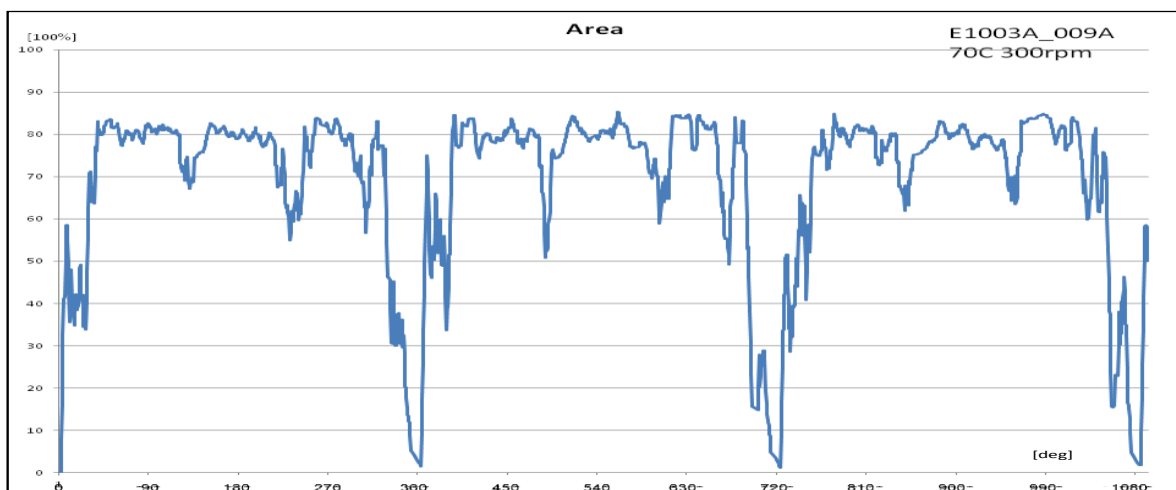


Figure 78 – Area Covered, E1003A_009A, 0.005L/Min, 70C, 300RPM

Figures 75 to 80 show the pattern that cavitation follows for the majority of the lubricant samples when these are tested under the same conditions for the entire matrix of the 19

lubricant that were originally tested. The testing of all the lubricant samples supports that there is a direct link between Kinematic Viscosity and cavitation. Kinematic Viscosity of engine oils is a critical property that relates to the fuel economy and durability of a running engine. The drivers behind lowering KV viscosity are global regulations to improve fuel economy and lower greenhouse gases in vehicles. Lower KV tends to improve fuel economy and lower emissions but higher KV offers better wear protection so a careful balance must be identified when formulating an engine oil. Sufficient KV is critical in preventing engine wear in the critical ring/liner interface area by maintaining a protective oil film between the moving parts. The kinematic viscosity is measured at different temperature increments, with the most widely used one being the HTHS viscosity (High Temperature High Shear) which is the viscosity at 150C, a temperature closer to engine operating conditions.

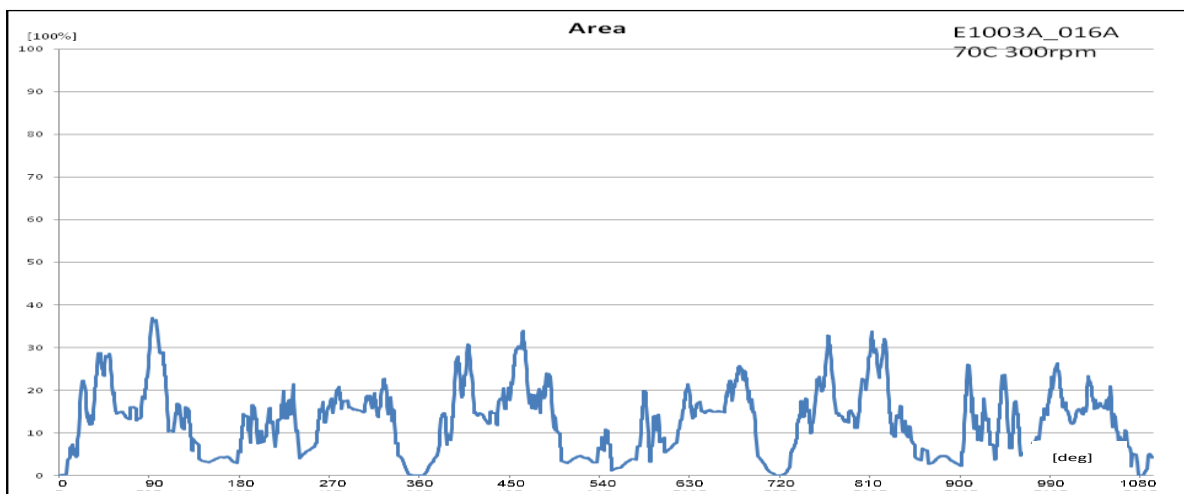


Figure 79 – Area Covered, E1003A_016A, 0.005L/Min, 70C, 300RPM

The kinematic viscosity is also linked to the way the lubricant cavitates, where a lubricant with high KV will present a lower total area of cavitation and lower KV a higher area of cavitation. This is also depended on the formulation of each lubricant thus why at the end of this chapter there is an additional lubricant-by-lubricant comparison between lubricants of the same base group where the formulations and their link to the physical properties and cavitation are further analysed. The patterns that the area of cavitation follows are repeatable as per the testing conditions, something that is also explained in further detail in the repeatability chapter of this report. The patterns are also repeatable for every cycle and they show similar behaviour at each step of the cycle. When all the different lubricants are compared against each other it is noted that the area covered by cavitation in all the individual tests is not the same across all the lubricants, but this depends on their individual

properties and formulation. The differences become more obvious at the point where the lubricants are compared against each other. The differences start with the overall lubricant behaviour and are directly linked to their individual formulations.

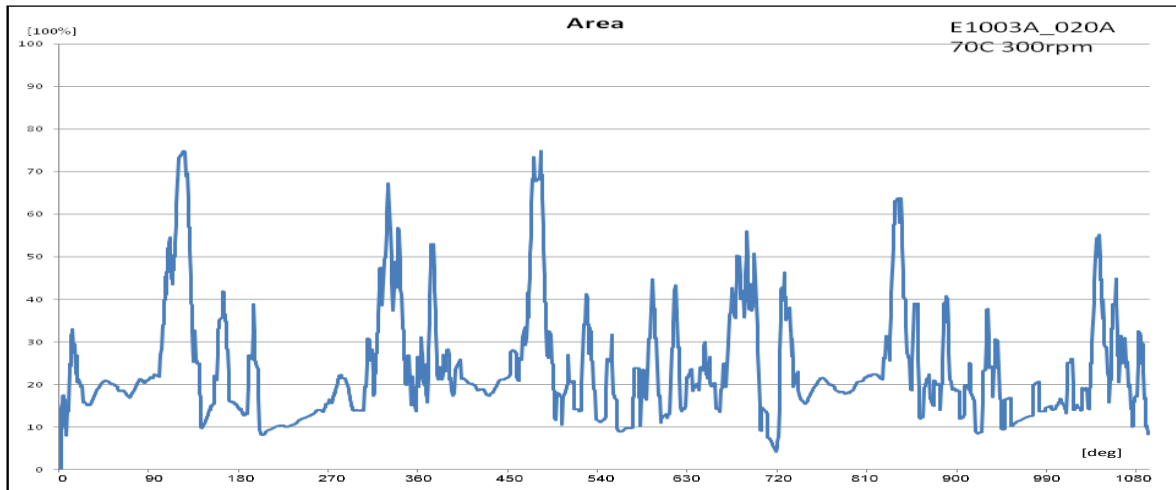


Figure 80 – Area Covered, E1003A_020A, 0.005L/Min, 70C, 300RPM

Area covered 0.005L/Min 70C 600rpm

The following set of images present the behaviour of cavities for the area they cover when tested on the lubrication test-rig at a speed of 600RPM and a flow rate of 0.005l/min while the temperature is at 70C. The data are in a percentage of the total ring area against the rotational crank angle. Figure 81 presents the area that the developed cavities occupy at a flow rate of 0.005l/min for lubricant sample E1003A_003A. This flow rate is the rate at which the lubricant is fed into the cylinder-liner and piston-ring interaction. The feed is performed through a number of small injectors located very near the interaction.

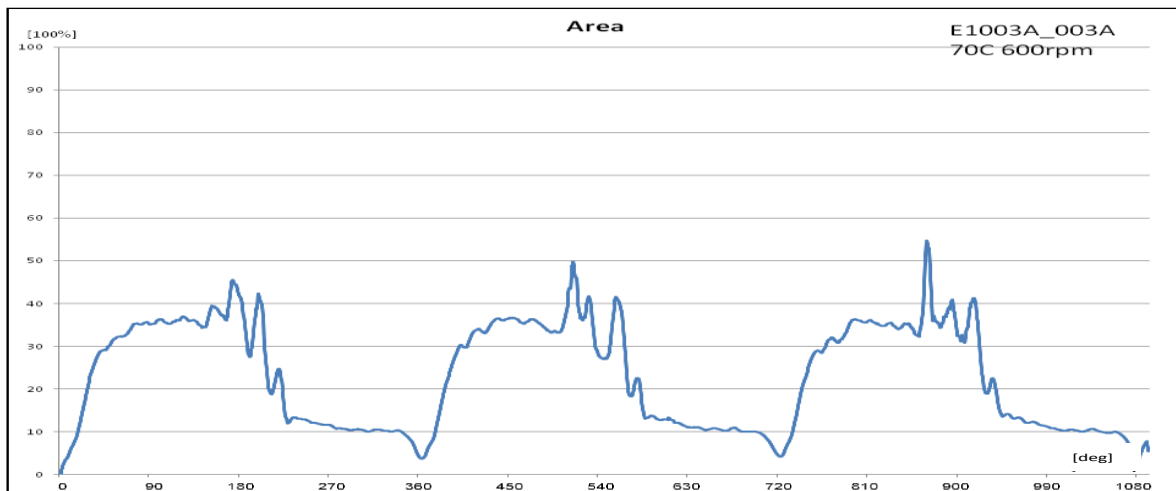


Figure 81 – Area Covered, E1003A_003A, 0.005L/Min, 70C, 600RPM

Lubricant 003A despite the higher speed presents a very similar curve as it did at the lower speed. This is an observation that is true for all the lubricants tested in this batch, with one exception. Lubricant 020A appears as it is following a different pattern than in the lower speed. This is mainly due to the software performance which appears to be better at the lower than the higher speed. The higher the speed the greater the oil film between the piston ring and the cylinder liner as described by A. Dhunpant. The greater oil film thickness will allow for a greater area where the light can be reflected thus making it easier for the software to detect the information. Figure 82 shows lubricant E1103A_004A which presents great similarity with 003A for the same speed. These two lubricants despite being of a different base group present a lot of similarities in relation to their KV70, as they are the two lubricants with the highest KV70 in the entire lubricant matrix.

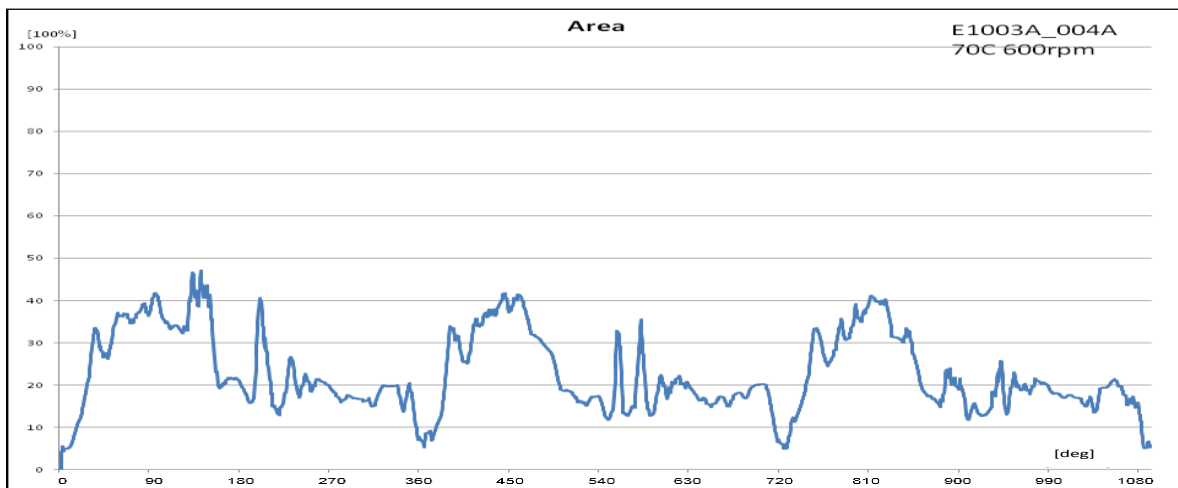


Figure 82 – Area Covered, E1003A_004A, 0.005L/Min, 70C, 600RPM

Lubricant 003A has a KV70 of 45 cSt and 004A a KV70 of 40 cSt. They also present different densities and viscosities with 003A having VI equal to 104 and Density equal to 0.89 where 004A has VI equal to 144 and Density of 0.85. Their differences become obvious every 180 degrees where each cycle ends. Lubricant 003A will reach a cavitating area of about 50% of the total area of the ring and then will gradually collapse until it enters the next cycle where 004A will also reach a cavitating are of about 50% but then this will student drop until the next cycle where new cavities have developed.

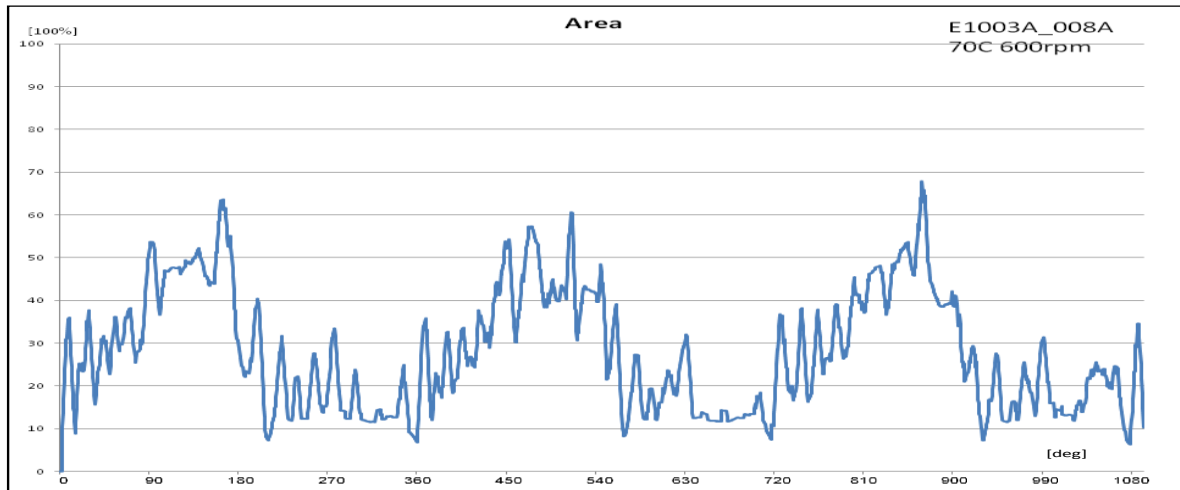


Figure 83 – Area Covered, E1003A_008A, 0.005L/Min, 70C, 600RPM

Even though 004A presents a more disturbed curve it also shares a lot of similarities with lubricant 003A. The most distinct observation is that they both follow a repeatable pattern that is directly linked to the position of the liner. In automotive engines, the position of the piston is measured in degrees of angular crank shaft movement. In the case of the lubrication test-rig the moving part is not the piston but the liner thus, the position at each individual moment is in relation to the movement of the liner.

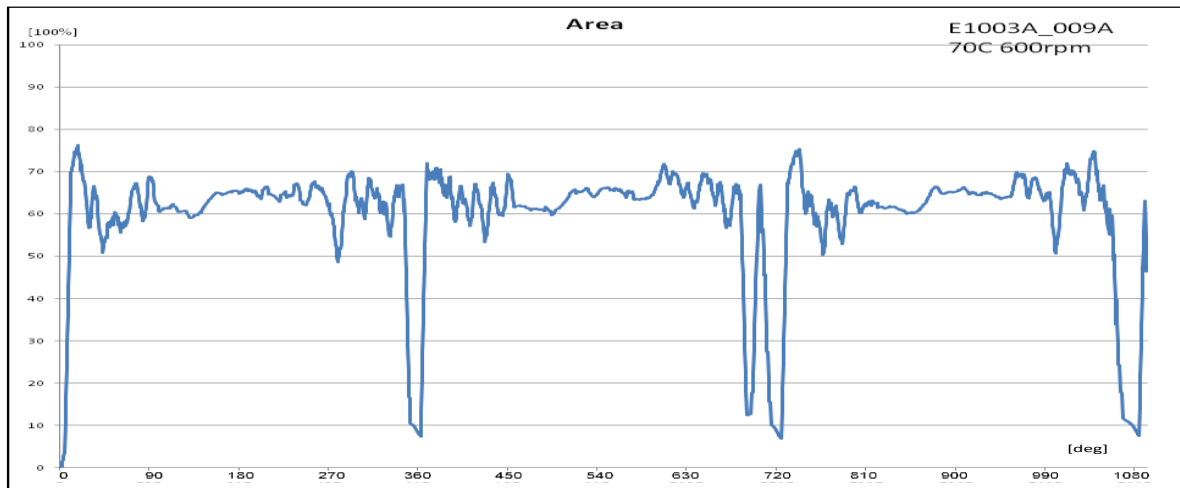


Figure 84 – Area Covered, E1003A_009A, 0.005L/Min, 70C, 600RPM

Figure 83 presents sample E1003A_008A for a total of 3 consecutive cycles. The behaviour of cavitation in regard to the area it occupies is directly linked once again to the position of the liner. This specific sample presents a profile that is more disturbed than the rest of the samples. What is observed is that lubricant 016A shows the same disturbance over its profile. This is particularly interesting as these two lubricants are part of the same base group with the

same add-pack. Sample 016A has an additional viscous modifier but their individual properties in regard to KV are very close to each other with 016A having a lower KV70 of 19 cSt where 008A of 20 cSt which explains the higher cavitating area of 008A. Despite the repeatability of the behaviour of these two samples, the pattern of the curve is spiking at a higher rate than samples E1003A_003A or E1003A_004A. The specific behaviour of each lubricant is also linked to the basic formulation of the sample as described earlier on. A distinct example is lubricant E1003A_009A where it presents a curve pattern very much different to the other lubricants in the batch but very similar to the pattern it presents for the lower speed at 300RPM. It is worth mentioning again that lubricant 009A is the lubricant with the lowest KV70 in group 1. The area under the graph is much higher than all the other samples and there is also a greater overlap in the cavities generated on the upstroke and down stroke. It has been indicated that the basic operation of the lubrication test-rig is based on the basic principles of a reciprocating internal combustion engine. The motion of the liner directly affects the generation of cavities at every part of the cycle. Depended on the movement and the direction of the liner the cavities will initiate either on the upper or the lower side of the ring.

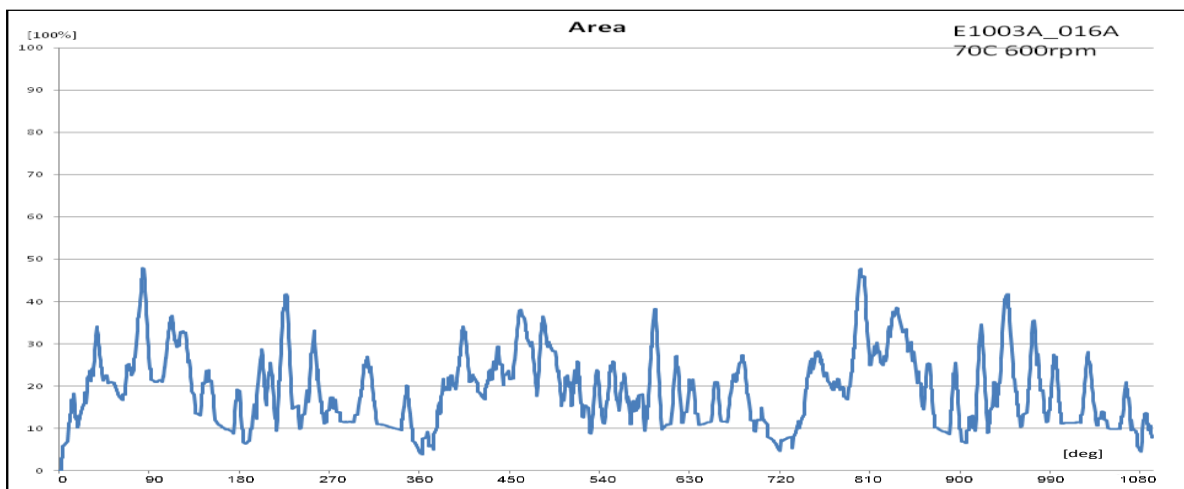


Figure 85 – Area Covered, E1003A_016A, 0.005L/Min, 70C, 600RPM

This observation dictates that when cavities are generated on one side of the ring, they have already collapsed on the other. This is not the case with lubricant E1003A_009A. This specific lubricant shows that there is a point between the cycles where cavities are present on both sides of the piston-ring simultaneously. That is mainly due to the fact that despite the new cavities that have been generated on the upstroke the collapsing cavities on the down stroke have not fully collapsed yet. This continues to the point where the recently generated

cavities have fully developed. This is again linked to the low KV70 that this lubricant presents for this specific group. The low KV suggests that this lubricant will offer reduced frictional losses and emissions but when it comes to component protection it will not offer the same level as the second lubricant in the same group (003A) with the higher KV. Figure 85, presents the area of cavitation for lubricant sample E1003A_016A. This specific lubricant shows a very “disturbed” profile and a lot of similarities with lubricant E1003A_008A. The similarities in their behaviour related to cavitation show a very similar profile. This can be link to their basic formulation as they both belong to base group 3 with the same add-pack. Lubricant 016A has an additional viscous modifier that increases its viscosity to the highest value in the group which also explains the higher cavitating area of 008A. The next lubricant 020A in figure 86 is the next lubricant in the matrix that features a viscous modifier as 016A does. Lubricant 020A is based on group 4 which is the same group as lubricant 004A. They both have the same add-pack but 020A has an additional viscous modifier.

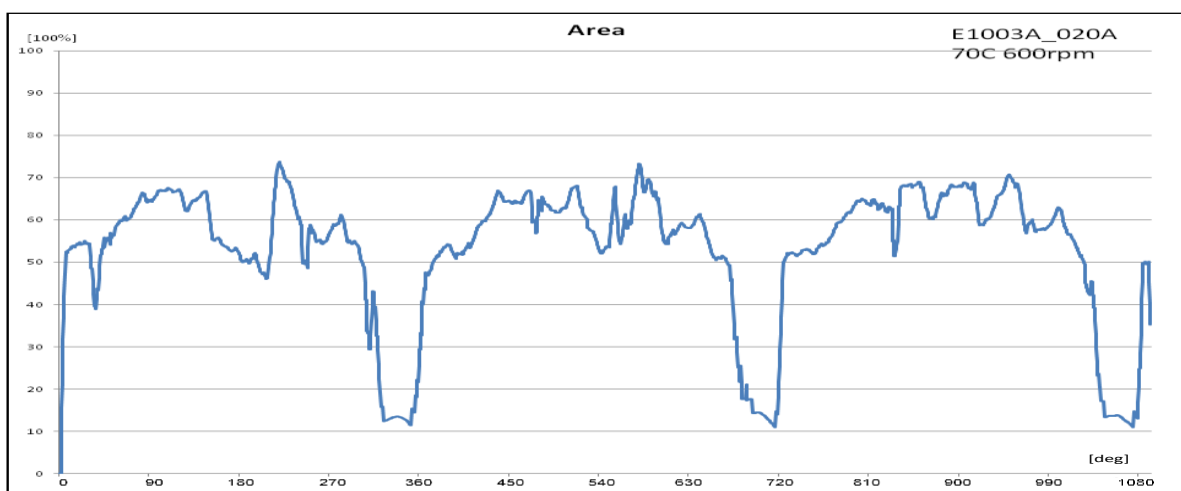


Figure 86 – Area Covered, E1003A_020A, 0.005L/Min, 70C, 600RPM

Lubricant 004A has one of the higher KV’s in the group and where both lubricants 004A and 020A feature similar densities and viscosities. The lubricant with the higher KV presents area of cavitation and pattern that fall close for the two tested speeds. When it comes to lubricant 020A this is not the case, the lubricant presents a much higher area of cavitation which comes close to the one observed with sample 009A. Based on that observation it is worth mentioning that lubricants 009A and 020A present no fundamental similarities in regard to their formulation except that they both feature the lowest KV within their individual groups. The findings support that there is a direct link between lubricants and cavitation with kinematic viscosity and mainly KV70 as the testing occurs at 70C. The comparison becomes

more apparent when the lubricants compared are based on the same oil group than samples from different oil groups which can present different behaviours for similar values of the features mentioned above. For this exact reason, the comparison continues at the end of this chapter for lubricants within the same group.

Number of Cavities 0.005L/Min 70C 300rpm

In this section figures 87 to 92 present the number of cavities as they develop at every part of the cycle. The number of cavities is directly linked to the formulation of the lubricants as well as the testing conditions. The extraction of the number of cavities is one of the trickiest attributes acquired from the data. The detection of cavity length and area posed to be a much easier task as these features cover a larger area on the image frames thus making the job of the Matlab algorithm easier as it gives a wider area to detect. The processing software faced certain limitation that did not allow for the extraction of data along the full cycle for this particular metric. Prime examples are lubricants 008A and 016A in figures 89 and 91 where the processing software faced difficulties in extracting the full cycle.

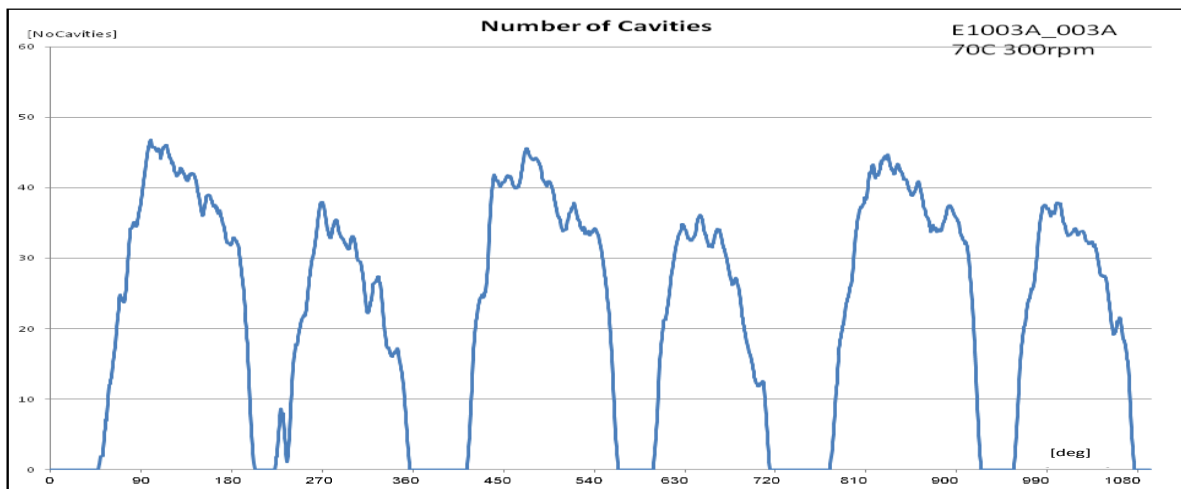


Figure 87 – Number of Cavities, E1003A_003A, 0.005L/Min, 70C, 300RPM

This is a very interesting observation as both of these lubricants are part of the same base group with the later one featuring an additional viscous modifier. Another interesting observation is that the lubricant with the added viscous modifier though earlier on it presented a higher cavitating area it now offers smaller but with more cavities than the one without the viscous modifier. This might seem confusing but when the width is added to the equation this difference makes more sense.

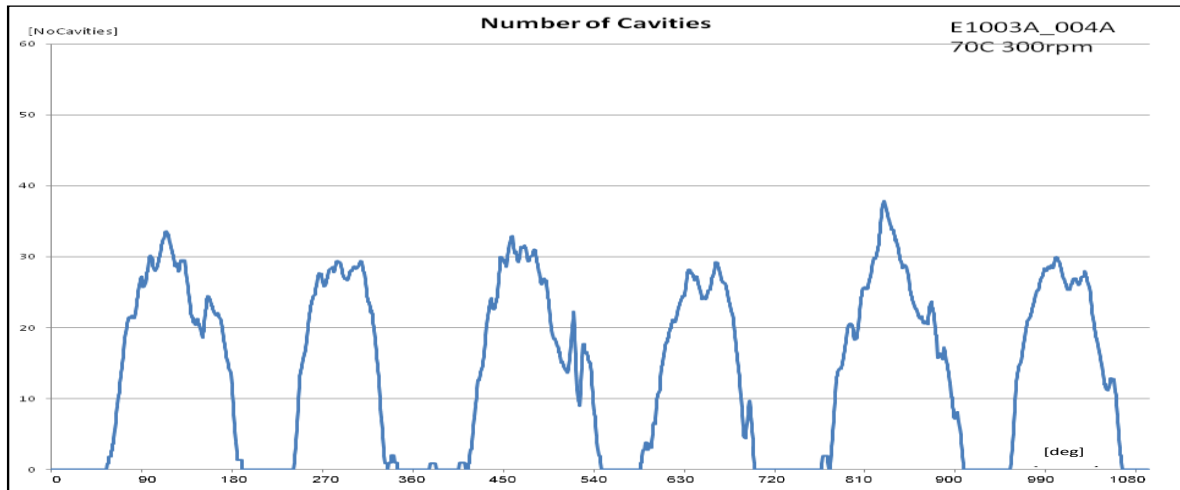


Figure 88 – Number of Cavities, E1003A_004A, 0.005L/Min, 70C, 300RPM

The sample with the viscous modifier might offer less cavities but these are of a greater length and cover a greater area on the piston ring. The reasoning behind the difference in the shape is assumed to be due to internal forces that prevent the generated cavities from merging together in order to form bigger cavities, but this is an area where the calculation of Reynolds number along with the density would add a greater value. This conclusion is based on the work performed by D. Quere at ESPCI university in Paris in 2005 where they carried out testing to identify the link between the shape of a cavity and subsequently the length and width to the physical properties for the fluid.

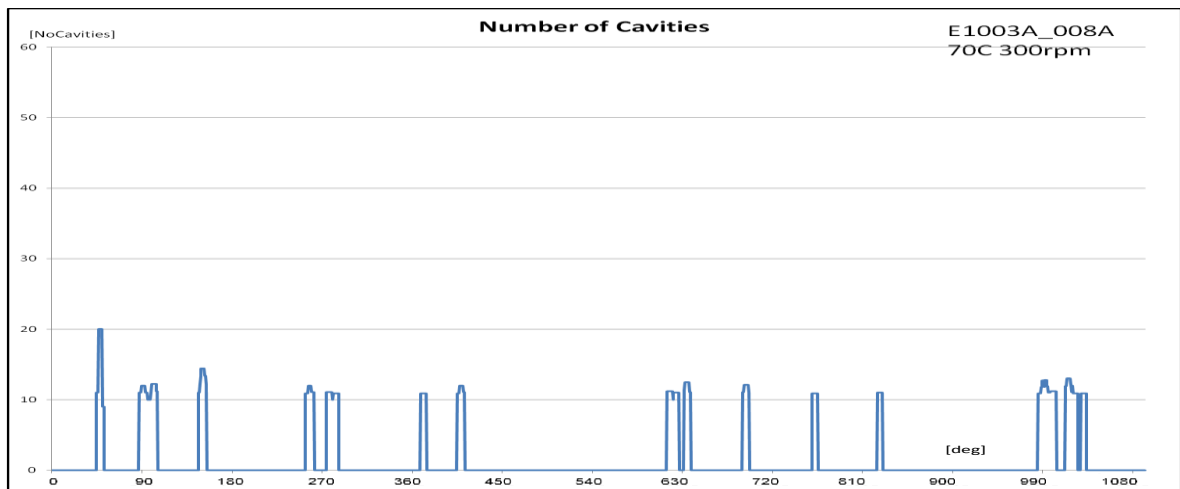


Figure 89 – Number of Cavities, E1003A_008A, 0.005L/Min, 70C, 300RPM

They suggest that there is a direct link between the density and Reynolds number. Considering this two samples have very similar features and values the calculation of such a parameter will shed some extra light to why the lubricant with the additional viscous modifier

presented a larger number of cavities. As explained at earlier stages of this report values related to the pressure, friction and oil film thickness were not extracted for the testing thus why Reynolds number cannot be accurately calculated for each individual sample. The analysis of the remaining lubricants showed that the number of cavities is particularly affected if lubricants of different formulations are tested and compared against each other. The temperature, the flow rate and all the specific testing conditions play their part and influence the total number of the cavities generated. Figure 87 shows the number of cavities present for a total of 3 cycles, a full 360 degrees' cycle for each of the graphs shows two high peaks. Each area under the peak is related to the number of cavities present in each individual stroke. The first peak in figure 87 shows the number of cavities on one side of the ring and the second peak is the cavities generated on the opposite side of the ring in the next stroke. It is easily observed that the behaviour follows a repeatable pattern.

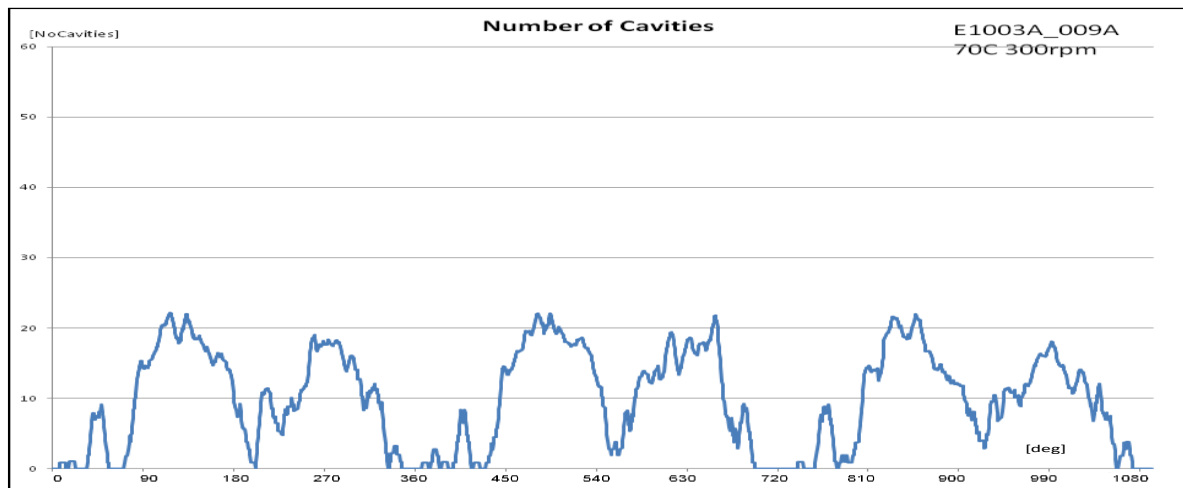


Figure 90 – Number of Cavities, E1003A_009A, 0.005L/Min, 70C, 300RPM

What is particularly interesting is that while analysing the cavitating area the specific sample presented an overlap between the cavities on the upstroke and the down stroke. The cavities at some stage in their collapse and development pass through the finger type cavities and form a cavitating sheet. This cavitating sheet is captured by the software as a single cavity thus why the gaps in the number of cavity graphs usually appear. The same graph shows that the cavities generate and collapse at the same rate and with the same profile in both the upstroke and downstroke. This is also the case with the remaining samples in the batch except the two that were mentioned earlier on where the processing software failed to capture data for a full cycle. In the majority of the tested lubricants the cavities present on the upstroke are

higher than the number of cavities on the down stroke. Similar behaviour is observed in figure 88 and lubricant E1003A_004A.

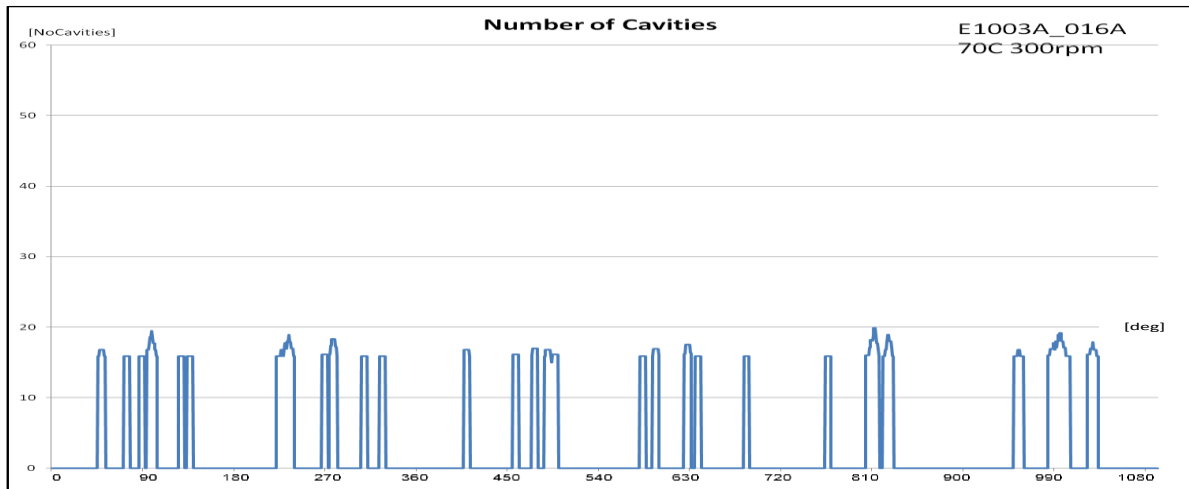


Figure 91 – Number of Cavities, E1003A_016A, 0.005L/Min, 70C, 300RPM

This specific lubricant is part of the 4th base group as is sample 020A. In a similar manner, as with lubricants 008A and 016A where they were both part of the same group but the lubricant with the viscous modifier presented a lower number of cavities, the lubricant with the viscous modifier once more presents a lower number of cavities. This suggests that there is a direct link to the number for cavities and the viscous modifier used in the samples. Unfortunately, due to confidentiality the composition of the viscous modifier has not been made available something that would have added a great insight to why this viscous modifier has such an effect on the number of cavities present in the lubricant.

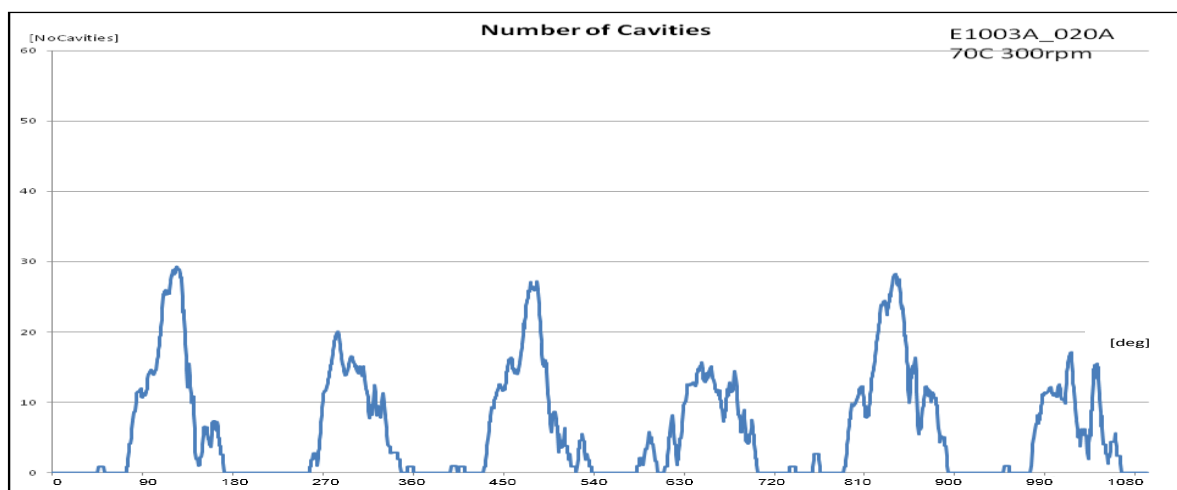


Figure 92 – Number of Cavities, E1003A_020A, 0.005L/Min, 70C, 300RPM

Between lubricants 003A and 004A, lubricant E1003A_003A presents more cavities in the up-stroke than the down-stroke where lubricant E1003A_004A shows similar number of cavities in both the up-stroke and the down-stroke. These two lubricants feature similar KV70s but very much different viscosities and densities. They are also part of different base groups, group 1 and group 4 respectively. Figure 89 and lubricant E1003A_008A as described earlier on is a good example of the difficulties that the processing algorithm faced when processing the raw data. The vast amount of data captured made the manual processing of the data an impossible manual task and the use of a custom-made algorithm was the only solution of ensuing accurate and efficient processing. The use of a computer software to automate the processing of the data comes with a few compromises. One of these compromises is the certain limitations that are related to the specific behaviour of each lubricant. Some of the tested lubricants feature finer cavities which makes their detection by the software a challenging task. The smaller the width the harder it is for the software to pick up the boundaries of the individual cavities. In the specific case of lubricants E1003A_008A and E1003A_016A in figures 89 and 91 respectively the processing algorithm failed to capture the number of cavities for the full cycle. There were individual instances where the algorithm picked the number of cavities at certain points of the cycle, but it could not capture the full profile of the curve, there is a relation between lubricants of the same group and the number of cavities. The lubricants presented in this section are later on analysed in groups as per their basic composition and these are compared to the way they cavitate.

Number of Cavities 0.005L/Min 70C 600rpm

The following figures represent the number of cavities generated while testing the samples at a temperature of 70C, a speed of 600RPM and a flow rate of 0.05l/min. The lubricants from figures 93 to 98 have all been tested under the same conditions. All the lubricants showed very similar behaviour with the main differences being the magnitude in the number of cavities. The higher speed has offered better quality results for all the tested lubricants. Big contributing factor is the grater with the cavities feature in the higher speed. A distinct example is lubricants 006A and 008A where the software managed to capture data for the full cycle in comparison to the lower speed where it had only offered sporadic data at different parts of the cycle.

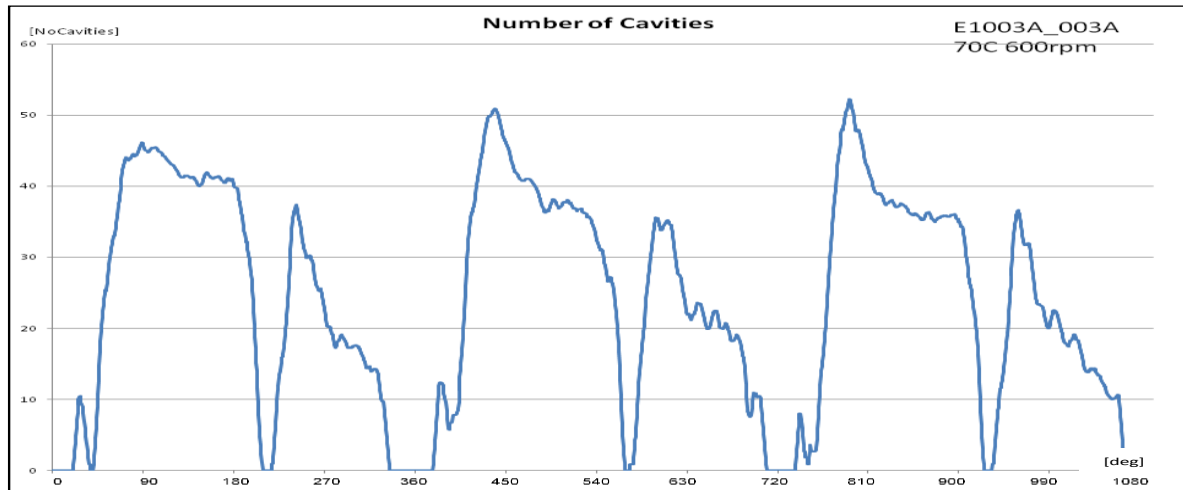


Figure 93 – Number of Cavities, E1003A_003A, 0.005L/Min, 70C, 600RPM

Figure 93 shows the number of cavities that are generated for lubricant E1003A_003A and what is immediately observed is the difference in the number of cavities between the up-stroke and the down-stroke. This observation is the same for all the lubricants in the batch and when it is compared with the lower speed the comparison shows that despite lubricants like as 004A showed cavities of similar numbers the higher speed constantly offers greater number of cavities on the upstroke that the down stroke for every sample of every cycle. This phenomenon is mainly based of the way the test-rig has been designed. The cylinder liner is free from restrictions on its upper part while it pivots on the lower one. The higher the speed the greater the hydrodynamic effect which increased the oil film thickness as this is supported by A. Dhunput and the work he did on oil film thickness on the test rig. One more observation that A. Dhunput made was that despite the fact that the ring has a curved profile that it is not the only factor that contributes to the gap created between the piston ring and the cylinder liner. Since the cylinder is pivoting on the bottom dead centre and while it is known that the higher the speed and the higher the lift of the cylinder liner, this will create a triangle which will always introduce a gap on the top side of the ring greater than the lower side of the ring. Furthermore, the higher the speed the more noticeable the effect. This is the main reason behind the noticeable difference between the down stroke and up stroke while the speed increases.

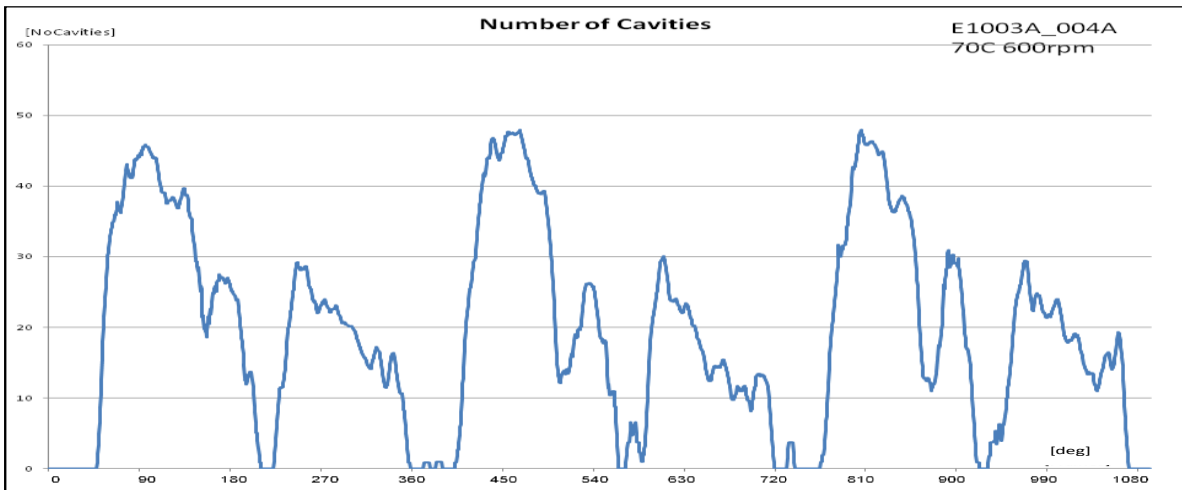


Figure 94 – Number of Cavities, E1003A_004A, 0.005L/Min, 70C, 600RPM

Despite the number of the cavities generated the profile for all the runs shows great similarities. Figure 93 presents the number of cavities generated for 3 consecutive cycles for the sample E1003A_004A. Lubricant 004A is part of base group 4 which contains also lubricant 020A. When comparing these two lubricants it is obvious that at this speed the number of cavities and the profile of the curve shows a lot of similarities. This is something that has not been observed at the lower speed. At the lower speed, the number of cavities between the two lubricants showed a few differences and this came down to the additional viscous modifier and the individual KV70 since the remaining were very close. At this higher speed, the differences seem to be ironed out and the lubricants come very close to each other. It will be a useful addition the repetition of the measurements at a higher speed to confirm that this observation is linear, and it increased along with the rotational speed.

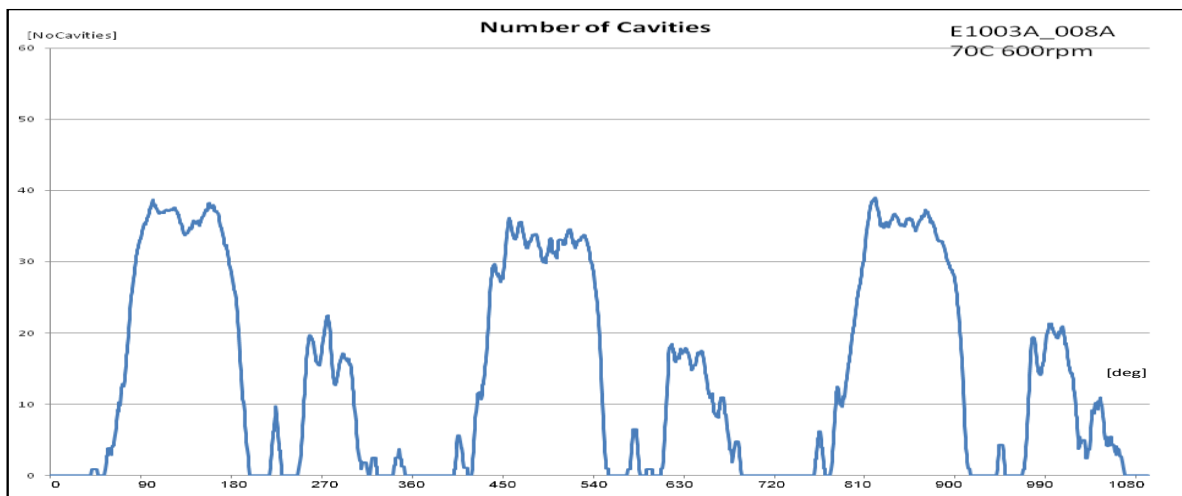


Figure 95 – Number of Cavities, E1003A_008A, 0.005L/Min, 70C, 600RPM

This is not thought the case with lubricants 003A and 009A. These lubricants as with 004A and 020A are of the same base group and they both feature the same viscous modifier. Their main differences though are with their individual values related to KV70 as Density and Viscosity are relatively close. These two lubricants offer KV70 of 45 cSt for lubricant 003A and 21 cSt for lubricant 009A. When comparing the data for both, lubricant 003A and 009A offer similar number of cavities throughout the cycle, what is different though is the profile of the curve which relates to how soon these cavities develop. Lubricant 003A develops the same number of cavities much sooner than 009A which eventually will reach the same value but at a later stage. For both lubricants, the upstroke cycle will always offer a greater number of cavities than down stroke. The similarities between these two lubricants are obvious. These similarities continue with the rest of the samples at the same test conditions. There is a predictable behaviour with lubricants that is presenting a higher number of cavities at the up-stroke rather than the down-stroke. Lubricant E1003A_008A in figure 95 when compared to the rest of the batch has a feature that differs from all the other samples at the same test conditions. The peaks of the curves appear to be flatter than all the other samples. The reason behind this behaviour is the fact that this lubricant maintains a relatively steady number of cavities once these are fully developed in each stroke. This is an event mainly seen on this specific sample. This sample is part of base group 3 which also contains lubricant 016A. In earlier sections, it has been a common observation that the lubricants within the same group would offer similar characteristics on the graphs, this is not true for these two lubricants. Lubricant 008A appears to be developing a greater number of cavities at an earlier stage and is capable of maintaining them for a longer period of time within the cycle, where lubricant 016A will develop them much later and will retain them for a much shorter period of time.

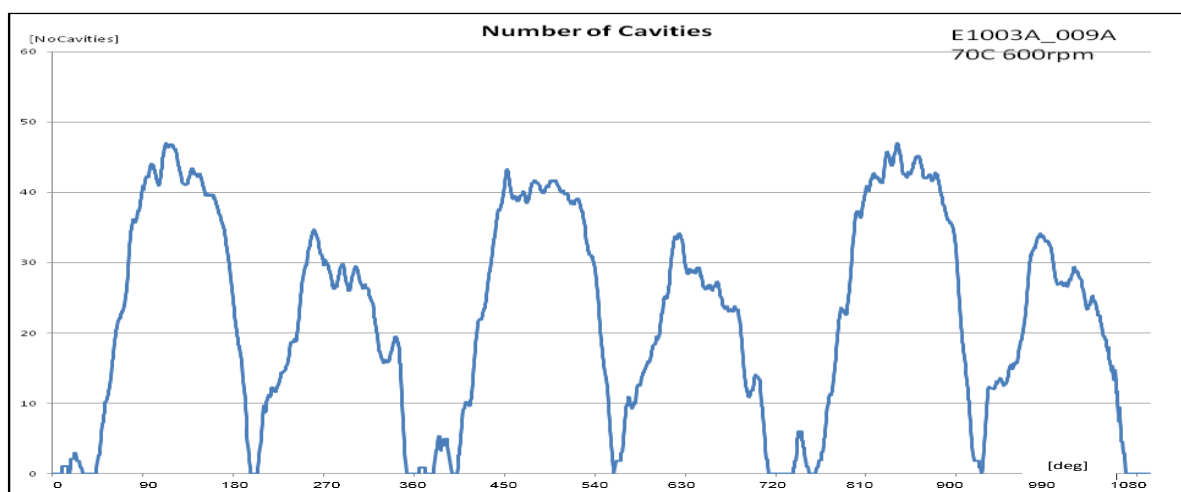


Figure 96 – Number of Cavities, E1003A_009A, 0.005L/Min, 70C, 600RPM

In general, there is a significant difference in the number of cavities between the up-stroke and the down-stroke where the number of cavities is significantly smaller in the down-stroke than the up-stroke. In figure 96 lubricant E1003A_009A shows a significant increase to the number of cavities compared to the previous lubricant in figure 95. The cavities are increasing in number very early in the cycle and maintain their number for a longer period than in the previous sample. Figure 96 shows a less disrupted profile than the previous lubricant.

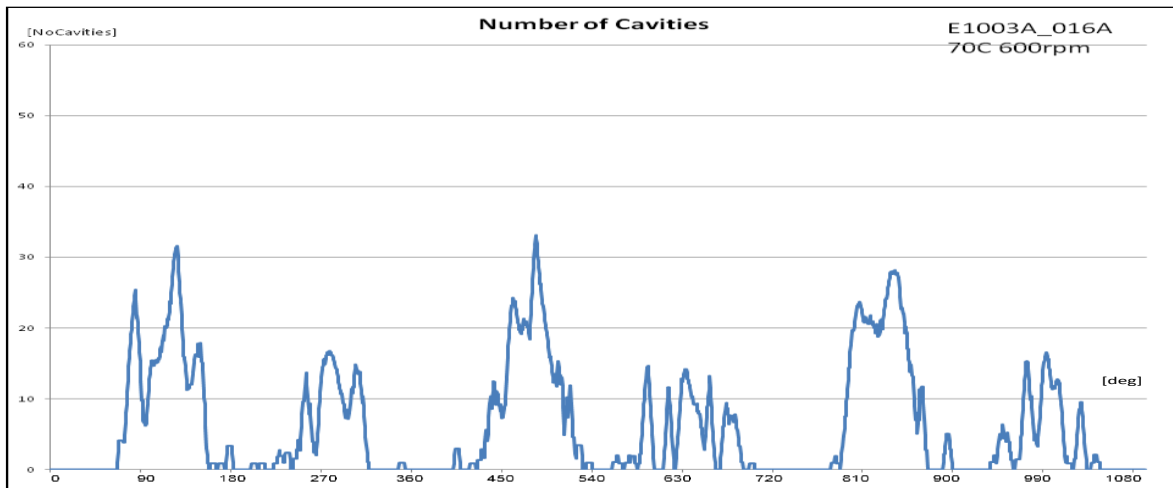


Figure 97 – Number of Cavities, E1003A_016A, 0.005L/Min, 70C, 600RPM

There are fewer gaps between the spikes and there are cavities present for a longer period throughout each cycle. All the differences are mainly linked to the physical composition of each lubricant. It must be noted that these two lubricants are not from the same base group but they both feature similar KV70 at around 21 cSt for 009A and 20 cSt for 008A, while having some of the lowest KSs in the entire batch. If these findings are compared with the total area analysed later on it is observed that lubricant 009A have covered a greater area than 008A. The figures on the number of cavities paint a similar picture, where the cavities at the up stroke are very similar between the two sample but the number at the down stroke appear significantly reduced. At a later stage, the width measurements show that both lubricants present similar cavity widths throughout the cycles. To complete the picture the measurement of the oil film thickness would have added a greater value in this comparison as this dimension is missing to conclude any distinct outcomes from the behaviour of the lubricants and the lubricant composition.

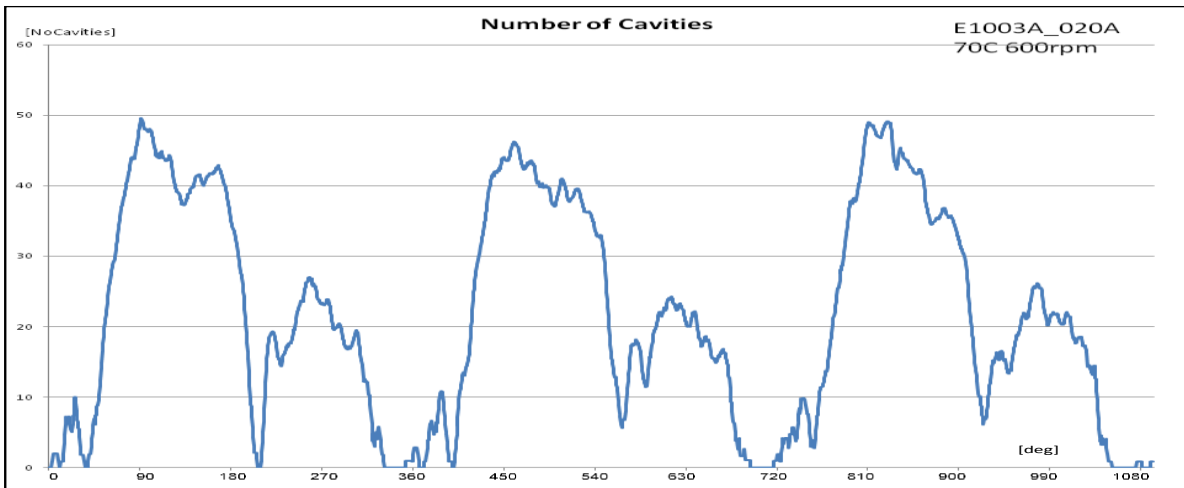


Figure 98 – Number of Cavities, E1003A_020A, 0.005L/Min, 70C, 600RPM

The next sample in figure 97 is on the opposite side of the spectrum. E1003A_016A shows a minimal number of cavities throughout each cycle, there are less cavities present than any of the previous samples. Sample 016A is a quite special sample within the batch, it is the only sample that contains a viscous modifier but at double the concentration of the 020A which is the only other sample with a viscous modifier. For the same sample, the curve that represents the number of cavities throughout the cycle appears more unstable than with the rest of the batch. The main cause is possibly the addition of an extra viscous modifier which is not present in most of other samples, E1003A_016A is one of the two lubricants in this batch of tested oils that has an additional viscous modifier. The other lubricant that uses the additional viscous modifier is sample E1003A_020A, though the concentration between the two is different. More specifically the Viscous Modifier in lubricant E1003A_016A has double the concentration of lubricant E1003A_020A. Figure 98 shows lubricant E1003A_020A which has been tested under the same conditions as the rest of the lubricants in this section. Both lubricants have the additional Viscous Modifier, but their overall performance is fundamentally different. That is mainly down to their different basic composition. Each of these lubricants belongs to a different base Oil Group. Lubricant E1003A_016A is of the base Oil Group 3 and lubricant E1003A_020A is of the base Oil Group 4.

Cavity Width 0.005L/Min 70C 300rpm

The following graphs from figure 99 to figure 104 are presenting information related to the cavity width for each individual lubricant for a total of 3 consecutive cycles. The profile of the graphs for the cavity width is distinct among the tested feature and is identified by the two spikes at the point of generation and the point of collapse. Figure 99 and lubricant

E1003A_003A present the distinct profile just described of the graphs related to the width of the cavities. It has been noted that the cavities start at a greater width than the one they maintain for the majority of each stroke.

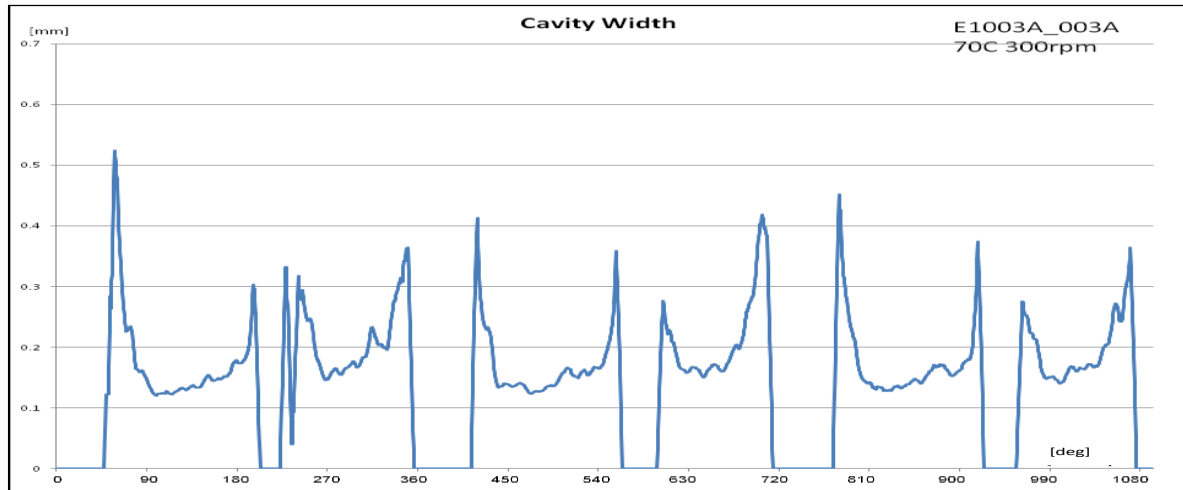


Figure 99 – Cavity Width, E1003A_003A, 0.005L/Min, 70C, 300RPM

This is caused by the way the cavities are generated. The cavities start their lifecycle with the release of air that is trapped within the lubricant. Air is dissolved in most of the fluids available and lubricants are not an exception. In average, an automotive lubricant contains 20% of air dissolved in its volume. When lubricants are stressed under extreme operating conditions the air dissolved is released and along with the high energy involved the air bubbles grow to what can be described as cavitation. These cavities are developed in a few basic stages that have been described and detailed in earlier chapters of these report. One of the first stages of the cavity generation is the development of Fern cavities. Unlike the fully developed cavities that present a finger like shape with their length being significantly larger than their width the Fern cavities expand towards every direction. This results in cavities being significantly wider at this stage than when they have fully developed. At the point of generation and as the cavities expand their width and length increases at similar rates. The more the cavities progress into the stroke the more they start to take their finger like shape. The cavities to expand and increase in while they decrease in width. This is the main reason why the graphs present the distinct “double-horn” profile seen in the majority of the lubricants tested at 300RPM. In the same respect, the second peak of the “horn” is related to a similar effect. Once the cavities have developed and increased in length while they reduce in width there is a point in cycle where the cavities start to collapse. The second peak is mainly the result of the way these cavities are collapsing.

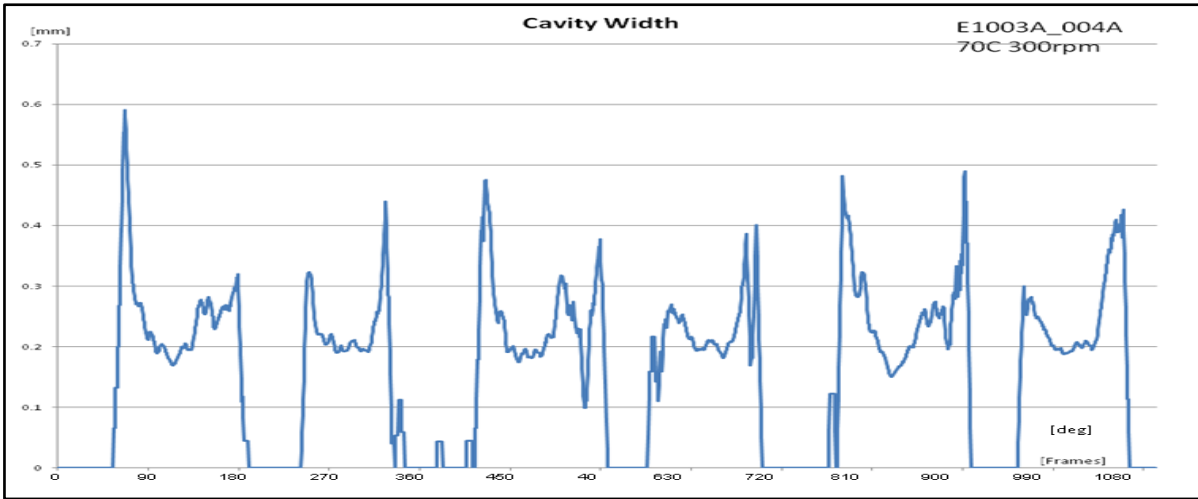


Figure 100 – Cavity Width, E1003A_004A, 0.005L/Min, 70C, 300RPM

The cavities are directly affected by the linear motion of the liner. After the liner, has reached maximum velocity and starts decelerating the cavities will start collapsing. First, the developing cavities are expanding in all directions until they fully develop into finger cavities but that occurs until the liner starts to decelerate and this is the point where the cavities start to collapse. At this point the cavities start to decrease in length and while the liner is decelerating the cavities start to slowly collapse.

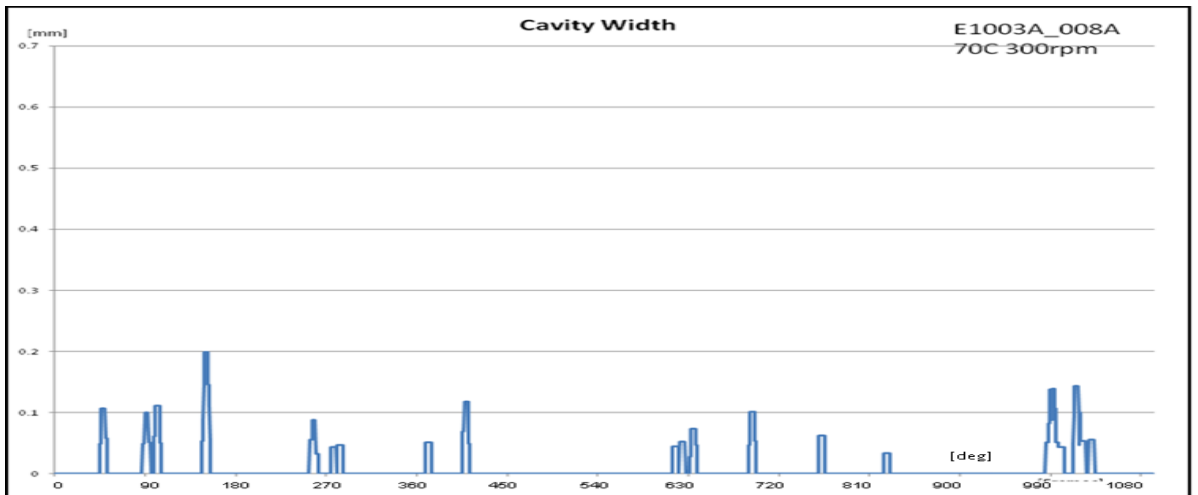


Figure 101 – Cavity Width, E1003A_008A, 0.005L/Min, 70C, 300RPM

The collapse is not instant; the cavities maintain their volume but at the same time they also decrease in length. While they decrease in length they start to increase in width. This continues up to the point where the liner has decelerated enough so that the cavities are not able to maintain their volume due to the reduced kinetic energy. At this point the cavities finally reduce in size and collapse. This collapsing of the cavities and the increase in width is

the cause of the second spike in the graph. While analysing the number of cavities for the lower speed of 300RPM there were two samples that had posed a difficulty for the processing algorithm to track. These two lubricants were the 008A and 016A. The same behaviour is observed when these two lubricants were analysed for their width at the same speed. It was mentioned earlier on that the limitation of the software to capture the number of cavities has been the failure of the software to successfully capture the width of the cavities, figures 101 and 103 present the data related to that event cause. The software was able to capture sporadically the cavity width, but it failed for the majority of the cycle. Both of the lubricants in these two figures are of the same base group 3.

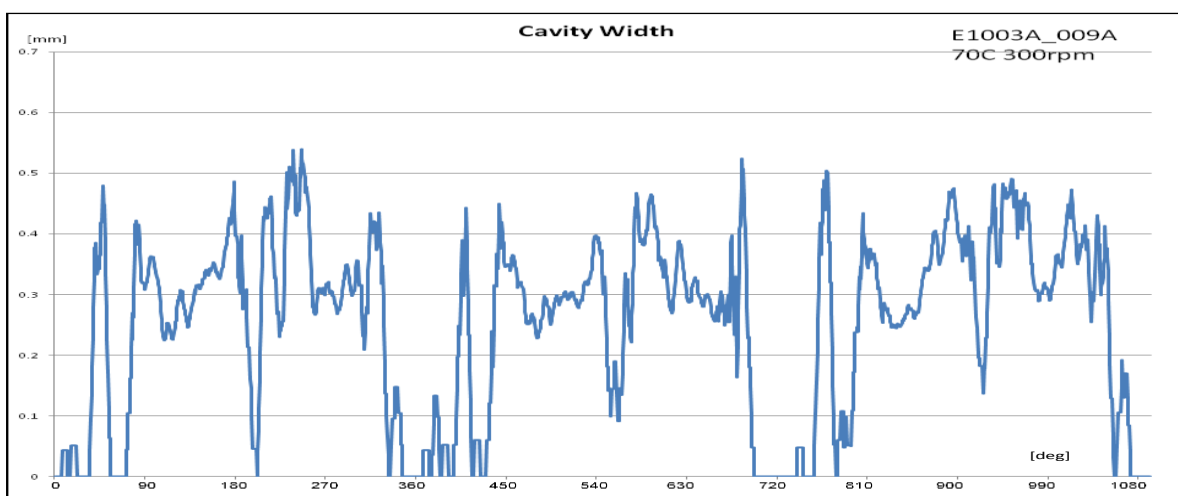


Figure 102 – Cavity Width, E1003A_009A, 0.005L/Min, 70C, 300RPM

Figures 99 and 102 show another two lubricants of the same group. Both sample 003A and 009A belong to the 1st base group and they both feature an additional add-pack without a viscous modifier. It is made obvious by the data that sample 009A is maintaining a higher width than 003A and features a more disturbed profile throughout the cycle. Samples 003A and 009A when their kinematic viscosities are observed, 003A has a KV70 of 45 cSt and the 009A of 21 cSt, The later sample following the observation on the area of cavitation and number of cavities was expected to be more prone to cavitation a link observed directly from the data. Lubricants 004A and 020A are also two lubricants of the same group. They both belong in group 4 and they both feature identical densities. When they are compared against each other it is noted that sample 020A does not follow the same pattern as the rest of the lubricants in the group. The same lubricant is one of the two lubricants that has an additional viscous modifier. The second lubricant that features a viscous modifier is lubricant 016A but

unfortunately the software could not extract enough information for the comparison to take place.

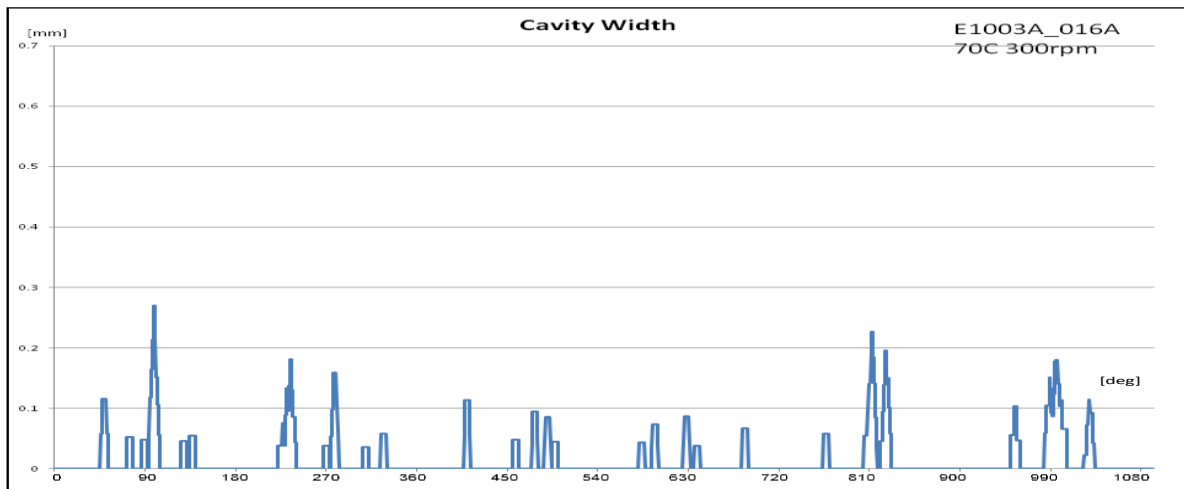


Figure 103 – Cavity Width, E1003A_016A, 0.005L/Min, 70C, 300RPM

When 020A is compared against 004A though it is understood that the additional viscous modifier has played a crucial role in the behaviour of the lubricant. Sample 020A shows that it does not cavitate in the same way as the rest of the batch. The fern cavities generated are of a smaller width and they stay at the initial fern stage from much shorter than compared with 004A. The cavities develop much sooner to finger cavities and once they develop they slowly decrease until they collapse. The viscous modifier has altered the properties of the lubricant to an extent where it does not behave as the rest in the same base group.

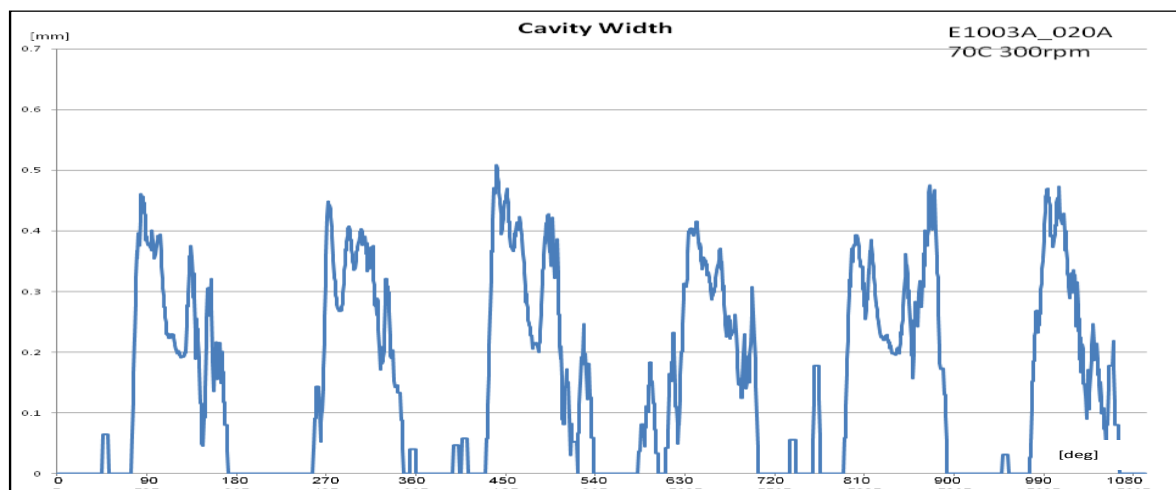


Figure 104 – Cavity Width, E1003A_020A, 0.005L/Min, 70C, 300RPM

Cavity Width 0.005L/Min 70C 600rpm

In this subsection, the following figures present the behaviour of the generated cavities in regard to their width. The test conditions are 0.05l/min flowrate and 70C at 600RPM. Figures 105 to 110 present the width of all the individual cavities from the point of generation up to the point where they collapse. The data are presented in a total of 3 consecutive cycles, which support the repeatability of the behaviour of the occurring phenomena. Figure 105 and figure 106 present the first samples of the lubricant matrix. These two lubricants despite being of a different base group with different basic properties present a very similar curve, this is also observed with the remaining lubricants. The only lubricant that presents a different behaviour is lubricant 016A which is one of the two lubricants with a viscous modifier and the one with the higher concentration of the additive.

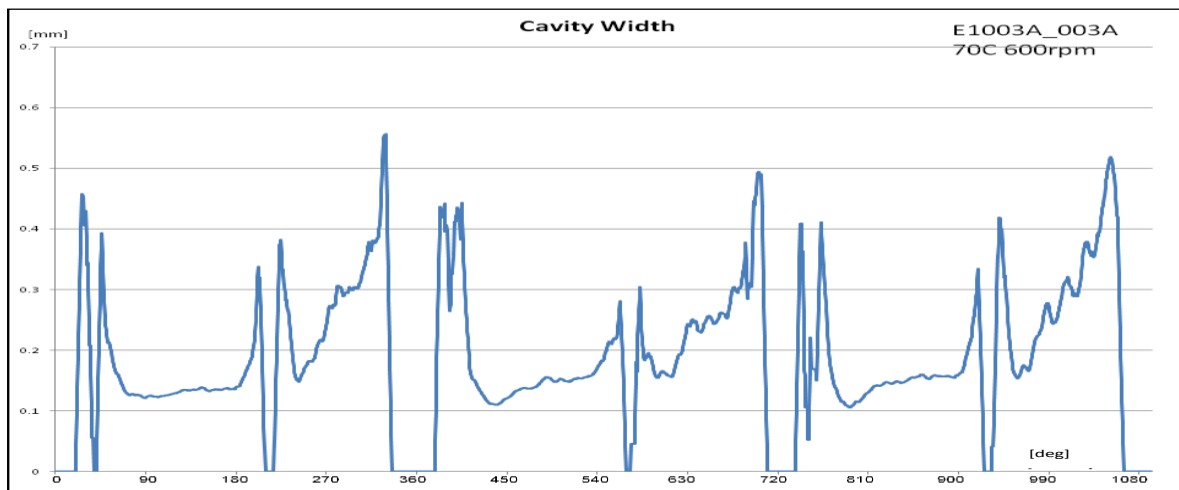


Figure 105 – Cavity Width, E1003A_003A, 0.005L/Min, 70C, 600RPM

The remaining lubricants present the “bull-horn” shaped curve first saw on the analysis of the cavitation width for the lower speed. As with the analysis of the number of cavities the higher speed offers a much better curve for all the graphs. Figures 105 and 108 present lubricants 003A and 009A, these two lubricants are part of the same base group and they both have the same add-pack but none of them has the additional viscous modifier. When figure 108 is inspected it is observed that the curve follows a pattern that is repeated every 180 degrees.

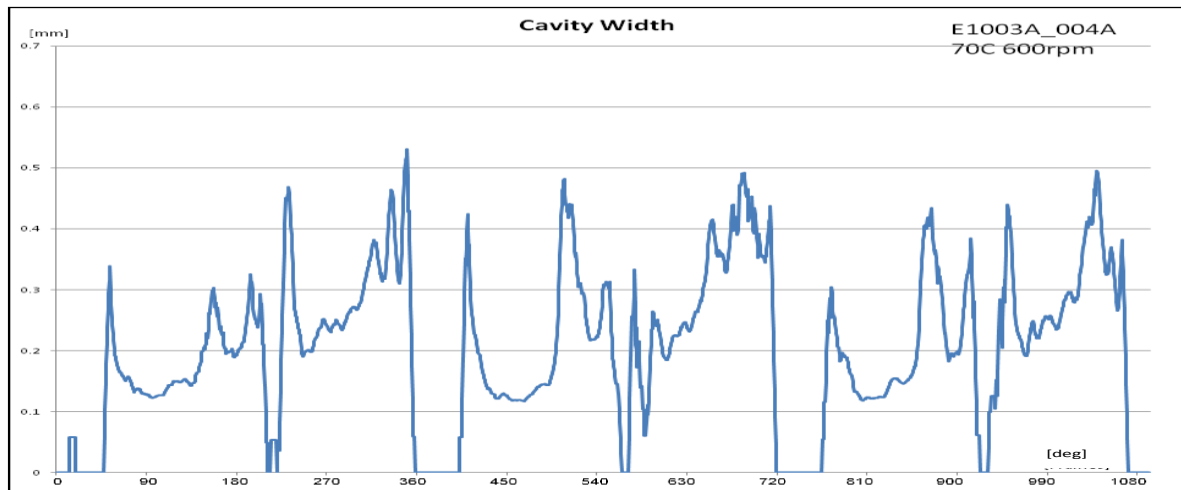


Figure 106 – Cavity Width, E1003A_004A, 0.005L/Min, 70C, 600RPM

This pattern shows that the leading spike of the curve is of a higher magnitude than the trailing spike of the same curve. When this is compared with figure 105 and lubricant 003A the differences become obvious. The curve in this figure follows a different pattern. This pattern is repeated every 360 degrees and is different for the upstroke and the down stroke. In this pattern, the initial stroke shows a leading spike of a higher magnitude and a trailing spike of a lower magnitude. Moving on to the next stroke the pattern is reversed, in this instance, the leading spike is of the low magnitude and the trailing spike of the greater one. This spike is directly linked to the way the lubricant cavitates and how this is linked to the width of the cavities along the cycle. Lubricant 003A during the first stroke develops cavities that are wider during their generation rather their collapse and on the next stroke it develops cavities that have a smaller width than when they collapse. Lubricant 009A as seen in figure 108 will always have cavities that are wider at the point of generation than the point of collapse. Considering that these two lubricants have viscosities and densities very close to each other and since they are part of the same base group the differences come down to the Kinematic Viscosity. Referring back to the number of cavities present for these two lubricants in an earlier section the number of cavities for these two lubricants has been relatively similar throughout the cycles but where they differ is at the area of cavitation.

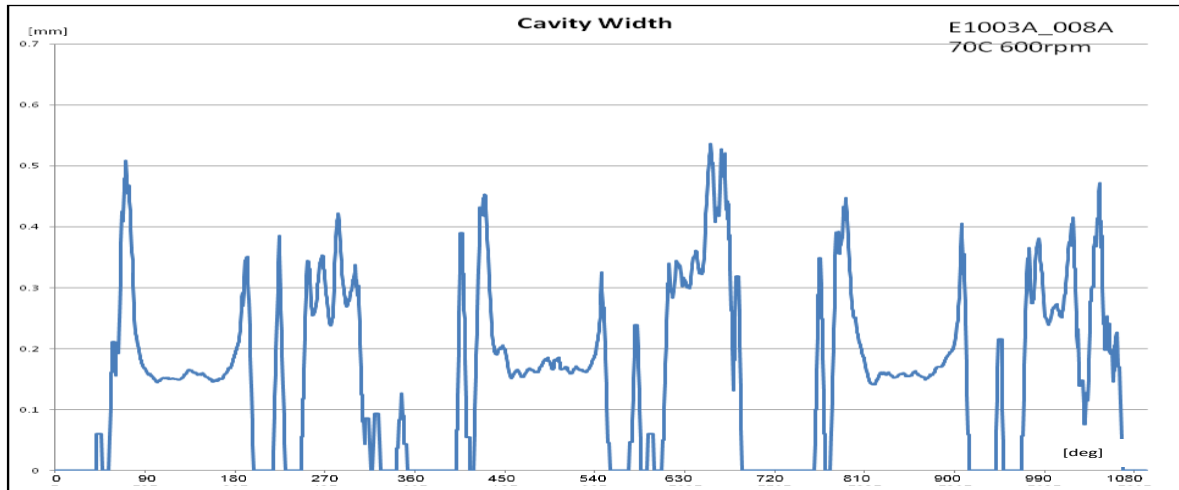


Figure 107 – Cavity Width, E1003A_008A, 0.005L/Min, 70C, 600RPM

When the area of cavitation is compared between 003A and 009A at 600RPM the area of 009A is much higher than 003A. To be more precise the area of 003A at its maximum peak could reach for a short period of time the 40% of the piston ring where the area of 009A would very early in the cycle develop at 70% and will remain there for the majority of the cycle. The different kinematic viscosities as also described in the discussion of the area has an effect in the way the lubricant cavitates.

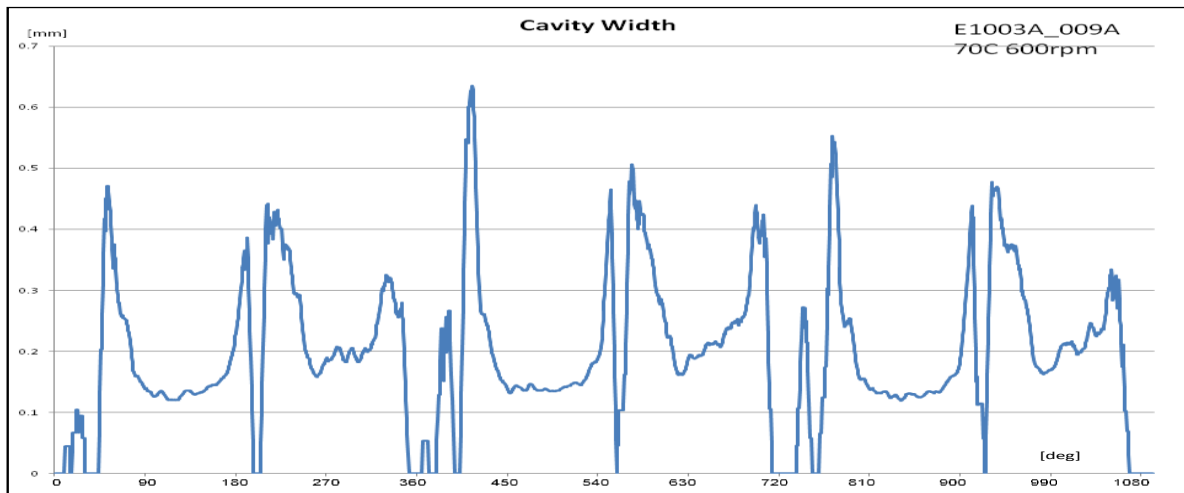


Figure 108 – Cavity Width, E1003A_009A, 0.005L/Min, 70C, 600RPM

Another observation in figures 105 and 108 is the gaps between the strokes is the stage of the cycle where the cavities have collapsed on one side of the ring, but no new cavities have generated in the opposite side. The cavity behaviour is linked and affected by the liner movement but that is not the case with the cavity response as well. The cavities respond with a delay in regard to the movement of the liner, meaning that even though the liner has

changed direction in certain samples the cavities are not immediately affected by that change. The majority of the samples showed a small delay when the liner changes direction to the point where the cavities react to that change. That is more obvious when the point where the cavities collapse is compare with the point where the liner starts moving in the opposite direction, a good example is figure 108.

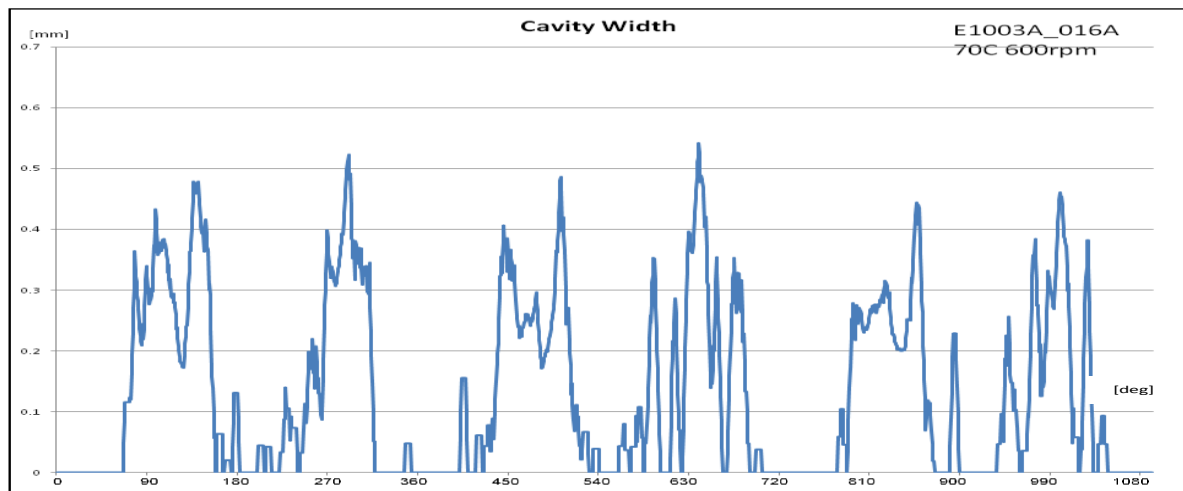


Figure 109 – Cavity Width, E1003A_016A, 0.005L/Min, 70C, 600RPM

Similar to the rest of the figures in this subsection this figure represents the average width of the cavities at any given point for a period of 1080 degree. The attention is drawn to the 180 degrees' mark and at the point where the liner has momentarily stopped, at this point the liner has stopped and changed direction. The 180 degrees turning point is a well-established fact and a fundamental design feature of every reciprocating conventional internal combustion engine that uses a piston and a crankshaft. In the same figure is noted that even though the liner direction has changed the cavities still maintain a certain width. Moreover, the cavities do not only reduce in width, but they also expand further for a short period before they finally collapse.

Figures 106 and 110 show another two lubricants that belong in the same group. Lubricants 004A and 020A belong in group 4 with 020A being one of the two lubricants that features a viscous modifier. The first lubricant in figure 106 has a quite distinct behaviour where the cavities seem to be overlapping from the first two strokes but not for the first two cycles. To further explain the observation the liner starts moving from 0 to 180 degrees and then at 360, at this point the profile of the cavity width appears to be continuous but when the piston passes further than the 360 degrees the cavities do not overlap with the next cycle. This exact same behaviour is observed with lubricant 020A. This lubricant also shows an overlap

between the two strokes of a cycle but not between the two cycles. This phenomenon can be linked to the design specification of the test-rig and to the piston rings distinct profile. When these two lubricants are compared closer it is observed that the overlap is more obvious for lubricant 020A. This is something that can also be linked to the area of cavitation at earlier chapter where lubricants 020A and 009A presented the higher cavitation area though the entire batch, reaching almost 70% of the total ring area.

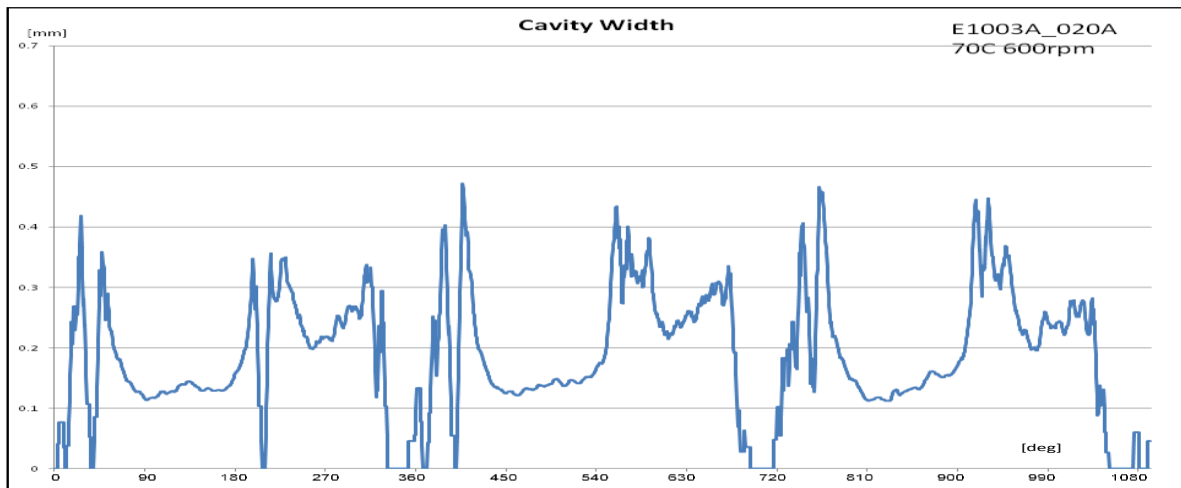


Figure 110 – Cavity Width, E1003A_020A, 0.005L/Min, 70C, 600RPM

The final base group contains lubricants 008A and 016A in figures 107 and 109 respectively. The 016A is the second lubricant with a viscous modifier and double the concentration of 020A. Once again as with the rest of the properties lubricant 016A offers a different curve than the rest of the lubricants. This lubricant not only has the additional viscous modifier but also the higher viscosity from the entire matrix. The very high viscosity explains why this lubricant is less prone to cavitation and why this is observed in the measurement of the area, the number of cavities and the width. Lubricant 008A on the other had offers a much more consistent curve and a pattern much closer to the rest of the lubricants. Lubricants 016A and 008A have a very special connection within the matrix, they are both of the same base group, they both have identical densities and values of Kinematic Viscosities very close to each other for 70C. Their main difference is the viscous modifier and the values of viscosity for both, where 008A has a viscosity of 139 and 016A a viscosity of 161. Their in-between comparison shows that the viscous modifies in this case has affected both the viscosity of the lubricant and its ability to resist cavitation compared to 008A.

Cavity length 0.005L/Min 70C 300rpm

In this section, the following figures from 111 to 116 present the average cavity length for the up-stroke and the down-stroke for the 6 tested samples. The Cavities generated during the up-stroke have been marked in “Blue” and the cavities generated during the down-stroke in “Red”. The captured length in contrast with the rest of the graphs presented in this report has been recorded separately for the up-stroke and separately for the down-stroke side.

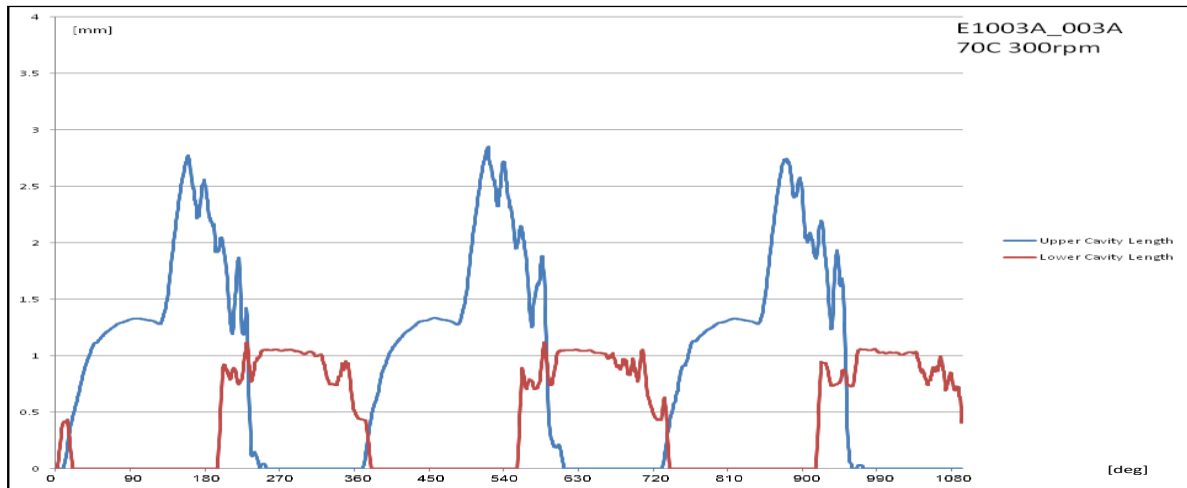


Figure 111 – Cavity Length, E1003A_003A, 0.005L/Min, 70C, 300RPM

The main reason behind that separation lies with the specification that had been set with the objectives of the project. When the first iteration of the software was developed, the length tracking module was the first module of the algorithm developed. For this exact reason, the cavity length module seats in the core of the software.

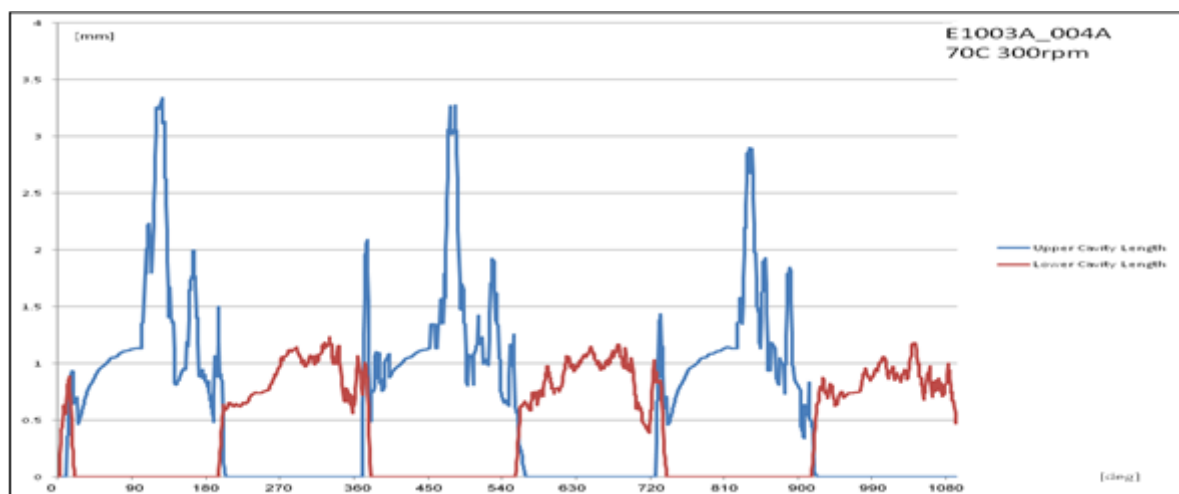


Figure 112 – Cavity Length, E1003A_004A, 0.005L/Min, 70C, 300RPM

It has been understood since the early stages of the project that the cavity length will offer more value if separated for the down-stroke and up-stroke side, as some of the lubricants have shown cavity overlap between the strokes. When the initial tests were carried out it was found that all the graphs recorded except the cavity length could be successfully represented as a sequence of up-stroke and down-stroke sequential data. All the data related to the lubricants were recorded at a constant rate through 3 consecutive cycles, this is not the case with the cavity length. For the cavity length, the software is treating the up-stroke and the down-stroke as two separate events and records the behaviour occurring on these areas in a different manner that with the rest of the dimensions. From all the parameters extracted from the samples, the length is one of the more interesting ones.

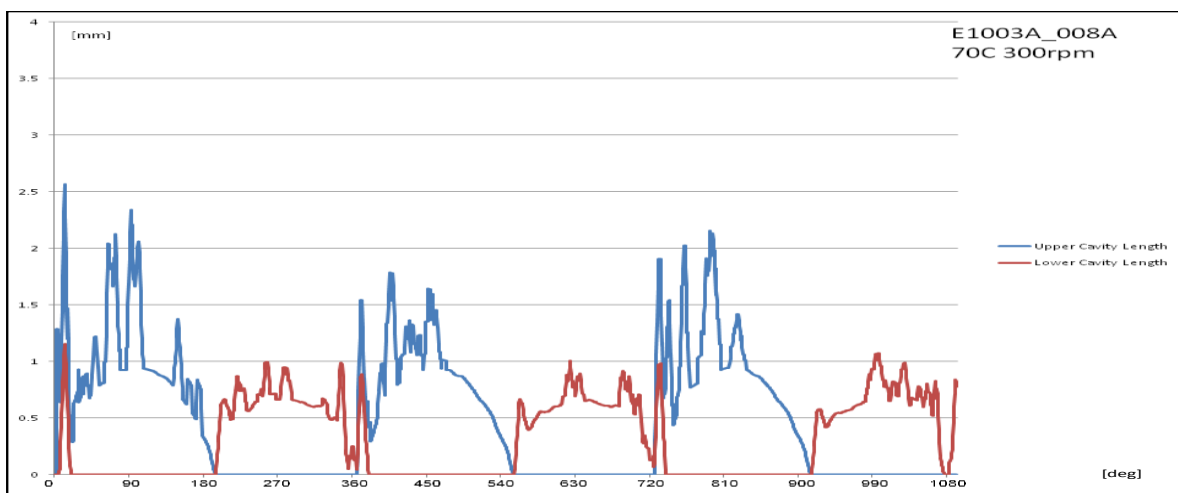


Figure 113 – Cavity Length, E1003A_008A, 0.005L/Min, 70C, 300RPM

Figure 111 and 112 shows two lubricants that are part of a different base group. Lubricants 003A and 004A are the only two lubricants that present a significant overlap between the up-stroke and the down-stroke. The overlap means that at some point in the cycle there are cavities present both on the top side of the ring and the bottom side of the ring. These two lubricants might not share the same base group but what they feature the highest KV70 in the group. It has been observed that the lubricants with the higher KV70 will offer a greater overlap than the rest of the batch. The first lubricant of the two (003A) is part of base group 1, the other lubricant in that group is 009A in figure 114. What is interesting in these two lubricants is that one features the highest KV70 in the batch and the other one of the lowest in the batch. Lubricant 009A with the low KV70 has presented a very small overlap and has also a much steeper curve that peaks much sooner in the cycle and remains relatively flat for the majority of the stroke before collapses. The other lubricant through 003A paints a

completely different picture. The cavities reach a much shorter length for both up-stroke and down-stroke while they only peak for a short time at the points of maximum acceleration. What is even more interesting between both samples is that this only affects the cavity length on the upstroke. During down-stroke the curves appear to be relatively close for these two lubricants.

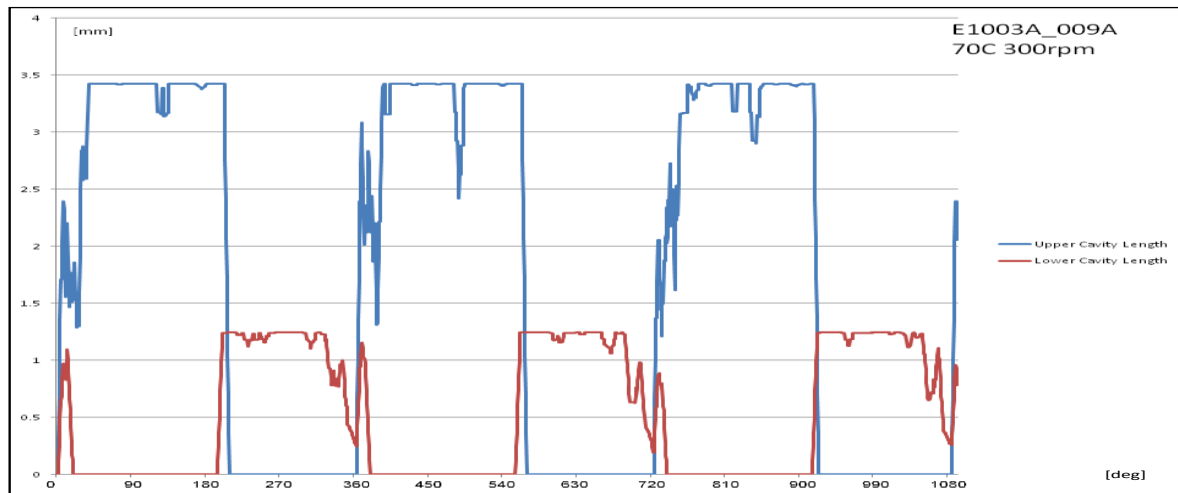


Figure 114 – Cavity Length, E1003A_009A, 0.005L/Min, 70C, 300RPM

Other lubricants do not offer that same level of overlap between the strokes as in figure 113 and sample 008A. In this figure, the cavities are generated at exactly the same point where the cavities on the opposite side collapse. This lubricant along with 016A are part of the 3rd base group. In this group 016A is one of the two samples that features a viscous modifier at a very high concentration, the other lubricant with a viscous modifier is 020A but has half the concentration of 016A. When samples 008A and 016A are compared against each other the differences are immediately noticeable. Sample 016A shows cavities that are very close between the up-stroke and the down-stroke and the same observation holds for sample 008A. What is very interesting is that despite sample 016A having the additional viscous modifier both samples have similar KV70 and density. What is even more interesting is that not only the curves follow similar profiles, but their magnitudes are relatively close. As with the analysis of the width, the number of cavities and the area, show that when lubricants of the same base group are tested under the same conditions the value of KV is a good indicator to whether a lubricant will offer cavities of a greater magnitude or not and to whether they would start earlier in the cycle or not.

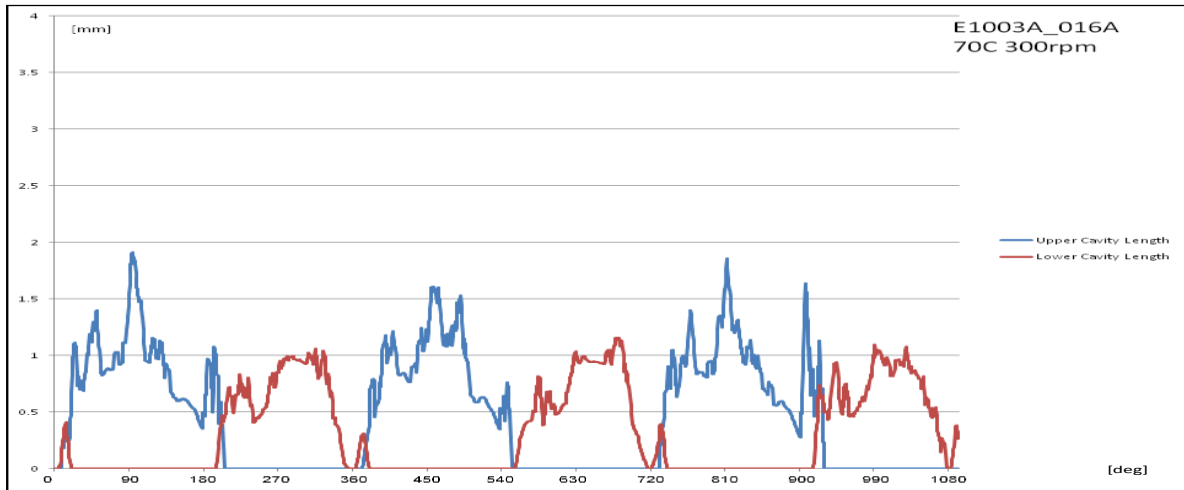


Figure 115 – Cavity Length, E1003A_016A, 0.005L/Min, 70C, 300RPM

The next sample in the batch that features a viscous modifier is sample 020A in figure 116. This sample is in the same group as lubricant 004A in figure 112. When these two lubricants are compared, they have a lot of similarities as the comparison of lubricants 003A and 009A, where 003A with the higher KV70 presented smaller cavity length and also maintained that length for a shorter period of time compared to 003A. In the same way 004A with the higher KV70 offered a smaller overall length than 020A. What is very interesting is also the comparison of 003A with 004A and 009A with 020A. Samples 003A and 004A feature some similarities with 009A and 020A. When these are compared with each other the samples 003A and 004A feature the highest KV70s in the batch and also similar cavity-length curves. The same is observed from the comparison of 009A to 020A with the only differences that these two lubricants feature KV70s exactly in the midrange of the batch. It is supported that there is a possibly link between the way lubricants cavitate and KV. This is stronger in lubricants that are based on the same group but even when different groups are compared against each other there are comparable similarities that are found which further support the claim.

The cavity length figures indicate that the cavity generation is directly linked and dependent to the individual formulation of each lubricant. The cavity length is also an important link to the previous work performed on the test-rig by previous researchers. The lubrication test-rig used for the testing of the lubricants has been in the possession of City University for a number of years. In these years, many researchers have performed work on it which has generated a vast database offering an enormous amount of information on the phenomenon of cavitation. The tests were performed in such a way that from all the aspects recorded during

all the individual project, the length would be the most reliable to extract and correlate with the formulation of each lubricant. Since the scope of those projects was not the optical algorithmic processing of the data those images do not offer the required resolution for the software to process them successfully, which indicates that only the features that are above a certain threshold would be analysed and these are the cavitating area and the cavitating length. Moreover, the results show that the lubricant formulation affects at a great degree the start and the end of each cavitation phenomenon with the KV being a very good indicator. This phenomenon has been linked mainly to the testing operating conditions, while another link could be established between the formulation of the lubricant and the start and finish of each cavitation event. The formulation affects the way the cavities are generated, the cavities present a certain pattern of behaviour relative to the movement of the piston. In addition to the generation and collapse points, the cavity length data offers highly important information on the way the cavities behave throughout each cycle and how these are linked to each lubricant's physical properties.

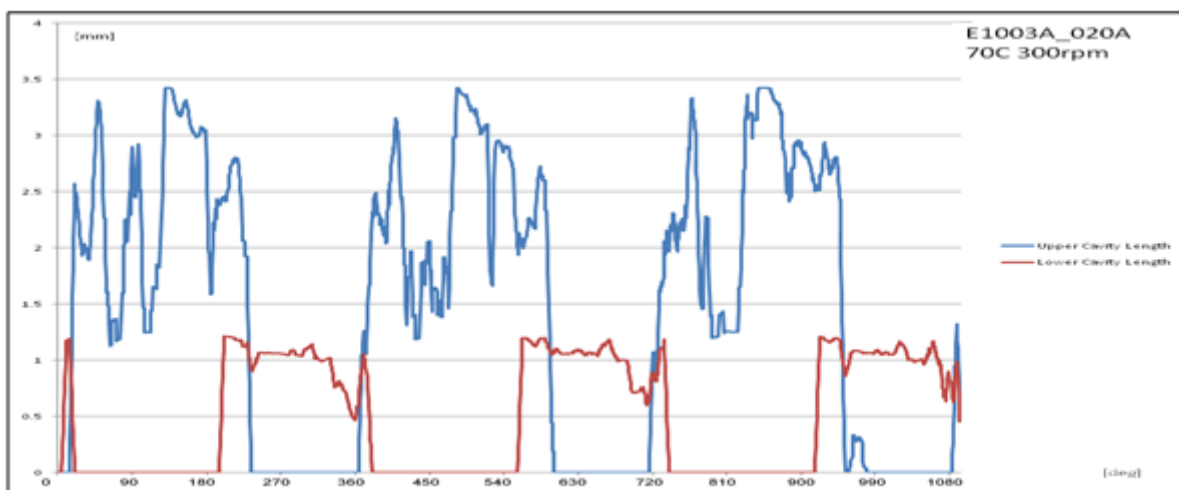


Figure 116 – Cavity Length, E1003A_020A, 0.005L/Min, 70C, 300RPM

As an example, when figures 111 and 114 are directly compared against each other their in-between differences are obvious. The profile of the cavity-length curves presents great differences. If then the attention is directed towards the point where the cavities are generated and collapse it is immediately noticed that despite the different cavity behaviour the cavities are generated and collapse at exactly the same point regardless their in-between behaviour. The information provided by this observation not only establishes a link between the cavity generation/collapse with the lubricant formulation but also links the behaviour of the cavities when these are fully developed. The different add-packs and viscous modifiers are

empirically known to have an effect on the lubricant formulation where now each individual component can be linked to a specific behaviour.

Cavity length 0.005L/Min 70C 600rpm

The following figures 117 to 122 present the cavity length in a space of three consequence cycles for a total of 1080 degree. The figures present the average cavity length at each different degree step for all the three cycles recorded. The total of the represented data supports an interesting fact directly linked to the formulation of all the lubricants presented in this report. They show key aspects of the lubricant behaviour that are associated to the way the lubricant was formulated. The most intriguing part is the effect that the different additives and KV have on the performance of the lubricants, while this project presents data that support a connection between all of them.

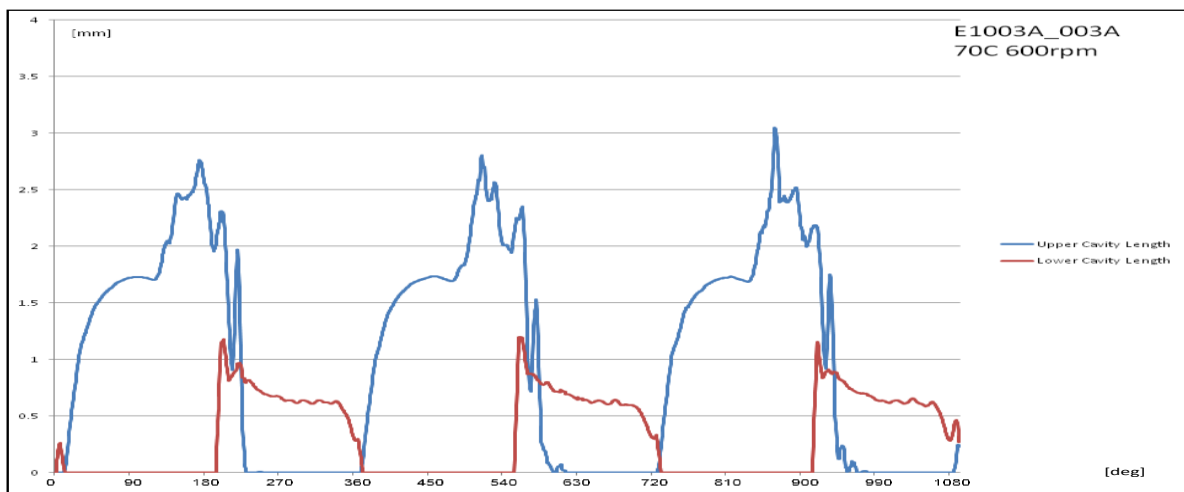


Figure 117 – Cavity Length, E1003A_003A, 0.005L/Min, 70C, 600RPM

The way the cavity length reacts to all the different test conditions is very similar between the 300RPM and 600RPM. As an example, lubricant 003A in figure 117 at 600RPM and lubricant 003A at 300RPM in figure 111 show very similar cavity length and profile despite the increase in speed. Furthermore, there are samples that not only they did not present similar lengths but the 600RPM data offered smaller cavity length than the 300RPM.

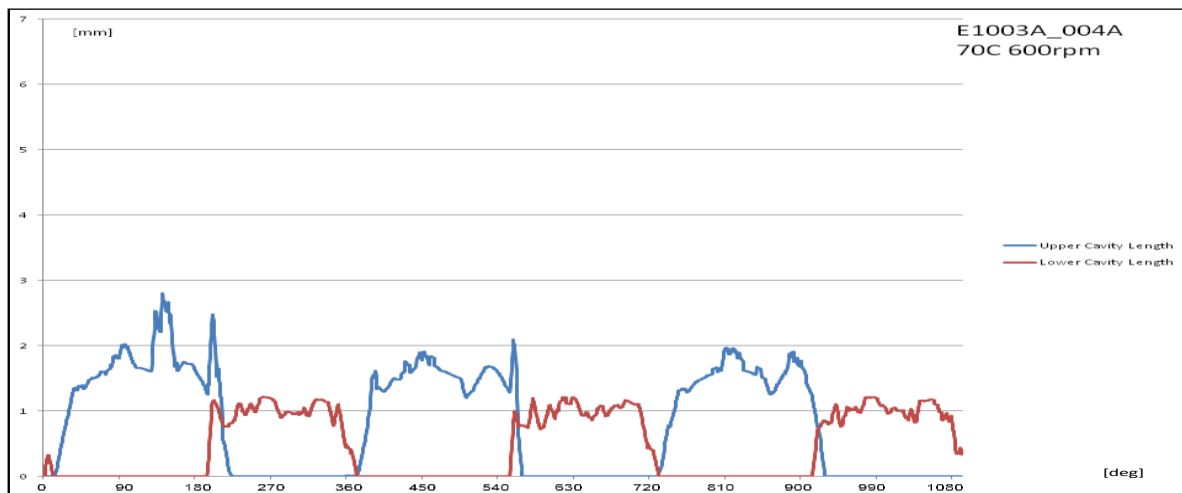


Figure 118 – Cavity Length, E1003A_004A, 0.005L/Min, 70C, 600RPM

A prime example of this sort of behaviour is lubricant 009A in figures 114 and 120 for 300RPM and 600 RPM respectively. In this comparison, it is observed that the cavity length for this lubricant has decreased by 0.5mm between the 300RPM and 600RPM.

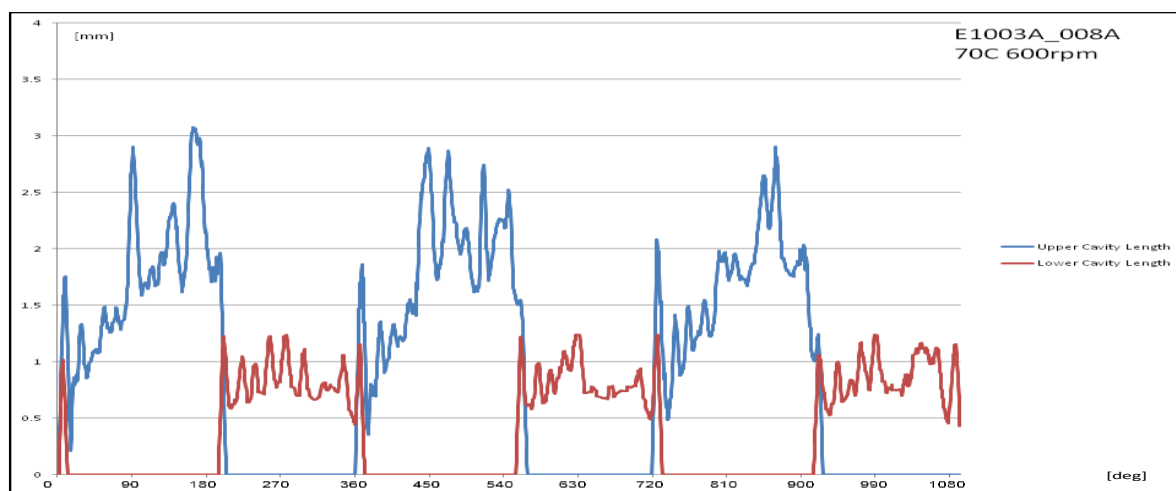


Figure 119 – Cavity Length, E1003A_008A, 0.005L/Min, 70C, 600RPM

This is also consistent with the comparison of the width earlier on in this section for the two different speeds where similar behaviour was observed. A possible explanation could be the increased gap at greater speeds between the liner and the ring. Due to hydrodynamic forces as observed by A. Dhunpant the lubricants will present a greater oil film thickness than the lower speed. The higher oil film thickness will also mean a greater gap between the cylinder and the ring. The greater gap can explain why the cavities might offer a smaller length or width.

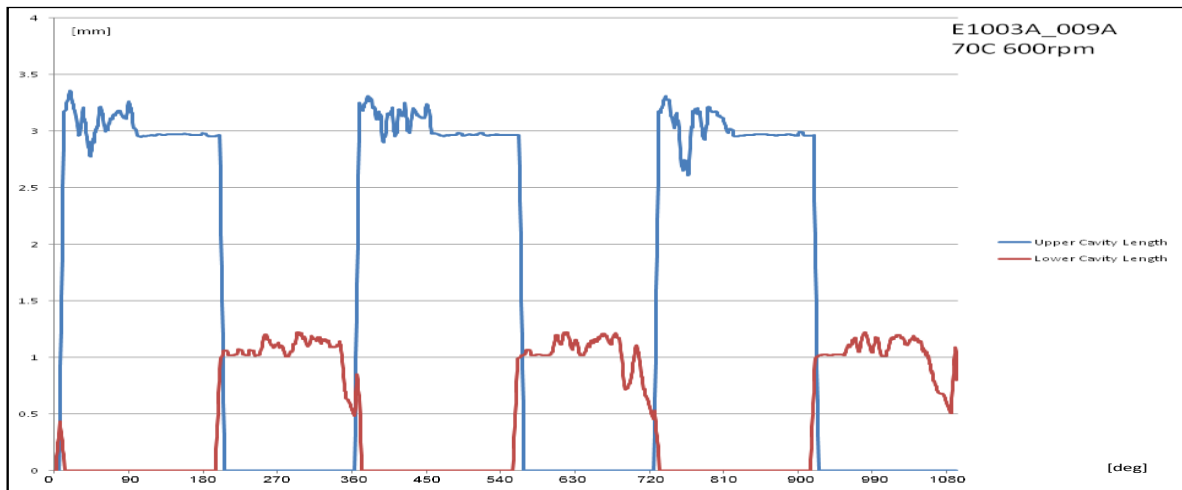


Figure 120 – Cavity Length, E1003A_009A, 0.005L/Min, 70C, 600RPM

In general, the graphs at these higher speeds show a more “unstable” profile than the lower speeds. The increased vibrations along with the forces introduced by the increased velocity of the liner cause disruptions in the profile of the data. The data follows a fluctuation that is represented in the graphs in the form of a wave. Figure 117 and figure 122 present the two distinct behaviours that the lubricants can follow among all samples. In the same way lubricants E1003A_003A, E1003A_004A, E1003A_008A and E1003A_016A in figures 117, 118, 119 and 121 respectively can be grouped together as they show similar profiles. The second grouping could be lubricants E1003A_009A and E1003A_020A in figures 120 and 122. These lubricants and their formulations dictate whether the lubricant will present a late cavity generation or a late cavity collapse. They also indicate the way the cavities behave between those points of generation and collapse. Different formulations result in different behaviours, one example is figures 119 and 122. Both lubricants are based on the same basic lubricant and they both have the same add-pack at the same concentration. The only component they do not share is the Viscous Modifier. Lubricant E1003A_016A features an additional Viscous Modifier, where lubricant E1003A_008A is missing that additive. The processed data present a completely different picture for these two lubricants. They might both share the same basic formulation, but that additional Viscous Modifier has made a massive difference in the total behaviour of the lubricant. The lubricant with the viscous Modifier has followed a more settle behaviour by maintaining a lower cavity length. Wheatears the lubricant without the Viscous Modifier has developed much longer cavities and in certain parts of the cycle double their length in comparison. It also seems that the cavities in lubricant E1003A_008A maintain their length later in the cycle and they extend in length even further as they go towards the end of the stroke. It has been observed that not only the

additives have an effect on the behaviour of the lubricant. One example is lubricant E1003A_003A in figure 117 and E1003A_008A in figure 119. These two lubricants feature the same add-pack at the same concentration and they also have the same viscous modifier at the same concentration as well. When these two lubricants are compared, they present some distinct differences. Lubricant E1003A_003A presents a much smoother profile than lubricant E1003A_008A, also the overlap between the strokes is greater in lubricant E1003A_003A which means the cavities are more stable and maintain their length for longer even in the next stroke.

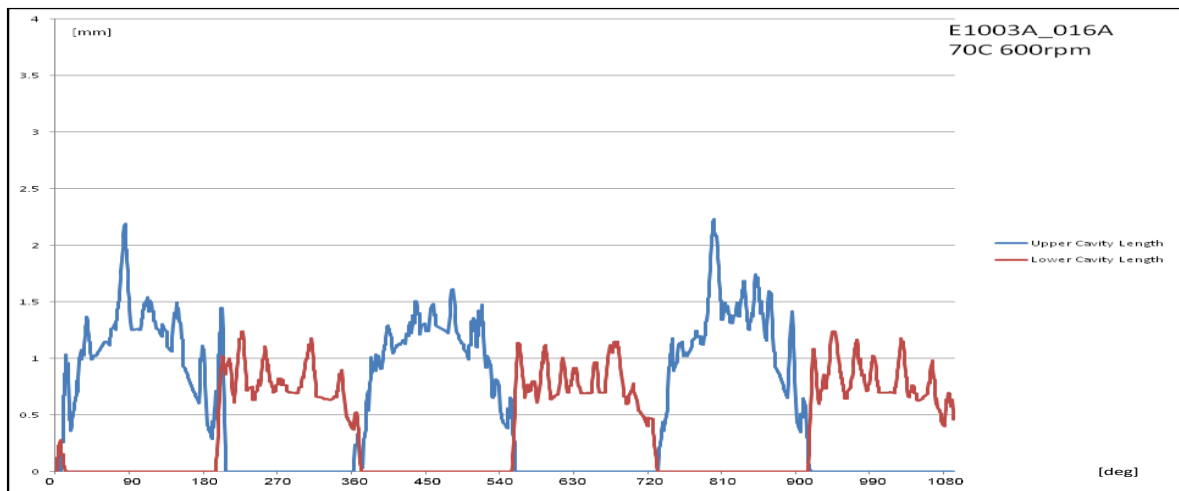


Figure 121 – Cavity Length, E1003A_016A, 0.005L/Min, 70C, 600RPM

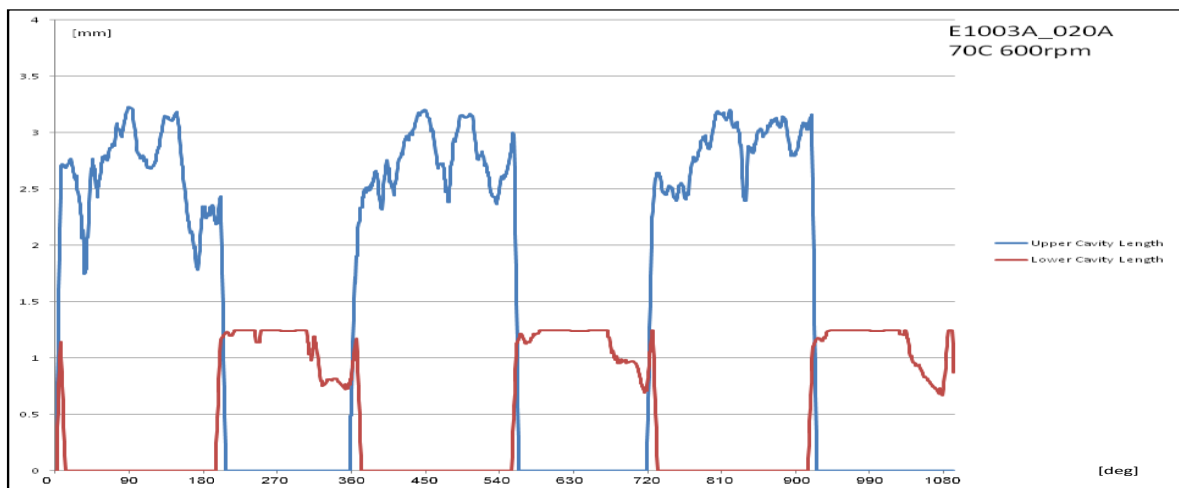


Figure 122 – Cavity Length, E1003A_020A, 0.005L/Min, 70C, 600RPM

Summary

The analysis summary outlines the behaviours of the lubricants and details the basic differences between the individual samples against their formulations. The results are compared in pairs as per their base group where the effects of the different formulations are highlighted under the effect of the various test conditions. The data presented in this section were generated on the City University's lubrication test-rig with the use of specialised high speed and lighting equipment. The data were captured mainly in the form of visual data that were later processed with the help of custom algorithms developed in Matlab. The data were further processed in order to filter out any associated noise and the final results were presented in graphs for their direct comparison. In many cases, lubricant names have been shortened from their full code name to the last four characters of that name, for example, E1003A_003A may be referred to as 003A. This comparison only presents a sample of the data generated in the course of the project. The data have been extracted from the captured images with the use of a custom Matlab algorithm. The results have been visualised in graphs and these graphs are presented in figures 75 to 122. Later the results have been analysed and the conclusions drawn are presented in pairs depending on their formulation. These pairs are grouped into different categories according to the test conditions. Due to confidentiality issues the lubricant formulations have not been published and the lubricants as well as their add-packs are referred to by their BP code names. The code names and their individual relative formulations are listed in table 4, the full lubricant matrix consists of 19 lubricant samples, these are divided into 4 base lubricant groups. These 4 base lubricants in some cases feature a number of different add-packs which can alter their basic properties. The following paragraphs detail and discuss the comparison of the tested lubricants into groups according to their formulation and test conditions. Below is also a summary of the discussion found on each test condition in the earlier pages of this report. At the end of the summary there is a direct sample by sample comparison grouped per base lubricant group.

The first two lubricants of the Matrix, lubricants E1003A_003A and E1003A_009A are almost identical, though they both feature a different type of Viscous Modifier. Both of these lubricants are part of the same lubricant base group with the same add-pack but when it comes down to their individual properties the two samples have very similar densities, though all the other features such as Kinematic viscosity are different. During testing, lubricant E1003A_003A was found to have covered an area of 40% compared to the total area of the piston-ring where lubricant E1003A_009A covered an area of almost 80%. This observation

can also be linked to their kinematic viscosities. Sample E1003A_003A has a KV70 of 45 cSt and when this compared to sample E1003A_009A with KV70 of 21 cSt is observed that though the density of the base lubricant is the same the additional viscous modifier has affected the kinematic viscosity at 70C. Furthermore, for this particular lubricant it is noted that the lower the kinematic viscosity the greater the cavitating area. Another important feature of these two lubricants is the KV70. Kinematic viscosity of engine oils is a critical property that relates to the fuel economy and durability of a running engine. The drivers behind lowering kinematic viscosity are new global governmental regulations to improve fuel economy and lower greenhouse gases in new vehicles. Lower kinematic viscosity tends to improve fuel economy and lower greenhouse gases, but higher kinematic viscosity provides better wear protection, a careful balance must be found when formulating an engine oil. Kinematic viscosity is critical in preventing engine wear in the critical ring/liner interface area by maintaining a protective oil film between the moving parts. For the two lubricants in comparison, E1003A_003A has a KV70 of 45 cSt where E1003A_009A has a KV70 of 21 cSt. Though the lower KV70 of E1003A_009A will probably offer better fuel economy and reduced emissions it will also offer reduced component protection as at the same operating conditions it presented double the cavitating area of E1003A_003A. Though E1003A_003A covered a smaller cavitating area than E1003A_009A, E1003A_009A presented a greater number of cavities. Which means that E1003A_003A developed more cavity fingers than the E1003A_009A, though the latest offered double the cavitating area. The viscous modifier in the case of these two lubricants has affected the behaviour of the cavities inside a lubricant and this phenomenon was observed in every repetition of the run. BP did not reveal the type or composition of the viscous modifiers or the add-packs used within each sample but indicated whether two samples had the same viscous modifiers or add-pack and the relative concentration of each. Based on this information it was found that it is not just the presence of the viscous modifier that affects the behaviour of the lubricant but also the type that is used.

Lubricants E1003A_004A and E1003A_020A as with the previously compared E1003A_003A and E1003A_009A are also of the same base group and they both feature the same additives as E1003A_020A but with an additional viscous modifier. E1003A_020A presented a cavitating area that reached 20% of the total area of the ring where E1003A_004A with no viscous modifier, cavitation of 40%. Lubricants E1003A_008A and E1003A_016A are two samples that fall under the same base group. E1003A_016A in

contrast with E1003A_008A has an additional Viscous Modifier. In fact, E1003A_016A features the same Viscous Modifier as lubricant E1003A_020A though at double the concentration. When comparing lubricants E1003A_008A and E1003A_016A where one of them has the additional Viscous Modifier but they both show similar kinematic viscosities it was found that regardless the different formulation they both covered an area of 20%. This indicates that kinematic viscosity plays a crucial role to the behaviour of lubricants.

When the speed increased from 300RPM to 600RPM the behaviour of the lubricants for some samples changed. Lubricant E1003A_003A did not show a lot of differences in the area of cavitation between the 300RPM and 600RPM but the cavitation development curve at 600RPM was steeper and cavities remained developed for longer. This indicates that while the speed increases, cavitating area increases but the time they require to develop decreases. On the contrary E1003A_009A appears to cover a smaller area at 600RPM than it did at 300RPM and while these two lubricants are using different viscous modifiers they possess very similar formulations. Lubricants E1003A_004A and E1003A_020A are two samples with the same base formulation and the same add pack while E1003A_020A has an additional viscous modifier. When E1003A_004A was tested showed roughly the same cavitating area as at 300rpm. This indicates that despite the increase in speed there was no change in the percentage of the area the cavities occupied but while the area stayed the same, the width and the number of the cavities changed. Cavities at 600rpm had a smaller width and came at greater numbers than 300rpm. When lubricant E1003A_020A was tested though the results showed the opposite behaviour compared to E1003A_004A. Furthermore, while E1003A_020A cavitated, it covered a greater area at 600rpm than it did at 300rpm and while the number of cavities had increased the width decreased. Also, the cavities at 600rpm stayed at their maximum length for a longer period than they did at 300rpm. Lubricants E1003A_008A and E1003A_016A are two lubricants that belong in the same base group. As with the earlier comparison of samples E1003A_004A and E1003A_020A, in the same way E1003A_016A features an additional Viscous Modifier over sample E1003A_008A. In fact, E1003A_016A has the same Viscous Modifier as lubricant E1003A_020A but at double the concentration. Lubricant E1003A_008A showed overall a higher cavitating area at 600rpm than it did at 300rpm. The same effect has been observed with lubricant E1003A_016A at 600rpm against 300rpm. Both lubricants have showed an increased number of cavities and width between the two speeds.

It has been observed that lubricants are experiencing cavitation when they are subjected to extreme forces and the findings of these report have indicated that the way cavities are generated can be altered with the use of additives, while KV70 is a good indicator of their performance while these lubricants are in the same base group. Each additive affects the cavity behaviour in a different way while equally important to the type of the additive is the amount of that additive present within the lubricant. The different tests considered more than the contribution of additives in the behaviour of cavities, it also investigated the effect that different base compositions have on lubricants and their behaviour. The collective summary is that the cavities are affected by several factors, these factors range from the temperature of the lubricant and the speed of the piston to the basic composition of each lubricant and their physical properties.

Samples 003A vs 009A at 300RPM

Lubricant E1003A_003A and lubricant E1003A_009A are of the same base lubricant group (Group 1) and they both feature the same add-pack (add-pack 1). The lubricants mainly differ in one parameter, which is their KV70. When these two lubricants were tested under the same conditions there were significant differences in the way they cavitated. The main difference in the results was the area these two covered when cavitating. The lubricant sample 003A covered an area of 40% of the total area of the piston-ring where lubricant 009A covered an area of almost 80%. Even though the lubricant 003A covered a smaller area than the lubricant 009A, the 009A presents greater number of cavities than 003A. Regarding the width of the cavities generated in both lubricants there were not many differences, both samples showed similar cavity width. At this point it has to be noted that both lubricants are of the same base Oil Groups and they both contain the same add-pack. The difference in KV70 has contributed in the behavioural difference observed when their processed results are compared. It is suggested that KV is a good indicator of the behaviour of cavities inside a lubricant when this is subjected under forces that cause it to cavitate.

Samples 004A vs 020A at 300RPM

Sample 004A and 020A are two lubricants that fall under the same base Oil Group (Group 4). These lubricants are not only under the same lubricant group but also feature the same add-pack (Add Pack 1). An interesting point with this comparison is that despite both lubricants featuring the same add-pack and that are part of the same group, 020A has an added viscous modifier. The testing of the two lubricants showed a different behaviour. When the 020A was tested, this lubricant presented cavitation that covered at its maximum the 70% of the total

ring area. The addition of the Viscous Modifier had a surprising effect on the behaviour of the lubricant as when the 004A was tested only showed cavitation that covered an area of around 40% to 50% of the total ring area. At this point though it needs to be noted that even though the 020A reached areas covered by cavitation of 70% this was at the point where the optical liner was changing direction. This means that for this lubricant the collapsing cavities had not fully collapsed while new ones were generated on the opposite side of the ring. Thus, the 70% cavitating area has been the result of the respective areas on both sides on the piston-ring. If the graphs are closely examined the spikes appear every 98 degrees of crank angle, these spikes represent the addition of the cavitating areas on both sides of the ring. At these point cavities are present on both sides of the ring as sometimes during testing the cavities that are collapsing are still present even though the liner has reached TDC or BDC and has changed direction while cavities have already generated on the opposite side. It is also noted that the 020A lubricant shows an area of cavitation that covers the 20% to 30% of the total ring area. Finally, the total number of cavities and the width of the cavities for both lubricants are similar throughout all the cycles and the same pattern has been observed in all the tests. The major difference presented here is related to the way the cavities maintained that width. Furthermore, 020A during a full cycle presented shorter cavities which reached their maximum length at a later stage in that cycle.

Samples 008A vs 016A at 300RPM

The lubricant sample 008A and the lubricant sample 016A are two lubricants that belong in the same lubricant base group. As with the comparison of the lubricant samples 004A and 020A, sample 016A features an additional Viscous Modifier in contrast to sample 008A. In fact, the 016A has the same Viscous Modifier as lubricant 020A but at double the concentration. Despite one of the lubricants featuring an additional Viscous Modifier they both show very similar kinematic viscosities. These two samples when compared against the rest of the lubricant matrix they both showed the lowest values as far as the area, the width and the length of the cavities are concerned. Furthermore, the testing showed that regardless the different formulation they both showed an area of cavitation that covers about the 20% of the total ring area. In addition to that point the length of the cavities has presented another similarity that these two lubricant samples share. These two lubricants proved difficult for the Matlab algorithm to process. The software was not able to extract all the data as the generated cavities were too small for the software to detect. As noted due to the software limitations there is not a continuous set of data in regard to the total number of cavities but all the other

attributes of the lubricant behaviour have been appropriately captured. Thus, the values for the area and the length of the cavities are accurate and when compared it is noted that the Viscous Modifier in this case has not affected the results even though it was expected to.

Samples 003A vs 009A at 600RPM

Sample 003A does not present a huge difference with the maximum area of cavitation between the 300RPM and 600RPM. The curve at 600RPM is steeper and stays at higher values for a longer period. This indicates that even though the speed increases this does not cause cavities to expand at a greater area than before. They do spread at this area though much sooner than when at 300RPM. In contrast 009A appears to cover a smaller area at 600RPM than it did at 300RPM. Both lubricants show about the same number of cavities throughout the three cycles as they do for the width of the cavities. The length of the cavities follows the same pattern as at 300RPM with one in relation to the area of cavitation. The cavities reach their maximum length much sooner at the higher speeds. Lubricant E1003A_003A and lubricant E1003A_009A are of the same base lubricant group (Group 1) and they both feature the same add-pack (add-pack 1). Where these two lubricants show a difference in their composition is with the Viscous Modifier. The data supports that the Viscous Modifier contributes to those differences in the samples behaviour.

Samples 004A vs 020A at 600RPM

Sample 004A and sample 020A are two lubricants that fall under the same base Oil Group (Group 4). These lubricants not only belong in the same lubricant group but also feature the same add-pack (Add-Pack 1). Both lubricants feature the same add-pack and are part of the same base lubricant group but the 020A has an added viscous modifier. Following the testing of these two lubricants at 600rpm the data presented two different sets of results. When lubricant 004A was tested showed roughly the same area of cavitation as it did at 300rpm. This means that despite the increased speed there was no change in the percentage of the area the cavities were occupying on the total area of the ring. Even though the area remained the same, this did not occur with the width and the number of the cavities. Cavities at 600rpm appeared thinner and greater in numbers than at 300rpm. On the other hand, when lubricant 020A was tested the results showed the opposite behaviour than what had been observed with lubricant 004A. Furthermore, lubricant 020A as it cavitated it covered a greater area at 600rpm than it did at 300rpm and the number of cavities had increased against the width which before had decreased. Finally, the cavities at 600rpm stayed at their maximum length for a longer part of the cycle than they did at 300rpm.

Samples 008A vs 016A at 600RPM

The samples 008A and 016A are two lubricants that belong in the same lubricant base group. As with the comparison of lubricant samples 004A and 020A the sample 016A features an additional Viscous Modifier against sample 008A. Sample 016A features the same Viscous Modifier as lubricant 020A but at double the concentration. Lubricant 008A overall showed a greater cavitating area at 600rpm than it did at 300rpm. The same effect has been observed with lubricant 016A at 600rpm against 300rpm. Both lubricants have showed an increased number and width of cavities when comparing the two speeds together. A note has been made to point out that this comparison is not considered entirely accurate as the software used to extract the data did not pick the complete number of cavities at 300rpm. This result is mainly due to limitations in the capabilities of the software itself. Despite the efforts to amend this issue and improve the accuracy of the software there was not a significant improvement to the way the algorithm captured the phenomenon for this specific sample. Further work is needed to either develop a more sophisticated algorithm in order to better capture the behaviour of cavities when those are relatively small or repeat the tests with greater magnification using more capable equipment and higher resolution.

Summary Conclusion

In total 19 lubricant samples were received by BP, these 19 samples completed the full matrix of lubricants tested throughout the length of the project. Out of these 19 samples 6 of them have been included in this report. These 6 lubricants were not randomly selected but they were chosen in a way that these will represent the entire lubricant matrix received. That was supported by the fact that some of the lubricants had similar compositions and similar performance. The lubricants were tested in a total of 12 different operating conditions. These conditions were; 3 different speeds, 2 different temperatures and 2 different flow rates. These were limited down to 2 different speeds for the purpose of this report. The complete lubricant matrix had to be analysed in order to derive a solid conclusion. There is the need to fully compare all the samples tested to paint a better picture of the way physical properties affect cavitation. There is also the need of re-coding the software in order to make it more “sensitive” into picking the finest of cavities as with lubricants 008A and 016A where there was a difficulty in identifying those events. As a conclusion, the outcome of the project is successfully giving information related to the performance of the lubricants in a way this has not been approached by previous researchers. This has offered a better understanding of how

different additives and different formulations affect the cavity behaviour and the properties of the lubricants and how cavitation can be linked with kinematic viscosity.

5.2 Repeatability Test of E1003A_021A

The repeatability of the results is crucial to the outcome for the project. It is important to be able to repeat the measurements that have been carried out to make sure the results are valid and are not based on random events. The following set of images in figure 123 show data related to the testing of lubricant E1003_021A at 600RPM at a temperature of 70C and a flowrate of 0.05L/Min. The images are at the same crank angle from different test runs which were captured on different dates. Bellow in table 5 are listed the values extracted and related to the images in figure 123. As an example, the values show that the runs present a difference of 2.5% at maximum between that as far as the area is concerned. The values for all the related properties are very close between the different runs. These data support that the tests are repeatable and consistent when these occur in different dates.

Frames Number	Actual Area Covered 100%	Number Of Cavities Number	Width Of Cavities mm	Upper Cavity Length mm	Lower Cavity Length mm
1	39.53	25	0.22	3.20	2.16
2	39.94	26	0.21	3.22	2.16
3	39.93	25	0.21	3.08	2.00
4	40.77	24	0.23	3.21	2.16
5	39.86	26	0.21	3.15	2.16
6	39.36	26	0.20	3.20	2.16
7	40.06	23	0.23	3.18	2.16
8	40.16	25	0.21	3.08	2.00

Table 5 – Repeatability between different test runs, E1003_021A, 600RPM, 70C, 0.05L/Min

The same observation occurs when the data are compared against different cycles of the same run. Figure 124 shows the Mean and Standard Deviation for the following features; area, width, number of cavities, upper cavity length and lower cavity length. The conditions are the same as in figure 123 which are the speed of 600RPM, at the temperature of 70C and at the flowrate of 0.05L/Min. The lubricant is also the same as in figure 123, with a product code of E1003_021A. Figure 124 presents in blue the mean for 8 consecutive cycles for the same run and in black the standard deviation at each point of the cycle. The X-Axis is in Frames per data point where 607 frames are equal to a full cycle of 360 degrees. The step is left at frames per data point and not converted to degrees to maximise the resolution of the results and calculation for mean and standard deviation. Figure 124 illustrates that the standard deviation is relatively small for all the individual properties when the mean values show continuous

changes with the crank angle which indicates that the results have similar behaviour cycle by cycle in those regions.

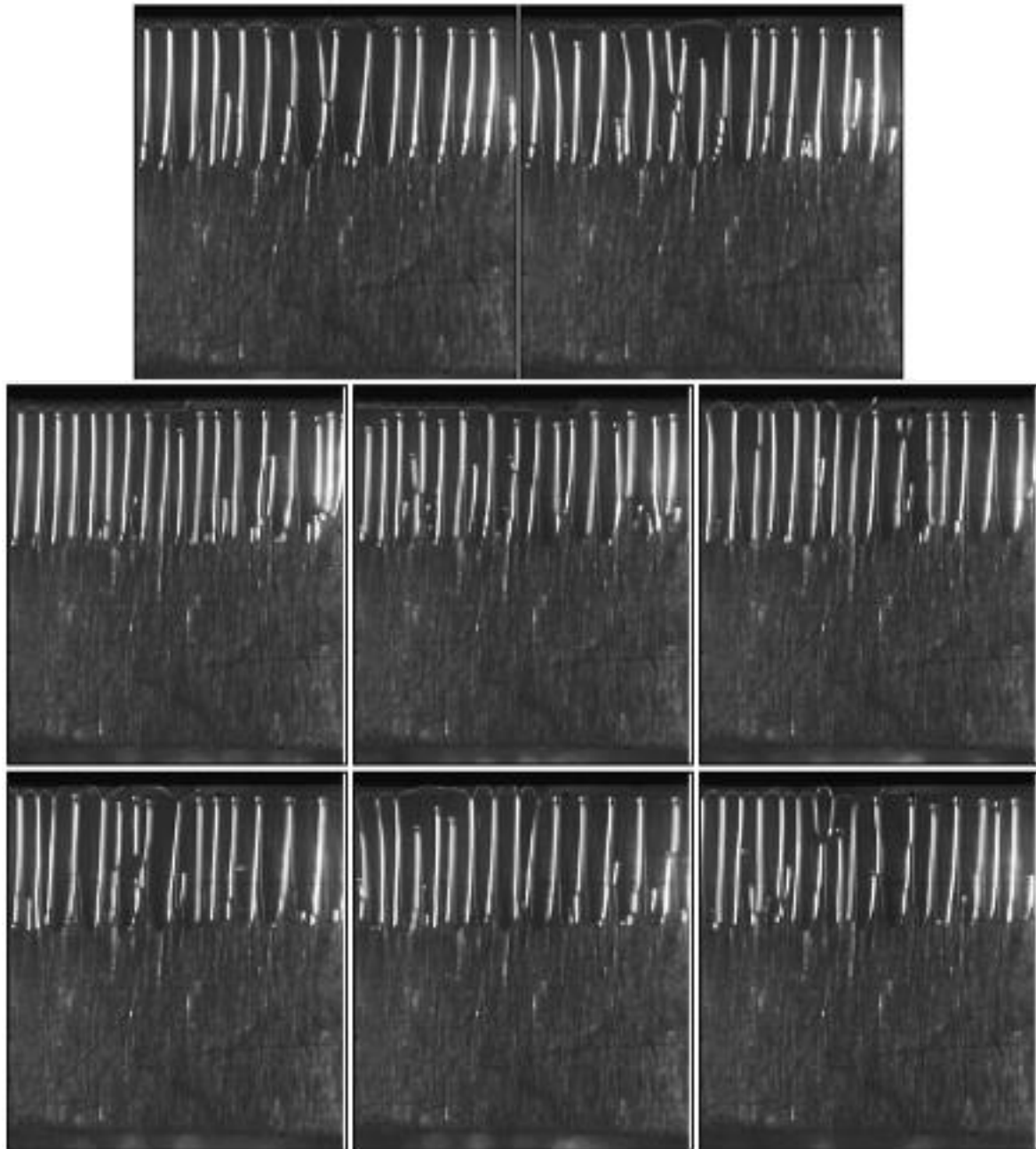


Figure 123 – Repeatability between different test runs, E1003_021A, 600RPM, 70C, 0.05L/Min

By calculating the standard deviation and the mean the absolute uncertainty can be calculated as the standard deviation multiplied by 1.96 with 95% confidence level and the percentage uncertainty error can be calculated as the absolute uncertainty divided by the mean, which ultimately will give the absolute error;

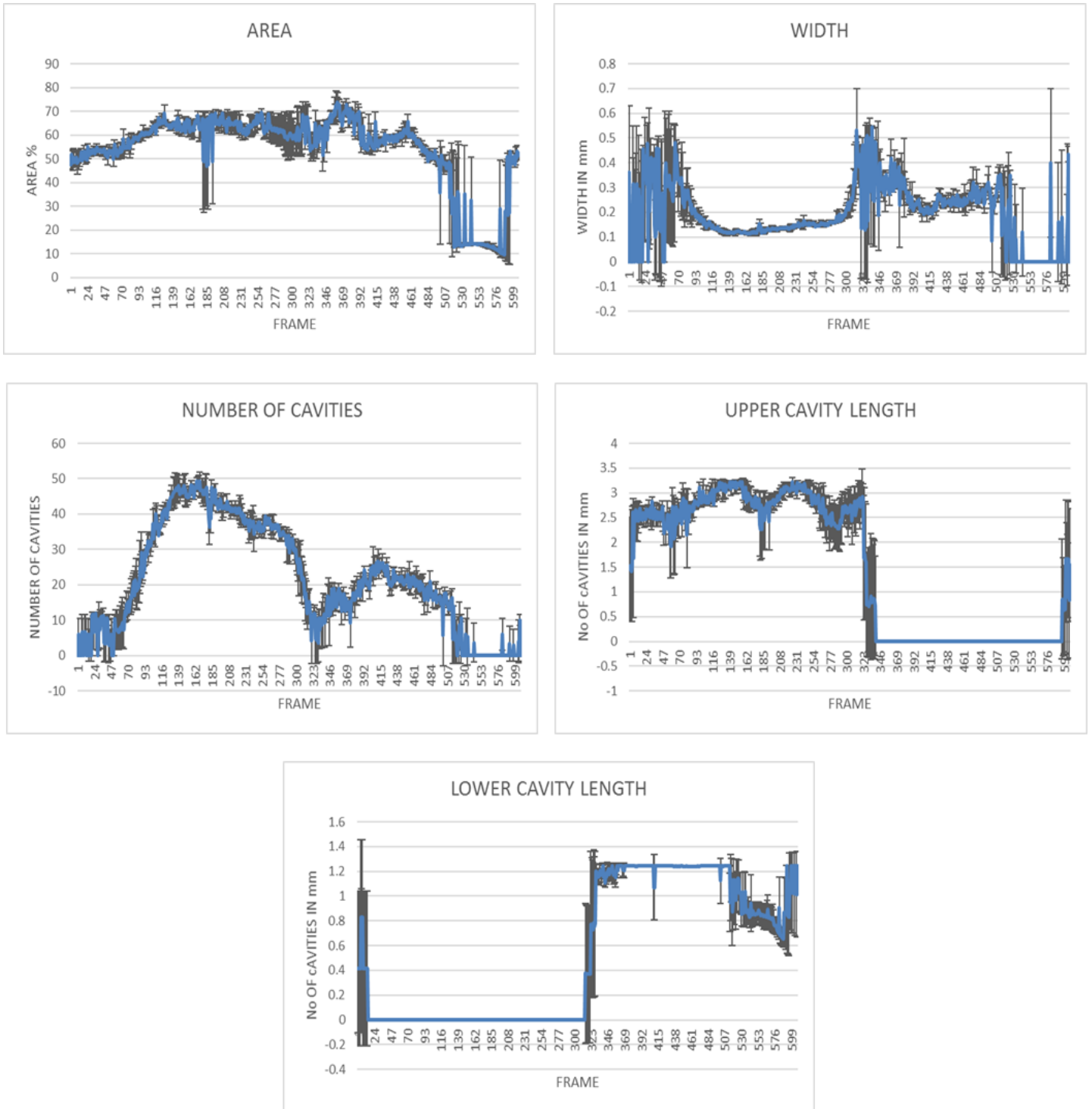


Figure 124 – Mean and Standard Deviation for 8 consecutive cycles E1003_21A, 600RPM, 70C, 0.05L/Min

- Area, The area has an average mean of 53.97mm and an average standard deviation of 2.93mm, this gives an absolute uncertainty of 5.74mm at 95% confidence and an absolute error of 10%.

- Number of Cavities, The Number of cavities have an average mean of 21 cavities and an average standard deviation of 2 cavities, this gives an absolute uncertainty of approximately 4 cavities at 95% confidence and an absolute error of 18%.
- Width, The width has an average mean of 0.19mm and an average standard deviation of 0.03mm, this gives an absolute uncertainty of 0.05mm at 95% confidence and an absolute error of 30%.
- Upper Cavity Length, The Upper Cavity Length has an average mean of 1.5mm and an average standard deviation of 0.16mm, this gives an absolute uncertainty of 0.31mm at 95% confidence and an absolute error of 20%.
- Lower Cavity Length, The Lower Cavity Length has an average mean of 0.5mm and an average standard deviation of 0.05mm, this gives an absolute uncertainty of 0.098mm at 95% confidence and an absolute error of 20%.

The values above indicate that on average the area presents an error of 10%, the width of 18%, the number of cavities of 30%, the upper cavity length of 20% and the lower cavity length of 20% for every 8 cycles the testing is repeated. These values and the difference refer to the average difference presented between the different runs for 8 consecutive cycles. These values are considered to be a very good indication that the results are repeatable within 10% to 30% for every 8 cycles that are recorded depended on the lubricant property investigated.

It has to be noted that the tests are repeatable when operating conditions are the same. An extra parameter and also an operating condition that affected the outcome of these tests has been the ambient (room) temperature which noticeably influenced cavitation. The test-rig being open to the environment was affected by atmospheric temperature which means that, for example, a 70C run during the summer and a 70C during the winter will present variations of around 10-15C in room temperature which is difficult to control.

5.3 Optical-Engine and Lubrication Test-Rig Correlation

The experimental part of the project was divided into two sections. The first section produced data generated on the lubrication test-rig and the second produced data generated on the optical-engine. The focus of the project was the built and test of a fully firing optical-engine. The project continued with the tests that where performed on the lubrication test-rig with a set of 19 samples received from BP. The parametric study gave additional experience with the use of the optical equipment and the measuring techniques that were later applied on the optical-engine. The time spend on the lubrication test-rig generated a large amount of data

and information on the behaviour of lubricants and how this are linked with their formulation and additives. One of the observations was that the behaviour of the lubricant regardless its formulation, would present similarities between the tested samples, depended on the testing conditions. When the testing continued on the optical-engine, similar patterns were observed at similar operating conditions between the optical-engine and the lubrication test-rig.

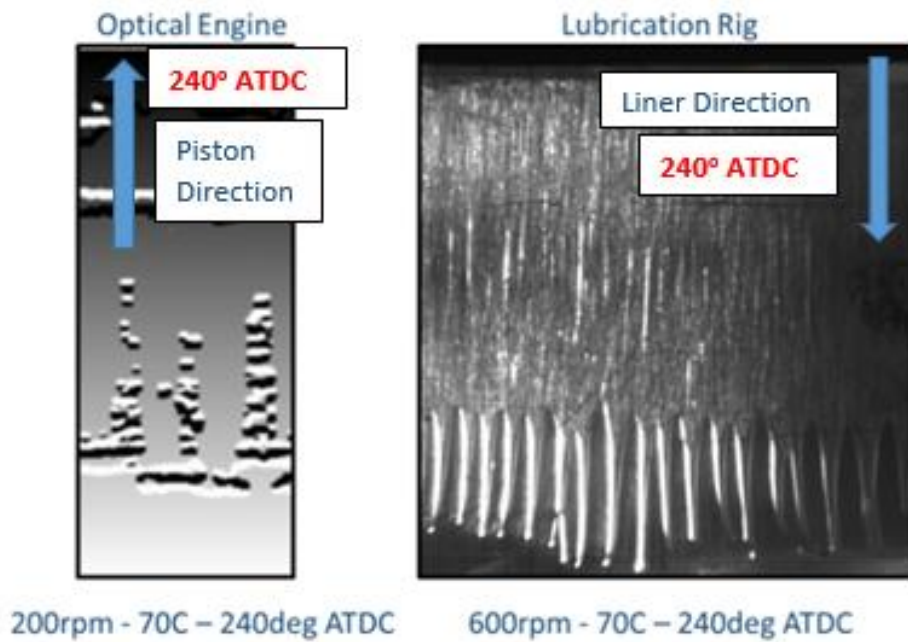


Figure 125 - Side by Side optical-engine and lubrication test-rig Cavity Comparison

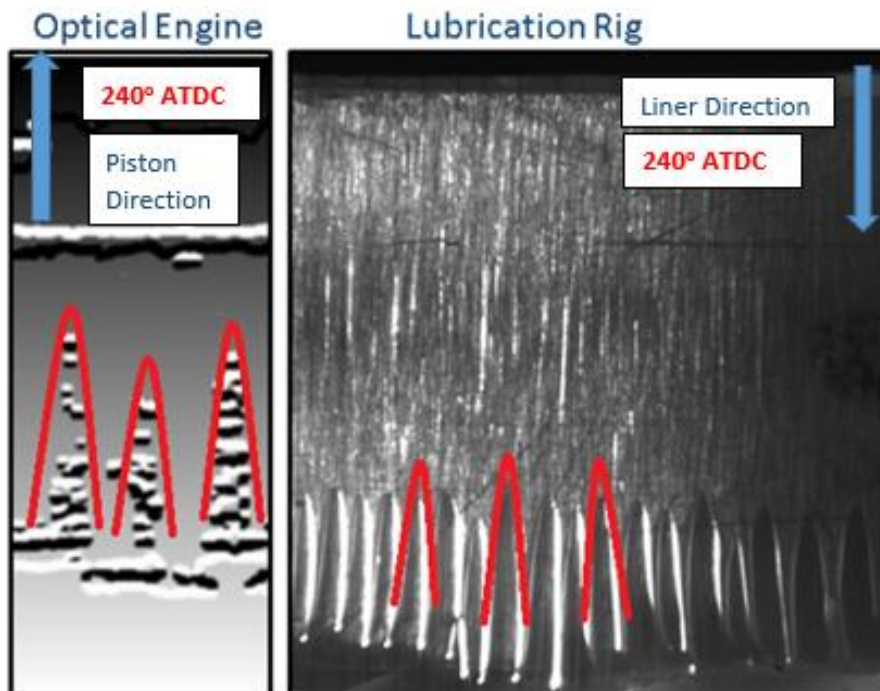


Figure 126 - Side by Side optical-engine and lubrication test-rig Cavity Comparison

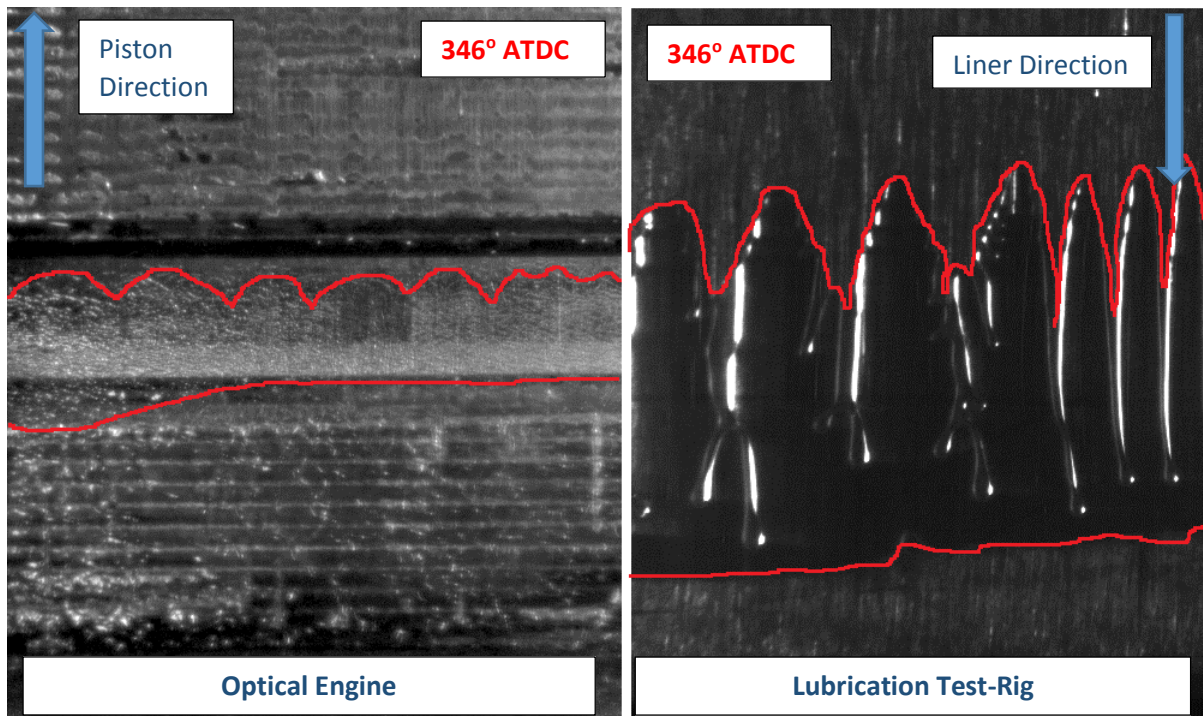


Figure 127 - Side by Side optical-engine and lubrication test-rig Cavity Comparison

That led to the investigation of a possible correlation that might exist between the optical-engine and the lubrication test-rig in an attempt to give an added value to the extended research done on the lubrication test-rig throughout the years. The possibility of an existing link between the lubrication test-rig and the optical-engine would be of high value since the lubrication test-rig is a device that allows for the quick and cost-efficient testing of lubricant samples in a simplified manner. The test-rig can produce data linked to the physical properties of each lubricant that can later be quantified and compared. The lubrication test-rig is accompanied with an extensive literature and work done by a number of researchers and there is a plethora of data available that would offer important knowledge and a big step towards the better understanding of the phenomenon of cavitation. The following images indicate that there is a link between the lubrication test-rig and the optical-engine at similar testing conditions. As seen in figures 125 and 126 both the engine and the lubrication test-rig present similar cavitation structure at similar testing conditions. It has been calculated that due to the geometrical differences between the engine and the rig the piston speed is equal between the two devices when the engine operates at 200rpm and the test-rig at 600rpm. Unfortunately, due to the test-rig's speed limitations the comparison could not continue past the 200rpm versus 600rpm for the engine and the rig respectively. Provided that the appropriate measures have been obtained and the tests are performed in accordance to the methodology specified, all the data generated on the lubrication test-rig it is suggested that

they can be considered as an idealised representation of the behaviour of cavities as these would occur in the optical-engine. Furthermore, any previous works performed on the test-rig should be possibly to link to the optical-engine. Figure 127 shows the cavities at a late stage of the upstroke and at 346 degrees after top dead centre. The frames compare the optical engine next to the lubrication test-rig where it shows the formation of a cavity sheet at a point which is 14 degrees before the top dead centre and the beginning of the next stroke. The direct comparison in figure 126 and 127 supports that both the engine and the test-rig present similar behaviour in the cavity structure at similar testing conditions. This observation suggests a link between the optical-engine and the test-rig and classifies the lubrication test-rig as a reliable source of data when the purpose is the investigation of the cavitation phenomenon that takes place in the piston-ring and cylinder-liner interaction on internal combustion engines.

5.4 General Characteristics of the Cavity Flow

5.4.1 Reynolds Number

Reynolds number is an important quantity in fluid mechanics, it is used to predict flow patterns in different fluid flow situations. Reynolds number is defined as the ratio of inertia to viscous force and it helps to characterize the type of fluid flow, low Reynolds number ($Re < 2000$) will indicate a dominate of viscous force and the flow is referred to as laminar flow and a high Reynold number is when the inertia force is dominate, and the flow is referred to as turbulent flow. Reynolds number is defined as

$$Re = \frac{\rho u D}{\mu} = \frac{u D}{\nu}$$

where u and D , are the characteristic velocity and length respectively and ν is the fluid kinematic viscosity.

Arcoumanis *et al.* (1997), Richardson and Borman (1992) and Priest *et al.* (2000) have demonstrated that the boundary conditions applied when solving Reynolds equation for the piston ring/liner interaction can have different results on the analysis and thus the prediction of hydrodynamic pressure profiles, lubricant film boundaries, lubricant film thickness, oil flow and friction could vary significantly, Dhunput (2009).

The Reynolds number for the test-rig is proposed to be estimated using the maximum speed and the minimum oil film thickness at the mid-stroke of the cycle. The current study did not

focus on the effect of oil film thickness on cavitation, thus information on the oil film thickness was not captured. Typical values have been taken from Dhunput's thesis where he measured oil film thickness on the same test-rig while using a similar experimental setup.

The typical Reynolds number at the rotational speed of 600 rpm for the test-rig is around 0.04 indicating a laminar flow inside the fluid film.

Applying similar analysis to an engine running at 2000 rpm, with an expectation of a half of the lubricant film thickness as what found in the test-rig, the Reynolds number is around 0.2 indicating the viscous force is dominant in the lubricant film; and flow of lubricant film can be treated as a laminar flow.

5.4.2 Weber Number

Weber number (We) is a dimensionless number which is often used in the analysis of fluid flows, especially where there is an interference of two different fluids.

$$We = \frac{\rho v^2 l}{\sigma}$$

Weber number can also be expressed as a measure of the relative fluid inertia to its surface tension. The Weber number indicated whether the kinetic energy or the surface energy is dominant. Since the Weber Number represents an index of the inertial force to the surface tension forces acting on a fluid element, it can be useful analysing thin films flows and the formation of droplets and bubbles. For a spherical droplet the Weber number can be derived using the kinetic energy compared to the surface energy Dongqing Li Prof. (2008)

Using the same typical values as in the estimation of the Reynolds number, the Weber number is found around 0.05 for the test-rig. The low value of Weber number indicates that the initial force is much smaller comparing to the surface tension. The disintegration of lubricant film observed in flow visualization is not a result of the initial force.

5.4.3 Cavitation Number

The cavitation number is a dimensionless number used in fluid flow calculations and is expressed as the relationship between the local pressure drop caused by a restriction and the kinetic energy per volume of the flow. The cavitation number is also used for the characterization of the energy losses of the flow. Previous literature on the test-rig explains how the cavitation number is the ratio of the injection pressure minus the back pressure over the back pressure minus the vapor pressure. This equation mainly finds its application in the

investigation of fluid flow when the fluid is passed through a piezo electrical injector Arcoumanis et al (1997). Similar study in the university of Valenthia has also expressed the same relationships as the injection pressure minus the back pressure over the injection pressure minus the vapor pressure. The literature supports that both methods of quantifying the cavitation number are acceptable and it depends on the application it is used, Patouna (2012).

For the purpose of the test-rig and optical engine calculations, the cavitation number will be calculated by using the first method with a modification of P_r replacing the injection pressure.

$$CN = \frac{P_r - P_{back}}{P_{back} - P_{vapour}}$$

In the test-rig, the peak pressure of pressure profiles between the cylinder liner and the piston ring is used as the reference pressure P_r . A typical value of P_r was found around 5 bar by Dhunput (2009), which gives the CN to be around 4. For the engine test, the CN is estimated using the in-cylinder pressure as the reference pressure. The back pressure is approximated to be 1 atm. Under those assumptions, the CN in an engine test will be around 9 when the in-cylinder pressure is 10 bar.

In orifice flows such as flows in injector nozzles, the cavitation will be initiated at around a number of 1.5 and its intensity increases as the CN increases. The Cavitation Number has not been used in any previous studies of engine lubrication. The comparative analysis above is a simplified analogy using the existing knowledge in orifice flows for the understanding of the flow physics in hydrodynamic lubrication.

5.4.4 Young-Laplace

Young Laplace is a nonlinear partial differential equation that describes the capillary pressure difference sustained across the interface of two static fluids. The Young Laplace equation related the pressure difference to the shape of the surface and it is widely used in the study of static capillary surfaces. The ΔP is the pressure difference across the fluid interface, considering an interface separating two immiscible fluids that are in equilibrium with one another. Figure 128 shows the cross section of a cavity which is equal to 0.16mm. The pressure difference would be 400 Pa if cavitation fingers were static. Although above consideration of Re , We and CN are very useful in analysing the cavitating lubricant flow, the lack of actual data in their calculation prevents to make a useful and meaningful

interpretation of the results obtain in this work. For consistency we present and discuss the current results in both the model rig and optical engine based on their speed in rpm and a correlation between the speed in the rig and that of the engine has been established.

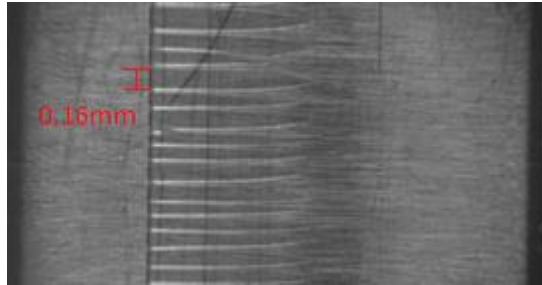


Figure 128 - Typical Cavitation of the Model Rig (Dhunput, 2006)

5.5 Optical-Engine

The testing of the optical-engine generated a large amount of information in the form of visual data. For this report a representative sample of this data has been presented. The specifications of the engine, lubricant and optical setup are shown in tables 6, 7 and 8. The information used has been chosen in a way that it will offer a clear view and an understanding of the project, its outcome and its importance to the understanding of phenomena that take place inside an internal combustion engine. These phenomena have a significant impact on the performance, efficiency and reliability of internal combustion engines, in addition they also have an impact on the environment and the planet. The engine emissions are a problem that all modern manufacturers need to address. This chapter will detail and analyse the phenomena that mainly affect many reciprocating internal combustion engines regardless their type, use or size. These two phenomena are the “lubricant cavitation” and the “blow-by”. Cavitation in lubricants is the phenomenon where the lubricant present inside an engine is subjected to extreme conditions which force it to release the air trapped inside its volume. The air is released in the form of bubbles that when collapse they are followed by a release of energy which can locally damage nearby components. Even though the initiation of those bubbles is due to the release of the entrapped air they collapse at a stage where they contain an air/lubricant vapour mixture. In addition to the damage caused by the collapse of the cavities the phenomenon of cavitation also affects the primary function of the lubricants.

Hydra Engine Technical Specifications	
Type	Single Cylinder, Liquid Cooled, 4-Cycle, Spark Ignition
Bore	80.26mm
Stroke	88.90mm
Swept Volume	0.4498m ³
Rated Speed	5500rpm
Max Power	18kW @ 5500rpm
Max Torque	39 Nm @ 3000rpm
Compression Ratio	9.5:1
Fuel	Rated for "Gasoline 95 RON" Used "Iso-Octane" for Testing
Valve Timing:	Inlet Opens > 10deg BTDC
	Inlet Closes > 48deg ATDC
	Exhaust Opens > 48deg BBDC
	Exhaust Closes > 10deg ATDC
Lubricant Used	Castrol GTX 10w-40 Part Synthetic

Table 6 - optical-engine specifications

Optical Engine Lubricant Specifications	
Name	Castrol GTX 10w-40
Density @ 15C, Relative	0.866 g/ml
Viscosity, Kinematic 100C	14.7 mm ² /s
Viscosity, CCS -25C (10W)	6900 mPa.s (cP)
Viscosity, Kinematic 40C	98.9 mm ² /s
Viscosity Index	155
Pour Point	-36 °C
Flash Point, PMCC	204 °C
Ash, Sulphated	1.3 % wt

Table 7 - Lubricant specification used on optical-engine

Optical Setup	
Camera	Photron SA 1.1 High Speed Camera
Max Resolution	1,024 x 1,024 pixels @ 5,400 fps
Max Shutter Speed	64 x 16 pixels @ 675,000 fps
Optical Lenses	Nikon 125mm & Nikon 50mm
Light source	Arri Lamp (225w, 575w & 1.8kW)
Camera Support	3 Axis (X,Y,Z) Fully Adjustable Milling Machine Bed
Focusing Lenses	Converging-Diverging, 350mm Diameter, 300mm Focus C-Mount
Optics Cooling Fans	3 x Cooling Fans 120mm 7-12V
Camera Computer	Intel Core 2 duo 2.93GHz, 4gb Ram, Ethernet to Camera Port

Table 8 - High Speed camera used for the optical-engine testing

Some of the main purposes of the lubricants used in internal combustion engines is to reduce friction, wear, cool the piston and seal the combustion chamber. Proper lubrication is critical to interacting component because the lack of lubricant can lead to catastrophic results. The moving engine components could come in contact and wear one another to the point of failure and cause irreversible damage to the engine.

Motorised	Speed					Viewing Window								
	208RPM	800RPM	1000RPM	2000RPM	3000RPM	1	2	3	4	5	6	7	8	
Temperature														
30C	X	X	X	X	X	X	X	X						
40C	X	X	X	X	X	X	X	X	X	X	X	X	X	X
50C	X	X	X	X	X	X	X	X						
60C	X	X	X	X	X	X	X	X						
70C	X	X	X	X	X	X	X	X	X	X	X	X	X	X

Table 9 - Motorised Test Conditions

One of the most critical areas inside an engine is the “piston-ring and cylinder-liner interaction”. It is one of the most hostile areas inside an engine mainly because it is subjected to high temperatures and the forces generated by the combustion. The engines are design in such a way that adequate lubrication is guaranteed. The lubricant is present in the form of a very fine film, enough to prevent metal to metal contact but not to splash off into the cylinder and enter the combustion chamber. When cavities are generated in this fine film the lubricant is giving its place to the cavities. These cavities mainly being composed by a gas are not capable of offering to the components the protection they require. This can lead from poor operation up to possibly severe engine damage and in some cases, total engine failure. Even

in best designed engines the control of the lubrication especially in the “cylinder-liner and piston-ring interaction” is far from ideal. This is not just due to insufficient engine design but also poor lubricant performance. The materials used for modern day lubricants might have tremendously evolved in the recent years but they still present limitations for the needs of modern internal combustion engines.

Firing	Speed					Viewing Window							
Temperature	208RPM	800RPM	1000RPM	2000RPM	3000RPM	1	2	3	4	5	6	7	8
30C													
40C			X			X	X	X	X	X	X	X	X
50C													
60C													
70C			X			X	X	X	X	X	X	X	X

Table 10 - Firing Test Conditions

This results into lubricants often entering the cylinder and with the help of the piston finding their way into the combustion chamber where they take part into the combustion. This phenomenon is called “Lubricant Blow-By” and is directly linked to lubricant consumption. Based on observation by Inagaki (1995) and Duszynski (1999) and also on work carried out for the purposes of this report, blow-by can occur in two ways.

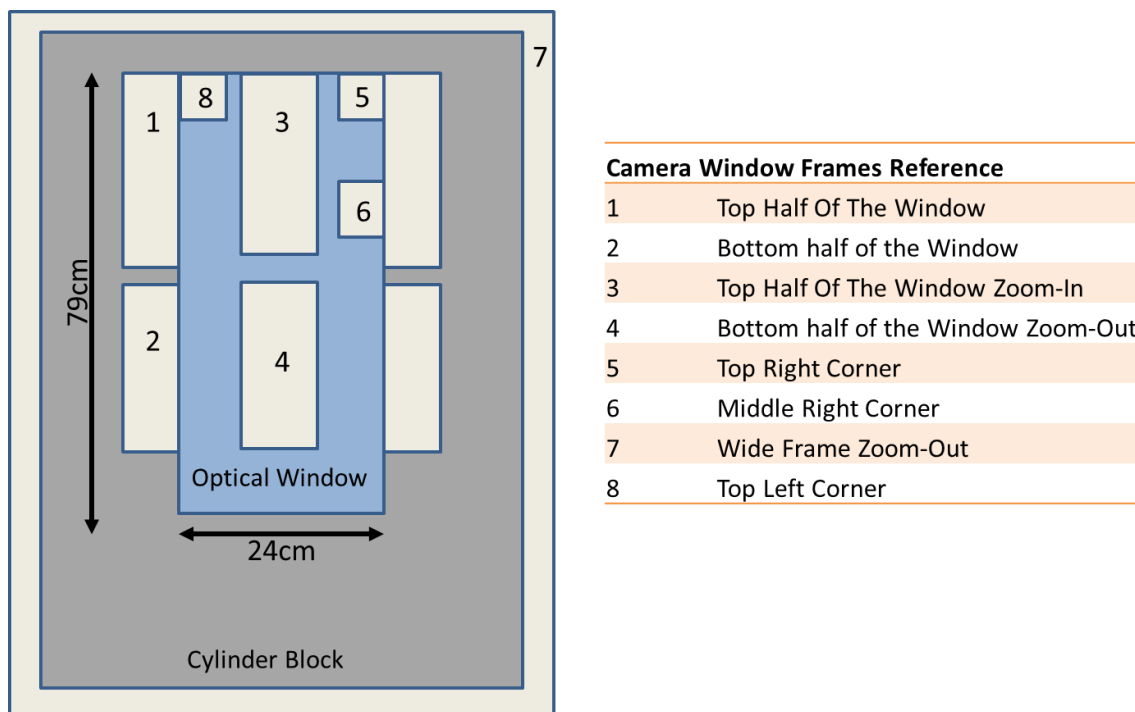


Figure 129 - The Camera Positions used for capturing the visual data

It can either be lubricant passing the piston-rings and entering the combustion chamber or fuel and combustion products passing down the rings and into the oil sump. Both of these

scenarios are highly undesirable as they affect the performance and reliability of the engine. When the lubricant enters the combustion, it has a negative impact on the output emissions while the products of a combusting lubricant can damage the internal components. On the other hand, when unburnt fuel and exhaust gases pass into the oil sump they contaminate the oil which highly affects its performance (Inagaki, 1995).

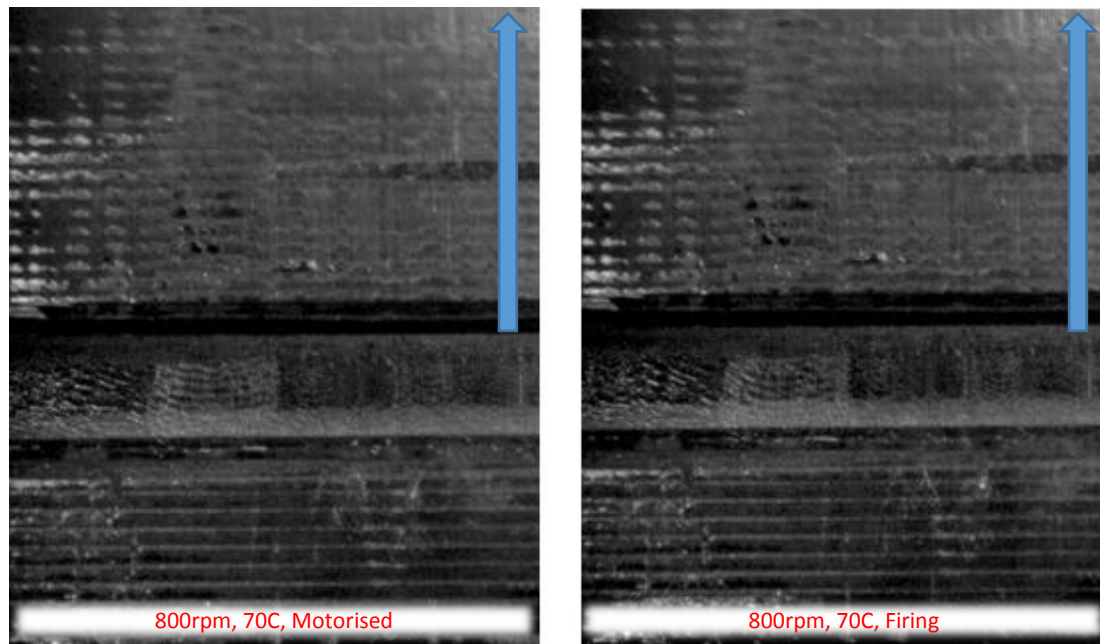


Figure 130 - Firing vs Motorised operation, 800RPM, 70C

The visual capabilities of the optical engine built for this project give the opportunity for the investigation of phenomena that take place in conventional engines in the area between the piston-rings and the cylinder-liner. The focus of the project is on two main areas, the lubricant cavitation and the lubricant blow-by. The following sections investigate the behaviour of cavitation at different engine speeds and temperatures. Tests have been performed for both motorised and firing conditions as shown in Table 9 and Table 10 respectively. The map of the optical windows location is shown in Figure 129. The first area of investigation is the top half of the cylinder and the second area the bottom half. In addition to the investigation of cavitation there are additional data capturing phenomena such as blow-by with lubricants entering the combustion chamber and taking place into the combustion, all listed, detailed and explained in the Results chapter of this report. The motorised tests followed the entire matrix as this is detailed in table 9. This is not the case for the firing operation and table 10. The firing operation was conducted for a selected portion of the operating condition used for the motorised operation. In the firing operation combustion

products, would cause the optical window to lose its optical capabilities due to the build-up of combustion residuals.

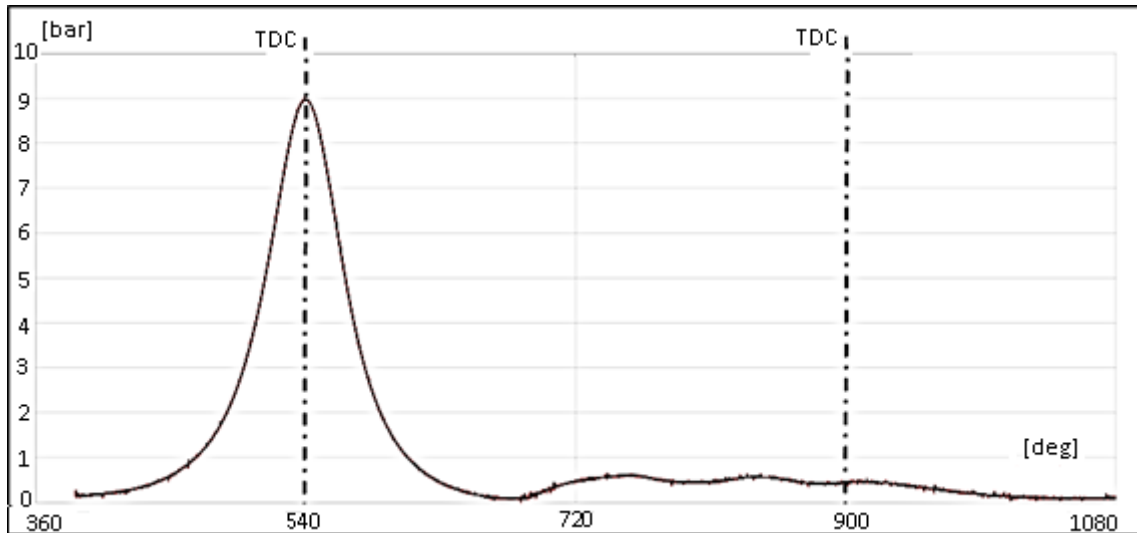


Figure 131 - The optical-engine pressure trace, Motorised, 1000RPM, 70C, 720deg

The effect the combustion residuals have on the optical window affects its visual clarity and thus the time between the testing dramatically increases due to the fact that the window needs thorough cleaning before the following run. Figure 129 presents the different optical frames used for the purpose of this report. There were eight frames used in total.

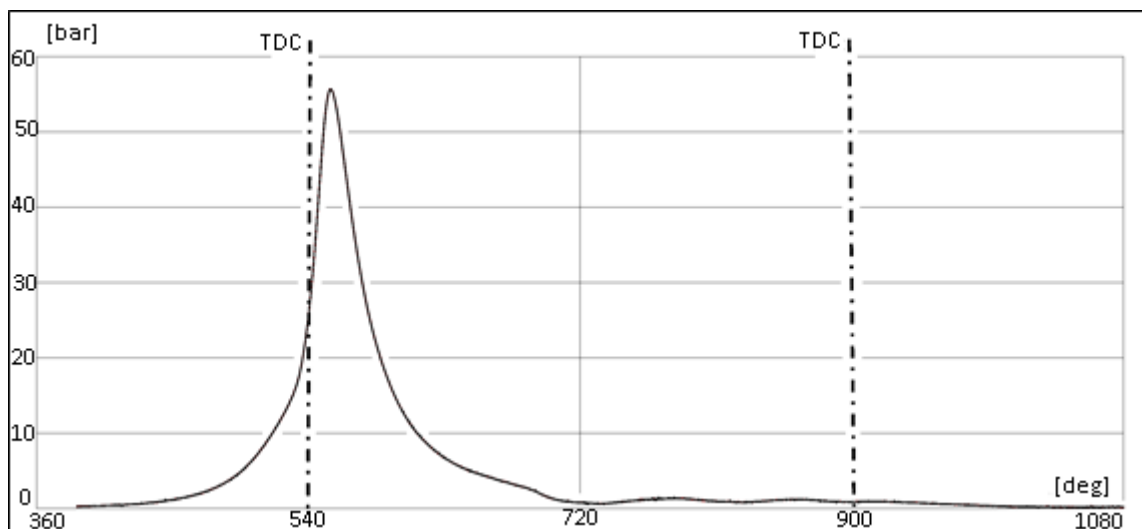


Figure 132 - The optical-engine pressure, Firing, 1000RPM, 70C, 720deg

The following figure shows the position and the frame captured by the camera in relation to the optical window. Figure 130 illustrates in blue the optical window and the numbered areas are the frames captured by the high-speed camera. Throughout the test runs it has been observed that there were no significant differences between the firing and the motorised

operation as far as the cavity generation is concerned. Figures 133 and 134 show the velocity and acceleration of the piston for the optical engine.

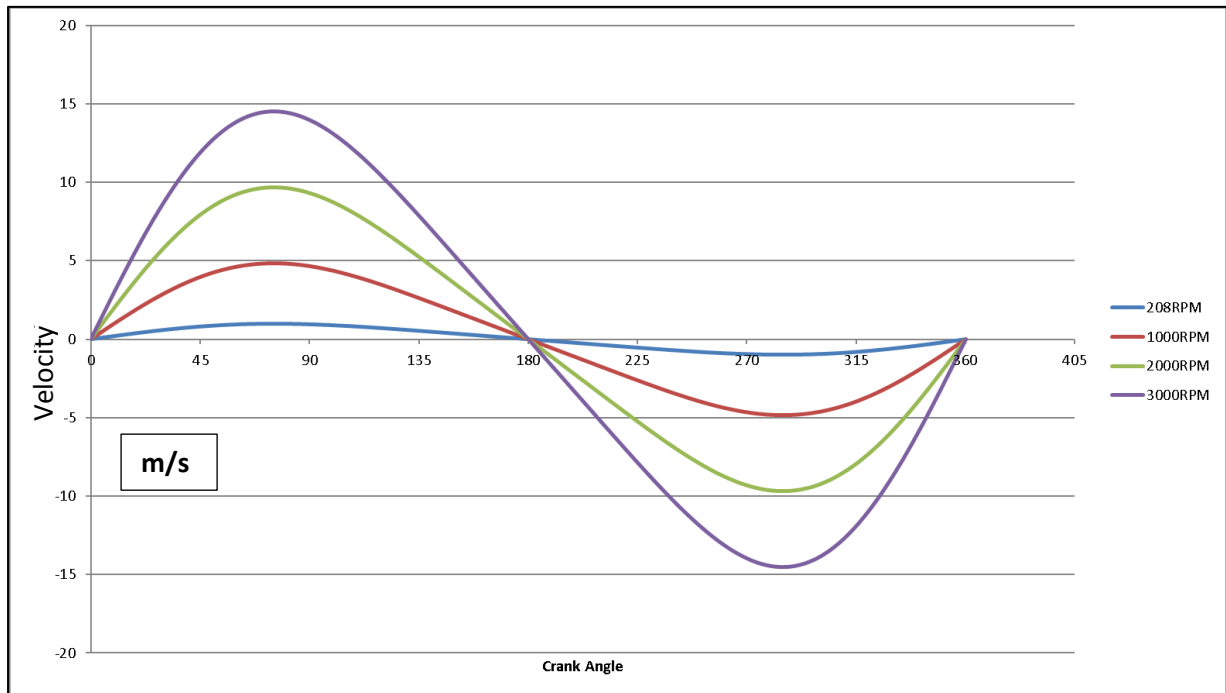


Figure 133 - Optical Engine Piston Velocity Profile

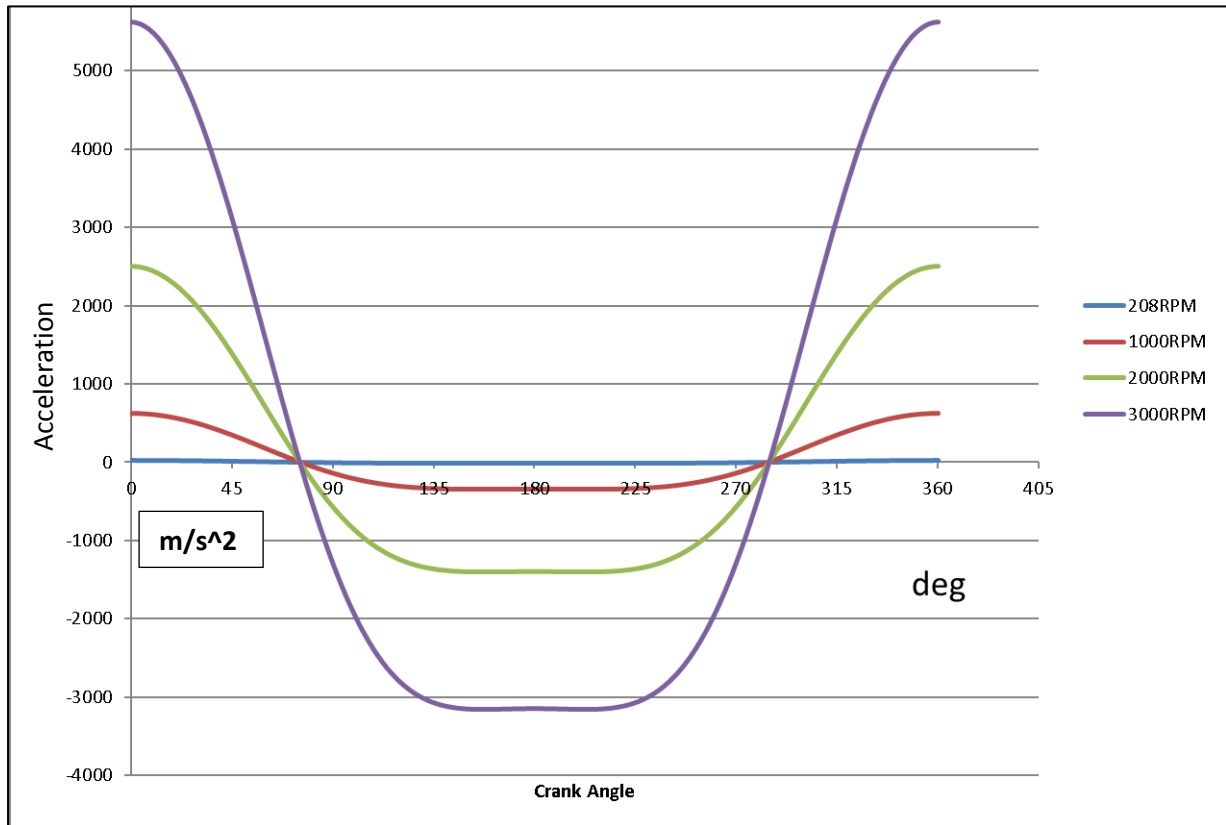


Figure 134 - Optical Engine Piston Acceleration Profile

Figure 130 is a representative example of that observation where the two frames between the two operating conditions are compared. The two frames have been captured under firing and under motorised operation at 800rpm and at a temperature of 70C. The optical frame refers to figure 129 as position number 4. Based on this observation the decision was made to present data mainly related to the motorised testing, when the phenomena of cavitation were investigated, as the motorised images featured better quality. The combustion residuals would in some cases affect the clarity of the optical windows which would affect the clarity of the images captured. Figures 131, 132 and 139 show the pressure trace of the in-cylinder pressure for both the motorised and the firing conditions. Figure 131 shows the pressure trace of the motorised operation. A specific characteristic of this operating condition is that the pressure has its peak at the TDC. This occurs as the in-cylinder pressure only increase due to the movement of the piston. Thus, the pressure peak would be at the highest point of the pistons journey (TDC). Figure 132 shows the pressure trace of the firing operation. It is distinct that the peak of the pressure trace is no longer at the TDC but a few degrees after TDC. This occurs as the fuel does not fully combust at the TDC. In a firing engine in-cylinder pressure would reach multiple times the pressure of the motorised after the TDC when fuel has fully combusted. The engines operating conditions are directly linked and affect the cavitation of the lubricant in the piston-ring/cylinder-liner interaction. The phenomenon of cavitation takes place when a fluid is subjected under extreme forces. In the case of an internal combustion engine that fluid is the lubrication oil. One of the first observations was that cavitation is not always occurring inside an operating four-stroke internal combustion engine. A four-stroke internal combustion engine operates in four strokes and two cycles. The meaning of that is that the engine needs four strokes of the piston to complete two cycles. These are the intake/exhaust cycle and the power cycle. In the intake/exhaust cycle the engine exhausts the combustion products from the previous cycle and takes in fresh air and fuel for the next cycle. In the next power cycle, the air/fuel mixture is compressed and ignited, and the process repeats itself while the engine is in operation. It has been observed that cavitation occurs only during the power cycle and more specifically when the in-cylinder pressure exceeds the atmospheric pressure. This observation remains unclear to whether cavitation is not occurring or if the cavities were in a magnitude that could not be captured by the high-speed imaging equipment used. The in-cylinder pressure exceeds the atmospheric pressure during the power cycle when both intake and exhaust valves are closed while the volume of the cylinder has decreased. The variation of the in-cylinder volume depends on the position of the piston thus, the in-cylinder pressure changes are directly linked to the piston's movement. Cavitation only

appears in the compression-expansion stroke but that is not the only phenomenon that is occurring during that specific part of the cycle. It seems that there are more phenomena that occur inside an engine when the in-cylinder pressure moves away from the atmospheric pressure and those are detailed and described in the paragraphs below. The following phenomenon mainly occurs under a fully motorised operation, where the engine is driven with the help of an electric motor. It has been observed that when the piston is moving downwards past the TDC the fuel present in the cylinder fully atomises in the form of aerosol. Under this motorised condition the fuel that enters the cylinder does not burn due to the lack of ignition. The unburned air-fuel mixture enters the cylinder and is compressed by the piston in the confined volume of the combustion chamber. As described when the piston is then moving downwards momentarily there is a phenomenon that is observed where there is the appearance of a fuel aerosol caused by condensation. After the piston, has travelled close enough to the BDC the “fuel aerosol” disappears. The development of that phenomenon is illustrated in figures 135 to 138. In the same figures the aerosol appears during the compression stroke and while under motorised operation. The fuel evaporates and appears as a white “smoke” up to the point where the valves open and the pressure reaches atmospheric.

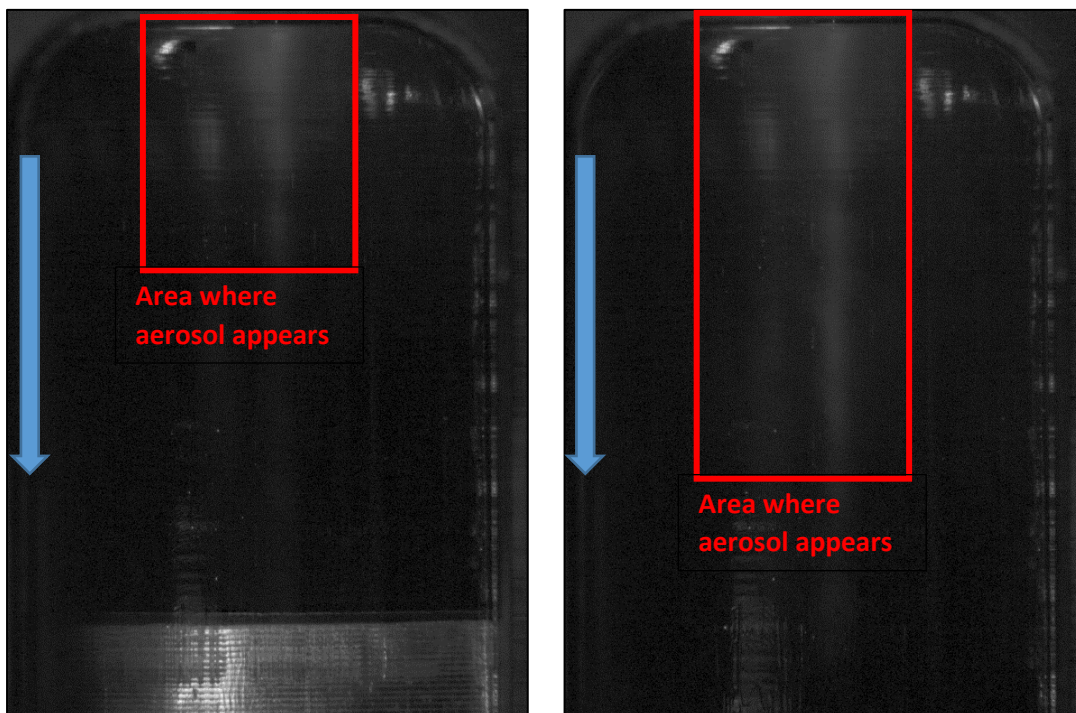


Figure 135 - Aerosol effect, 208rpm, 70C, Motorised

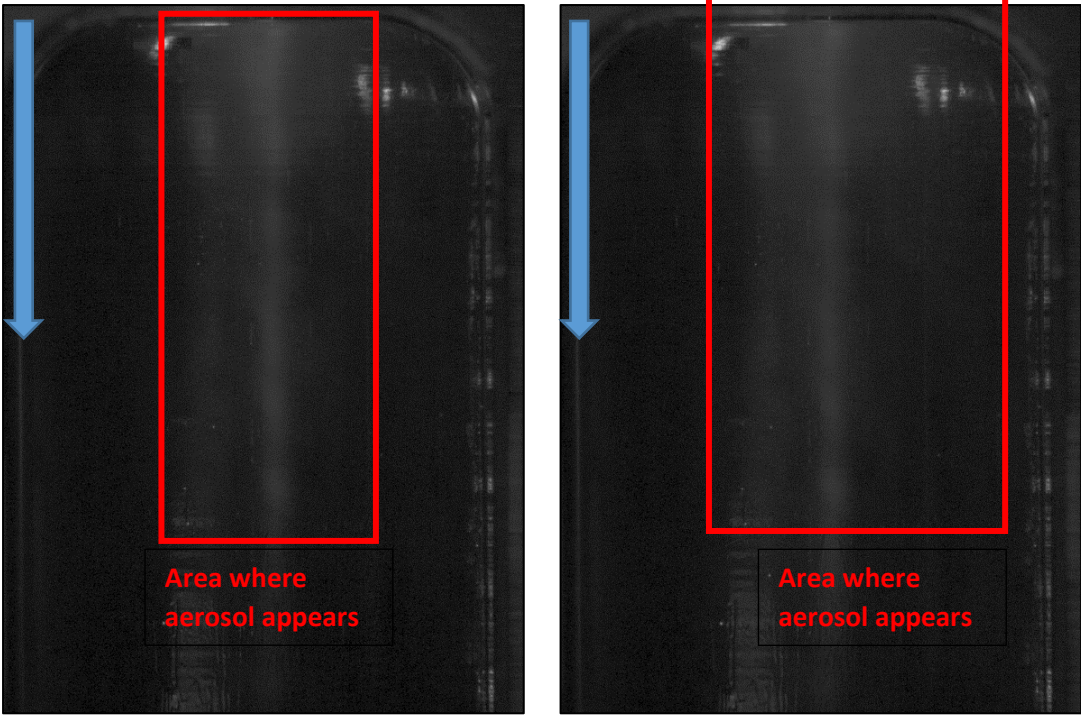


Figure 136 - Aerosol effect, 208rpm, 70C, Motorised

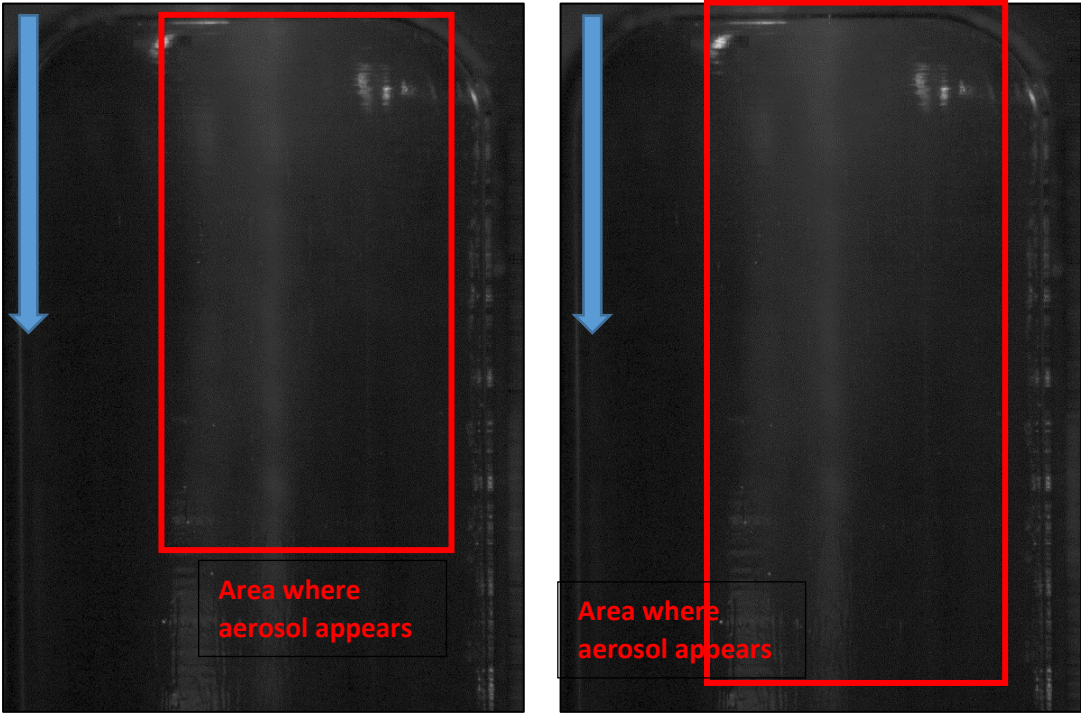


Figure 137 - Aerosol effect, 208rpm, 70C, Motorised

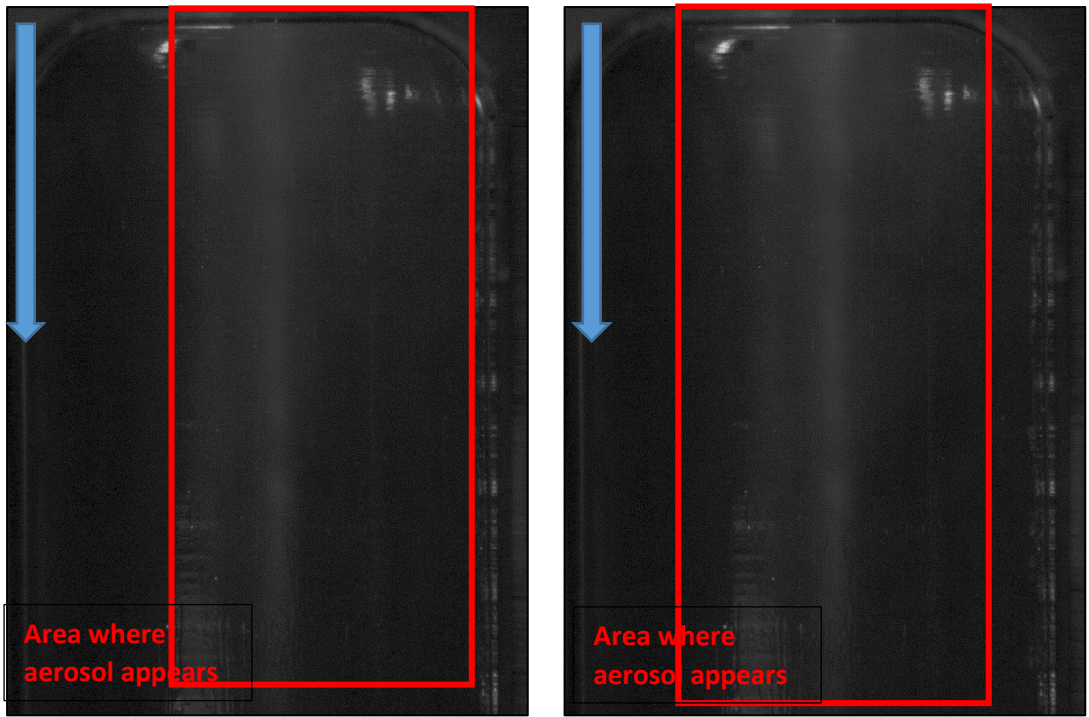


Figure 138 - Aerosol effect, 208rpm, 70C, Motorised

During the intake/exhaust cycle and more specifically when the in-cylinder pressure reaches the atmospheric pressure while a set of valves are open there was no cavitation appearing. The reason behind this phenomenon is considered to be the lack of increased in-cylinder pressure during the intake and exhaust cycle.

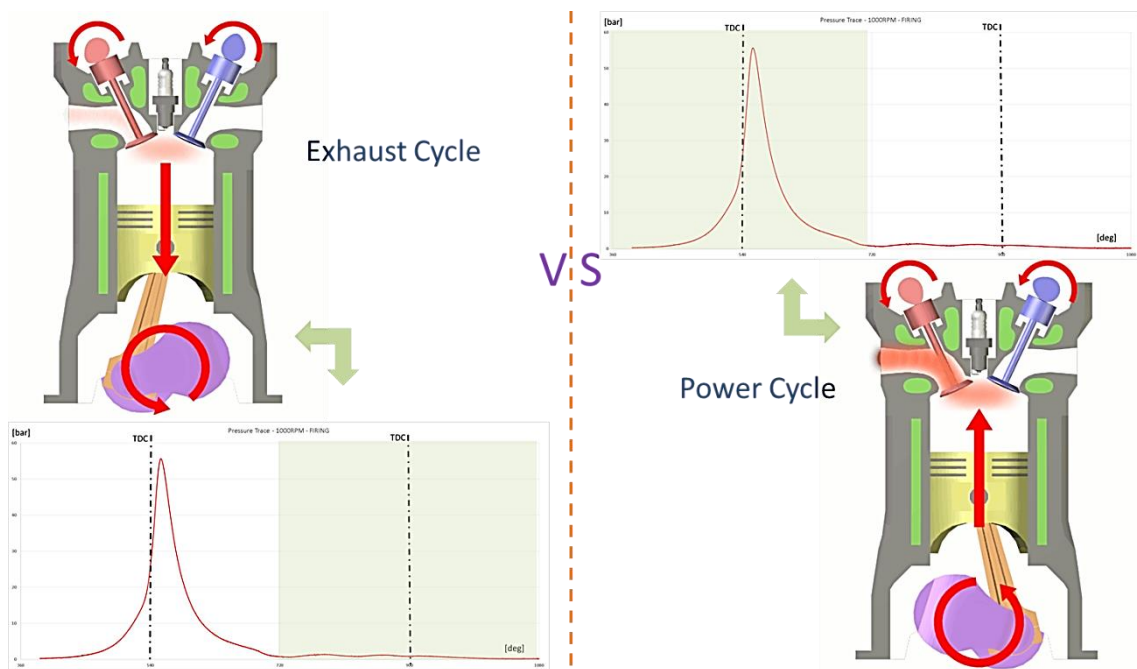


Figure 139 - Exhaust/Intake Cycle VS Power Cycle

The fundamental operation and design of the piston-rings is based on the principal that the in-cylinder pressure is acting on the back of the rings forcing them for a better seal. Thus, the higher the in-cylinder pressure the better the seal. This applies to all the rings resulting to better control of the lubricant film left of the cylinder walls. The force behind the rings causes the gap between the rings and the liner to decrease significantly. This decrease in the gap between the rings and the liners causes the lubricant present in the area to pass through a very narrow and confined space that places the lubricant itself under a high pressure that along with the surface imperfections causes the lubricant to cavitate. It is observed that the cavity generation is highly linked to the changes in the in-cylinder pressure. Lubricants not only have to maintain their properties throughout the engine cycle and provide sufficient lubrication, they also must withstand extreme forces and the cavitation process that take place inside an internal combustion engine. The continuous search for more sophisticated and better lubricants is one of the leading factors that contributed to the need for the specific project. Since cavitation is not observed in every cycle the results will only cover the power cycle including the compression and power strokes. To better understand the difference in the cavitation of the lubricant between the two cycles the following sequence of images show the behaviour of the lubricant when trapped between the cylinder-liner and piston-ring interaction for both the inlet/exhaust and the power strokes.

5.5.1 Intake/Exhaust Cycle

During this cycle the following set of images from figure 140 to figure 145 show that there is no cavitation taking place in the cylinder-liner and piston-ring interaction at either the up-stroke or down-stroke of the piston. There is also the possibility that the generated cavities are of size that cannot be captured by the optical setup used. In order to clarify this, further testing has to be performed with possibly the use of fluorescence additives. The following images from [-61] to [+71] degrees crank angle have been captured under motorised operation without fuel injection. The engine speed is constant at 1000rpm and the temperature of the lubricant is maintained at 70C with the use of the in-build heaters. The main reason motorised operation was used to present the cavity behaviour, is due to the fact that the combustion gasses would affect the clarity of the images. The effects of the combustion have been considered later section of this report. The images from [-61] to [+71] degrees clearly show that despite the engine operating at 1000rpm there is no cavitation taking place. All three rings show exactly the same behaviour, regardless if the movement is up-stroke or down-stroke. The effect is the same. It is concluded that while one set of valves

is open, cavities do not appear on the surface of the rings. That can be partially due to the fact that the in-cylinder pressure which is close to the atmospheric pressure does not allow for the cavities to generate and grow or that the cavities are generated at such a small scale that are not captured by the setup used. Another cause of this phenomenon and which is believed to be the more dominant is the gap between the rings and the liner. The piston-rings are designed on the principle that the in-cylinder pressure assists them in a way that the higher the in-cylinder pressure the better they seal the combustions chamber.

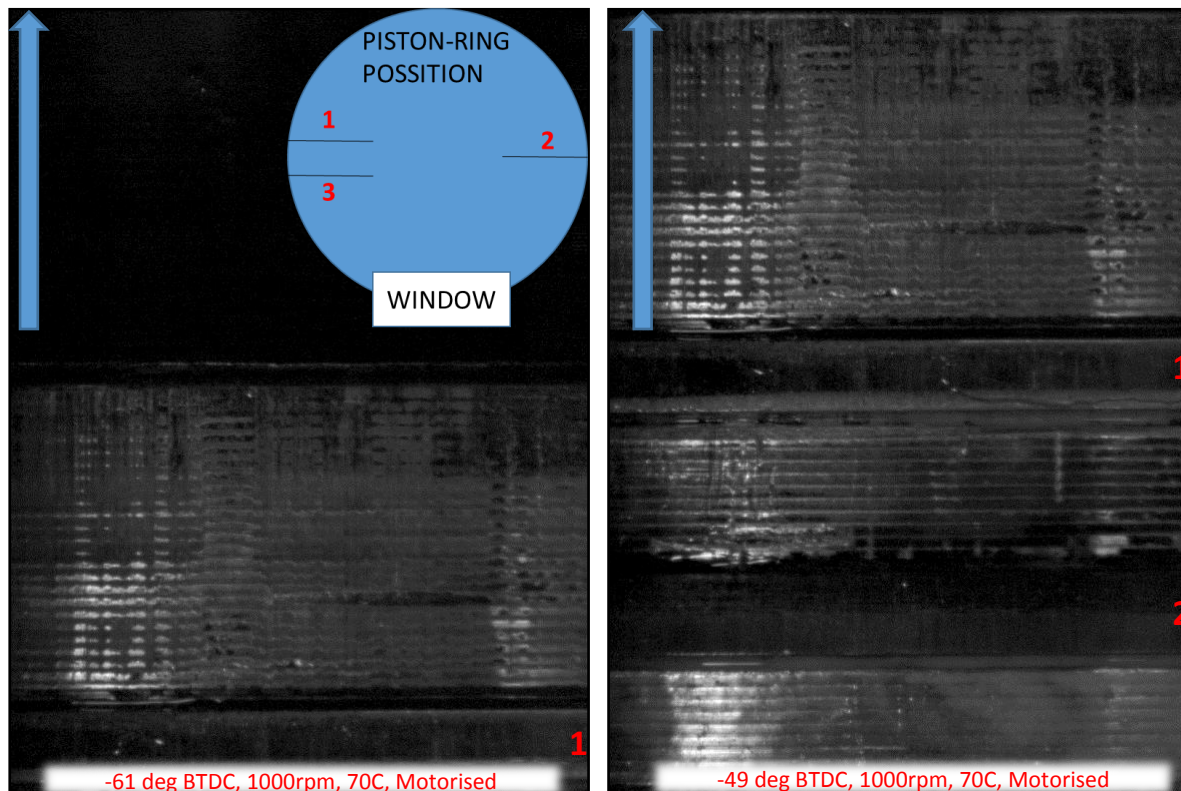


Figure 140 - BTDC, 1000rpm, 70C, Motorised

This occurs because the in-cylinder pressure is acting on the back of the piston-rings and forces them onto the cylinder walls. The higher the in-cylinder pressure the higher the force acting behind the piston-rings thus, the better they seal. While the piston is following, a reciprocating motion the rings move at the same speed and direction since they act as part of the piston itself. During engine operation, the piston never comes in contact with the cylinder walls. In the event that something like that happens the consequences can be catastrophic for the engine. The basic engine operation principle is that the rings come in contact with the cylinder walls and they provide a smooth sliding surface between the piston and the liner. They also provide a way of sealing off the combustion chamber and preventing combustion products and in-cylinder gasses escaping into the crank case. While the piston-rings and the cylinder-wall have been polished at a degree that ensures minimal friction, the direct contact

needs to be avoided at all times. This is where the lubricants are of use. The lubricant interferes between the sliding surfaces and prevents the metal to metal contact. While the lubricant transport mechanisms have been fully detailed and analysed in the early chapters of this report, the end result is that there is always a fine film of lubricant present on the cylinder walls. This film regardless its thickness is crucial to the engine operation.

The piston and the rings are following a reciprocating motion, and considering that the piston-rings and the cylinder-liner are in contact separated with only by the lubricant interfering between them, the oil film is actually forced between the piston-rings and the cylinder-liner while the engine is in motion. The higher the in-cylinder pressure the higher the forces acting on the back of the piston and the higher the in-cylinder pressure the smaller the gap that the lubricant needs to squeeze through. The ring-gap while the engine is at the intake or exhaust phase is not small enough for the lubricant to reach the required pressure for the cavities to generate and develop. From testing done on a test-rig it has been observed that there is a direct link between cavitation, the piston-ring and the cylinder-liner gap.

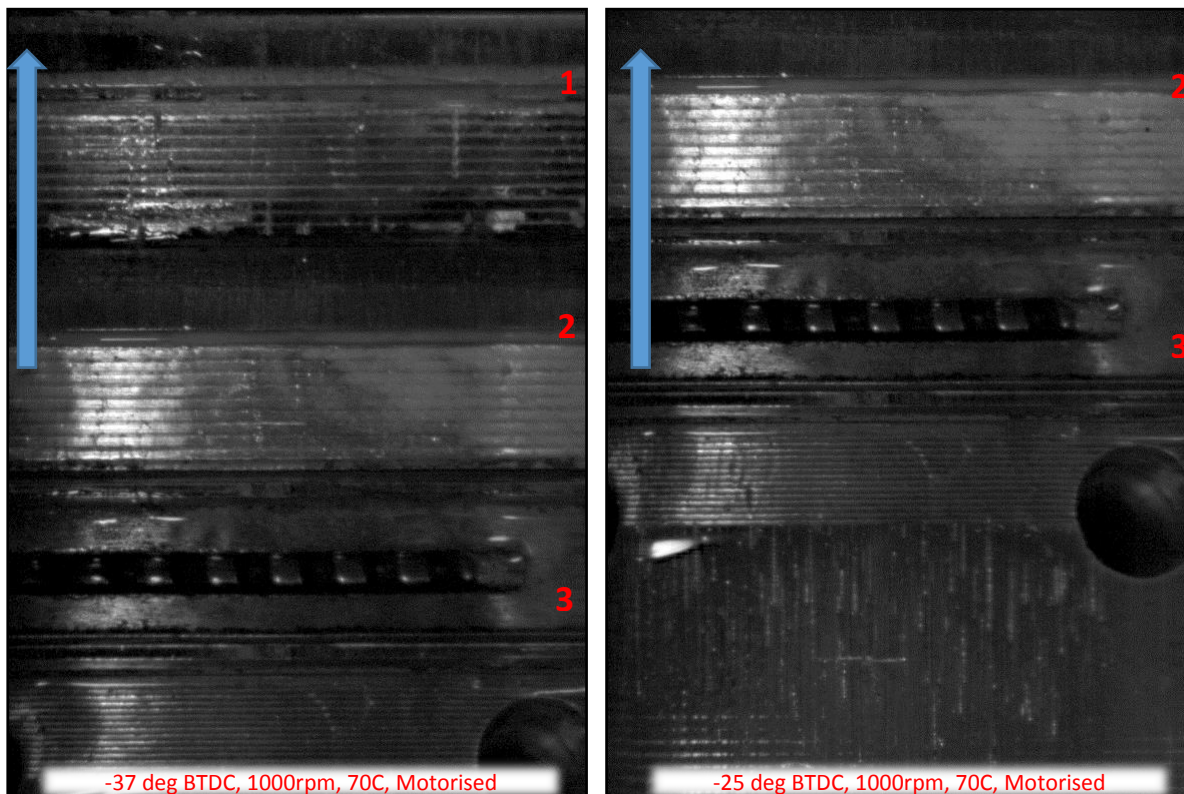


Figure 141 - BTDC, 1000rpm, 70C, Motorised

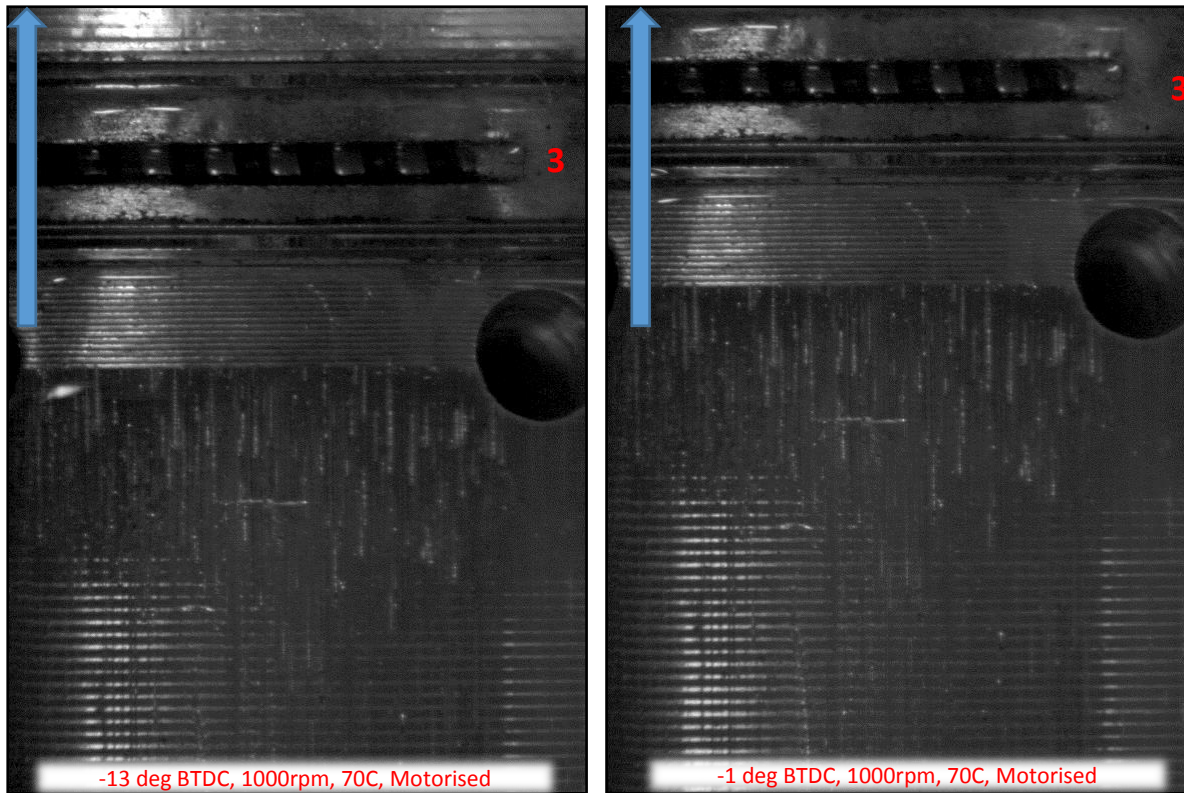


Figure 142 - BTDC, 1000rpm, 70C, Motorised

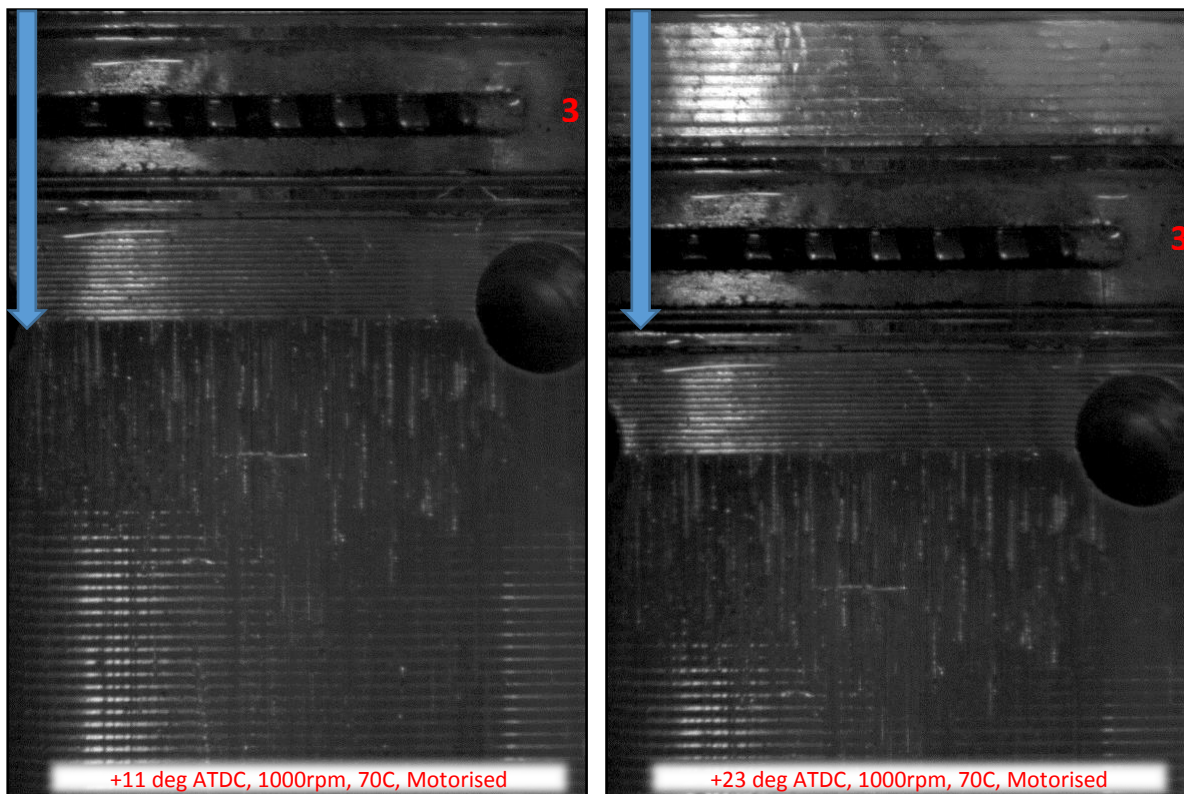


Figure 143 - ATDC, 1000rpm, 70C, Motorised

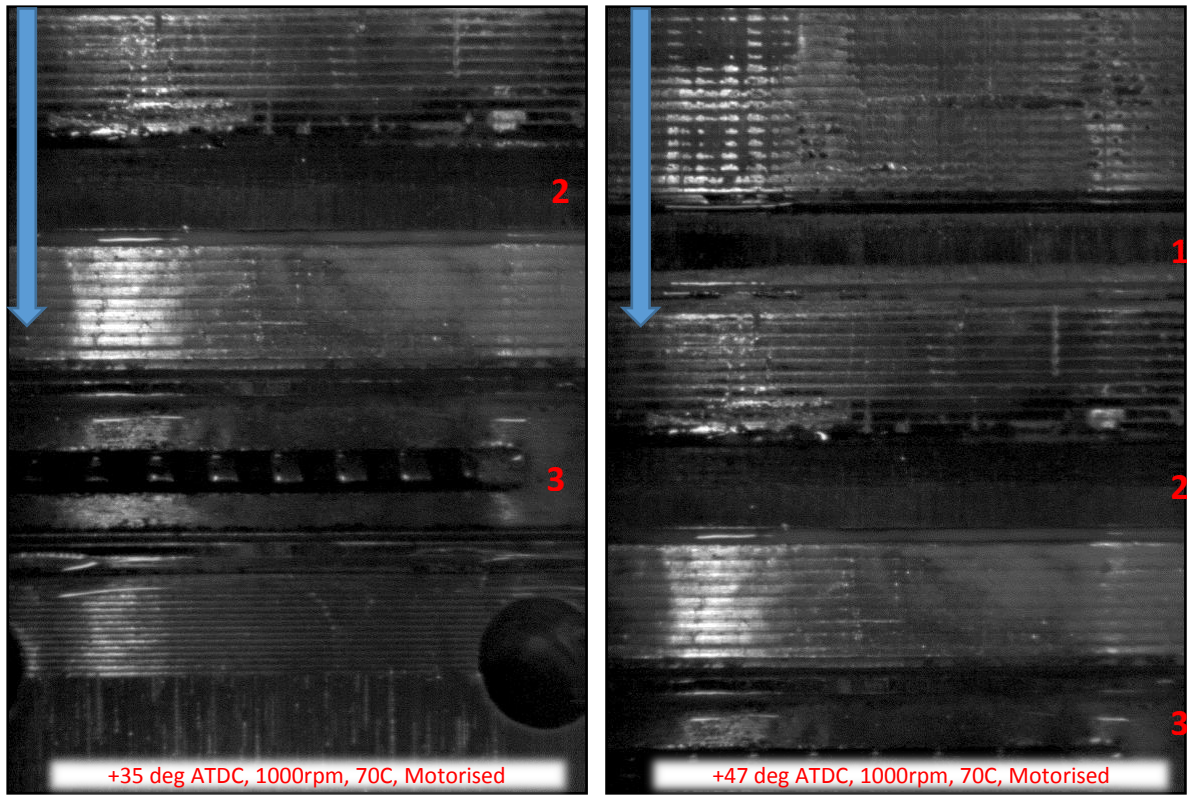


Figure 144 - ATDC, 1000rpm, 70C, Motorised

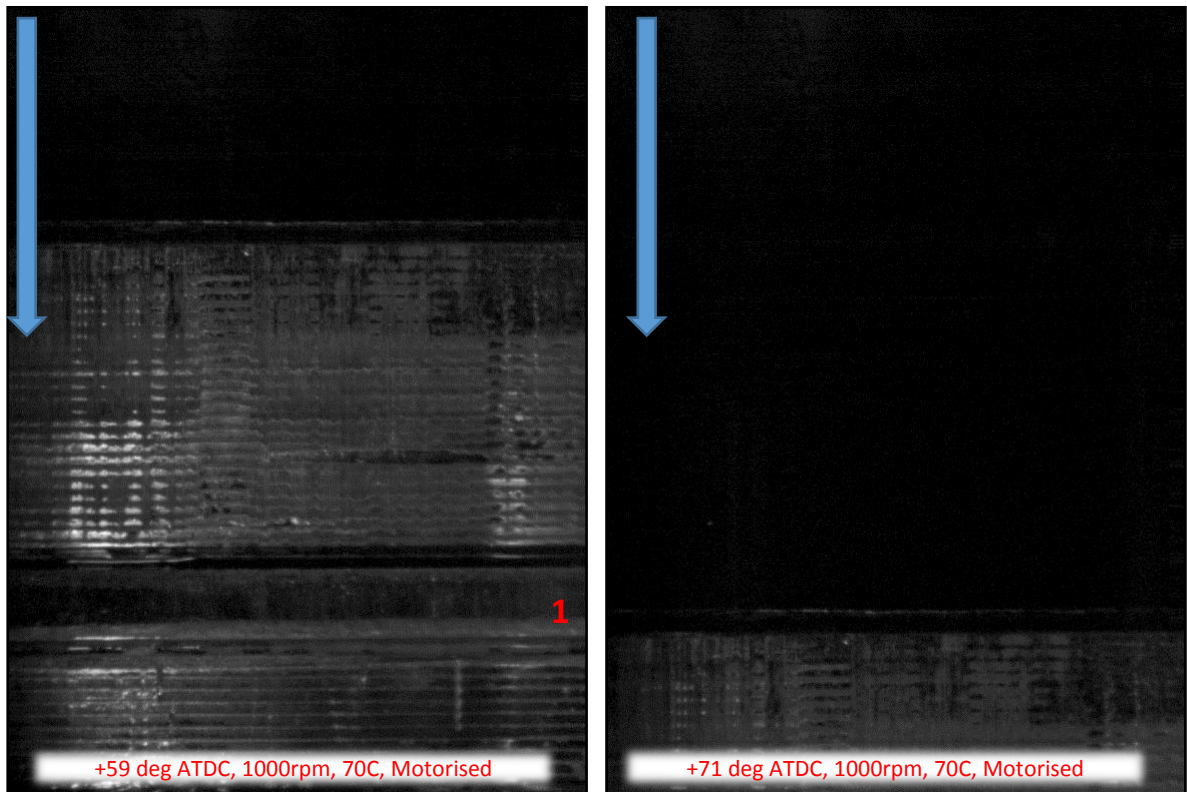


Figure 145 - ATDC, 1000rpm, 70C, Motorised

As a conclusion, the decreased in-cylinder pressure allows for a larger gap between the cylinder-liner and the piston-rings that do not allow the lubricant to reach the conditions needed for the lubricant to cavitate. Usually cavitation is directly linked to the pressure changes that a fluid is subjected to. The pressure changes along with surface imperfections result to the release of air already trapped inside the fluid in the form of bubbles and with the sudden pressure change and energy generated these bubbles grow and form cavities. These cavities are the cause of many engine related problems. These range from poor engine performance to critical engine failure. Going back to the observation that there is no cavitation on every cycle during the operation of an internal combustion engine this is a step towards the better understanding of this phenomenon which up to now was only known through the assumption that it occurs inside and engine but never having the actual evidence when it does. This discovery is an important step toward a possible solution that would minimise the effect of cavitation on the performance and reliability of internal combustion engines. The final conclusion is that lubricants due to each individual factor detailed above do not show any signs of cavitation while the in-cylinder pressure is equal to the atmospheric. The phenomenon is directly linked to the position of the inlet and outlet valves.

5.5.2 Power Cycle

During the power cycle the following set of images from figure 146 to figure 151 show that there is cavitation taking place in-between the cylinder-liner and piston-ring interaction at both the up-stroke and the down-stroke of the piston. The [-61] to [+71] degrees crank angle images have been captured under motorised conditions without fuel injection. The engine speed is constant at 1000rpm and the temperature of the lubricant is maintained at 70°C with the use of the engines in-build heaters. There is clear evidence that cavitation is not observed during the power cycle, where there is a massive increase in the in-cylinder pressure. The increase is due to the fact that the in-cylinder volume is decreasing as the result of the piston's upward movement. It can be derived that the images captured during the power cycle offer a completely different view when compared with the results of the intake/exhaust cycle. In all the captured images it is evident that cavitation occupies a big part of the area of the ring and it is eminent that the increased in-cylinder pressure has a direct effect on cavitation. It has been known that cavity generation is directly linked to pressure and it occurs in lubricants when these are subjected to extreme pressure changes. These pressure changes with the help of the surface imperfections present in the surrounding components cause the air trapped inside the fluid to be released in the form of bubbles. These bubbles after their generation will

continue to grow due to lubricant evaporating along the bubble boundaries up to the point where they collapse. While the bubbles collapse they release a large amount of energy in the form of a shock wave which is targeted at a very small area. This can cause significant damage even to the toughest nearby components. Finding a solution that will eliminate or minimise the effect of that phenomenon would be beneficial towards the performance and reliability of those engines. The images present that the increased in-cylinder pressure has a dramatic effect on the behavior of cavitation. It has been noted that the in-cylinder pressure changes are causing the lubricant film present on the cylinder walls to cavitate. The main cause of this phenomenon is believed to be the effect that the in-cylinder pressure has on the piston-rings. While the in-cylinder pressure builds up in relation to the movement of the piston the pressure forces the rings onto the cylinder wall resulting in a better seal. The better seal automatically results to a finer space between the piston-rings and the cylinder-liner causing the lubricant present to flow through a confined space. The lubricant under these conditions starts to cavitate causing the film to break and produce the set of visual data presented in this section. Another phenomenon equally interesting as the phenomenon of cavitation is the effect the in-cylinder pressure has on the fuel itself, when the fuel does not combust inside the cylinder. Fuel has been injected in the motorised tests in order to study the effect of the fuel on the lubricants. What has been observed is that the fuel would enter the combustion chamber at the point where the inlet valves open. This is a feature found mainly with port injection internal combustion engines. The fuel enters the combustion chamber at the same time as Air. While the fuel enters the cylinder and the inlet valves close the piston would start moving upwards and would compress the air fuel mixture till the point it reaches the top dead center. At the top dead center the piston would stop and would start moving backwards towards the bottom dead center. At this point what is observed is that the fuel that has been compressed due to the rapid change in the in-cylinder pressure it would momentarily evaporate and would appear in the form of an aerosol until the piston has moved further down the cylinder where the smoke would disappear. This is a phenomenon that was observed during the testings and it appeared on every cycle with fuel present inside the cylinder while all the ports were closed. There is need for further investigation in order to determine the exact cause of this phenomenon and the effect it has on internal combustion engines. Due to the fact though that the majority of engines are not motorised the fuel would almost never leave the combustion chamber un-burned. It has been indicated that there would be no significant effect of this phenomenon to the operation of firing engines.

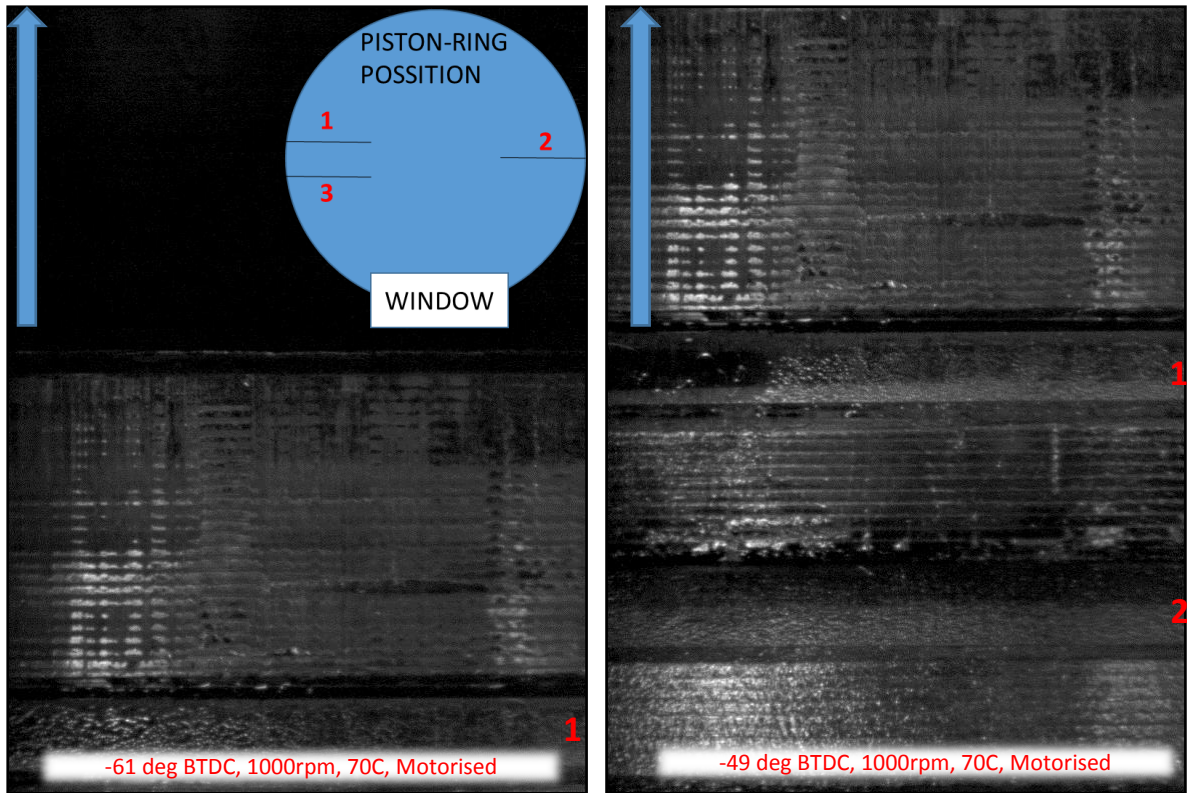


Figure 146 - BTDC, 1000rpm, 70C, Motorised

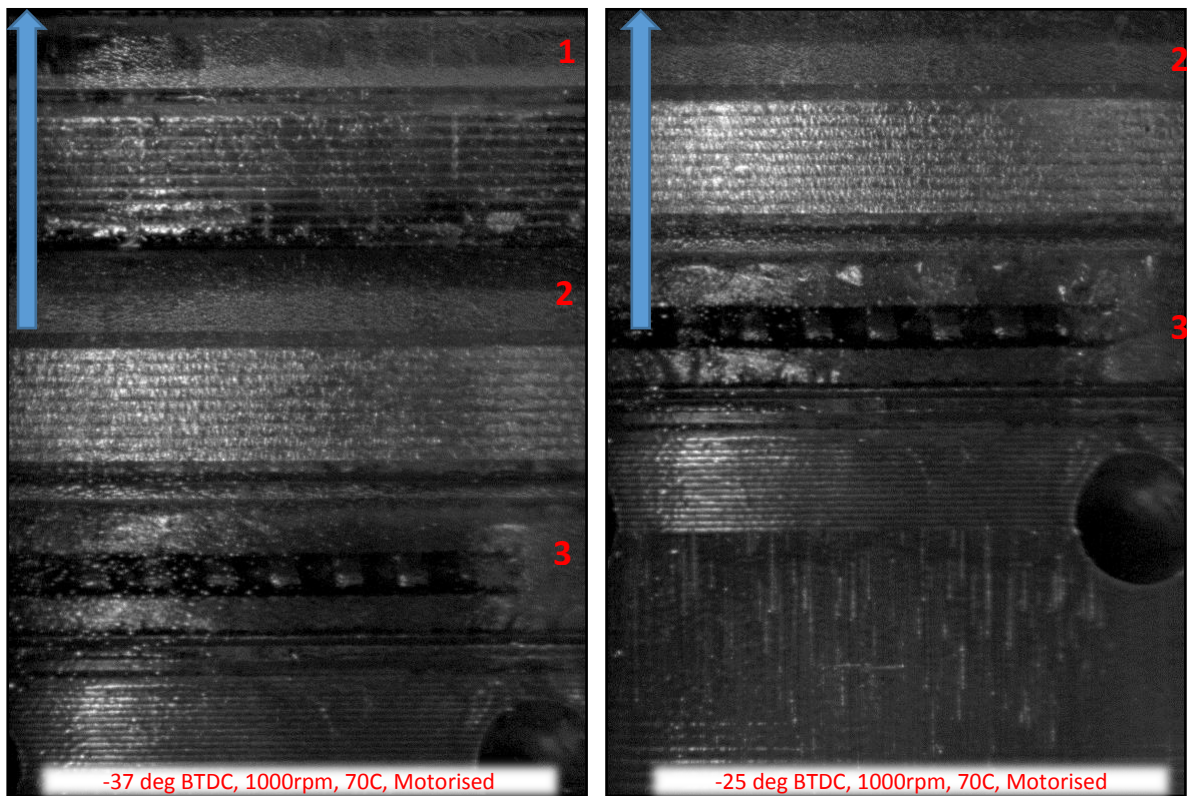


Figure 147 - BTDC, 1000rpm, 70C, Motorised

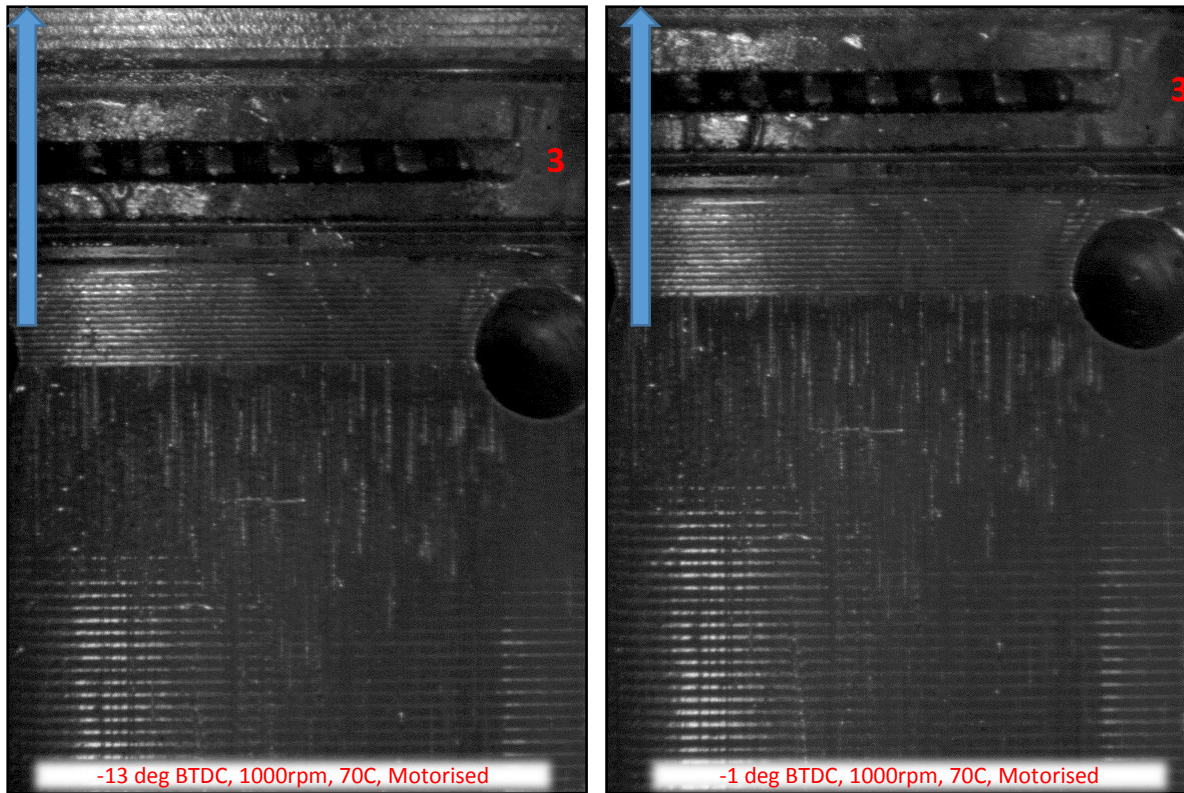


Figure 148 - BTDC, 1000rpm, 70C, Motorised

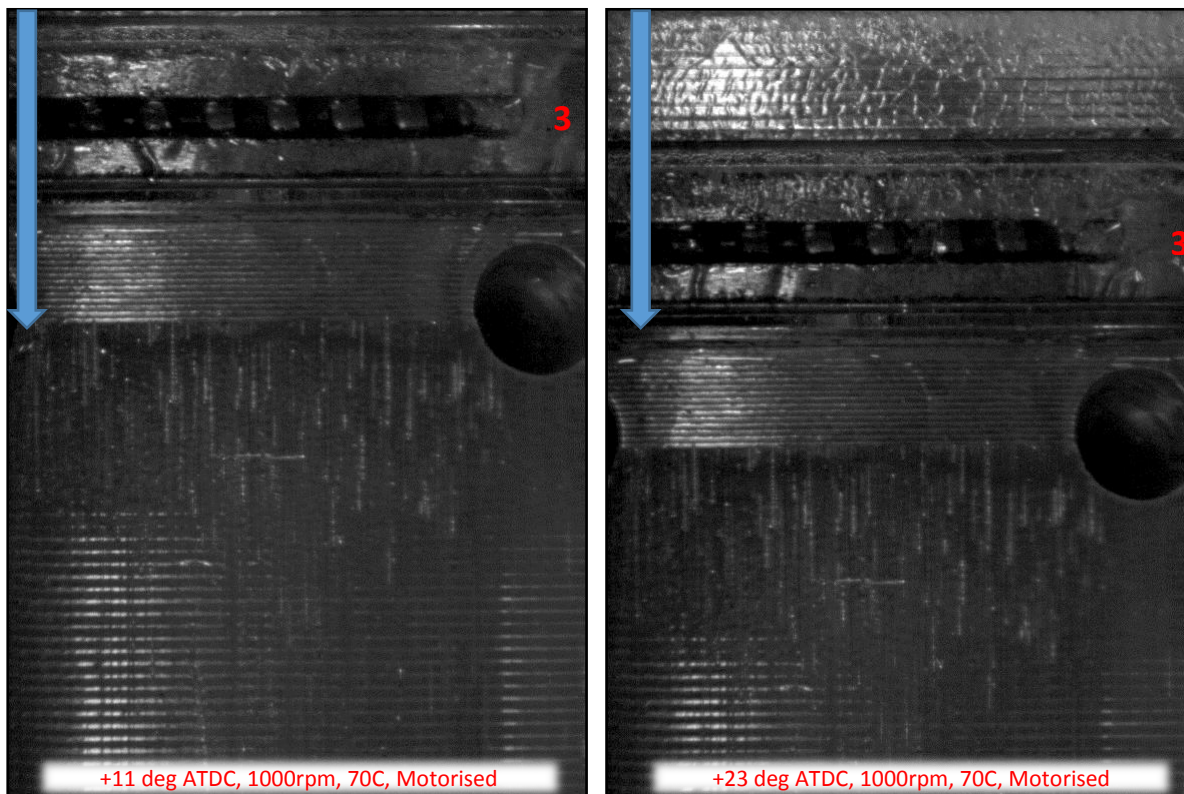


Figure 149 - ATDC, 1000rpm, 70C, Motorised

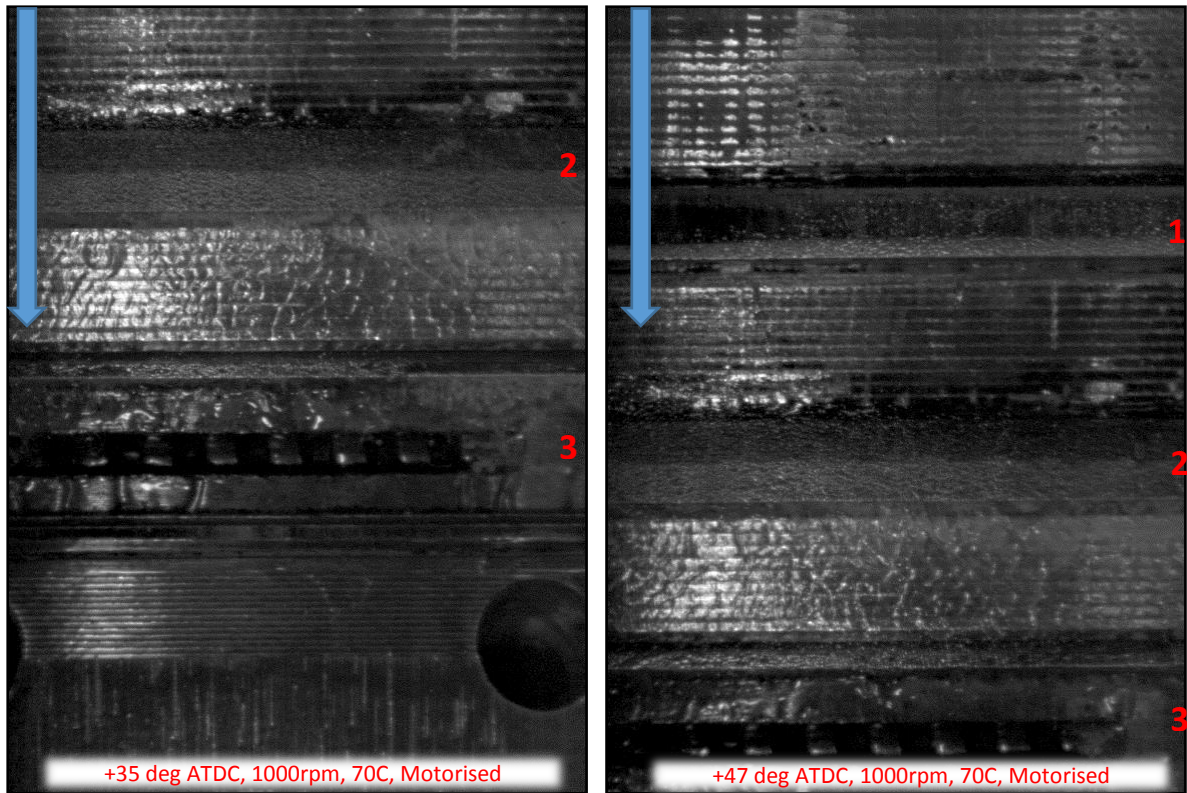


Figure 150 - ATDC, 1000rpm, 70C, Motorised

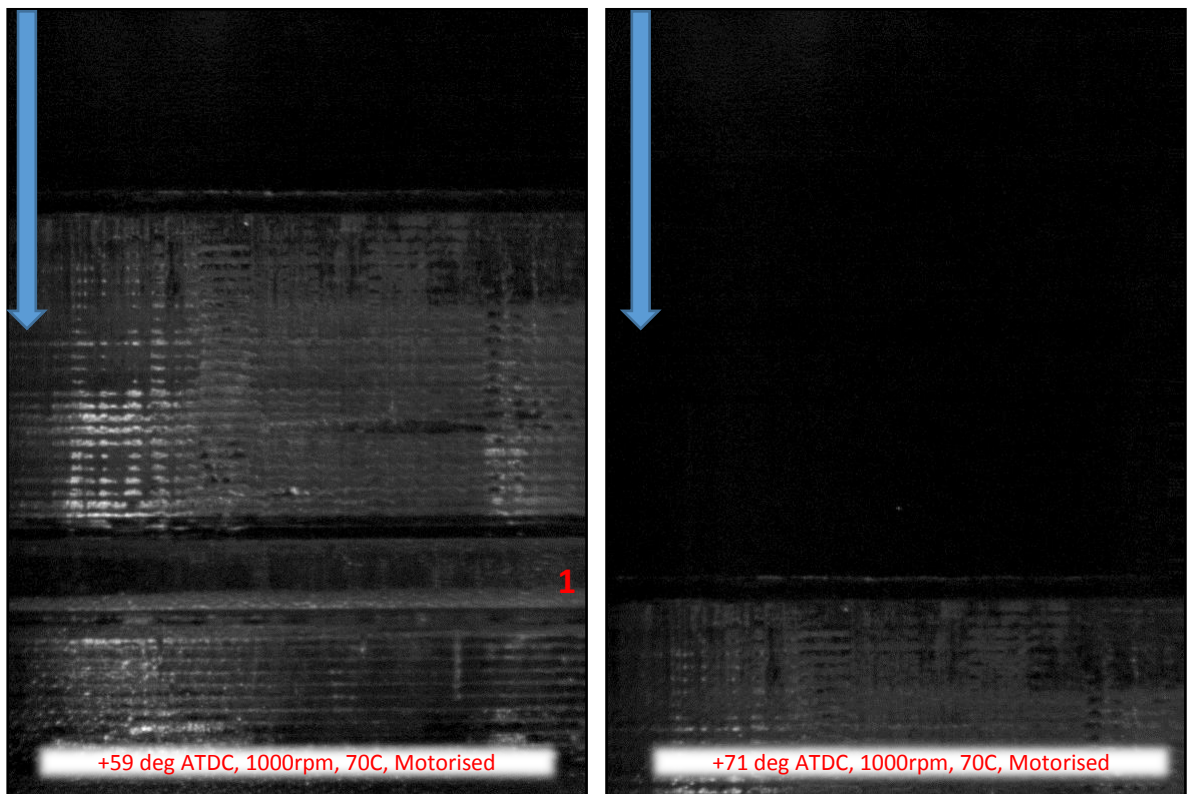


Figure 151 - ATDC, 1000rpm, 70C, Motorised

On the contrary further investigation is needed as it seems that the pressure difference is causing the fuel to atomise. Effect highly desirable for the better combustion of the fuel, especially on port fuel injected engines. One more aspect that would possibly make use of such type of research is the possible effect of those phenomena at certain stages where the in-cylinder fuel has not fully combusted and would possibly still be in the cylinder well into the expansion stroke. This usually occurs when fuel has not fully atomised while entering the cylinder or at high speed applications where fuel does not have the time to fully combust. The final conclusion has to be the effect that the in-cylinder pressure has on the phenomenon of cavitation in internal combustion engines and how the pressure affects its behaviour. Cavitation is a phenomenon that is known to affect the performance, efficiency and reliability of internal combustion engines. These findings have given a new perspective on the view of cavitation in relation to the internal combustion engines. The cavities do not seem to affect the engines on every cycle and possibly this is a way of finding a solution to the negative effects of cavitation on the engines. The fact that cavitation does not take place on every cycle and the fact that cavitation is linked to the changes in the in-cylinder pressure could possibly be a step towards improved engine designs. Finally, the findings of the project are considered to be important as the project gave an insight to an area of the engine rarely investigated before due to its particular location. It is supported that cavitation does affect internal combustion engines and sometimes with catastrophic results. A view is offered to the way cavitation behaves inside an engine and most importantly that it does not affect every consecutive cycle as initially thought.

5.5.3 Cavity Generation

The following set of images show how cavities are generated in the piston-ring and cylinder-liner interaction when the engine is in operation. For convenience, the affected areas on the three rings have been noted and highlighted with yellow markers. The images in figures 152 and 153 have been captured under motorised conditions without fuel injection. The engine speed is constant at 1000rpm and the temperature of the lubricant is maintained at 70°C with the use of the in-build engine heaters. The camera has been focused on the bottom part of the cylinder-liner, window number 4 as these are specified in figure 129. This set of images present the specific areas in yellow anotation wherever cavities are generates on the piston-rings. The cavities do not cover the entire area of the rings at all times during every stroke. This is highly depended on the in-cylinder pressure, the position, the velocity and the acceleration of the rings. It has been oberved that cavities heve not been generating at random

points either. Even though their behavior is slightly unpredictable while they develop, this becomes more eminent at high engine speeds, though the point where they generate does not seem to be random.

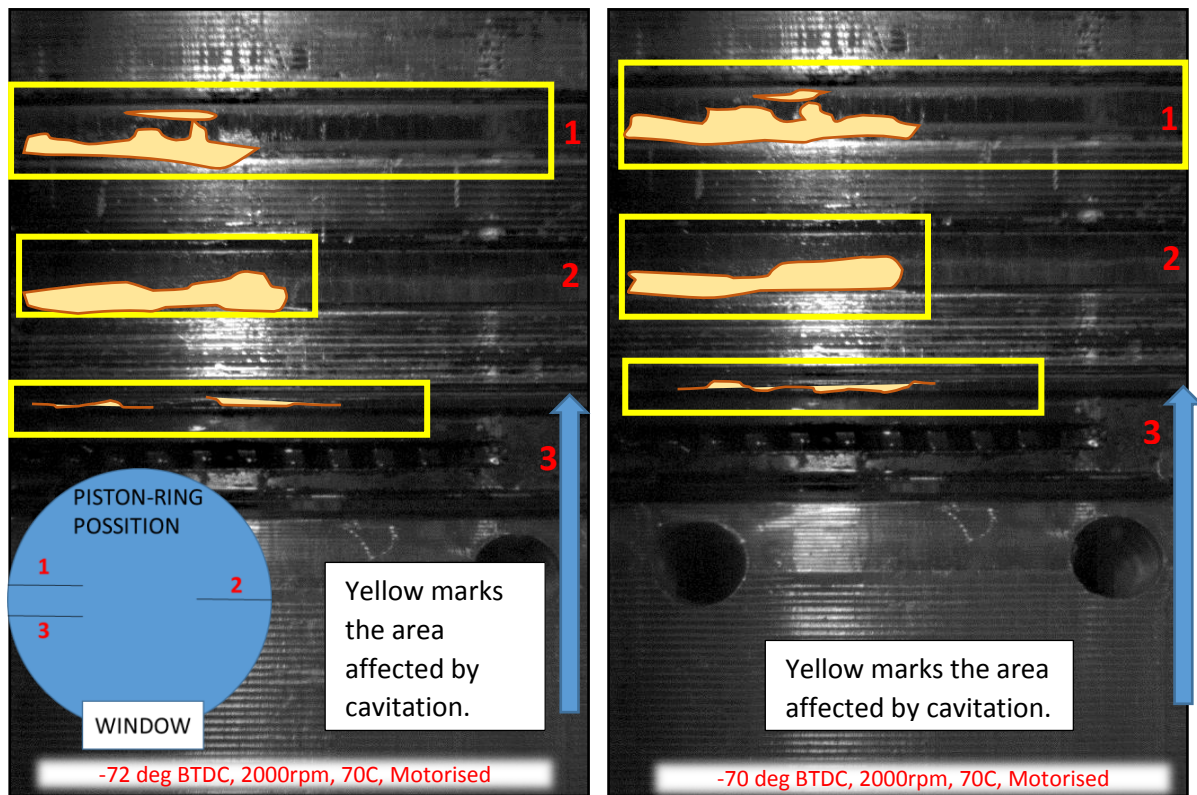


Figure 152 - BTDC, 2000rpm, 70C, Motorised

Cavity generation seems to favor certain parts of the rings. These are believed to be points where the ring surface has certain imperfections that promote the cavity generation. Cavities are initialised by the release of air already trapped inside a fluid and for the separation to begin imperfections need to exist on the nearby surfaces. After the fluid has passed over an imperfection it would cause the air trapped inside it to be resealed and that is followed by fluid evaporation through the bubble boundaries that would grow the cavities till the point of collapse. The cavities that collapse will release a shock wave capable of damaging even the toughest engine components. The yellow markers highlight the affected areas. The affected areas are where cavities have developed. The cavity generation is more distinct in a video where the consecutive images play at a higher framerate but that is not easy to observe on still images. For this purpose the affected areas have been noted and highlighted with markers to give a better understanding of how cavities are generated and develop. In figure 153 is noted that even though the piston has passed the mid-point of the cylinder the cavities still do not cover the entire surface of the ring. The cavities start to develop at the area of the

ring where there are surface imperfections. The main cause of them starting at the same side and more specifically of the left side of the frames is that despite the best efforts to make the joint between the quartz glass and the metal liner as smooth as possible it seems that at a microscopic level there are surface imperfections present due to the transition from the metal to the quartz window. The cavities would initiate at the left side of the frame and gradually progress towards the right side of the frame till they cover the entire area of each ring in the area visible through the optical window. The cavities would generate and expand through the rings to the point where they would collapse by either the change in the pistons direction or they would escape from the area of the piston-ring and cylinder-liner interaction forced by the blow-by gasses that some times pass though the rings due to the increased in-cylinder pressure. At this point the cavities are forced out of the interaction and are pushed to the area between the rings where they collapse due to the pressure change. The cavity generation and collapse are highly depended to the specific speed, in-cylinde pressure and postion of the piston.

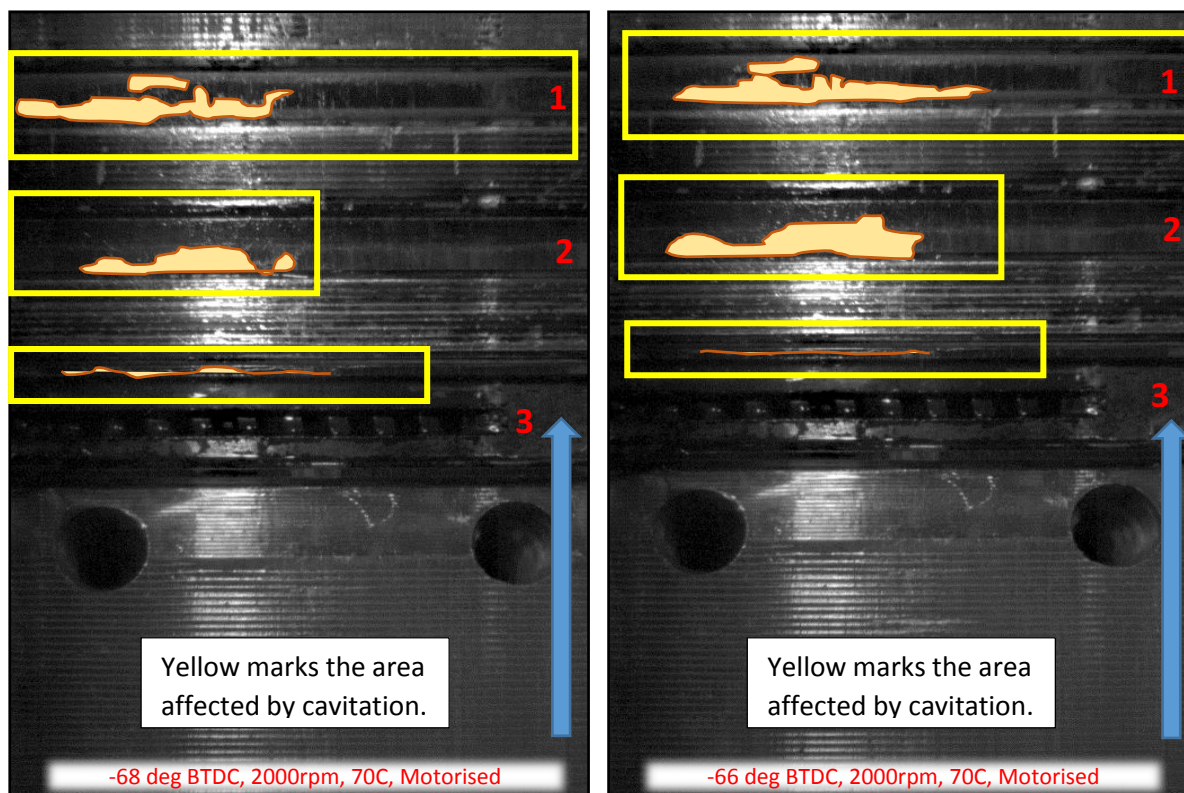


Figure 153 - BTDC, 2000rpm, 70C, Motorised

5.5.4 Temperature Effect

The following set of data presents the effect the temperature has on the cavitation behaviour at a number of different test conditions. The temperature is referred to and measured at the

inlet of the coolant before it enters the water jacket in the cylinder liner. These temperature is maintained with the use of the cooling and heating systems of the engine. The engine is heated up and then the cooling system is driving down the temperature to the desired value. It has been noted that cavitation is directly linked to the viscosity of lubricants and the viscosity is highly depended on the temperature. Usually, the higher the temperature, the lower would be the viscosity. That is not valid just with lubricants but with the majority of liquids. When the engine is not fired, the lubricant temperature is at the same temperature as the engine itself. As a result, the higher temperature will decrease the viscosity. The following images show the difference in cavitation for a number of different temperatures for the same lubricant at the same speed of 800 rpm and at the same crank angle. The temperatures range from 30°C to 70°C and the lubricant is the same lubricant used in all of the engine tests, the BP Castrol GTX 10w-40. Figure 154 shows the differences between the 30°C and 40°C. The differences in the area are not evident by naked eye as the area of cavitation has changed shape from one frame to the next. For this purpose, a script was written in Visual Basic that would calculate the area of cavitation for each of the different frames. In figure 154 the area calculated by the software is in red on the top left corner of the frame. The area is given as a percentage of the entire ring visible on the same frame. The ring even though it appears to be of a rectangular, flat shape, is actually not. The ring has a circular profile and the centre of rotation is along the vertical axis in the middle of the frame. A calculation based on square meters or square centimetres would not be accurate as there would be a difficulty when bringing the curvature of the ring into the calculations. The most appropriate representation that would carry the minimum risk and offer maximum accuracy is to represent the area of cavitation in a percentage of the total ring visible on the frame. In this way, the calculations are ensured to be accurate while still maintaining a solid measure of comparison between the different frames. In figure 154 it is noted from the values calculated by the software that there is a difference in the area the cavities occupy. The cavities at 40°C cover the 62.53% of the total ring area and at 30°C cover the 57.26% of the total ring area. That is more than a 5% difference and since the speed, crank angle and type of lubricant are the same this difference is linked to the increase of the lubricant temperature. In a similar way figure 155 represents a 10°C difference between the two presented frames. That is between the 40°C and 50°C. Again, the difference in the area covered by cavitation is close to a 4% increase for a 10°C temperature increase, which brings it closer to the results observed in figure 154. The jump

from 40°C to 50°C is a crucial one, this is where the cavities start showing uniformity as far as their shape is concerned.

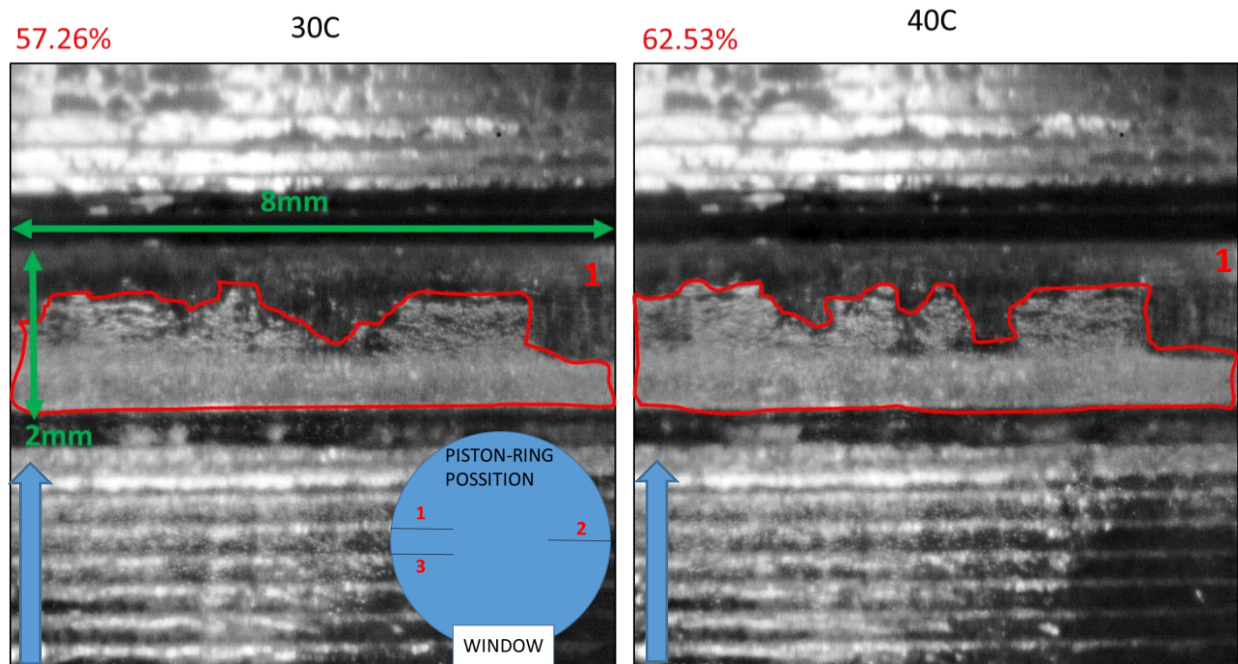


Figure 154 - Temperature Effect 30C VS 40C, 800RPM

Up to 40°C the cavities change their total shape and seem more unstable after they pass the 50 °C mark. The cavities form a uniform rectangular area and this continues to the 60°C and 70°C, both represented in figure 157. Back to figure 155 and the 40°C vs 50°C the differences are obvious and clear. The cavities at 50°C cover a uniform rectangular area and they do not show any of the unevenness seen at 40°C. Furthermore, the next figure, figure 153 shows the 50°C against 60°C. It is obvious that the cavities have retained a uniform front and back boundaries and they do not show any break in the area of cavitation. Even though the entire area of the ring is not covered by cavities, this is the maximum area of cavitation that will ever be observed throughout the cycle. It is known by previous work done on the City University's lubrication test-rig and presented in the results section of this report that the cavities never cover the entire area of the piston-rings. In fact, they only cover the side of the ring that is facing the direction of the piston's movement and they extend up to the middle of the ring if not slightly further. In the case of figures 154 to 157 the piston is moving upwards. These observations were made on the lubrication test-rig and the engine is not an exception. In a similar way, the cavities do not cover the entire face of the piston-ring at any point of the cycle.

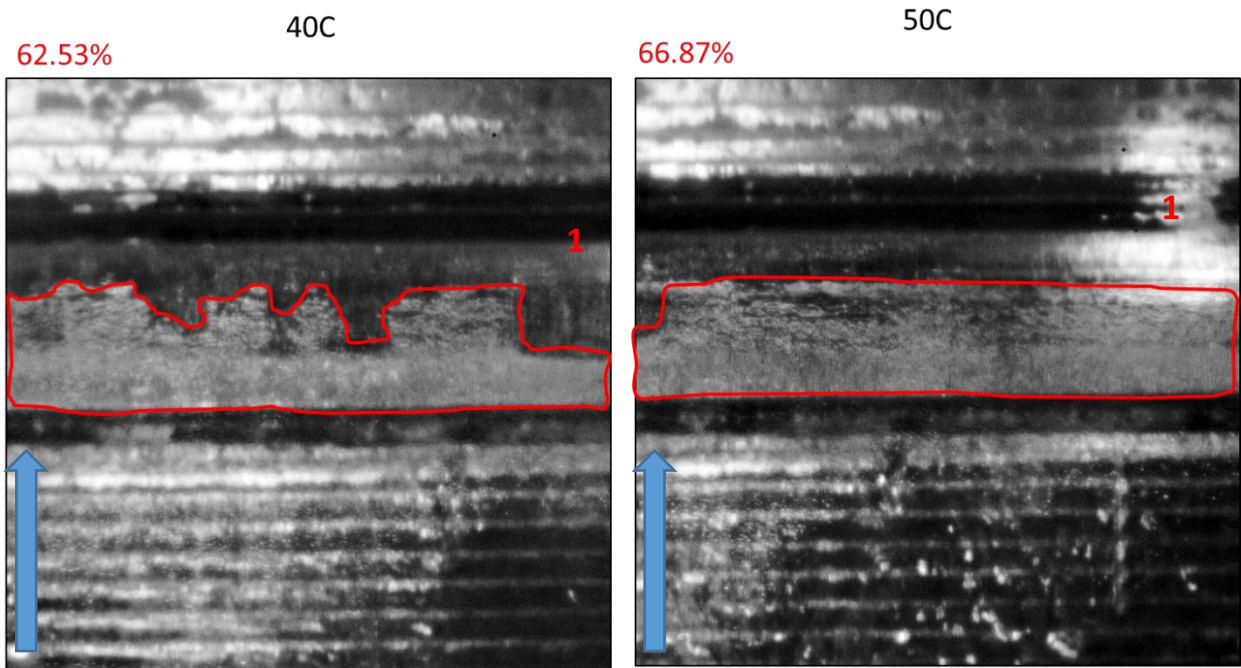


Figure 155 - Temperature Effect 40C VS 50C, 800RPM

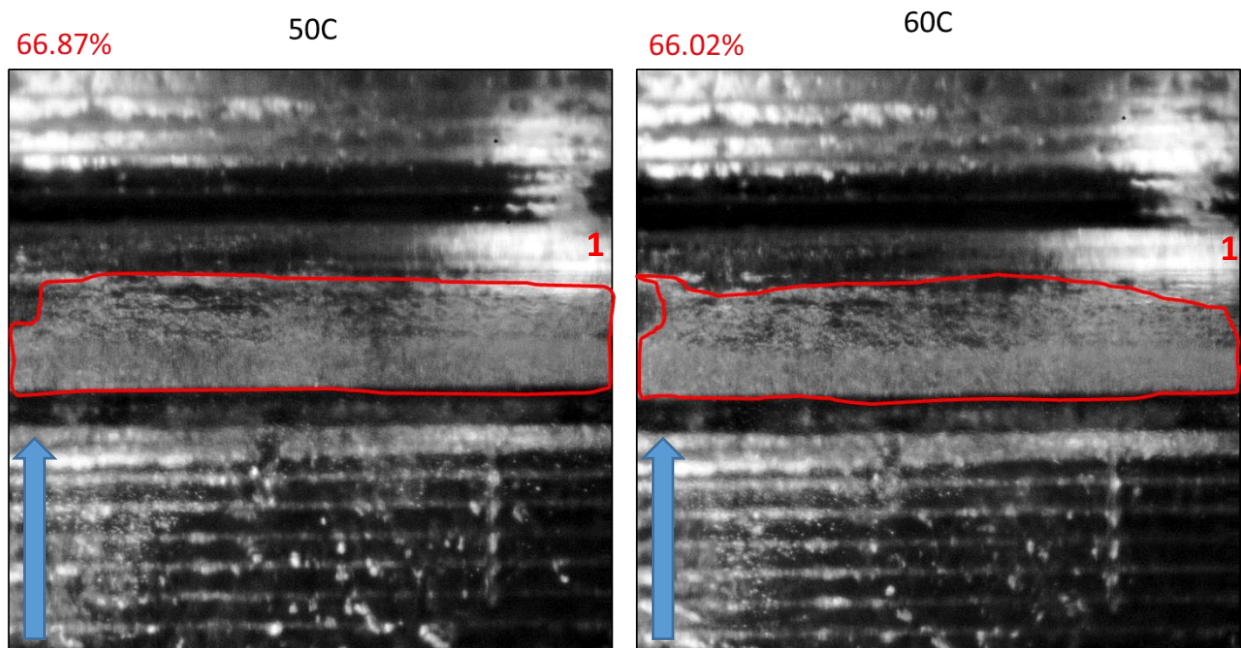


Figure 156 - Temperature Effect 50C VS 60C, 800RPM

In a change of events the cavitating area will not grow as the temperature increases. Figure 157 shows the difference between the 60°C and 70°C. It is supported by the area values calculated that the area at 70°C has decreased from 66.02% down to 57.8%. That is a decrease of more than 8%. This is higher than the differences seen for lower temperatures and moreover at this point there is a decrease observed in the area of cavitation. This is a very

interesting phenomenon, the general rule dictates that since the temperature is rising the viscosity drops which should promote cavitation. Thus, it has been identified and presented that temperature has an imminent effect on cavitation from the point of generation to the point of collapse, though not in all cases as expected.

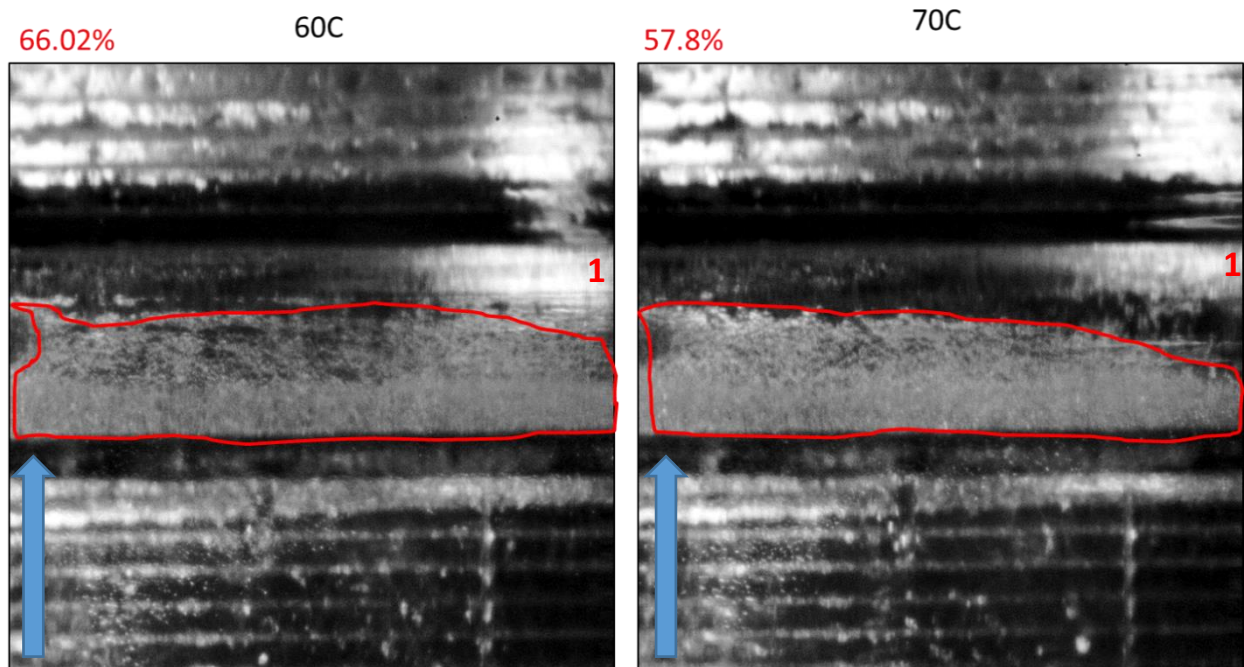


Figure 157 - Temperature Effect 60C VS 70C, 800RPM

5.5.5 Speed Effect

The piston speed is one of the factors that are proven to affect the behaviour and generation of cavities. This section details a set of data representing the behaviour of cavitation in a range of different speeds at the same crank angle and the same temperature. The lubricant is the one used for all the engine testing and is the commercially available BP Castrol GTX 10w-40. The way the data are compared with each other is by the area the cavities are covering as a proportion of the total ring area. The area has been calculated with the use of an algorithm composed for the purpose of this report. The software calculated the area the cavities cover and further calculated the proportion of the total ring area affected. Starting with figure 158 the differences are obvious. The cavities at 208rpm are barely visible on the surface of the ring whereas at 1000rpm they already cover the majority of its area. The difference is a massive 70% and there can be no argument that there is a significant change in the cavitation area from 208rpm to 1000rpm. Conventional gasoline engines do not usually operate at 200rpm speeds as their idle is usually found between 600rpm and 800rpm, but many diesel engines though idle at such a low speed and that is one of the reasons this low

range speed was investigated while comparing to the test-rig results. As mentioned the differences between the 208rpm and 1000rpm are obvious. This is not the case though with higher speed, and more specifically 1000rpm and 2000rpm in figure 159. It seems that there is little to no effect by the increase in engine speed from 1000rpm to 2000rpm in figure 159. The area of cavitation between these two speeds is very similar.

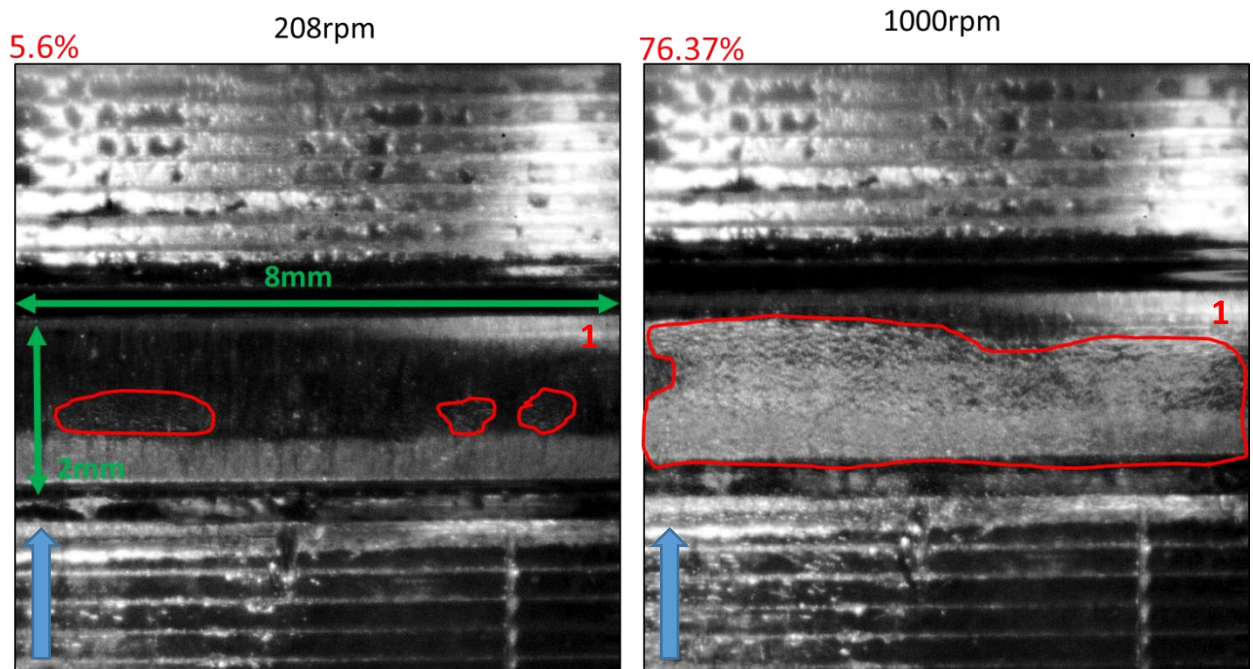


Figure 158 - 208RPM VS1000RPM, Speed Effect, 70C

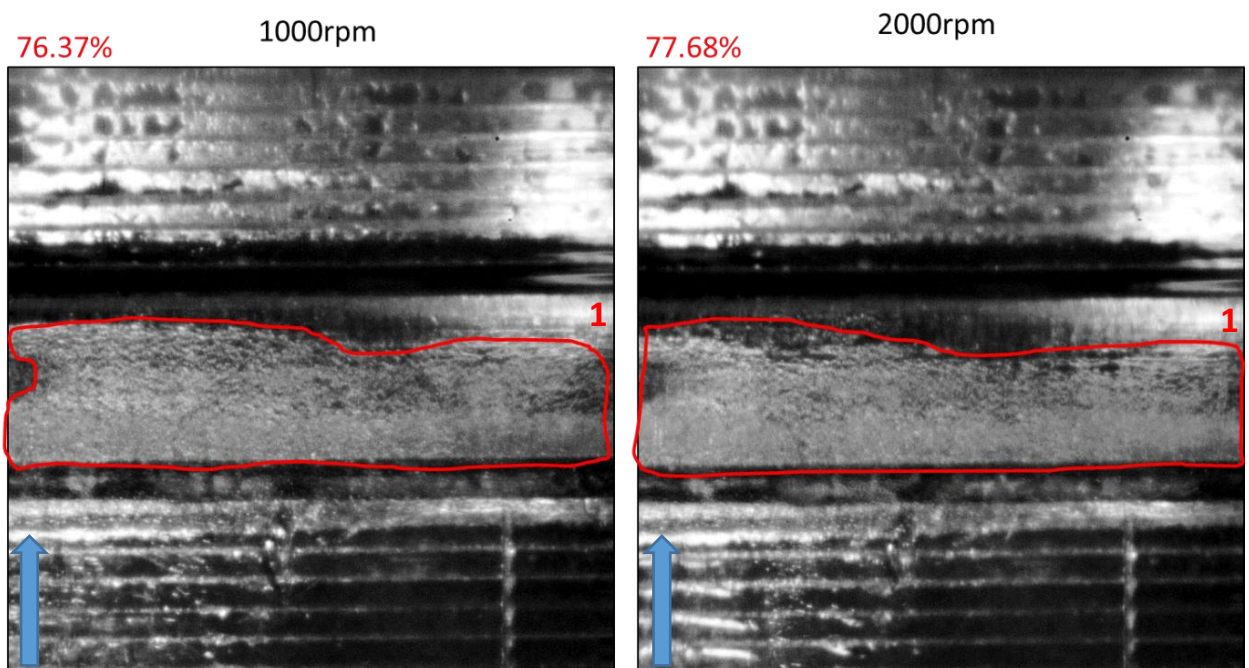


Figure 159 - 1000RPM VS 2000RPM, Speed Effect, 70C

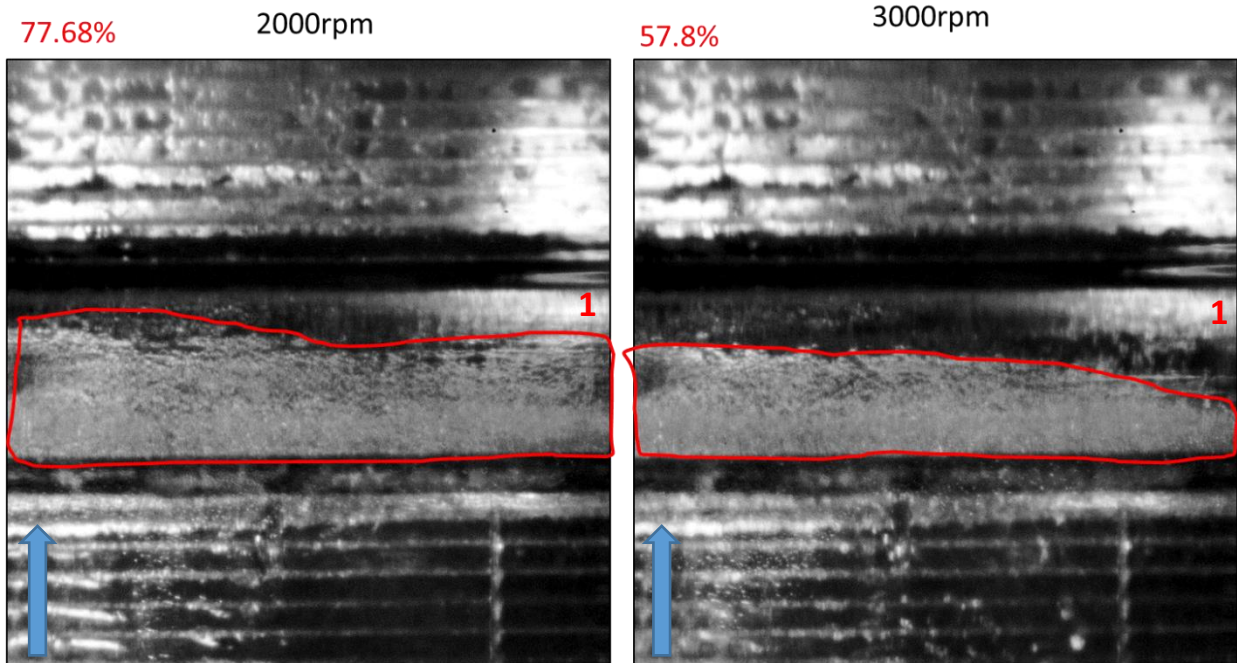


Figure 160 - 2000RPM VS 3000RPM, Speed Effect, 70C

The area of cavitation at 2000rpm is 1% higher than the lower speed of 1000rpm. These again changes once more at the 3000rpm and in figure 160. Figure 160 show that there is a big difference at 3000rpm and there is a cavitation area decrease of almost 20%. This is in contrast to what it was initially expected. The initial expectation was that the cavities will cover higher area at higher speeds. The data extracted from the engine though support otherwise. Further investigation is needed to identify the cause behind the decrease of the cavitating area while the engine speed is increasing.

5.5.6 Blow-by Effect

Blow-by is the phenomenon where the combustion gasses and products pass through the piston-rings and find their way into the crank case. This phenomenon is undesirable within an internal combustion engine, mainly due to the fact that the escaped gasses result to in-cylinder pressure drop. The pressure losses could significantly affect the performance of an engine. Another drawback of blow-by is that the combustion gasses, which are mainly burned hydrocarbons, can contaminate the internal components located in the crankcase while, the majority of these products can affect the quality of the engine lubricant. The combustion products can build up on the surfaces of internal components such as the bearings with catastrophic results. The quality of the lubricants can seriously be affected once the combustion products dissolve in their volume. The combustion products are capable of altering the lubricants basic characteristics meaning that the lubricant will not perform as

intended under operating conditions. That might cause poor engine performance and possibly serious internal component damage. As the combustion gasses find their way into the crank case by passing through the piston-rings the same can occur the opposite way. In the same way as combustion gasses can pass through the piston rings down to the crank case, the lubricant from the crank case can pass through the rings and into the combustion chamber.

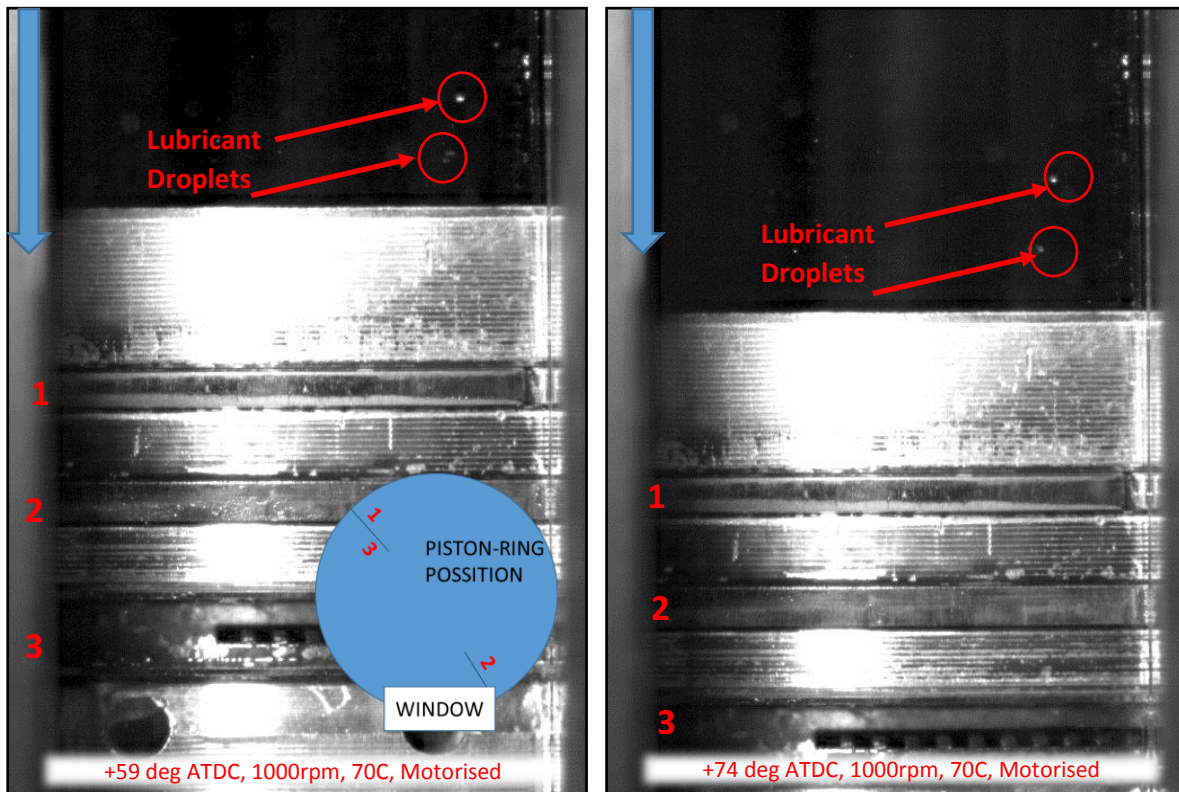


Figure 161 - ATDC, 1000rpm, 70C, Motorised

This is a phenomenon also called blow-by, even though it relates to different side-effects on the engine itself. The majority of piston-equipped, internal combustion engines that use lubricants for their operation will use a type of oil injector under the piston to constantly feed lubricant on the piston it self. The piston is equipped with oil pass holes that deliver the lubricant onto the cylinder walls and with the help of the piston-rings, the lubricant is spread onto the cylinder walls in the form of a very fine film. Excess lubricant would pass through the piston-rings and would find its way into the combustion chamber. Lubricants are mainly composed of hydrocarbons. While these hydrocarbons enter the combustion chamber they mix with the fuel and take part in the combustion. The burnt lubricant later exits the combustion chamber along with the rest of the combustion products. Engine emissions are a major issue for car manufacturers. Regulations on emissions in the recent years have become very strict and manufacturers need to ensure that their products are in-line with the

latest government regulations, otherwise they might face serious repercussions. The lubricant inside the engine cylinder takes part in the combustion and later escapes through the exhaust ports, into the exhaust system and out in the environment. One of the most critical components in the exhaust system is the exhaust catalyst. The exhaust catalysts are sensitive engine components and are highly affected by products that are derived from the combustion of an air-fuel-lubricant mixture. The burned lubricant would contaminate the catalyst and therefore significantly reduce the performance of the exhaust catalysts. The failure of an exhaust catalyst would usually lead to increased garage bills as catalysts contain precious metals which make them particularly expensive.

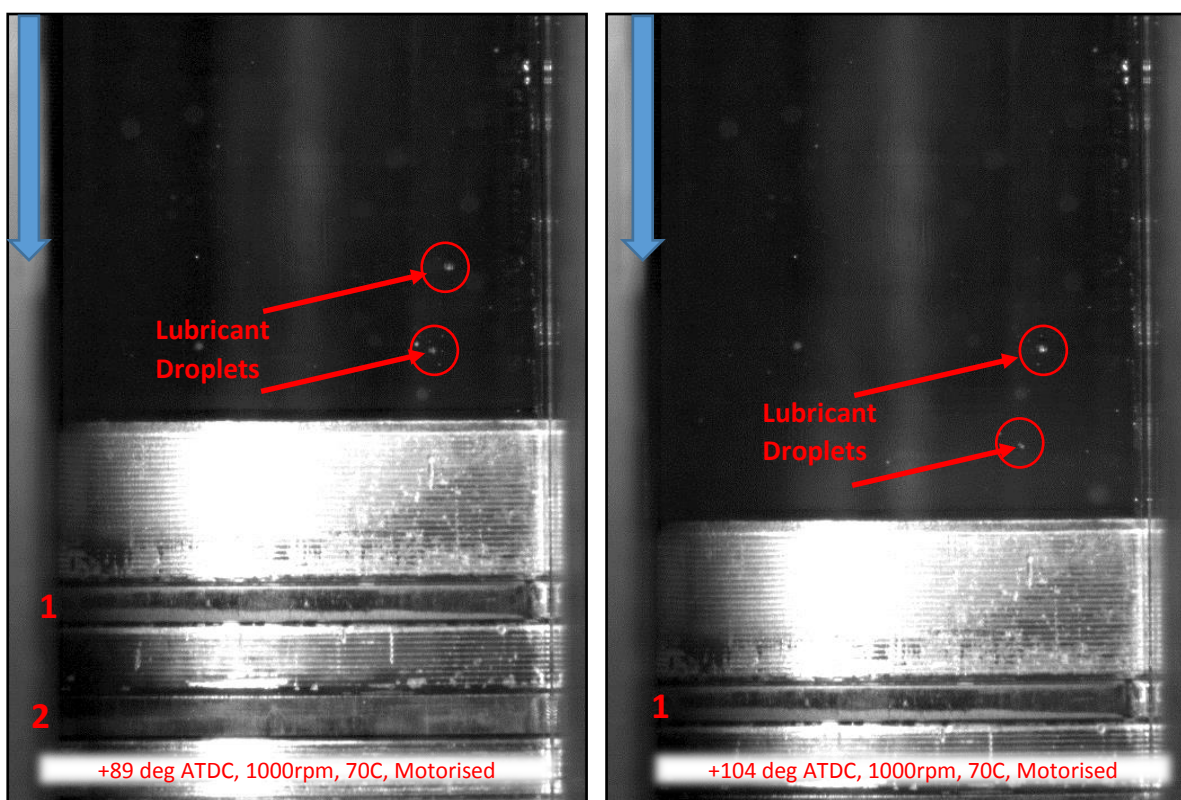


Figure 162 - ATDC, 1000rpm, 70C, Motorised

The burned lubricant would also affect the output emissions of an engine. Since lubricants are hydrocarbons the addition of such a component into the combustion would significantly increase the output emissions of an engine. Both are side-effects that are not desirable by the engine or the lubricant manufacturers and need to be addressed through extensive research and testing. Due to the objectives of the project the investigation of these phenomena mainly focuses on the journey the lubricant follows from the crankcase, pass the piston-rings and into the combustion chamber. The majority of research done in the past with similar focus had only target phenomena taking place inside the cylinder and not the phenomena taking

place onto the cylinder walls. This resulted into substituting some of the engines critical components with compatible parts such as PVC piston-rings on quartz liners. One example is the engine used by the University of Brighton for LIF and Mie Scattering measurements for fuel in liquid and vapour phases.

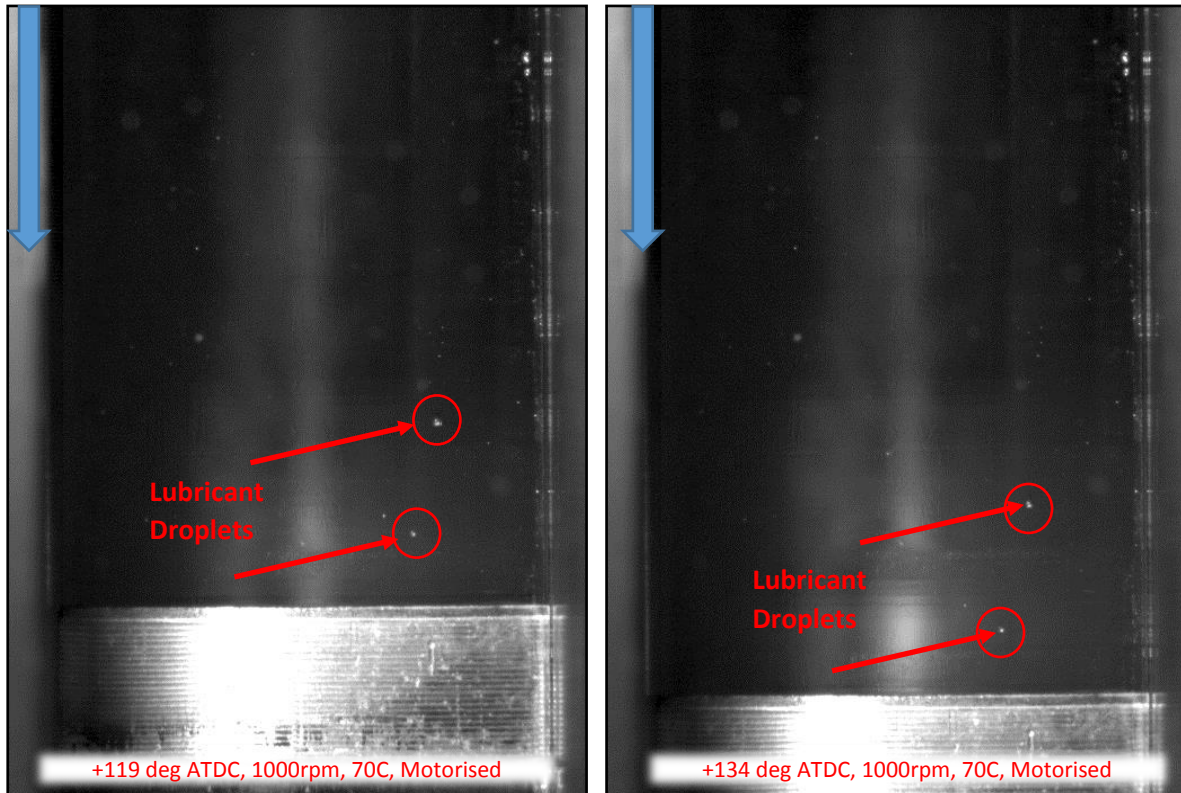


Figure 163 - ATDC, 1000rpm, 70C, Motorised

This type of rings feature no gaps and offer a much better seal than the rings used in automotive internal combustion engines. Thus these engines do not face any pressure loss through the rings while testing. The point where this project has added value is in the use of original engine components such as an actual ring-pack. With the use of an actual ring-pack a variety of phenomena were observed that have not been identified on other experimental setups.

One of these phenomena is the blow-by of the lubricant past the piston-rings and into the combustion chamber. It has been observed that blow-by does take place in internal combustion engines. This outcome is the result of using an actual ring-pack for all the test cases and ring-gaps, similar to the ones found in commercial internal combustion engines. The sequence of images in figures 161 to 163 show two lubricant droplets that have escaped from the crankcase and have passed into the combustion chamber. These two droplets started their journey through the cylinder at the point where the piston reached the top dead centre.

Practically the lubricant observed in these images originally came from the oil sump which is located in the lower part of the engine. This lubricant used mainly on internal engine components to offer component protection and friction reduction. The lubricant is delivered to the individual internal components through a system of tubing around the engine. One of these tubing guides the lubricant to the bottom or skirt of the piston. Once the oil comes in contact with the piston it gets absorbed in a series of small holes located on the actual piston skirt. These holes guide the oil from the back of the piston to the front and more precisely on the front of the skirt and to the back of the oil control rings. The reciprocating motion of the piston and the pressure differential force the oil through the piston ring gaps and slowly guide it on top of the first piston-ring. Once the oil has reached the top ring it will stay in that area until the piston has reached the top dead centre. Once the piston passes the top dead centre and starts moving in the opposite direction the inertia of the oil still present on top of the first ring will force it to leave the piston and enter the combustion chamber. This is exactly the phenomenon observed in figures 161 to 163. In figure 161 the piston is at 59° and 74° after the top dead centre and the two droplets can be seen to travel through the cylinder. The same continues into the next two frames in figure 162 where the two droplets still continue their path through the cylinder. The speed of the piston is higher than the speed of the droplets and these two will not meet before the piston has reached the bottom dead centre and the piston is moving in the opposite direction. That is in the case that the droplets continue moving towards BDC and do not collide with the cylinder walls. In figure 163 the two droplets have moved apart compared to the previous figure and their in between distance has changed. That is mainly an effect of vortexes that occur inside the cylinder due to the vacuum created by the piston. Their relative movement becomes clearer once the consecutive images are played in a video sequence. The droplets have been marked with red arrows and properly annotated to assist with their visualisation.

The path that the lubricant travels into the combustion chamber has been tracked and analysed to assist in the further improvement of the design of internal combustions engines to minimise or eliminate the lubricant blow-by. The basic design of the piston in the engine allows the lubricant to find its way though the piston skirts, up to the oil passages, embedded on the piston itself. The oil would pass though these holes to the back of the scraper ring. The oil control ring is equipped with slots that allow the lubricant to pass though them and onto the cylinder wall. The oil control ring is also responsible of controlling the delivery of the oil onto the cylinder wall. There are some points in the cycle where oil can escape the oil control ring

and would pass in the gap between the oil control ring and the second compression ring. While the lubricant is in this space it will continue to move forced by the movement of the piston until the point where it reaches the gap of the second ring and then it makes its way up to the area between the first and the second ring. From there it follows a similar path and by passing the gap of the first ring it finds its way on the top of the first ring. The escaped lubricant stays there for most of the up-stroke but when the piston reaches the TDC and mainly due to the inertia of the lubricant and the piston the lubricant will fly off the piston and would find itself traveling through the cylinder.

5.5.7 Ring Rap and Blow-By

The following set of images from figure 164 to figure 169 show the blow-by through the gaps of the first and the second and the third piston rings which have been aligned for the purpose of the project. The main passage of the lubricant was found to be the gaps between the rings which allowed for the exchange of oil between the oil sump and the cylinder. It has been observed that the lubricant will pass the gaps between the rings and with the kinetic energy introduced by the piston along with the pressure differential the lubricant will find its way into the combustion chamber with a plethora of negative effects for the engine itself. This section further details and illustrates the mechanisms that allows a lubricant to utilise the gaps as a passage to the combustion chamber. The sequence of images present evidence that support the occurrence of blow-by where lubricant passes through the ring-gaps. The engine used for the experiment is a custom design with a custom setup, one of those customisations is the position of the piston-rings and their gaps. It has been observed that regardless the position of the gaps the lubricant will eventually find its way through them and into the combustion chamber. The effort was made to assist and accelerate that phenomenon which usually takes a few strokes to complete in eventually the length of one stroke. This has been achieved by placing all the ring-gaps in line with each other. By bringing all the ring-gaps inline, it has been observed that lubricant would complete the journey from the crankcase to the combustion chamber in a single stroke.

In the first frame in figure 164 the piston has almost reached the top dead centre as part of the compression stroke. During the compression stroke, both of the inlet and outlet valves are closed, and the combustion chamber is pressurised. The further the piston travels towards the top dead centre the higher the in-cylinder pressure. At -2 degrees before the top dead centre and considering that the engine is operated under motorised condition the pressure of the combustion chamber has reached its maximum value. With a compression ratio of 9.5 to 1

the volume of the cylinder has reduced by 9.5 times and the pressure has equally increased. The high pressure is forcing the gases that are trapped into the cylinder to find their ways down to the sump through the back of the rings and the ring gaps. While the engine is in operation and as it can be seen in the second frame of figure 164 the gaps between the rings are occupied by lubrication oil. The high-pressure gasses while on their way towards the crankshaft will carry with them parts of the lubricant and will return it in the crankshaft case. In the event that the engine was in firing mode the high-pressure gasses would carry more than lubrication oil. The combustion products and possibly unburned fuel would follow the same path and will find their way down the piston, as the lubrication oil does in figure 165. In figure 165 the piston has passed the top dead centre and even though the pressure has started to drop the in-cylinder pressure is still at a very high level. In figures 166 and 167 the high-pressure gasses continue to push the lubricant through the ring gaps towards the crankshaft. What is particularly interesting is that the gases/lubricant mixture as soon as it leaves the bottom ring it finds its way down to the sump through the oil feed holes on the skirt of the piston.

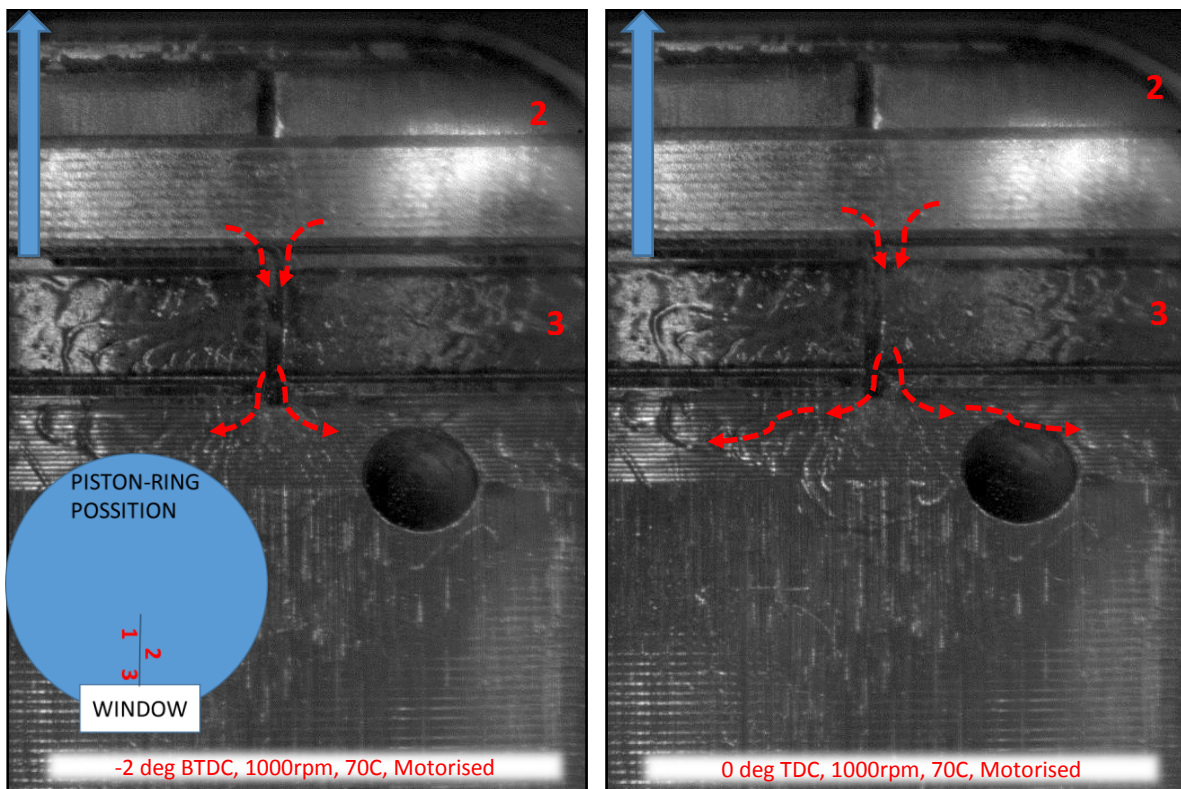


Figure 164 - 1000rpm, 70C, Motorised

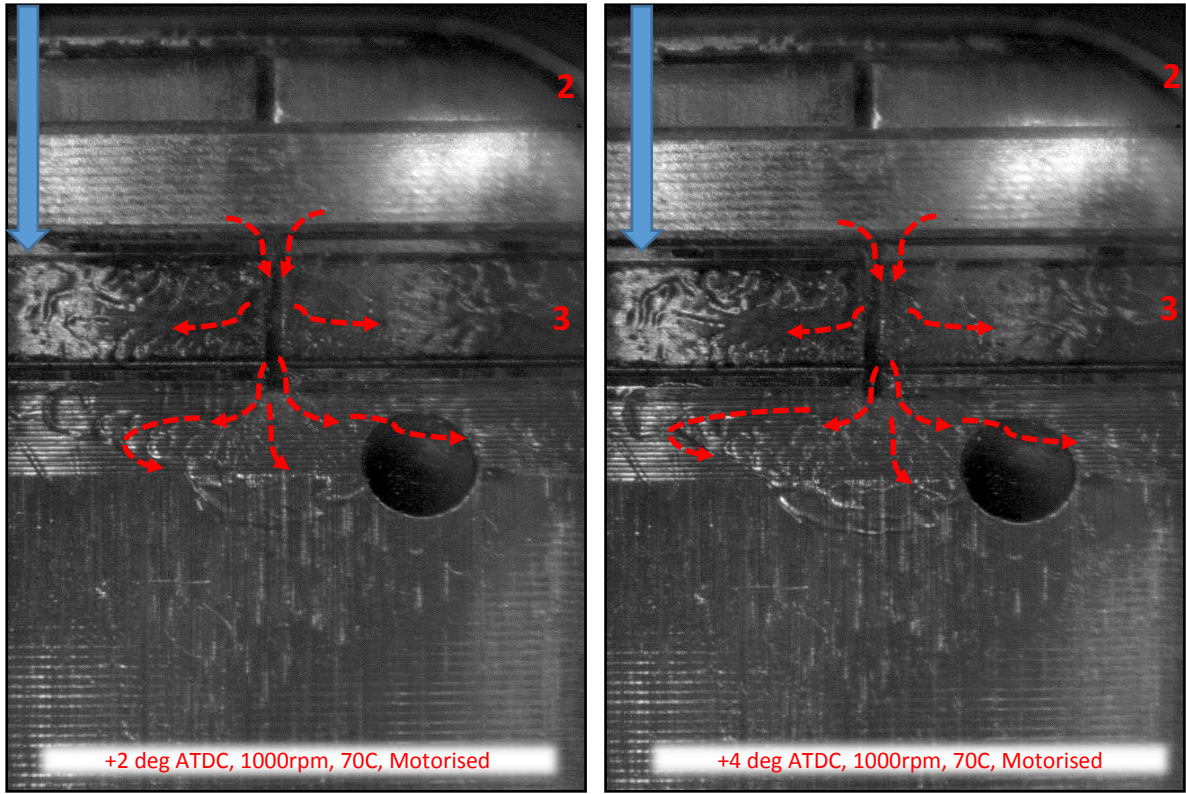


Figure 165 - 1000rpm, 70C, Motorised

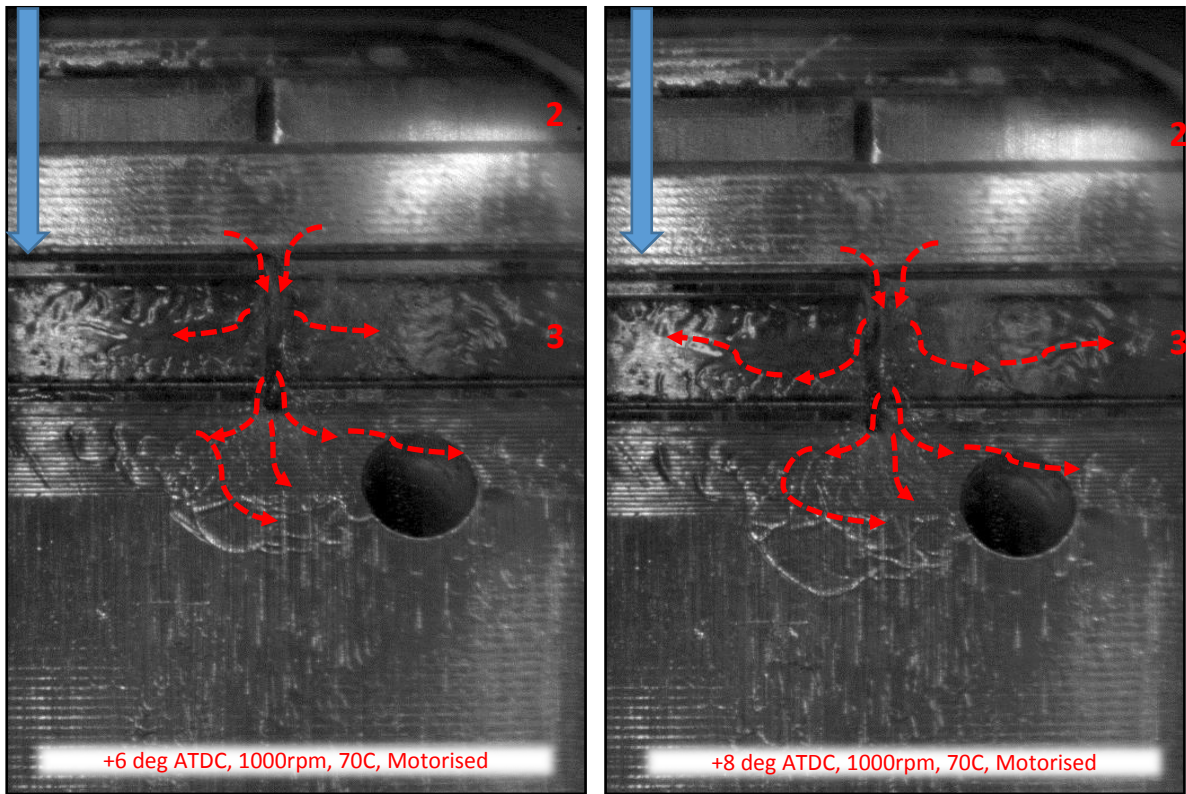


Figure 166 - 1000rpm, 70C, Motorised

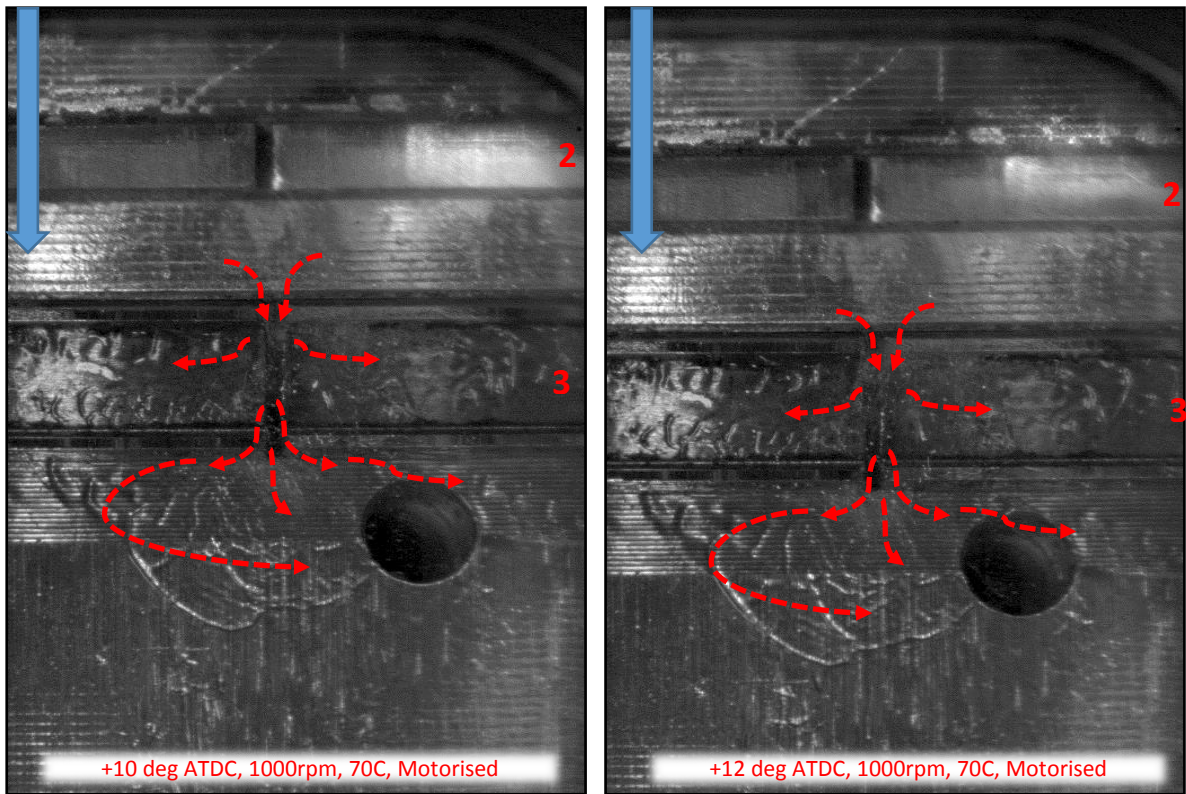


Figure 167 - 1000rpm, 70C, Motorised

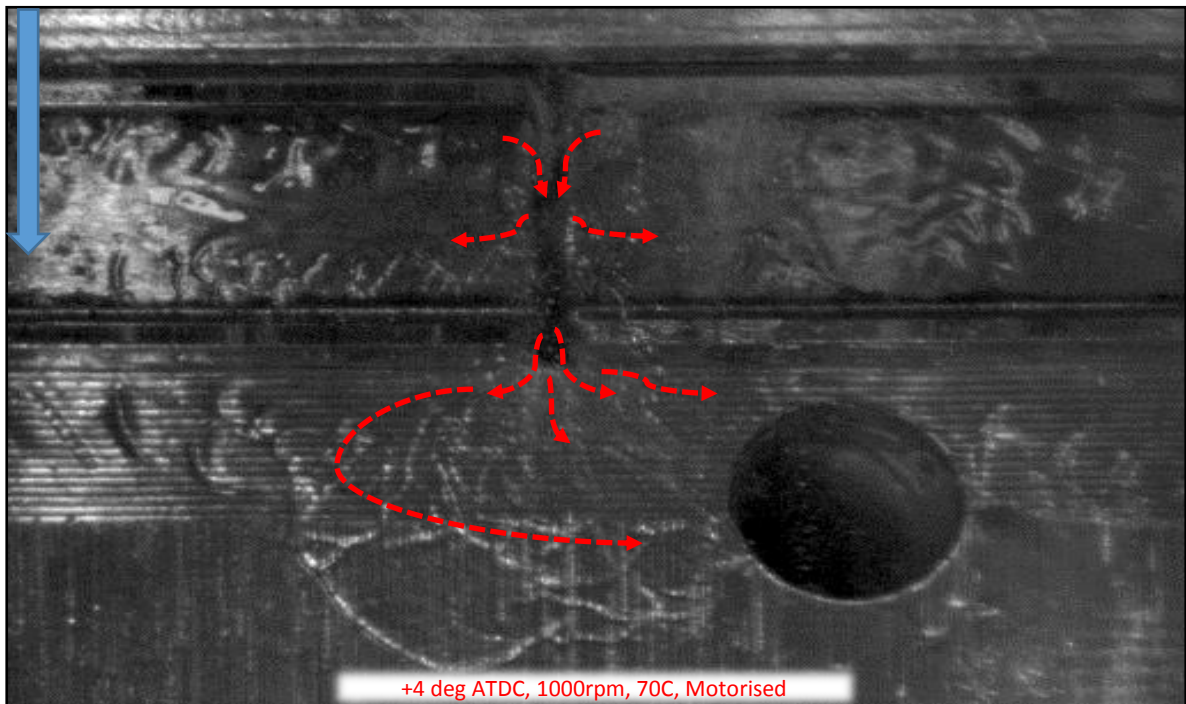


Figure 168 - 1000rpm, 70C, Motorised

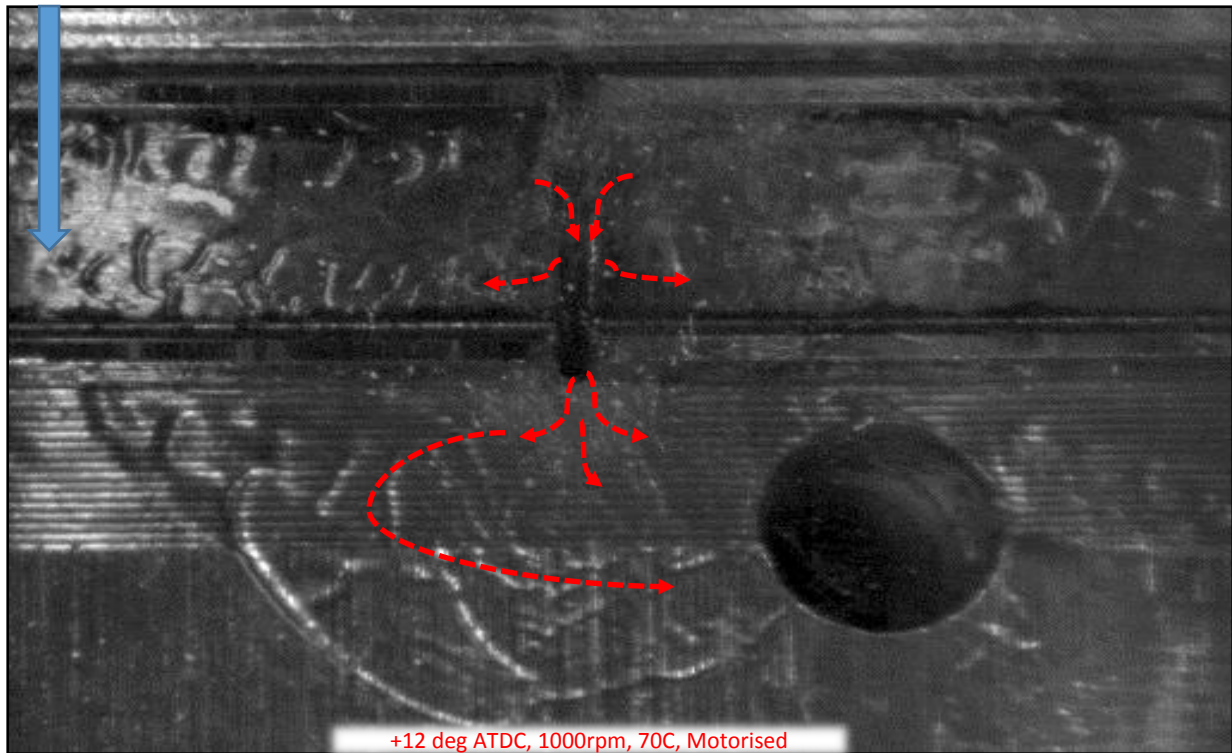


Figure 169 - 1000rpm, 70C, Motorised

This can be explained by the fact that this hole offers an easier escape towards the sump rather than the area between the skirts and the cylinder liner. It is also observed that the gasses in figure 164 and at 0 degrees seem to carry with them less lubricant than in figure 167. This indicates that the gasses a few degrees after the top dead centre travel faster than at the top dead centre, even though the in-cylinder pressure is higher closer to the top dead centre. This is believed to be due to the way the piston meets the combustion chamber once the piston has reached the top dead centre. At the top dead centre, the piston is very close to the cylinder head offering a very small area where the gasses could escape. Once the piston starts moving downwards the bottom dead centre the gap between the piston and the combustion chamber increases offering a better route of escape for these high-pressure gasses. The images above illustrate the journey the lubricant follows from the crankcase to the combustion chamber. The lubricant starts from the bottom ring and more specifically the gaps behind the ring. The oil passes through these gaps and finds itself through the third bottom piston-ring, then the oil escapes and finds its way in the gap between the bottom and second piston-ring. While the second gap between the third and second piston-rings is filling up with oil there is oil already passing the second piston-ring and finds its way to the gap between the first and second piston-ring. While the lubricant is passing through the ring-gaps it is creating vortices around the ring-gap edges. That is an additional indication that the ring-

gaps are the main path of lubricant transportation from the crankcase to the combustion chamber. The passage of the oil is assisted by the high-pressure gases that are moving from the cylinder to the crank case due to the increased in-cylinder pressure. The unique setup of the engine is the reason behind the successful execution of the testing needed for the project and the fact why the collected set of data have offered an insight to an area of the engine usually restricted. The phenomenon of blow-by is highly important to the engine manufactures and the lubricant, phenomenon that has been successfully captured and detailed in the pages of this report.

5.5.8 Firing

After the initial motorised testing, the tests on the engine continued under full firing operation. During the full firing operation, the engine was igniting the injected fuel on every cycle. The dynamometer was used to place a load on the engine. The load applied was a proportion of the total power output of the dynamometer and it was applied by using the dynamometer as a brake. By not letting the engine operate freely the operating conditions were closer to the operating conditions of automotive engines. Another use of the dyno was to start up the engine. As with the majority of the engines, this engine needed to be started with the use of an electric motor before it could sustain itself into operation. The dyno has been used to first bring the engine up to speed before the fuel system was switched on. The fuel system was let to run until the pump had reached its operating pressure. After switching on the fuel pump, the next stage is to initiate the ignition, while the ignition is operating the final stage is to switch on the fuel injectors that provide the fuel needed for the engine to operate. Once the engine is in operation under its own power the dyno is switched from a starter motor mode to applying the load on the engine.

Optical-engines are useful instruments when investigating phenomena taking place inside an engine but unlike the non-optical engines they have a distinct vulnerability. That vulnerability is also their most important feature, their optical window. Under firing operation, the load on the window increases by a great margin while its life expectancy dramatically decreases. The specific engine has a 9.5 to 1 compression ratio, which increases 5 times when the engine is fired. In the course of the project four optical windows were consumed in total. That was mainly due to the fact that the metal rings would come in contact with the quartz window and wear it to the point where the damage would be of that extend that the in-cylinder pressure spikes would cause the window to crack. Due to the nature of quartz as a material and due to

its crystal structure as soon as a small imperfection is introduced on one of its surfaces this imperfection would propagate into a crack, up to the point where the window would fail.

Fully Firing optical-engine	
Engine Speed	1000rpm
Engine Load	2.1kW
Air/ Fuel Ratio	14.1
Fuel Type	Iso-Octane

Table 11 – Fully firing optical engine test conditions

Time constraints along with the shortage of supply of the optical windows meant that the engine did not go through the same amount of testing under firing as it did under motorised operation. After several testing's, it has to be noted that the firing of the engine did not affect the behaviour of the cavities at a great extent. At this point it is worth also mentioning that the engine could not operate on full firing mode for prolonged periods of time partially due to the window needing cleaning in short time intervals and partially due to the caution taken towards the safety of the optical windows and the engine itself.

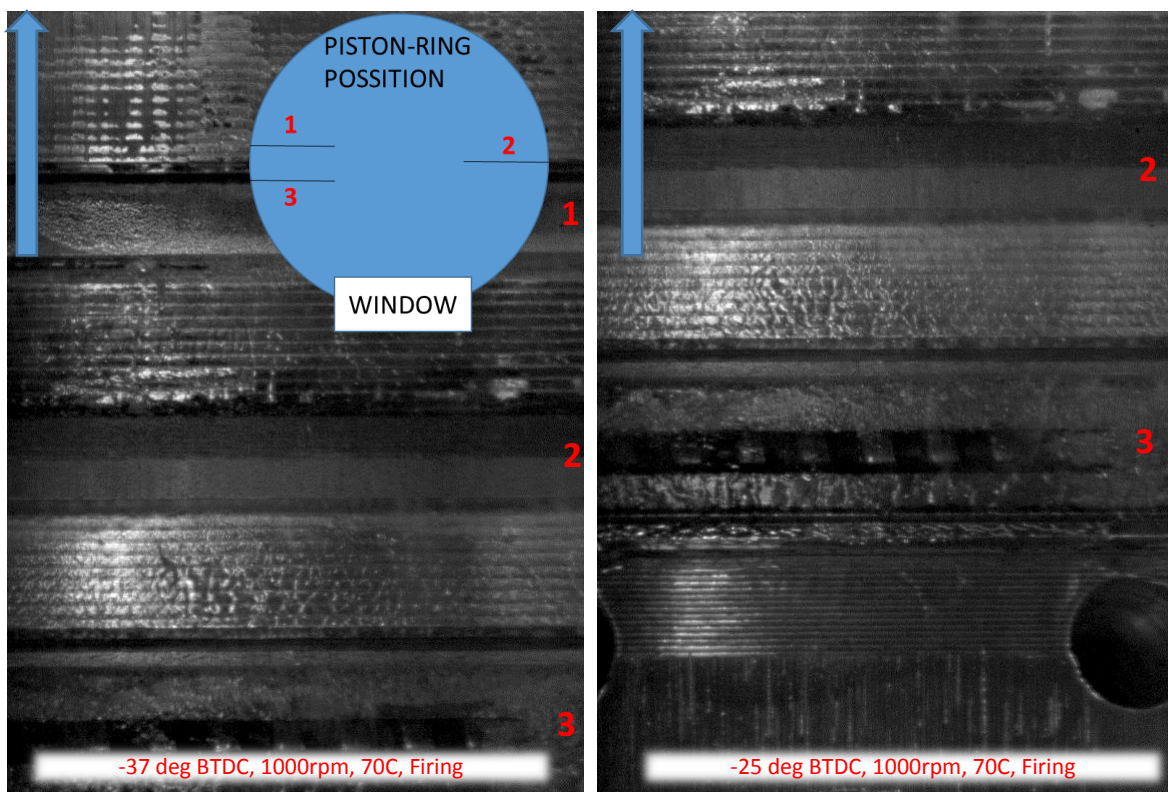


Figure 170 – 1000rpm, 70C, Firing

Table 11 and the sequence of images from [-37] to [+71] degrees crank angle in figures 170 to 174 show the test conditions and the behaviour of cavitation while the engine is under full firing operation. During full firing the engine has been igniting the fuel on every cycle causing the in-cylinder pressure to explode at levels much higher than what the engine experiences under motorised operation. The engine used has a 9.5 to 1 compression ratio. When the engine was firing, these values increased 5 to 6 times over the motorised ones. Under firing operation, the engine would as well experience a shift in the pressure pick, meaning that the pressure pick would no longer be at TDC but it occurred at a later stage as shown and explained in the “Optical Engine” section of these report. In all the images the effect of cavitation is obvious in the area over the piston-rings. During all the runs there was no significant visual difference between the full firing and the motorised tests as described in the “Optical Engine” section earlier in this report. This always refers to the data between the firing and the motorised operation at similar operating conditions. Two of the most critical condition that had a significant effect on the behavior of the cavities were the engine speed and the temperature. Due to the unpredictable and chaotic behavior of the cavities on the optical engine it has not been possible to apply the software solution implemented on the investigation of the cavities on the City University’s optical test-rig. For that reason a separate software was developed in Visual Basic which is further explained in the “Processing Software” section of this report. Despite the fact that the cavities on the test-rig and the optical-engine followed similar patterns at similar speeds the test-rig capabilities are quite limited compared to those of the engine. The engine would reach much higher speeds and at these speeds the cavities would scatter and stop following a clearly visible pattern. There is clear evidence of cavities occurring on the face of the piston-rings. As described in earlier section of this report the cavitating oil would leave the face of the ring and pass in the areas between the piston-rings where it would either escape towards the crank case or it would find its way into the combustion chamber. The “-25 degrees BTDC” frame, figure 170 shows lubricant trapped in the area between the piston-rings. Due to the special design of the oil-control ring there is oil also trapped in between the two edges of the ring itself. Oil control rings can either have a flat face or in the majority of the engines a slot in the middle of their face running around the profile of the ring. The specific ring used on this optical engine features a slot running across its profile. This allows for better oil control and delivery. Due to the protruding edges it is not uncommon to see lubricant trapped in the area between the two edges. Unlike the lubricant trapped in the area between the piston-rings, the lubricant trapped in the oil control ring can easily escape. The oil control ring is equipped with

slots that not only allows for the delivery of fresh oil onto the cylinder walls, but also allow for the drain of the excess oil back into the crank case. It has been observed that the increased cylinder pressure has a significant effect on the way the cavities are generated and behave in the motorised tests.

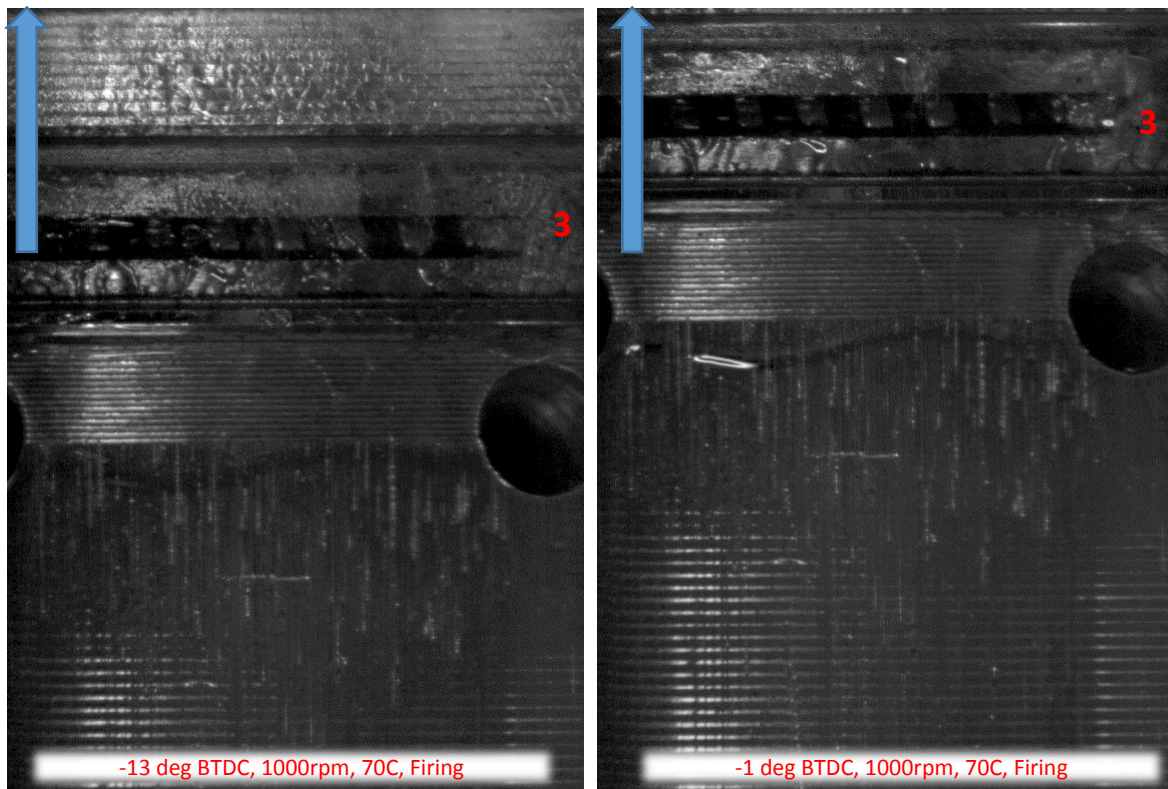


Figure 171 – 1000rpm, 70C, Firing

It has been also observed that the added pressure caused by the combustion of the fuel has no significant effect on the cavitation and it does not affect the way it behaves. The project mainly focused on the investigation of cavitation in the area between the piston-ring and cylinder-liner interaction and not on the effect of combustion on cavitation. Further work is needed on the investigation of the differences between the effects of combustion on the cavities generated inside a firing engine and how these differ from the case of the motorised operation. At this point it has to be noted that the findings of this specific study do not indicate a significant difference between the two but for a validity perspective the extra time has to be invested to reinvestigate the findings. The proposed projects need to take under consideration the findings of the current project and needs to implement a new approach in the investigation of how the cavities behave in the two different cases of motorised and firing operation and highlight their differences, if any. Additional high-speed visualisation techniques might reveal more information regarding this phenomenon.

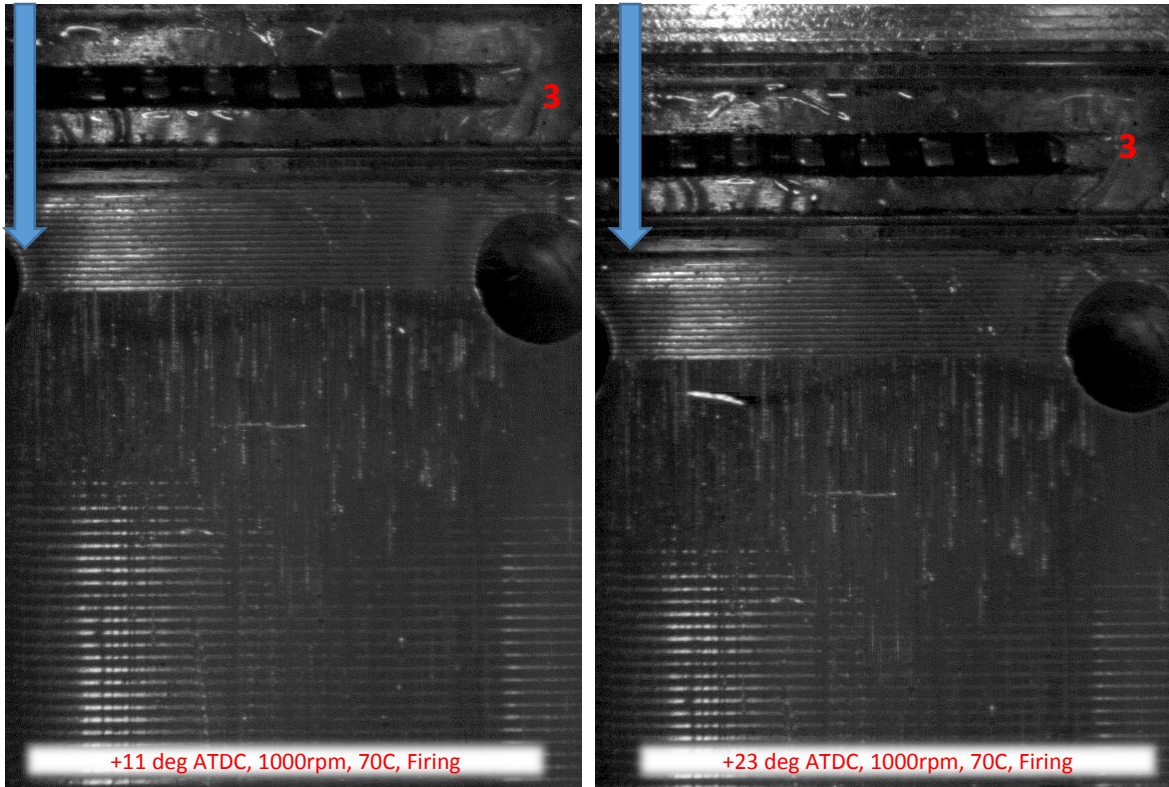


Figure 172 – 1000rpm, 70C, Firing

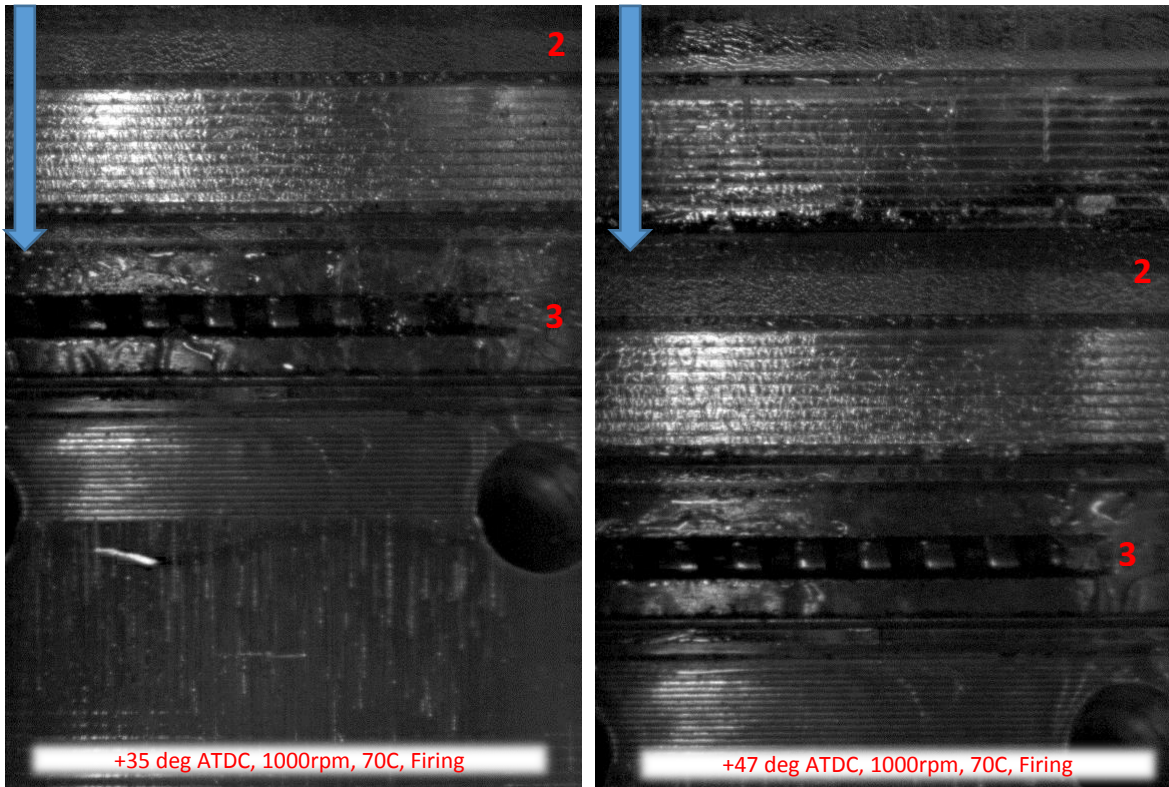


Figure 173 – 1000rpm, 70C, Firing

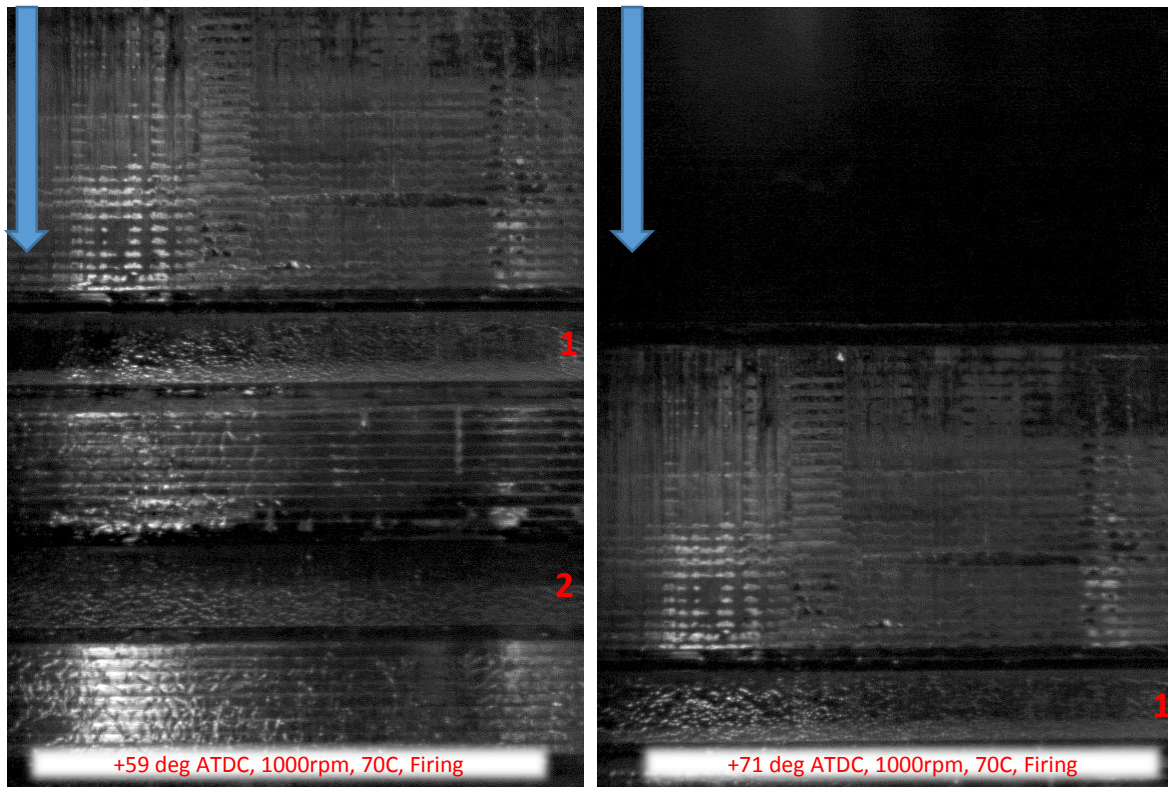


Figure 174 – 1000rpm, 70C, Firing

5.6 Error Analysis

This section of the report is focused on errors that might have been introduced during the testing and which must be taken under consideration when reviewing the results or repeating the experiments. Below are identified a few of the instruments used for data collection and data extraction and their reading errors are presented to give an understanding of the magnitude of the error that might have been introduced and what actions might have been performed to mitigate. The flowmeter used on the test-rig has been found to have a set amount of error which has been calculated by the manufacturer at $\pm 5\%$ of the total flowrate displayed. The capacitance used on the specific test-rig is a device that uses two conductive plates to measure the oil film thickness. This method requires very careful calibration before every measurement. The calibration is important to link the change in voltage with the change in length. The capacitance output is displayed in Volts with an accuracy of the first decimal place. This results into an error while acquiring the measurements of 0.05V which is 0.05% if 1 volt is measured. This will affect both the calibration and the final readings. The capacitance also relies on a micrometre to measure the change in length and correlate movement with voltage. The micrometre used for the calibration of the capacitance can be accurate within a $\pm 0.005\text{mm}$ for measurements of length. Shaft encoders were used to capture

the rotational movement of the engine and the test rig. The shaft encoder used has a resolution of 3600 pulses per revolution. This will result at an error of 0.05degrees of crank angle. This has been a very low measuring error and it would not affect the outcome of the tests. One of the main challenges has been to synchronise the high-speed camera with the engines position. For that reason, the high-speed camera was triggered with the use of digital signals generated by the crank shaft encoder. Thus, the error introduced would be the same as the one introduced by the crank shaft encoder and that would be equal to 0.05 degrees of crank angle. The vibrations generated by the operation of the single cylinder engine caused the images to shift and tilt from frame to frame. This was resulting in an error when the software was calculating some physical properties of the cavities. The error introduced by the image processing was accommodated as part of the code and it was implemented when writing the algorithm. The algorithm would detect the shift and the tilt, and it would accommodate from one frame to the next.

CHAPTER 6: CONCLUSIONS AND FURTHER DISCUSSION

The experimental investigation of cavitation formation and development at contact point between the ring and the liner in a lubricant test rig and the newly designed optical engine has been carried out at different operating conditions using two high speed cameras coupled with three ARRI high intensity light sources to visualise cavitation. The present research project has been divided into three stages; first the measurement in the lubricant test rig and then the design of the new optical engine followed by the testing and measurement in the optical engine. A summary of the main findings obtained from the results of this research programme are presented in the following sections. The project continued with the design and testing of the optical engine. The engine testing provided data that could assist in the better understanding of how lubricant cavitation can affect certain aspects of the engine in the way they operate and perform. Some negative effects that are related to the phenomenon of cavitation are increased emissions, blow-by, lubricant contamination and damage on internal components.

6.1 Summary discussions and conclusions of test-rig measurements

A lubrication matrix was tested with the sole purpose of determining the effect of different lubricant formulations and operating conditions on the behaviour of cavitation. The work on the test-rig produced a large amount of unprocessed data, a considerable amount of time was invested to find the best way that would allow for the most accurate and efficient processing of those data. The work involved the testing and visual investigation of the cavitation phenomenon for 19-samples, at different speeds ranging from 100 – 600 RPM. There was also an attempt to identify the behaviour of different lubricants and how their formulation affects cavitation. The results were processed with the use of sophisticated algorithms written specifically for the project in Matlab. Later the processed data were grouped and compared to highlight behavioural differences that could be linked back to their formulation. All 19 lubricants were tested under the same operating conditions but only a representative population of 6 was chosen for this report; the selection of these 6 lubricants has been based mainly on their performance and individual composition. This population featured a number of base lubricants with the addition of viscous modifiers and extra add-packs. The different lubricants were subjected to several tests that would stretch their physical properties to the point where they would start to cavitate. The data were obtained at different speeds and under a range of operating conditions, these conditions were 2 different flowrates at 0.02L/min and 0.05L/Min, 3 different speeds at 100, 300 and 600 RPM, and two different temperatures at

30°C and 70°C; full details can be found in Table 1 and Table 2. The followings are a summary of major findings:

- The data processing was performed with the use of algorithms developed in Matlab. The structure and logic of this algorithm changed dramatically throughout the different stages of the project to ensure the accuracy of the end results considering all the limitations, including the extraction of optical information by the software; full details are provided in Section 2.1.6. The final version of the software offered visual feedback to the user and gave the ability to override the processing if anomalies were observed.
- To ensure the presented data are of high quality, all tests were repeated 3 times to improve the clarity of the images. This involved the sourcing of better quality optics and higher intensity light sources that would allow for higher frame rates, lower exposures and brighter images.

The parametric study offered a set of valuable results when all the lubricants were tested on the lubrication test rig. The 6 out of the 19 lubricants included in this report have offered the following conclusions.

- The performance of each lubricant is directly linked to the lubricants formulation and the operating conditions. Lubricants of the same group show similar behaviour and the kinematic viscosity is a very good indicator of cavity performance. The data support that the addition of a viscous modifier can have a direct effect on cavitation. As an example, lubricants 004A and 020A had the same viscosity and density values but presented different cavity behaviour. The operating condition also interfere with the way lubricants cavitate though not always in the way expected, the increase of the speed does not always increase the cavitating area or cavity length.
- Kinematic viscosity is a good indicator to whether lubricants of the same base group would be more prone to cavitation. Previous literature suggests that viscosity can be directly linked to oil film thickness. A link can be supported between cavitation and Kinematic Viscosity.
- A viscous modifier can reduce the effect of cavitation. As an example, lubricants 004A and 020A are two lubricants of the same group where 020A has an additional viscous modifier. The area of cavitation for 004A varied from 10 – 50% but has a mean value of 20%, while lubricant 020A has an area of cavitation from 10 – 70%

with a mean value of 50%, a clear reduction in cavitation with the viscous modifier. This suggests that the addition of a viscous modifier delays the cavity generation which appears later in the cycle.

- Previous literature suggests that when the speed increases the oil film thickness increases as well. Although in the present investigation the oil film thickness was not measured, the observation showed that the increase in speed had not the same effect on the length of cavity. The length in fact decreased with speed which also supports the increase in film oil thickness and the gap between the piston ring and the liner.
- The Previous literature suggests that when lubricants have different viscosities the one with the lowest viscosity would have the smallest oil film thickness. This is not the same for the rest of the metrics such as cavity width and cavity length. Furthermore, kinematic viscosity has a direct effect on cavity formation. The lower the KV the higher the cavitating area, the length of the cavities and the width of the cavities.
- The consecutive images were processed with the use of a custom algorithms written in Matlab in order to obtain accurate quantitative information for cavity length, cavity width, cavitating area and number of cavities.
- The algorithm allows for the link of physical properties such as cavity length, width, area and number of cavities with physical properties extensively investigated by previous researchers, such as oil film thickness and friction. This could be made possible by extending the capabilities of the software and incorporating the oil film thickness and friction in the algorithm which could offer results that would give a view of the flow on 3 dimensions.
- The software developed can successfully process the visual data but must be coupled with appropriate optical setup which can offer the desired quality and optical clarity. The resolution and magnification of the optical equipment are very important to the way the software performs. Equally important are the light sources used and the position these are placed.
- One of the core objectives was to try and establish a link between the lubrication test-rig and the optical engine. A correlation between the results from the test-rig and the optical engine has been established based on the following conditions:
 - The lubricants tested on the test-rig and the optical engine presented similar behaviour and structure when both tests were at similar operating conditions.

- A link between the test-rig and the optical engine is supported and has been observed for test-rig speeds of 600RPM which correlates to engine speeds of 208RPM. This correlation is based on piston speed.

6.2 Summary of Design of the Optical Engine

The second part of the project focused on the investigation of cavitation within a fully firing optical-engine where the piston-ring and the cylinder-liner interact. This area is subjected to extreme forces, temperatures and pressures, these made the design of the optical engine far more difficult especially on the strength of the optical window, the thermal expansion and the tolerances and as a result the design of the engine has been a very careful and time-consuming procedure; full details of the design processes has been given in chapter 4 and below is a summary of the new design development/outcome.

The new optical engine was based on a modified Ricardo Hydra single cylinder engine where many parts such as the cylinder liner had to be redesigned (except the ring pack which had to be identical to the one used on the unmodified engine) to allow for the optical access to the piston ring and cylinder liner interaction. The optical window covers the full length of the liner over a width of 25mm; this visibility allows access not only into the contact point over the entire length of the liner, but also provides access to the combustion chamber to allow for flow visualisation and flow field measurements.

Many considerations have been taken into account as explained in chapter 4 but the challenging issues were the matting of the optical window with the cylinder liner and the piston rings, and the possibility of oil passing from the sump into the combustion chamber or vice versa, the transfer of the fuel into the sump (“blow-by” effect) which can affect the emission, performance of the lubricant and possible damage to the lubrication system or the engine’s internal components.

Once the design was finalised and the engine was manufactured and the auxiliary components had to be designed to fit the engine. The engine control software and the ECU had to be designed and build in such a way that would allow for the custom setup and operation of the engine as well as for the control of the optical equipment to be installed.

Overall the design of the optical engine was a great success and provided the means to fulfil the objectives of the project, the investigation of the phenomenon of cavitation within a fully firing optical-engine, and beyond with the following features:

- The new design provides full access to a very hostile area where the piston-ring and the cylinder-liner interact and in addition a good exposure to the combustion chamber, covers the full length of the liner over a width of 25mm which provides a great optical access, much greater than that given by XUL10Ar engine.
- The new engine was successfully operated without any issues up to speeds of 3000RPM for firing and motorised operation.
- The new control system to operate the engine with new software and the ECU capable of controlling both the engine operation as well as the optical equipment; the combined new control system and the optical engine would offer a useful and valuable testing device that would allow further investigation to be carried out
- The new optical engine operated at the same specification with in cylinder pressure the same as the unmodified engine. The in-cylinder pressure and the compression ratio showed that the mating of the window with the cylinder liner and the piston rings was successful.
- With careful and accurate design consideration, it was ensured the insertion of the optical window can work the metal piston rings assembly while maintaining the original engine tolerances.
- The new optical engine provides not only access into the contact point over the entire length for the investigation of lubricants cavitation, but also a great optical access into the combustion chamber where the charged motion, spray characteristics and combustion can be visualised or quantified using different optical diagnostics like LDV, PIV, PDA and LIF.
- The piston rings used were a full metal ring pack similar to the one fitted on the unmodified engine. The piston ring gaps play an important role in the way lubricants cavitate within an engine. Cavitation is directly linked to pressure and it occurs when the pressure of a liquid suddenly drops. The ring gaps are a leading factor in cylinder pressure losses, while cylinder gasses can escape down towards the sump. Leading piston ring manufacturers are aware of the pressure loss ring gaps cause and they usually provide a maximum ring gap tolerance with each product. The usual tolerance is 0.0035cm per cm of cylinder diameter to ensure maximum performance and appropriate lubrication. The effect piston rings have on the pressure differential between the cylinder and the sump will affect the pressure profile along the face of the piston rings thus affecting the cavity generation.

6.3 Summary discussions and conclusions of Optical Engine measurements

The final stage of the project involved the testing of the optical engine which would offer access to the usually inaccessible area between the cylinder liner and piston ring interaction under motorised and firing conditions; full details of the operating conditions are given in section 5.5. The followings are the main conclusions:

- The data showed that the lubrication oil from the sump uses the ring gaps to pass into the combustion chamber. The lubricant passes through the gap rings until it finds itself on the top of the top ring where as soon as the piston reaches the top dead centre and changes its direction the lubricant, due to its kinetic energy, will separate itself from the rings and fly within the cylinder.
- The captured video images showed that the rotation of the piston rings does not affect the phenomena of cavitation. The same data suggested that cavitation occurs only in two of the strokes for a four-stroke engine. The phenomenon seems to occur only in the stroke when the in-cylinder pressure is higher than the atmospheric. During this stroke, the in-cylinder pressure puts an extra force behind the piston rings forcing them to form a smaller gap with the cylinder wall, something that does not occur when the valves are open.
- The results showed that, cycle after cycle, cavitation occurs on the face of the piston rings within the gap mainly as a fully developed cavitating sheet in both up-stroke and down-stroke.
- Cavitation takes place on the face of all the 3 rings and not on the face of the piston. It has also been observed that cavitation does not form a uniform cavitating sheet along the face of the ring. This is due to the fact that the cylinders as well as the piston rings do not follow a perfect circular profile.
- While the engine is in operation under motorised conditions with the fuel system on, it was observed that the injected fuel inside the cylinder would momentarily atomise at the first stage of the expansion stroke to form a fuel spray. This suggests that one can use a PDA diagnostic system to characterise the fuel spray characteristics in terms of fuel droplets size and velocity distribution simultaneously.

6.4 Contribution to knowledge

Optical Internal combustion engines are used for the investigation of phenomena that occur during engine operation. Many of these engines operate under idealise conditions or key parts

are replaced in order to protect their optical windows thus, risking the possibility of deviating from the exact behaviour of the phenomena compared to an unmodified engine. The design, manufacture and testing of a fully firing optical engine, that would use a conventional metal ring-pack would offer both a unique measuring device and optical data of great value to the better understanding of the phenomenon. The main contributions of the project are presented below;

- The project developed a unique design of a fully firing optical engine that allowed for the optical visualisation of the piston ring and cylinder liner interaction. The design succeeded in offering an engine that has been both reliable and fully functional at the extend of replicating the operation of a conventional same specification engine.
- A lot of weight was given to the use of a metal 3 piston-ring, ring-pack in combination with the optical window. This project managed to achieve an ideal matting of the surfaces between the piston-ring and the optical liner and ensured that pressure losses would interfere with the results.
- The findings support a correlation between the lubrication test-rig and the optical engine. This link gives access to all the information that was been generated over the past years by a different number of projects performed on the same test rig.
- The data investigate assumptions and speculations made around the phenomena that take place in the cylinder liner/piston-ring area. The contribution of this project was the design and manufacture of an optical-engine that was very close to the specification of a conventional internal combustion engine. The majority of the work performed on optical-engines was performed with the use of full optical cylinders and PVC piston-rings. These rings do not feature the highly important ring-gaps found in conventional engines. These setups though safe and reliable do not fully replicate the behaviour of the phenomena that take place inside that engine.
- The use of a metal ring-pack offered the ability to observe the behaviour of lubricants while these cavitate or pass through the ring-gaps. The setup assisted in better understanding and observing the phenomenon of “blow-by”, something practically impossible with the full PVC ring setups.

This project has assisted with the observation of phenomena that occur in the cylinder-liner and piston-ring interaction. Moreover, it has produced data that can be used to further study the highly important phenomena of cavitation and “blow-by”. This research has produced an

important piece of literature for the future study of these phenomena. There is a lot of knowledge that has been gained from this project and in addition to the literature there is also the experience and expertise of building and operating an optical engine that simulates the same principles and specifications as a conventional internal combustion engine.

6.5 Aims and Objectives Assessment

- Design, manufacture and assembly of an optical internal combustion engine that would allow for the investigation of the phenomenon of cavitation while this takes place in the cylinder liner and piston-ring interaction. The engine must have as a core feature the use of a metal piston-rings similar to the ones used on automotive production engines. – *The design, manufacture and assembly of the engine was successful as the engine operated correctly, even from the initial test runs. The assessment of its performance was done in small increments where the operating conditions and load were gradually increased until the engine was operating at its full potential, the engine operated successfully at every increment, giving the confidence to later use it for the extraction of experimental data. Big success has been the matting of the optical window with the rest of the cylinder and the piston rings. The tolerances between the optical and the unmodified conventional engine have been very close to identical and this can be easily identified from the comparison of the pressure trace and the compression ratio between the two. This ensured that the engine operated to the specifications it was initially designed to. The optical engine was based on a conventional single cylinder Ricardo Hydra engine. The original engine made use of a 3-ring metal ring pack. The piston rings used were the exact same piston rings that the engine was equipped before the optical window modification and the success of the design was to ensure that they came in contact with the optical window to the extent that they would not damage the optical properties of the window or its structure and still maintain its original specifications.*
- Install, setup and successfully use high speed optical equipment on the engine to collect data from the piston ring and cylinder liner interaction. – *The installation and setup of the optical equipment was successfully implemented, and it produced high quality images from the piston ring and cylinder liner interaction which allowed for the further investigation of the phenomenon. The camera, the lighting and the engine were carefully setup and timed together to offer optimum results. The trickiest part was to guide both the light and the camera through the narrow window installed on the engine. This posed a lot of difficulty due to the limited space, but the data confirm the successful implementation.*

- Process the data collected on the optical engine to extract information that would reveal a link between cavitation and the operating conditions of an engine. – *The data extracted were successfully processed and analysed to derive conclusions related to the cavity behaviour inside an optical engine. Though the processing and analysis of the data has been successfully achieved additional work could be carried out that would extract more information from the samples such as lubricant velocity and oil film thickness that would allow for a more detailed analysis of the flow.*
- The completion of the parametric study that would use an existing test-rig, currently property of City, University of London to test a set of 19 lubricants. These 19 lubricants were received by BP while their formulations had been withheld and protected by a confidentiality agreement. Key point is the study of the phenomenon of cavitation and the extraction of information that had not been investigated by the work performed on the test-rig by previous researchers. – *All the 19 lubricants were tested on the lubrication rig with sole purpose the extraction of information that had not been considered by all the previous researchers who performed similar experiments on the test rig. This project succeeded into taking a step further than the measurement of the oil film pressure, the friction and the oil film thickness, which are metrics extensively investigated before. It used the visual data that were captured and combined them with sophisticated algorithms to extract information on the area of cavitation, the length of cavities, the width of cavities and the number of cavities.*
- The data from the test-rig must be compared to the data from the engine and their in-between correlation must be investigated. – *The data extracted from the test-rig were compared to the data extracted from the engine and their in-between relation was investigated. The data presented many similarities to the behaviour of the cavities in similar operating conditions and though extra work is needed to further investigate that link the findings successfully support that there is a close correlation.*
- Finally, a report must be produced that would summarise and discuss the findings of the project along with suggestions for future work. – *The final objective of the report has been the summation of the findings along with recommendations for future work. This part has been successfully completed and the findings as well as all the relevant information have been included as part of the current report.*

6.6 Critical Assessment of experimental process

During the course of the project the measurements had to be repeated numerous times to ensure optimum results. The test-rig measurements were repeated 3 times in total to improve the quality of the data. The software used for the processing of the test-rig data was developed in house for the needs of the project. The first set of the results extracted from the test-rig were captured with a setup similar to the one used by previous researchers and which was presented as optimum for the visualisation of cavitation. Once all the lubricants were tested the captured data were used to develop the Matlab processing algorithm. It soon became obvious that the software faced limitation that regardless how good its logic was it could not overcome due to the input data. For that reason, the optical setup had to be adjusted. The solution was given at the time with the use of greater angle lenses and lower aperture combined with more powerful light sources that would allow for a greater magnification in order to help the software identify the phenomena with a higher accuracy. The result as expected seemed promising as the newly developed software would work much better with the new set of results and would produce much better data that would track closer the cavities generated. Once all the lubricants were tested it was realised that there was a possibility of further improving the software and the derived results, an observation that came with the experience gained. The decision was taken to perform all the tests for a third time in order to achieve the best possible results. The tests were repeated once more while the software was further developed to achieve an even better tracking of the cavitation phenomena.

Though every effort was made to improve the results there is still potential to improve both the software and the data captured. As the software relies on pixel by pixel tracking, the use of a camera with a higher resolution would dramatically improve the quality of the results and the way the software tracks cavitation. Another modification that could have a positive impact would be the use of optical fibres to guide the light into the cylinder liner and piston ring area and ideally from both sides of the test rig. The test-rig is made out of stainless steel which at $\lambda = 589\text{nm}$ has a reflective index of $n = 2.5$ where lubrication oil only $n = 1.47$ (Bor et al, 1990). As found the test-rig has a higher reflective index than the lubrication oil and since the processing algorithm relies on the light intensity to track the cavities, the reduction of the reflective light on the surrounding components would have allowed for the thresholds on the algorithm to be adjusted to a more conservative setting that would also allow for an even better tracking of the cavities. The part of the software that handles and mitigates for the

reading errors would have to work less to post process the data which would have increased the accuracy and also reduced the processing time.

The same optical fibre light sources could have also been used on the optical engine. The illumination of the contact point between the cylinder liner and the piston ring was always a challenge throughout the testing of the engine. The light sources used were coupled with focussing lenses that would allow for the better focusing of the light beam and though the focusing lenses did a very good job in focusing the light there would be a great benefit to the use of new light source that would implement optical fibres to better guide the light. The main problem of the light sources used was not only the fact that with the addition of the focusing lenses the setup became bulky and difficult to setup, nor the fact that even with the lenses the focusing became a constant challenge but the fact that they produced a tremendous amount of heat that when focused would raise the temperature of the engine thus risking affecting the behaviour of the lubricants and the integrity of the engine. The optical fibres could also be used with high intensity light sources such as lasers which would allow for the measurement of the oil film thickness on the cylinder walls and between the cylinder liner and piston ring interaction, which could give an idea of the oil film thickness between the cylinder wall and the piston rings. The use of lasers would have also given a better tracking of the lubricant blow by, where a molecule is identified and then tracked throughout its path. The same technique could be used to calculate the speed of the flow through the cylinder liner and piston ring gap.

6.7 Recommendations for Future work

Despite the valuable knowledge gained with throughout the project there is a need for further work to be carried out in order to achieve a better understanding of the link between the formulation of the lubricants and the behaviour of cavitation. There are certain aspects that need to be further analysed and investigated that would bridge gaps possibly not covered by the current project. These revolve mainly around the formulation of lubricants and the way the data were acquired and processed. The tests on the optical engine have only been performed with an off the shelf lubricant sample that is commercially available and manufactured from BP. The possibility of composing new samples from base lubricants where their formulations could be controlled would offer a different insight to the way different lubricant formulations behave inside the engine. Another point where the current research can be improved is by improving the processing software developed for the project. The VBA code written for the processing of the engine data is mainly computing the area of

the image that is covered by cavitation. It would be of great benefit to develop a more sophisticated algorithm that would allow for the processing of the data while incorporating that curvature of the ring into the calculations. This is one aspect that was not added into the current software and would be of a great value, as it will increase the accuracy of the results. The engine as it was originally delivered came with a set of thermocouples installed on its original cylinder block. These thermocouples were connected on a control unit responsible for acquiring the readings. This control unit was malfunctioning, but the thermocouple setup could be a good addition to the newly manufactured cylinder block as it will allow for temperature distribution reading simultaneously with the optical data. This setup will unlock further capabilities of the engine that would allow for the better understanding of how the temperature distribution on the cylinder and the piston affects the cavity behaviour. The current temperature readings were based on the average temperature of the cylinder block but since cavitation is a phenomenon directly linked to viscosity and viscosity is depended on the temperature the uneven temperature distribution along the cylinder block might have an effect on the cavity behaviour itself. Another modification that needs to be considered is the addition of a force-feed induction that would allow for testing and would simulate the case where an engine has been supercharged or turbocharged. The need for smaller and more powerful engines and the current notion among the engine manufactures to turn to supercharging or turbocharging to achieve that, means that this type of research will add value to phenomena related to those types of engines. Finally, another area that needs to be further investigated is the improvement of the current Matlab algorithm to make it more sensitive to fine cavities that currently are not successfully recorded, another possibly solution would be the re-run of the tests to a greater magnification but for these cases the tests would have to be repeated and new equipment would have to be acquired.

REFERENCE

- Alfa Romeo. (2015, March 16). Alfa Romeo. Retrieved from Alfa Romeo:
http://wallpaperswide.com/alfa_romeo_engine-wallpapers.html
- all4honda. (2015, March 16). all4honda. Retrieved from all4honda:
<http://www.all4honda.com/webshop/14-civic-2001-2006/39-motor-tuning/354-inlaatraject/oem-honda-rbc-inlaatspruitstuk-k20a-motoren-details.html>
- Anubiz. (2015, March 16). Engine tune-up package for Japanese Single Cylinder Engines. Retrieved from Engine tune-up package for Japanese Single Cylinder Engines:
<http://www.anubizcarbturn.com/services/service-packages/japanese-bikes/>
- Arcoumanis, C., M. Duszynski and H. Preston. (1998b). Cold-start measurements of lubricant film thickness in the cylinder of a firing diesel engine using LIF. SAE Transactions 107(4).
- Arcoumanis, C., M. Duszynski, H. Flora and P. Ostovar. (1995). Development of a piston-ring lubrication test-rig and investigation of boundary condition for modelling lubricant film properties. SAE Transactions 104(4):1433-1451.
- Arcoumanis, C., M. Duszynski, H. Lindenkamp and H. Preston. (1998a). Measurements of lubricant film thickness in the cylinder of a firing diesel engine using LIF. SAE Transactions 107(4):898-906.
- Arcoumanis, C., P. Ostovar and R. Mortier. (1997). Mixed lubrication modelling of Newtonian and shear thinning liquids in a piston-ring configuration. SAE Transactions.
- autodiagnosticandpublishing. (2015, March 16). autodiagnosticandpublishing. Retrieved from autodiagnosticandpublishing:
<http://www.autodiagnosticandpublishing.com/feature/fuel-injector-testing.htm>
- Benchaita, M.T. , S Gonsel and F.E Lockwood. (1990). Wear Behaviour of Base Oil Fractions and Their Mixtures. Tribology transactions 33:371-383.
- Boness, R. J. and H. M. Hawthorne. (1995). Acoustic Emission from the Unlubricated Sliding Wear of Steel and Silicon Nitride. Tribology transactions 38(2):293-298.
- Boness, R. J., S. L. McBride and M. Sobczyk. (1990). Wear Studies Using Acoustic Emission Techniques. Tribology International 23(5):291-295.

- Bosch. (2015, March 16). Bosch . Retrieved from Bosch : <http://www.bosch-presse.de/presseforum/details.htm?txtID=6406&locale=en>
- BP-Castrol. (2015, March 16). BP-Castrol. Retrieved from BP-Castrol: <http://www.bplubricants.com/en/bp-lubricants>
- Brennen, Christopher E. (1995) Cavitation and Bubble Dynamics. New York: Oxford University Press.
- Brown, M. A., H. McCann and D. M. Thompson. (1993). Characterization of the Oil Film Behavior Between the Liner and Piston of a Heavy-Duty Diesel Engine. SAE paper 932784.
- Brown, S. R. and G. M. Hamilton. (1977). The partially lubricated piston-ring. *Journal Mechanical Engineering Science* 19(2):81-89.
- Brown, S. R. and G. M. Hamilton. (1978). Negative pressures under a lubricated piston-ring. *Journal Mechanical Engineering Science* 20(1):49-57.
- Brown, S. R., G. M. Hamilton and S.L Moore. (1975). Hydrodynamic pressure under a piston-ring. *Nature* 253:341-342.
- Burnett, P. J. (1989). Relationship between oil consumption, deposit formation and piston-ring motion for single cylinder diesel engines. SAE paper 920089.
- Caines, A. J. and R. F. Haycock. (1996) *Automotive lubricants reference book*: Society of Automotive Engineers Warrendale, PA.
- California, U. o. (2015, March 16). University of Southern California. Retrieved from University of Southern California: <http://www.marketplace.org/topics/sustainability/we-used-be-china/la-smog-battle-against-air-pollution>
- Cameron, A. (1971) *Basic Lubrication Theory*: Longman.
- Casey, S.M. (1998) Effects of engine operating conditions on oil film thickness and distribution along the piston/ring/liner interface in a reciprocating engine. In 1998 Fall Technical Conference of the ASME Internal Combustion Engine Division 133:47-56. Clymer, New York (ASME)
- Castleman, R. A. (1936). A Hydrodynamical Theory of Piston-ring Lubrication. *Journal of Applied Physics* 7(9):364-367.

chemhume. (2015, March 16). chemhume. Retrieved from chemhume:
<http://www.chemhume.co.uk/ASCHEM/Unit%203/15%20Equilibria/Equilibriac.htm>

chevyhardcore. (2015, March 16). chevyhardcore. Retrieved from chevyhardcore:
<http://www.chevyhardcore.com/tech-stories/engine/junkyard-ls-engine-builds-going-from-rags-to-riches/>

chilkatdesigns. (2015, March 16). chilkatdesigns. Retrieved from chilkatdesigns:
<http://www.chilkatdesigns.com/OilPan.html>

CHIS, A. R. (2015, March 16). How Wankel's Rotary Engine Works. Retrieved from How Wankel's Rotary Engine Works: <http://www.autoevolution.com/news/how-wankels-rotary-engine-works-19241.html>

Conley, M. (2015, March 16). Antique Steam & Gas engine SCANS. Retrieved from Antique Steam & Gas engine SCANS: <http://www.machineryscans.com/steam%20engines.htm>

Cooke, V. B. (1990) Lubrication of Low Emission Diesel Engines: Society of Automotive Engineers.

Coyne, J. and H. G. Elrod. (1970a). Conditions for the rupture of a lubricating film, Part 1. ASME J. Lubrication Technol 92:451–456.

Coyne, J. and H. G. Elrod. (1970b). Conditions for the rupture of a lubricating film, Part II: New boundary conditions for Reynolds equation ASME J. Lubrication Technol 92:156-167.

CROWE, P. (2015, March 16). BMW Concept 6 – 1600cc Inline 6 Cylinder Engine. Retrieved from BMW Concept 6 – 1600cc Inline 6 Cylinder Engine: <http://thekneeslider.com/bmw-concept-6-1600cc-inline-6-cylinder-engine/>

Dellis, P. (2005) "Aspects of Lubrication in Piston Cylinder Assemblies." PhD Thesis, Department of Mechanical Engineering: Imperial College of Science, Technology and Medicine. London.

Dellis, P. and C. Arcoumanis. (2004). Cavitation development in the lubricant film of a reciprocating piston-ring assembly. Proceedings of the Institution of Mechanical Engineers, Part J: Journal of Engineering Tribology 218(3):157-171.

Didot, F.E., E. Green and R.H. Johnson. (1987). Volatility and oil consumption of SAE 5W-30 engine oil. SaE paper 872126.

- Dorinson, A. and K. C. Ludema. (1985) *Mechanics and chemistry in lubrication*: Elsevier.
- Dowson, D, E.H Smith and C.M Taylor. (1980). An experimental study of hydrodynamic film rupture in a steadily-loaded, non-conformal contact. *Journal of Mechanical Engineering Science* 33(2):71-78.
- Dowson, D. (1979) *History of tribology*: Longman New York.
- Dowson, D. (1993). Piston assemblies: Background and lubrication analysis. *TRIBOLOGY SERIES* 26:213-213.
- Dowson, D. and C. M. Taylor. (1979). Cavitation in Bearings. *Annual Reviews in Fluid Mechanics* 11(1):35-65.
- Drinkwater, B., R. Dwyer-Joyce and P. Cawley. (1997). A study of the transmission of ultrasound across solid–rubber interfaces. *The Journal of the Acoustical Society of America* 101:970.
- Duszynski, M. (1999) "Measurement of Lubricant Film Thickness in Reciprocating Engines." PhD Thesis, Department of Mechanical Engineering: Imperial College of Science, Technology and Medicine. London.
- Dwyer-Joyce, R. S., P. Harper and B. W. Drinkwater. (2004). A Method for the Measurement of Hydrodynamic Oil Films Using Ultrasonic Reflection. *Tribology Letters* 17(2):337-348.
- Elrod, H. G. (1979). A general theory for laminar lubrication with Reynolds roughness. *ASME, Transactions, Journal of Lubrication Technology* 101:8-14.
- eMercedesBenz. (2015, March 16). Wikipedia. Retrieved from Wikipedia: http://en.wikipedia.org/wiki/History_of_the_internal_combustion_engine
- enginebasics. (2015, March 16). enginebasics. Retrieved from enginebasics: <http://www.enginebasics.com/Engine%20Basics%20Root%20Folder/Flywheel.html>
- enginetechnologyinternational. (2015, March 16). enginetechnologyinternational. Retrieved from enginetechnologyinternational: <http://www.enginetechnologyinternational.com/news.php?NewsID=32368>
- Floberg, L. (1965). On hydrodynamic lubrication with special reference to sub-cavity pressures and number of oil streamers in cavitation regions in cavitation regions. *Acta Polytechnica Scandinavica Mechanical Engineering Series* 19.

Floberg, L. (1973). Lubrication of two rotating cylinders at variable lubricant supply with reference to the tensile strength of the liquid lubricant. *Journal of Lubrication Technology, Transactions ASME, Ser F* 95(2):155-165.

Froelund, K., J. Schramm, T. Tian, V. Wong and S. Hochgreb. (2001). Analysis of the Piston-ring/Liner Oil Film Development During Warm-Up for an SI-Engine. *Journal of Engineering for Gas Turbines and Power* 123:109.

Frølund, K., J. Schramm, B. Noordzij and T. Tian. (1997). An Investigation of the Cylinder Wall Oil Film Development During Warm-Up of an SI Engine Using Laser Induced Fluorescence. *SAE Transactions* 971699.

FullRace. (2015, March 16). FullRace. Retrieved from FullRace: <http://www.full-race.com/store/turbos/garrett-gt-series/garrett-gt3788r-twinscroll-turbo.html>

Furuhama, S. (1959). A Dynamic Theory of Piston-Ring Lubrication (1st report, Calculation). *Bulletin of Japanese Society of Mechanical Engineers* 2(7):423-428.

Furuhama, S. (1985) Some Factors on engine oil consumption through a piston. In *Proc JSLE Int Trib Conf.*:301. Tokyo

Furuhama, S. (1987). Tribology of reciprocating internal combustion engines. *Jap. Soc. Mech. Engrs Int. J* 30(266):1189-1199.

Furuhama, S. and T. Sumi. (1961). A Dynamic Theory of Piston-Ring Lubrication (3rd report, Measurement of oil film thickness). *Bulletin of Japanese Society of Mechanical Engineers* 4(16):744-752.

Gitlin, J. M. (2015, March 16). The road ahead: How we'll get to 54.5 mpg by 2025. Retrieved from *ARS Technica*: <http://arstechnica.com/features/2012/10/the-road-ahead-how-well-get-to-54-5-mpg-by-2025/2/>

Green, D.A., R. Lewis and R. Dwyer-Joyce. (2006) The ultrasonic measurement of automotive component contact pressures. In *Tribology 2006: Surface Engineering and Tribology for Future Engines and Drivelines* London, UK (Institute of Mechanical Engineers)

Greene, A. (2015, March 16). AutoFoundry. Retrieved from AutoFoundry: <http://www.autofoundry.com/731/e-lenoir-patents-the-first-practical-engine-153-years-ago/>

- Greene, A. B. (1969). Initial visual studies of piston-cylinder dynamic oil film behaviour. *Wear* 13:345-360.
- Grice, N. and I. Sherrington. (1993). An Experimental Investigation Into the Lubrication of Piston-rings in an Internal Combustion Engine: Oil Film Thickness Trends, Film Stability and Cavitation. SAE Technical Paper Series 930688.
- Gümbel, L. K. R. (1921). Vergleich der Ergebnisse der rechnerischen Behandlung des Lagerschmierungsproblem mit neueren Versuchsergebnissen. *Monatsbl. Berliner Bez. Ver. Dtsch. Ing*:125-128.
- Hahn, H. W. (1957). Dynamically loaded journal bearing of finite length. Conference on Lubrication and Wear Clut.
- Hamilton, D. B., C. M. Allen and J. A. Walowit. (1966a). A theory of lubrication by microirregularities. *ASME, TRANSACTIONS, SERIES D-JOURNAL OF BASIC ENGINEERING* 88:177-185.
- Hamilton, D. B., J. A. Walowit and C. M. Allen. (1966b). A Theory of Lubrication by Microirregularities. *Transaction of the ASME, Journal of Basic Engineering, Series D*:177-185.
- Hamilton, G. M. and S. L. Moore. (1974). Measurement of the oil-film thickness between the piston-rings and liner of a small diesel engine (First Paper). *Proc. Instn Mech. Engrs* 188:253-261.
- Hamrock, B. J., S. R. Schmid and B. O. Jacobson. (2004) *Fundamentals of Fluid Film Lubrication*. 2nd Edition. New York: Marcel Dekker Ltd.
- Han, D. C. and J. S. Lee. (1998). Analysis of the piston-ring lubrication with a new boundary condition. *Tribology International* 31(12):753-760.
- Harigaya, Y., M. Ichinose and M. Suzuki. (1996). Effect of temperature on the lubrication characteristics between the piston-ring and the cylinder liner of internal combustion engine. The 1996 18th Annual Fall Technical Conference of the ASME Internal Combustion Engine Division. Part 2(of 5):17-24.
- Haugland, R. P (1999) *Molecular probes*. In *Handbook of Fluorescent Probes and Research Chemicals*. 7th Edition.

Herbst, H. M. and H. H. Priebsch. (2000). Simulation of piston-ring dynamics and their effect on oil consumption. SAE transactions 109(3):862-873.

Hill, B. (2015, March 16). DailyTech. Retrieved from DailyTech:
<http://images.dailytech.com/nimagecq5dam.web.1280.1280.jpeg>

Hoult, D. P. and M. Takiguchi. (1991). Calibration of the laser fluorescence technique compared with quantum theory. Tribology transactions 34:440-444.

Hoult, D. P., J. P. Lux, V.W. Wong and S. A. Billian. (1988). Calibration of Laser Fluorescence Measurements of Lubricant Film Thickness in Engines. SAE paper 881587.

Inagaki, H., A. Saito, M. Murakami and T. Konomi. (1995). Development of two-dimensional oil film thickness distribution measuring system. SAE paper 952346.

jscspeed. (2015, March 16). jscspeed. Retrieved from jscspeed:
http://www.jscspeed.com/catalog/Performance_Crankshafts_for_90_99_Mitsubishi_Eclipse_4G63-8773-1.html

Kennedy, G. (2015, March 16). Porsche Engine Teardown. Retrieved from Yahoo:
<https://autos.yahoo.com/news/porsche-engine-teardown-coolest-thing-ll-see-today-163216089.html>

Kim, S., A. Azetsu, M. Yamauchi and T. Someya. (1995). Dynamic Behavior of Oil Film between Piston-ring and Cylinder Liner: Visualization of Oil Film Rupture and Measurement of Oil Film Pressure Using Simulating Rig. JSME international journal. Series C, Mechanical systems, machine elements and manufacturing 38(4):783-789.

Klamann, D. and R. R. Rost. (1984) Lubricants and Related Products: Synthesis, Properties, Applications, International Standards: Verlag Chemie.

Kustas, F. M., J. N. Schwartzberg, S. H. Carpenter, C. R. Heiple and D. L. Armentrout. (1994). Acoustic emission monitoring of diamond-like carbon coating degradation during sliding wear. Surf. Coat. Technol.(Switzerland) 67(1):1-7.

Laurence, R. B., V. W. Wong and A. J. Brown. (1996). Effects of Lubrication System Parameters on Diesel Particulate Emission Characteristic. SAE Transactions 105(4):157-164.

Liskiewicz , T. W., A. Morina and A. Neville. (2008). Challenges in Lubricant Additives Technology. The Triz Journal.

- Luengo, G. , J. Israelachvili and S. Granick. (1996). Generalized effects in confined fluids: New friction map for boundary lubrication. *Wear* 200(1):328-335.
- Lux, J. P., D. P. Hoult and M. J. Olechowski. (1990). Lubricant film thickness measurements in a diesel engine piston-ring zone. *Lubrication engineering* 47(5):353-364.
- lysholm. (2015, March 16). lysholm. Retrieved from lysholm:
<http://www.lysholm.us/camaro.php>
- Maloney, B. (2015, March 16). Cradle Of Aviation Museum - Aircraft Engines. Retrieved from Cradle Of Aviation Museum - Aircraft Engines:
<http://www.williammaloney.com/aviation/cradleofaviationmuseum/AircraftEngines/pages/11WrightJ4RadialEngine.htm>
- Masjuki, H. H., M. A. Maleque, A. Kubo and T. Nonaka. (1999). Palm oil and mineral oil based lubricants—their tribological and emission performance. *Tribology International* 32(6):305-314.
- Meyer, E. (1998) *Nanoscience: Friction and Rheology on the Nanometer Scale*: World Scientific Pub Co Inc.
- mikunipower. (2015, March 16). mikunipower. Retrieved from mikunipower:
<http://www.mikunipower.com/>
- Miller, G.M. (1862). On a packing for Pistons of Steam Engines. *Proc Inst Mech. Engrs.*
- Moin, S. (2015, March 16). Shaik Moin. Retrieved from Shaik Moin:
<https://shaikmoin.wordpress.com/tag/four-stroke-engine/>
- Moore, S. L. and G. M. Hamilton. (1978). The Starved Lubrication of Piston-rings in a Diesel Engine. *Journal Mechanical Science* 20(6):345-352.
- Moore, S.L and G. M. Hamilton. (1980). The piston-ring at top dead centre. *Proceedings of the Institution of Mechanical Engineers* 194.
- motorcycle-superstore. (2015, March 16). motorcycle-superstore. Retrieved from motorcycle-superstore: <http://www.motorcycle-superstore.com/21116/i/wiseco-titanium-engine-valves>
- Myers, J. E., G. L. Borman and P. S. Myers. (1990). Measurements of oil film thickness and liner temperature at top ring reversal in a diesel engine. *SAE transactions* 99:339-366.

Nakashima, K., S. Ishihara and K. Urano. (1995). Influence of Piston ring-gaps on Lubricating Oil Flow Into the Combustion Chamber. SAE paper 952546.

NGK. (2015, March 16). NGK. Retrieved from NGK: <http://www.ngkntk.co.uk/>

onallcylinders. (2016, March 16). onallcylinders. Retrieved from onallcylinders: <http://www.onallcylinders.com/2014/02/07/camshaft-faqs-lobe-separation-intake-exhaust-centerlines/>

Ostovar, P. (1996) "Fluid aspects of piston-ring lubrication." PhD Thesis, Department of Mechanical Engineering: Imperial College of Science, Technology and Medicine. London.

Parker, D. A., J. V. Stafford, M. Kendrick and N. A. Graham. (1975) Experimental measurements of the quantities necessary to predict piston-ring-cylinder bore oil film thickness, and the oil film thickness itself, in two particular engines. In Piston-ring Scuffing conference:79-98. London, UK (Institute of Mechanical Engineers)

Parks, J. E., J. S. Armfield, T. E. Barber, J. M. E. Storey and E. A. Wachter. (1998). In Situ Measurement of Fuel in the Cylinder Wall Oil Film of a Combustion Engine by LIF Spectroscopy. *Applied Spectroscopy* 52(1):112-118.

PATRASCU, D. (2015, March 16). opoc Engine Explained. Retrieved from AutoRevolution: <http://www.autoevolution.com/news/opoc-engine-explained-22609.html>

perf-concepts. (2015, March 16). perf-concepts. Retrieved from perf-concepts: http://www.perf-concepts.com/cylinder_head.htm

Phen, R. V., D. Richardson and G. Borman. (1993). Measurements of Cylinder Liner Oil Film Thickness in a Motored Diesel Engine. SAE Transactions Paper 932789

pi-innovo. (2015, Mach 16). pi-innovo. Retrieved from pi-innovo: <http://www.pi-innovo.com/engineering/engine-emission-control>

Pitts, E. and J. Greiller. (1961). The flow of thin liquid films between rollers. *Journal of Fluid Mechanics* 11(01):33-50.

Priest, M. and C. M. Taylor. (2000). Automobile engine tribology-approaching the surface. *Wear* 241(2):193-203.

Priest, M., D. Dowson and C. M. Taylor. (2000). Theoretical modelling of cavitation in piston-ring lubrication. Proceedings of the Institution of Mechanical Engineers, Part C: Journal of Mechanical Engineering Science 214(3):435-447.

Pyke, E. A. (2000) "Investigation of piston-ring lubrication using laser induced fluorescence." PhD thesis, Department of Mechanical Engineering: Imperial College of Science, Technology and Medicine. London.

racetep. (2015, March 16). racetep. Retrieved from racetep:
<http://www.racetep.com/mr2tpart.htm>

Ramsbottom. (1854). On an improved Piston for steam Engines. Proc Inst Mech. Engrs:70-74.

Ramsbottom. (1855). On the construction of Packing Rings for Piston. Proc Inst Mech. Engrs:206-208.

Richardson, D. E. and G. L. Borman. (1992). Theoretical and experimental investigations of oil films for application to piston-ring lubrication. SAE, WARRENDALE, PA(USA). 1992.

RMC. (2015, March 16). RMC Automotive. Retrieved from RMC Automotive:
<http://www.rcmautomotive.com/id1.html>

rrconnectingrods. (2015, March 16). rrconnectingrods. Retrieved from rrconnectingrods:
<http://rrconnectingrods.com/steel-connecting-rods/steel-connecting-rods.html>

Ruddy, B. L., D. Dowson and P. N. Economou. (1982). A review of studies of piston-ring lubrication. Proceedings of 9th Leeds-Lyon Symposium on Tribology: Tribology of Reciprocating Engines:109-121.

Ryan Fletcher, A. H. (2015, March 16). Dynamite and Other Explosives. Retrieved from Dynamite and Other Explosives: <http://www.scientiareview.org/pdfs/275.pdf>

Sanda, S. (1998). Measurement of oil film thickness: The Fluorescence Method and Others. Japanese Journal of Tribology 43(7):893-902.

Sanda, S. and T. Someya. (1987) The Effect of Surface Roughness on Lubrication Between a Piston-ring and a Cylinder Liner. In Tribology - Friction, Lubrication and Wear: Fifty Years On 1:135-143. (Proceedings of the Institution of Mechanical Engineers, International Conference)

- Sanda, S., A. Saito, T. Konomi and H. Nohira. (1993). Development of Scanning Laser-Induced-Fluorescence Method for Analyzing Piston Oil Film Behavior. Proceedings of IMechE, C 465:155-164.
- Savage, M. D. (1977). Cavitation in lubrication. Part 1. On boundary conditions and cavity—fluid interfaces. *Journal of Fluid Mechanics* 80(04):743-755.
- Sawicki, J. T. and T. V. Rao. (2004). Cavitation Effects on the Stability of a Submerged Journal Bearing. *The International Journal of Rotating Machinery* 10(3):227-232.
- Schiemann, L. F., C. A. Andrews, V. A. Carrick and B. K. Humphrey. (1995). Developing Heavy Duty Diesel Lubricants to meet the extended Service Interval Challenge. SAE Paper SP-1121:159-172.
- Seki, T., K. Nakayama, T. Yamada, A. Yoshida and M. Takiguchi. (2000). A study on variation in oil film thickness of a piston-ring-package: variation of oil film thickness in piston sliding direction. *Journal of Society of Automotive Engineers of Japan* 21(3):315-320.
- Shaw, B. T., D. P. Hault and V. W. Wong. (1992). Development of Engine Lubricant Film Thickness Diagnostics Using Fiber Optics and Laser Fluorescence. SAE paper 920651.
- Shenghua, L., L. Jijun, A. Longbao and W. Rong. (1996). An Experimental Investigation of the Oil Film Lubricating Piston-rings. SAE Transactions 961912:32-37.
- Sherrington, I. and E. H. Smith. (1985). Experimental methods for measuring the oil-film thickness between the piston-rings and cylinder-wall of internal combustion engines. *Tribology International* 18(6):315-320.
- Sherrington, I. and S. Söchting. (2006) An experimental study of variability in the thickness of the hydrodynamic lubricant film between the piston-rings and cylinder bore of an internal combustion engine under steady operating conditions. In *Tribology 2006: Surface Engineering and Tribology for Future Engines and Drivelines* London, UK (Institute of Mechanical Engineers)
- Shuster, M., D. Combs, K. Karpip and D. Burke. (2000). Piston-ring Cylinder Liner Scuffing Phenomenon Studies Using Acoustic Emission Technique. SAE Transactions.
- Skinner, S. (1903). On the Occurrence of Cavitation in Lubrication. Proceedings of the Physical Society of London 19:73-81.

Smart, A. E. and R. A. J. Ford. (1974). Measurement of Thin Liquid Films by a Fluorescence Technique. *Wear* 29(1):41-47.

Sobester, A. (2015, March 16). Wikipedia. Retrieved from Wikipedia:
http://en.wikipedia.org/wiki/Components_of_jet_engines

SparkAuto. (2015, March 16). SparkAuto. Retrieved from SparkAuto:
<http://cazaautoparts.ca/guides.html>

Stachowiak, G. and A. W. Batchelor. (2000) *Engineering Tribology*: Butterworth-Heinemann.

Stieber, W. (1933). *Das Schwimmlager*. Ver. Dtsch. Ing.

subaruforester. (2015, March 16). subaruforester. Retrieved from subaruforester:
<http://www.subaruforester.org/vbulletin/f75/sti-radiator-cap-104046/>

Sun, J., R.J.K. Wood, Wang. L., I. Care and H.E.G. Powrie. (2006) Wear monitoring of lubricated sliding contacts by acoustic emission and electrostatic technologies. In *Tribology 2006: Surface Engineering and Tribology for Future Engines and Drivelines* London, UK (Institute of Mechanical Engineers)

Swales, P. D. (1974) A review of cavitation phenomena in engineering situations. In *Tribology, Cavitation and Related Phenomena in Lubrication*, Proceedings of the 1st Leeds-Lyon Symposium (Eds. D. Dowson, M. Godet and C. M. Taylor) Paper 1(i):3-9. The University of Leeds, England (Institute of Mechanical Engineers)

Swift, H. W. (1932). The Stability of Lubricating Film in Journal Bearings. *Proceedings Institute Civil Engineers (London)* 233:267-288.

Takiguchi, M., K. Nakayama, S. Furuhashi and H. Yoshida. (1998). Variation of Piston-ring Oil Film Thickness in An Internal Combustion Engine--Comparison Between Thrust and Anti-Thrust Sides. *SAE Transactions* 107(3):816-824.

Takiguchi, M., R. Sasaki, I. Takahashi, F. Ishibashi, S. Furuhashi, R. Kai and M. Sato. (2000) Oil Film Thickness Measurement and Analysis of a Three Ring-pack in An Operating Diesel Engine. In *Advances in Powertrain Tribology 2000 (CEC/SAE)*

Taylor, G. I. (1963). Cavitation of a viscous fluid in narrow passages. *Journal of Fluid Mechanics Digital Archive* 16(04):595-619.

ThinkLink. (2015, March 16). w 16 engine. Retrieved from ThinkLink:
<https://www.thinglink.com/scene/442631183654715393>

Thirouard, B. (2001) "Characterization and modeling of the fundamental aspects of oil transport in the piston-ring-pack of internal combustion engines." PhD Thesis, Department of Mechanical Engineering: Massachusetts Institute of Technology. Massachusetts, Cambridge.

Thirouard, B. P., T. Tian and D. P. Hart. (1998). Investigation of Oil Transport Mechanisms in the Piston-ring-pack of a Single-Cylinder Diesel Engine, Using Two-Dimensional, Laser-Induced Fluorescence. SAE paper 982658.

Tian, T. and V. W. Wong. (2000). Modeling the lubrication, dynamics, and effects of piston dynamic tilt of twin-land oil control rings in internal combustion engines. Journal of Engineering for Gas Turbines and Power (Transactions of the ASME) 122:119-131.

Tian, T., L. B. Noordzij, V. W. Wong and J. B. Heywood. (1996). Modeling piston-ring dynamics, blowby, and ring-twist effects. The 1996 18 th Annual Fall Technical Conference of the ASME Internal Combustion Engine Division. Part 2(of 5) 2:67-80.

Tian, T., V. W. Wong and J. B. Heywood. (1998). Modeling the dynamics and lubrication of three piece oil control rings in internal combustion engines. SAE transactions 107(4):1989-2006.

Ting, L. L. (1993a). Development of a Reciprocating Test-rig for Tribological Studies of Piston Engine Moving Components--Part II: Measurement of Piston-ring Friction Coefficients and Rig Test Confirmation. SAE paper 930686.

Ting, L. L. (1993b). Development of a Reciprocating Test-rig for Tribological Studies of Piston Engine Moving Components - Part I: Rig Design and Piston-ring Friction Coefficients Measuring Method. SAE paper 930685.

tomiokaracing. (2015, March 16). tomiokaracing. Retrieved from tomiokaracing:
<http://www.tomiokaracing.com/index.php/exhaust-manifold-for-evo-4-9.html>

TWO-STROKE ENGINE. (2015, March 16). Retrieved from TWO-STROKE ENGINE:
<https://prharikrishnan.wordpress.com/2014/05/26/difference-between-2-stroke-and-4-stroke-engine/>

V6 engine. (2015, March 16). Retrieved from Wikipedia:
http://en.wikipedia.org/wiki/V6_engine

- Van Dam, W. and W.M. Klelser. (1995). Lubricant Related Factors Controlling Oil Consumption in Diesel Engines. SAE paper 952547.
- Vijay, H. and V. H. Arakeri. (1973). Viscous effects on the position of cavitation separation from smooth bodies. *J Fluid Mech* 68(4):779-799.
- Wakuri, Y, S Ono, M Soejima and N Noguchi. (1979). Oil-film behaviour of reciprocating slider with circular profile (Observation of film by means by thin film interferometry). *Bulletin of JSME* 22(167):755-762.
- Wakuri, Y., M. Soejima, Y. Ejima, T. Hamatake and T. Kitahara. (1995). Studies on Friction Characteristics of Reciprocating Engine. *SAE transactions* 104(4):1463-1477.
- Wakuri, Y., S. Ono, M. Soejima and K. Masuda. (1981). Oil-film Behaviour of Reciprocating Slider with Circular Profile: Optical Measurement of Oil-film Separation Boundary. *Bulletin of JSME* 24(194):1462-1469.
- Washio, S., S. Takahashi and S. Yoshimori. (2003). Study on cavitation starting at the point of separation on a smooth wall in hydraulic oil flow. *Proceedings of the Institution of Mechanical Engineers, Part C: Journal of Mechanical Engineering Science* 217(6):619-630.
- wbautomotive. (2015, March 16). wbautomotive. Retrieved from wbautomotive: <http://www.wbautomotive.com/EFIAccessories.htm>
- What-When-How. (2015, March 16). Retrieved from What-When-How: <http://what-when-how.com/energy-engineering/reciprocating-engines-diesel-and-gas-energy-engineering/>
- Wikipedia. (2015, March 16). Wikipedia. Retrieved from Wikipedia: <http://en.wikipedia.org/wiki/Cavitation>
- Wing, R. D. and O. A. Saunders. (1972). Oil film temperature and thickness measurements on the piston-rings of a diesel engine. *Proc. Instn Mech. Engrs* 186:1-9.
- wiseco. (2015, March 16). wiseco. Retrieved from wiseco: <http://www.wiseco.com/Automotive/Pistons.aspx>
- Wong, V. W. and D. P. Hoult. (1991). Experimental Survey of Lubricant-Film Characteristics and Oil Consumption in a Small Diesel Engine. SAE paper 910741.
- Wong, V.W., S.M. Casey and G Tamai. (1999) Lubricant film characteristics in power cylinder and dependence on location, oil properties, and engine operation conditions. In

Proceedings of the 15th International Combustion Engine Symposium (International) 30:161-166. Seoul, Korea (SAE International)

Woods, H.A. and H.M. Trowbridge. (1955). Shell Roll Test for Evaluating Mechanical Stability. NLGI Spokesman 19:26-27 and 30-31.

Yilmaz, E., T. Tian, V. Wong and J. B. Heywood. (2004). The contribution of different oil consumption sources to total oil consumption in a spark ignition engine. S A E Transactions 2004-01-2909.

youthcollection47. (2015, March 16). youthcollection47. Retrieved from youthcollection47: <http://www.youthcollection47.com/engine-cooling-system-air-or-liquid-cooled/>

Yu, S. and K. Min. (2002). Effects of the oil and liquid fuel film on hydrocarbon emissions in spark ignition engines. Proceedings of the Institution of Mechanical Engineers, Part D: Journal of Automobile Engineering 216(9):759-771.